INVESTIGATING IMMUNOTHERAPY IN TRIPLE NEGATIVE BREAST CANCER

INVESTIGATING IMMUNOTHERAPY TREATMENTS AND THE IMMUNOLOGICAL SYNAPSE IN TRIPLE NEGATIVE BREAST CANCER

By ALYSSA R. VITO, B.Sc., M.Sc.

A Thesis Submitted to the School of Graduate Studies in Partial Fulfilment of the Requirements for the Degree Doctor of Philosophy

McMaster University © Copyright by Alyssa Vito, April 2021

McMaster University DOCTOR OF PHILOSOPHY (2021) Hamilton, Ontario

(Biochemistry & Biomedical Science)

TITLE: Investigating immunotherapy treatments and the immunological synapse in triple negative breast cancer

AUTHOR: Alyssa Vito, B.Sc. (Eastern Michigan University), M.Sc. (McMaster University)

SUPERVISOR: Professor K. Mossman

NUMBER OF PAGES: xxiii, 262

Lay Abstract

Triple-negative breast cancer (TNBC) has poor prognostic outcomes due to lack of expression of targets for therapy. As such, patients routinely undergo aggressive treatment regimens with many harsh side effects, including high levels of toxicity. Immunotherapy, a form of therapy that boosts the immune system to fight cancer cells, has gained increasing prominence largely due to its safety and low toxicity to the patient. In the work within this dissertation, we have developed therapeutic platforms and studied them in a murine model of TNBC. The completed studies show the use of clinical therapies, in combination with immunotherapy and investigate the fundamental biology associated with therapeutic outcomes. These findings contribute knowledge to progress clinical regimens for TNBC patients as well as to better identify patients that will respond to therapy. Although this proposal is specific to breast cancer, the underlying concepts can be applied to many other forms of cancer.

Abstract

Triple negative breast cancer (TNBC) is an aggressive subtype of the disease with dismal clinical outcome. Immune checkpoint blockade (ICB), which blocks inhibitory pathways on T cells, has surged to the forefront of cancer therapy with clinical success in a variety of cancer types. However, ICB for TNBC only benefits 10-20% of patients. Thus, a deeper understanding of the immune landscape in TNBC is required to develop efficacious therapies and delineate prognostic biomarkers of disease.

We have developed combination therapy platforms that sensitize TNBC tumors to ICB. Using a clinical chemotherapy (FEC) combined with oncolytic virotherapy (oHSV-1) we show enhanced tumor-infiltrating lymphocytes (TILs), upregulation of B cell receptor signaling pathways, suppression of myeloid-derived suppressor cells (MDSCs) and improved survival. In vivo depletion studies revealed that B cells were required to achieve cures with treatment. Furthermore, the absence of B cells resulted in the expansion of MDSCs. This crucial finding of the importance of B cells for mediation and downregulation of MDSCs is a novel and significant contribution to the field.

RNA sequencing revealed that two of the top upregulated genes in mice treated with FEC + oHSV-1 were S100A8 and S100A9, calcium binding proteins highly expressed in myeloid cells. These genes have controversial findings in the literature with both pro- and antitumorigenic functions being reported. Investigation of data from the Cancer Genome Atlas revealed that high levels of S100A8 and S100A9 correlate with improved prognostic outcomes in breast cancer patients. In line with the clinical data, our data suggests that increased levels of S100A8 and S100A9 results in improved responses

to immunotherapy treatments and that this increased expression is involved in macrophage-mediated epigenetic reprogramming of the tumor microenvironment.

Our second therapeutic platform used a radiolabeled biomolecule containing the beta-emitting radioisotope, lutetium-177. We found that two doses of radiotherapy, combined with ICB improved overall survival in murine TNBC tumors, increased TILs and suppressed circulating MDSCs. These findings offer insight into the newly explored field of combination radioimmunotherapy and again highlight the importance of suppressing MDSCs to alleviate tumor immunosuppression.

Acknowledgements

First, I would like to thank Karen for her supervision, mentorship and guidance throughout my Ph.D. Your own ambition, passion for science and genuine care for your trainees is evident in everything you do and truly inspiring to those of us lucky enough to work with you. Thank you for giving me endless opportunities, supporting me in my many ventures, always responding to your emails in record time and writing me countless reference letters for every opportunity imaginable.

I would like to thank my committee members, Dr. Sheila Singh and Dr. Jonathan Bramson for always upholding me to the highest of scientific standards at both the molecular and clinical levels and challenging me to think of innovative new ways to approach complex scientific problems.

I would like to thank all of the members of the Mossman Lab who I had the pleasure of calling colleagues. It is through all of your efforts fostering an environment for active, engaging scientific conversation that we are able to push our scientific ideas forward, push ourselves through the long dredge of graduate school and maybe even publish some impactful manuscripts along the way. In particular I would like to thank Dr. Samuel Workenhe for many intense scientific discussions (or debates may be a more accurate word to use), scientific guidance, support and mentorship that continued well after you moved on to your new position. I would also like to thank Nader El-Sayes and Omar Salem for all of their contributions to my projects, engaging scientific discussions and helping me with many, many hours of flow cytometry. I would like to thank Dr. Stephanie Rathmann and Dr. John Valliant for their contributions to the radiotherapy

project and in allowing me to dip my feet back into the world of radiochemistry to pursue an idea of bringing two niche scientific worlds together. I also want to thank Salma Al-Karmi for always believing in me, encouraging me and editing pretty much every single scholarship application I wrote.

Lastly, I would like to thank my family. Even though most of the time you have no idea what I do or what I study, you always support me and are my number one champions. Thank you to my parents for countless hours of babysitting (especially when it came time to write my thesis during the pandemic), my sister and husband for listening to me complain about anything and everything all day long, and my beautiful nieces and nephew who constantly give me energy to feed off of. I started my PhD with a three-year old at home and another one cooking in my belly. Aya and Malik, you are the driving force for everything I do and this thesis (should you ever read it) is borne of your boundless energy and love.

Table of Contents

List of Figures

List of Tables

List of Abbreviations and Symbols

15-PGDH	15-prostaglandin dehydrogenase
5-FU	5-fluorouracil
AC	Doxorubicin, cyclophosphamide
Akt	Protein kinase B
APC	Antigen presenting cell
Arg	Arginase
ATP	Adenosine triphosphate
BCR	B cell receptor
BSA	Bovine serum albumin
CAF	Cancer-associated fibroblast
CO_2	Carbon dioxide
CP	Immune checkpoint blockade
CR	Calreticulin
CTLA4	Cytotoxic T-lymphocyte antigen 4
DAMP	Damage-associated molecular pattern
DAPI	4',6-diamidino-2-phenylindole
DC	Dendritic cell
DMEM	Dulbecco's modified Eagle's media
DNA	Deoxyribonucleic acid
ELISA	Enzyme-linked immunosorbent assay
EMT	Epithelial-mesenchymal transition
ENTPD2	Ectonucleoside triphosphate diphosphohydrolase 2
EPAS1	Endothelial Per-Arnt-SIM
ER	Endoplasmic Reticulum
FBS	Fetal bovine serum
FDA	Food and drug administration
FEC	5-Fluorouracil, epirubicin, cyclophosphamide
FOXP3	Forkhead box P3
GC	Germinal centre
GFP	Green fluorescent protein
GM-CSF	Granulocyte-macrophage colony-stimulating factor
Gsk3	Glycogen synthase kinase 3
H & E	Hematoxylin and eosin
HIF	Hypoxia-inducible factor
HMGB1	High mobility group box 1
HRE	Hypoxia-responsive elements
HSP	Heat shock protein
HSV-1	Herpes Simplex Virus type 1
ICD	Immunogenic cell death
IEDDA	Inverse electron-demand Diels-Alder
IF	Immunofluorescence
IFNγ	Interferon gamma

IHC	Immunohistochemistry
i.p.	Intraperitoneally
i.t.	Intratumorally
KEGG	Kyoto Encyclopedia of Genes and Genomes
LASP1	LIM and SH3 domain protein 1
mAB	Monoclonal antibody
MALDI-MS	Matrix-assisted laser desorption ionization mass spectrometry
MDSC	Myeloid-derived suppressor cell
mTNBC	Metastatic triple negative breast cancer
mTOR	Mammalian target of rapamycin
NAC	Neoadjuvant chemotherapy
NK	Natural killer
NO	Nitric oxide
oHSV-1	Oncolytic Herpes Simplex Virus-1
OV	Oncolytic virus
PARPi	Poly(ADP-ribose) polymerase inhibitor
PBMCs	Peripheral blood mononuclear cells
PBS	Phosphate-buffered saline
PCA	Principal component analysis
PD1	Programmed cell death protein 1
PD-L1	Programmed death-ligand 1
PDT	Photodynamic therapy
PHD	HIF-prolyl hydroxylase domain enzyme
PI3K	Phosphatidylinositol-3-kinase
PNAd	Peripheral node addressin
PSMA	Prostate-specific membrane antigen
pVHL	Von Hippel-Lindau tumor-suppressor protein
RNA	Ribonucleic acid
ROS	Reactive oxygen species
RPMI	Roswell park memorial institute
RT	Radionuclide therapy
Sino	Sino Biological
STAT1	Signal transducer and activator of transcription 1
TAA	Tumor-associated antigen
TAM	Tumor-associated macrophage
TAP1	Transporter associated with antigen processing 1
TCA	Tricarboxylic acid
TCO	*Trans*-cyclooctene
TCR	T cell receptor
TDLN	Tumor-draining lymph node
Teff	Effector T cells
Tfh	Follicular T helper
TIL	Tumor-infiltrating lymphocyte

TIL-B	Tumor-infiltrating B cell
TME	Tumor microenvironment
TNBC	Triple negative breast cancer
Treg	Regulatory T cells
TSC2	Tuberous sclerosis complex 2
T-Vec	Talimogene laherparepvec
UPR	Unfolded protein response
VEGF	Vascular endothelial growth factor

Declaration of Academic Achievement

The manuscript contained in Chapter 2 titled "Hypoxia-driven immune escape in the tumor microenvironment" was initially submitted on March 6th, 2020 and published April 16th, 2020 in Cells. This review was conceived by me and co-authored with Nader El-Sayes. The concept of the review was to investigate tumor immunosuppression and ways in which a hypoxic environment drives immune escape and alters immune cell phenotypes. Additionally, we discussed ways in which hypoxia alters responses to immunotherapy treatments and strategies for developing novel therapies targeting hypoxia-induced pathways.

The manuscript contained in Chapter 3 titled "B cell involvement renders triple negative breast cancer sensitive to immune checkpoint blockade through downregulation of myeloid-derived suppressor cells" was initially submitted January 22nd, 2021 and at the time of submission was under review. The initial concept for this paper was borne of my idea to employ chemotherapy cocktails routinely used in the clinic for TNBC patients and combine this with our oncolytic virus. This was a true discovery paper and as we assessed the therapy, we followed the outcomes and followed the logical stepwise succession of experiments. RNA sequencing was performed by the Farncombe metagenomics facility and analyzed by Anna Dvorkin-Gheva (Figures 5, 7A, 8, Table S1). Cytokines analysis was performed by Eve Technologies (Figure 3) and the heatmap was generated by Omar Salem (Figure S3). Immunohistochemistry (IHC) was performed at the McMaster Immunology Research Centre Histology Core. IHC slides were then scanned and quantified by Spencer Revill (Figure 4, S4, S6A). Omar Salem assisted in some flow

cytometry experiments (Figures 6, S5, 7, S7). Nader El-Sayes assisted in some animal studies and flow cytometry experiments (Figures 8, S9). Ana Portillo performed the ELISA assay (Figure 6E), the protocol for which was designed by Dr. Ali Ashkar. Dr. Samuel Workenhe assisted in experimental design of some animal studies and the cytokines analysis assay (Figure 3). Immunofluorescence was performed by the BC Cancer Agency's Molecular and Cellular Immunology Core Facility (Figure S6). Dr. Yonghong Wan and Dr. Karen Mossman provided facilities, funding and scientific guidance. The remainder of the experiments and the writing of the manuscript were done by me.

The manuscript contained in Chapter 4 titled "S100A8/A9 as mediators of response to immunotherapy treatments" was unpublished and incomplete at the time of submission. The idea for this work came from my RNA sequencing experiments performed in the manuscript in Chapter 3. The Clariom S assay was performed by the Genetic and Molecular Epidemiology Laboratory at the David Braley Research Institute. Nader El-Sayes assisted in harvesting and processing tumors for the Clariom S assay. Dr. Karen Mossman provided facilities, funding and scientific guidance. The remainder of the experiments and the writing of the manuscript were done by me.

The manuscript contained in Chapter 5 titled "Combined radio-immunotherapy for treatment of TNBC" was unpublished and not yet submitted at the time of submission. The idea for this work came from collaborative discussions with Dr. Stephanie Rathmann, Dr. John Valliant, Dr. Karen Mossman and me. Development of the radiotherapy platform and optimization of radiolabeling conditions was performed by Dr. Stephanie

Rathmann. Natalie Mercanti radiolabeled the biomolecule for the final study of the manuscript (Figures 6, 7). Nader El-Sayes assisted in collecting tissues for IHC and flow cytometry studies (Figures 6, 7). Dr. Karen Mossman and Dr. John Valliant provided facilities, funding and scientific guidance. The remainder of the experiments were performed by me. Dr. Stephanie Rathmann and I wrote the manuscript together.

The remainder of the thesis was written by me, with editing and suggestions from Dr. Karen Mossman.

CHAPTER ONE: INTRODUCTION

1.1. Cancer

Cancer is a disease characterized by abnormal cell proliferation in an area of the body. This pathological hyperplasia allows for the development of tumor masses with the potential of dissemination into surrounding tissues and eventually, formation of metastatic lesions. The word cancer was originally coined by the Greek physician Hippocrates, who was considered the "Father of Medicine". Hippocrates used the term *carcinoma* (Greek for "crab") to describe ulcer-forming masses after observing that the cells extravasated in a finger-like manner, similar in appearance to a crab. The term cancer has stood the test of time and is still used in current clinical practice to describe the same findings that Hippocrates once denoted. While cancer is indeed used today to describe abnormal, malignant populations of cells, it has since become an umbrella term for the more than two hundred subtypes that all share the common biology of uncontrolled cell growth and proliferation in a part of the body.

While the rate of cancer incidence in Canada continues to climb, largely due to the growing and aging population, improvements in cancer detection and treatment have resulted in a substantial decrease in cancer mortality since its peak in 1988[1]. However, even with enhanced clinical management and decreases in overall mortality rates, cancer remains the leading cause of death among Canadians[2], accounting for 30% of all annual deaths. It is therefore plainly evident that additional efforts and strategies are required for the advancement of research, prevention, screening and treatment to address the overall burden of cancer on the Canadian population.

1.2. Breast Cancer

Breast cancer is the second most commonly diagnosed cancer in Canada[1] and the most common cancer among women worldwide, accounting for more than 2 million new cases and 600,000 deaths annually[3]. While incidence rates of the disease have fluctuated over the years due to increases in proactive breast screening programs, there has been a dramatic decline in mortality rates since the peak in 1986[2]. These improvements can largely be attributed to progress in early detection and treatment options[4]. Though current treatment regimens have shown consistent success with early-stage primary tumors, there are limited therapeutic options to successfully treat aggressive forms, prevent metastasis or completely cure advanced metastatic disease.

Breast cancer classification is dependent on three key biomarkers: the estrogen receptor, the progesterone receptor and human epidermal growth factor receptor 2. Triple negative breast cancer (TNBC), a subtype negative for the overexpression of biomarkers, holds an overall dismal clinical outcome with limited therapeutic options. As such, patients often undergo extensive treatments including invasive surgical resection and aggressive regimens of dose-dense chemotherapy and radiation therapy. These regimens come with a multitude of harsh side effects, including high levels of toxicity and an increased risk of developing other forms of cancer later in life. TNBC accounts for 10 – 20% of all breast cancers, has a higher risk in women under the age of 40, demonstrates substantial tumor heterogeneity and is often identified as being high grade[5]. There remains a critical knowledge gap for TNBC and in particular, with ways of improving clinical management of the disease.

1.3. Hallmarks of Cancer

In 2000 Douglas Hanahan and Robert A. Weinberg published a conceptual manuscript detailing what they considered to be the hallmarks of cancer[6]. In this work, they described six biological capabilities acquired during the multistep development of human tumors. The hallmarks, providing an organizational framework for the vast complexities of dynamic, neoplastic disease are: 1) sustaining proliferative signaling, 2) evading growth suppressors, 3) resisting cell death, 4) enabling replicative immortality, 5) inducing angiogenesis, and 6) activating invasion and metastasis. It was proposed that normal cells acquire these traits in succession through an evolutionarily driven process, and that the process of human tumor pathogenesis could be rationalized by the need of embryonic cancer cells to acquire the traits to enable tumorigenesis.

As the field of cancer research has rapidly progressed, clinical observations have revealed mechanistic concepts that were not covered in the initial hallmarks of cancer. As such, Hanahan and Weinberg revisited the topic in 2011, considering new traits that may be included to expand upon the functionality of recruited stromal cells to tumor biology. Assessment of the dynamic tumor microenvironment (TME), and the various cell types present, resulted in additional hallmarks being added to the list, namely; reprogramming of metabolic pathways and evasion of immune destruction[7] (Figure 1.1). As cancer research continues to delve deeper into the foundational biology associated with the disease, we will undoubtedly uncover more hallmark traits and factors driving tumorigenesis.

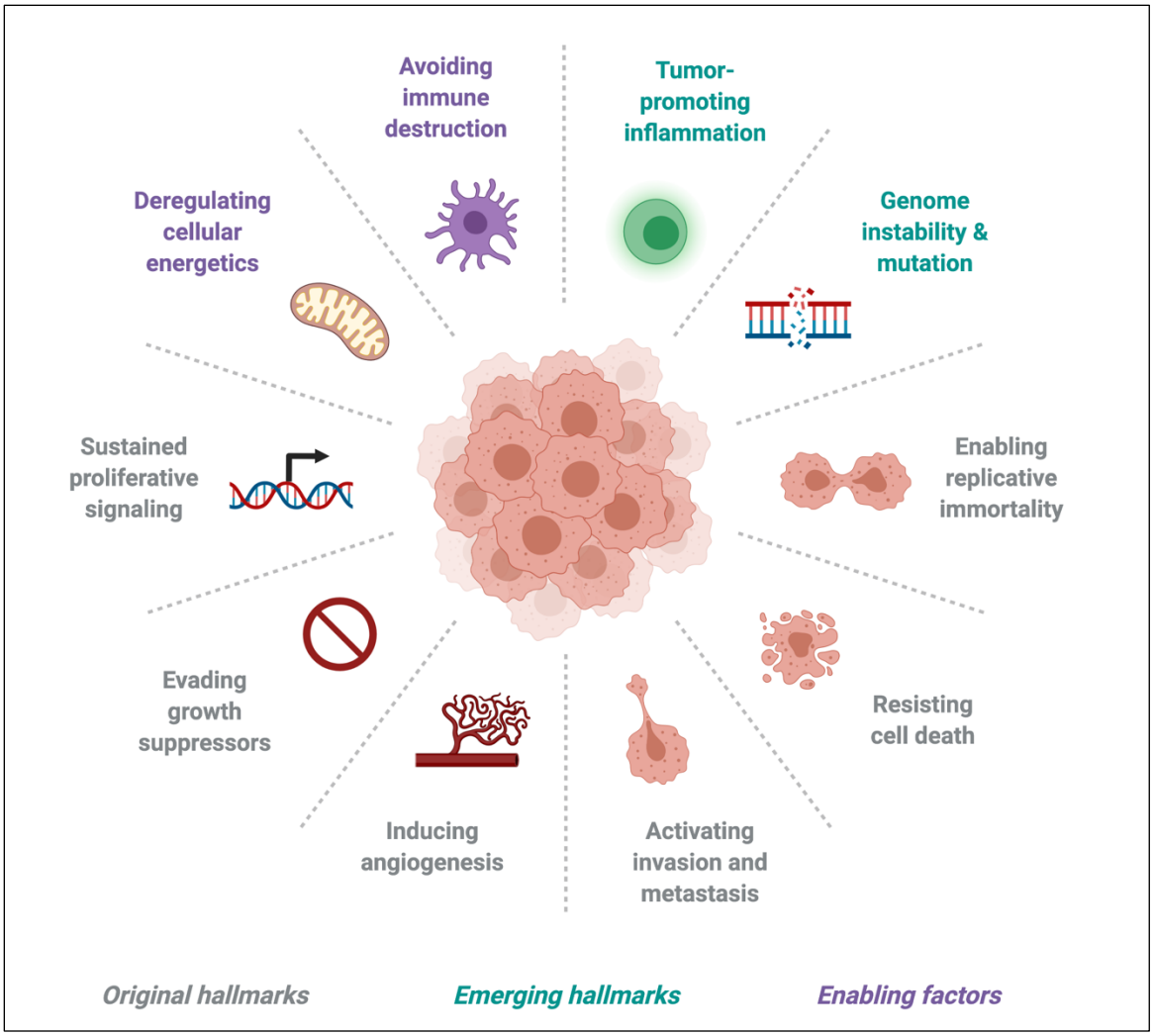

Fig. 1.1. The hallmarks of cancer. *Created using BioRender.com.

1.4. Immunotherapy

It is difficult to investigate human disease at the biological level without taking into account the immune system and its role in maintaining homeostasis within the body. The immune system serves as a means of "checks and balances", recognizing and eliminating foreign hosts and diseases. The ability to identify a wide variety of pathogens and distinguish them from native healthy tissue is vital for the immune system to maintain a healthy and efficient defense system. For more than 100 years it has been postulated

that natural immunity can eliminate cancer with no additional therapeutic intervention[8]. In recent decades, researchers have begun to investigate this concept in great detail and identify ways that the immune system can be harnessed and manipulated for the development of novel cancer immunotherapies[9].

The advent of immunotherapy has revolutionized the way we think about treating cancer, as we shift away from cytotoxic-based therapies to those of an immunostimulatory nature. This paradigm shift in the field is due in part to the safety profiles of immunotherapies, coupled with the astounding success rates of some types of immunotherapy in a wide variety of cancer types. While there are many different types of immunotherapy (Figure 1.2), each having a distinct mechanism of action, they all share the common principle of enhancing immune-mediated cell death[10,11]. However, the mechanism by which this overarching goal is achieved differs between different therapeutic platforms. While some therapies seek to initiate an immune response within the body (such as cancer vaccines), others strive to block immunosuppressive checkpoints, thus enhancing cytotoxic T cell-mediated killing (such as immune checkpoint blockade)[12,13]. Clinical trials employing certain types of immunotherapy have resulted in successful application across a broad range of cancers, but only a minority of patients with aggressive or advanced disease experience durable survival outcomes to treatment[14,15]. Thus, as immunotherapy continues to evolve and become more widespread clinically, it will be important to simultaneously collect data about which patients respond and identify the biological drivers within this distinct population.

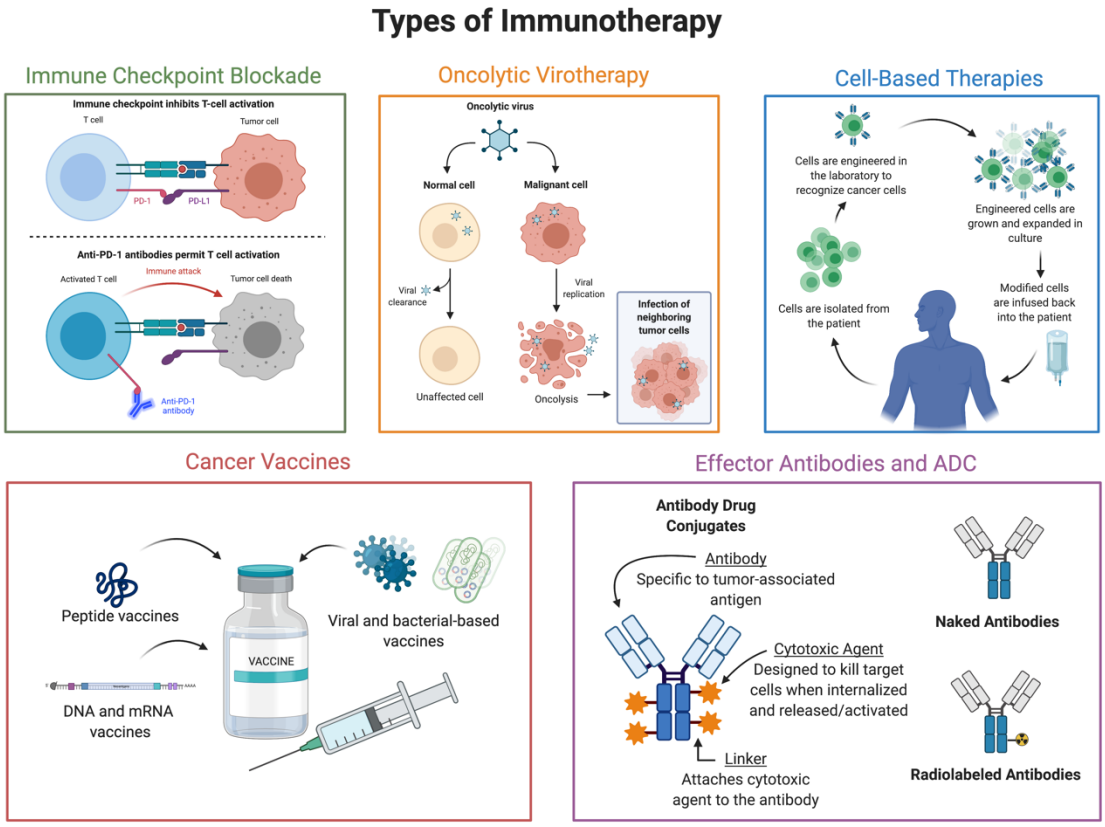

Fig. 1.2. Types of immunotherapy. *Created using BioRender.com.

1.5. Immunosurveillance, Immunoediting and Mechanisms of Antitumor Immunity

The theory of immunosurveillance, or rather the concept of natural antitumor immunity, has existed in the field of medicine for decades. However, the ability to prove this concept has been challenging and the experimental limitations in the quest to do so have undoubtedly been one of the largest barriers to progress in the field[16]. After a century of controversy, conversation, improvements in technology and innovative experimental design, evidence has mounted in support of immunosurveillance, at least in part. While it is now well established that the immune system plays a role in controlling tumor development, it is also now recognized to play a simultaneous part in the

facilitation of tumor growth. This dual and opposing role in the complex interactions between cancer and the immune system prompted Schreiber and colleagues to propose the theory of "immunoediting"; a three stage process of elimination, equilibrium and escape (Figure 1.3)[16].

In the initial stage of cancer immunoediting, the immune system recognizes transformed and mutated self-antigens expressed by tumor cells and mounts a tumor-specific immune response to eliminate them[17]. Immunotherapy takes advantage of this immune response and mediates tumor cell lysis releasing cell contents, viral particles and nucleic acids that subsequently alarm innate immune cells and associated stroma in the TME[18]. Released pathogen-associated molecular patterns (PAMPs) and damage-associated molecular patterns (DAMPs) initiate signaling cascades leading to the secretion of cytokines that aid in the activation and maturation of dendritic cells (DCs). DCs take up tumor-associated antigens (TAAs) from lysed tumor cells and express co-stimulatory molecules that enhance T cell proliferation and assist in determining whether T cells become activated or tolerized[17,19,20].

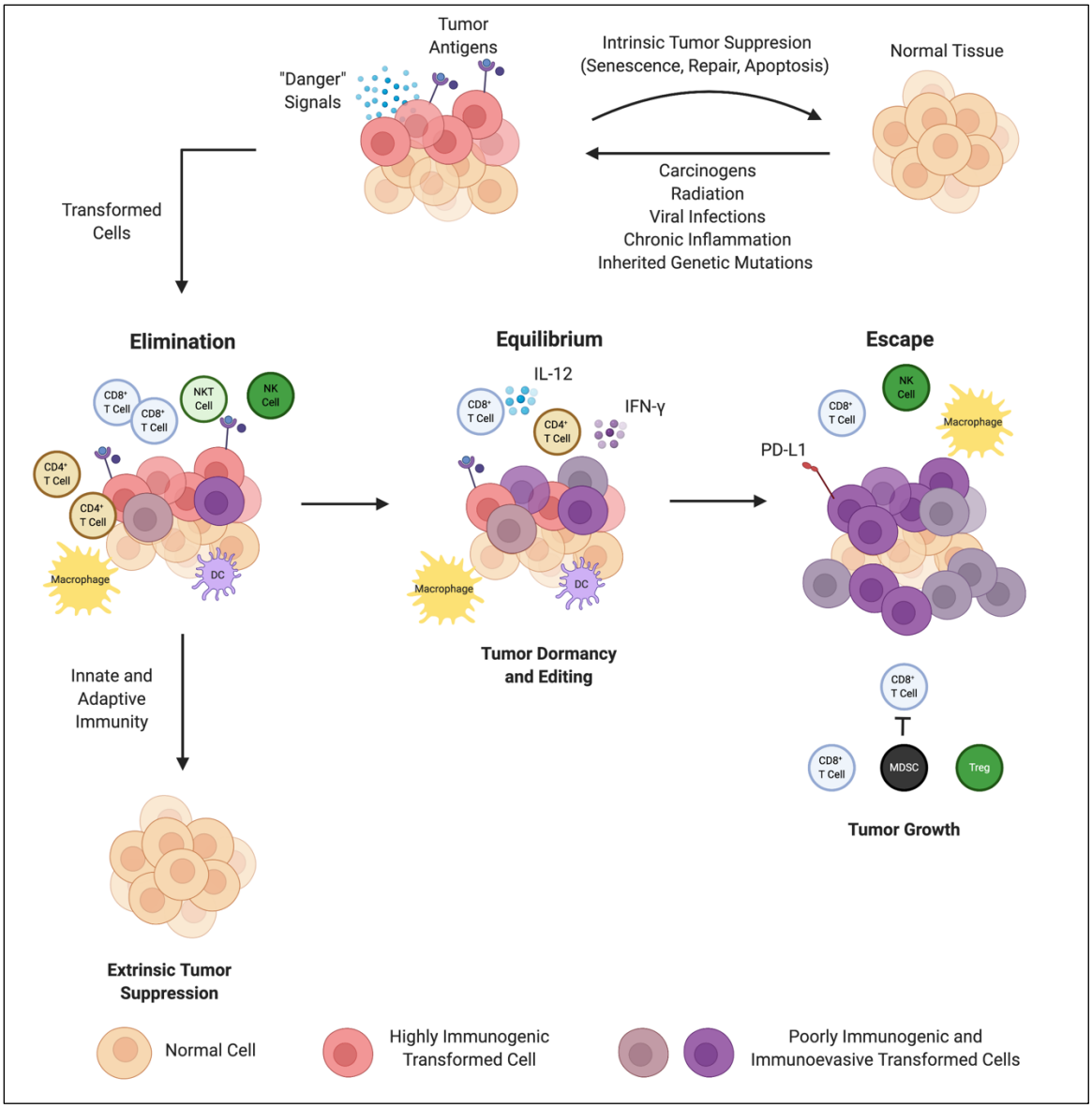

Fig. 1.3. The three E's of cancer immunoediting. DC = dendritic cell, MDSC = myeloid-derived suppressor cell, Treg = regulatory T cell. *Created using BioRender.com.

In human breast tumors, the extent of tumor-infiltrating $CD8^+$ T cells is directly associated with improved clinical outcome[21–24]. Conversely, high levels of immunosuppressive cell populations such as myeloid-derived suppressor cells (MDSCs), macrophages and $CD4^+$ T cells (regulatory T cells) are directly correlated with reduced

overall survival[21]. However, despite these clear correlations, the TME contains an extensive network of suppressive cytokines and growth factors that impair T cell entry and antitumor activity[25], allowing tumors to effectively escape and evade immune-mediated killing[16]. In an effort to combat this tumor immunosuppression, therapies must be designed that elicit immunologically desirable cancer cell death, creating an inflammatory TME for optimal antigen presentation and T cell activation.

1.6. MDSC-Mediated Immunosuppression in TNBC

Myeloid cells play an important role in the innate immune response through phagocytosis of pathogens (by macrophages), processing and presentation of antigens (by DCs), induction of an inflammatory response (by neutrophils) and promotion of wound healing (by platelets). Myelopoiesis is the process by which multipotent progenitor cells and oligopotent myeloid precursors differentiate into megakaryocytes, eosinophils, basophils, erythrocytes, monocytes and neutrophils[26]. Megakaryocytes undergo an intricate series of remodeling events, resulting in the release of thousands of platelets from a single megakaryocyte[27]. Newly formed monocytes migrate to distant tissues and further differentiate into macrophages and DCs[28] (Figure 1.4). While healthy individuals constantly have immature myeloid cells present, chronic inflammatory conditions such as cancer drive abnormal differentiation, resulting in the accumulation of MDSCs[29,30].

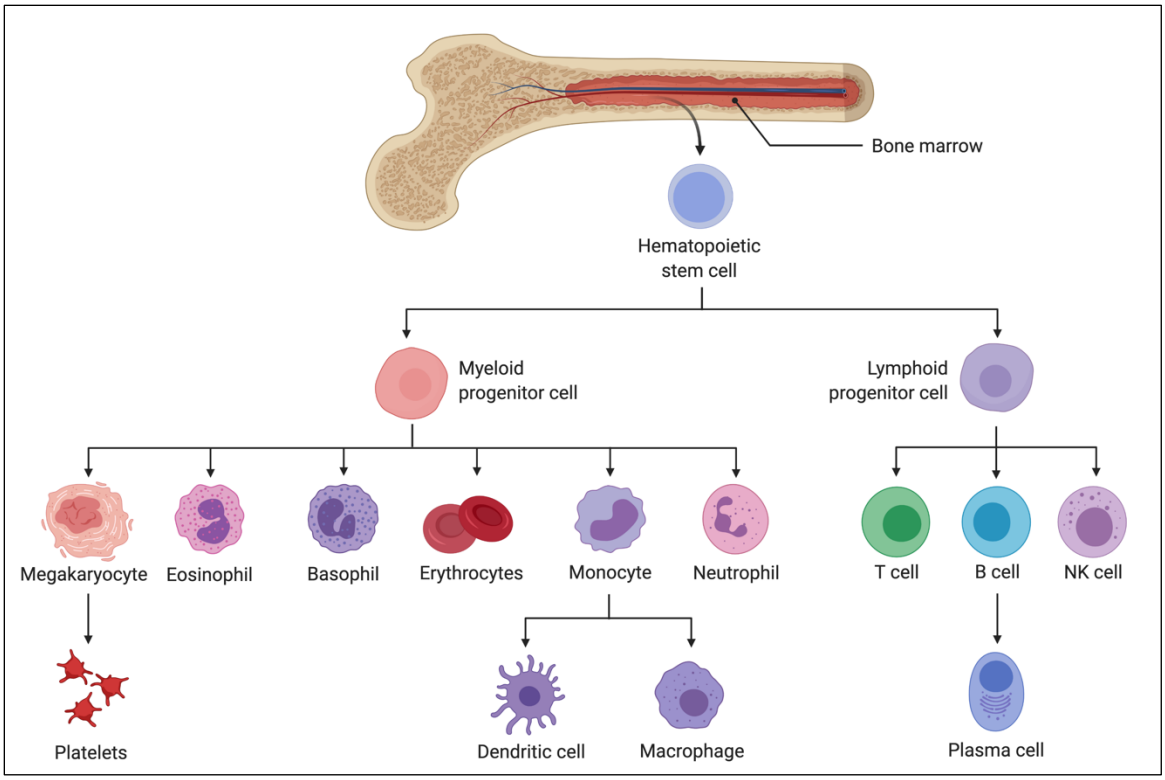

Fig. 1.4. Progenitor cell differentiation. *Created using BioRender.com.

In cancer, a decrease in the amount of peripheral myeloid cells drives myelopoiesis, increasing the migration of cells before they have completely differentiated[31]. This results in an influx of myeloid cells with strong immunosuppressive patterns and abnormal functions[32,33]. Due to their myeloid origin, this heterogenous population of cells has been termed MDSCs, representing a distinct population of immature myeloid cells that are activated under sustained inflammation. In breast cancer, MDSCs have been demonstrated as a major driver of immune escape and the main reason for therapeutic resistance and cancer relapse, particularly in the case of immunotherapy[34]. Circulating MDSCs in the peripheral blood of breast cancer patients are elevated in all

stages of the disease and directly correlated with clinical cancer stage and metastatic burden[35,36].

While clinical studies have demonstrated the prognostic relevance of TILs in many subtypes of breast cancer[37,38], TNBC patients are found to have more tumors with intermediate or high levels of TILs than other non-TNBC subtypes of the disease[39]. Increased TILs are associated with better response to therapy and improved overall survival[38]. Correlative effects of TILs are limited not only to their density in the TME, but more notably on the phenotypic state of the infiltrates. To this end, studies have documented TNBC tumors to be highly enriched with IL-17A, which functions to promote cellular immune responses but also plays an opposing role in reprogramming myeloid cell differentiation, leading to increased levels of MDSCs[40–42]. In a murine 4T1 TNBC tumor model, Dawod and colleagues showed that ectopic IL-17A expression by tumor cells enhanced tumor growth and metastasis[43]. This increased disease severity was coupled with a marked expansion of MDSCs, despite activation of NK cells, B cells, $CD4^+$ and $CD8^+$ T cells. Notwithstanding multiple attempts at therapeutic intervention, the only modality capable of restoring tumor control in their study was depletion of MDSCs[43], signifying their strong immunosuppressive nature and ability to resist therapeutic treatment.

1.7. MDSC Interactions with Other Immune Cells

MDSCs drive tumor immunosuppression through various interactions with other immune cell types. They have been widely shown to inhibit the activation and proliferation of cytotoxic T cells, diminishing the antitumor immune response, promoting

cancer progression and driving therapeutic resistance[44]. MDSCs have further been shown to inhibit the antitumor activities of NK cells and DCs, while simultaneously stimulating Tregs and TAMs, leading to tumor progression[45,46]. Additionally, some immune cells can actively be converted into MDSCs. Adoptively transferred NK cells in tumor-bearing mice lost their NK phenotype and were converted by granulocyte-macrophage colony-stimulating factor (GM-CSF) into an MDSC phenotype[47].

Myelopoiesis has been shown to be altered at the stem-cell level in tumor-bearing mice, resulting in the accumulation of MDSCs and a low number of mature B cells[48]. B cells continue to have a controversial role in tumorigenesis, with both pro- and antitumorigenic effects described in the literature[49]. Regardless of the role of B cells in tumor-bearing hosts, their diminished function by MDSCs has been well elucidated in the literature. Indeed, Xu and colleagues have shown that MDSCs accumulate around the germinal center in the spleen of tumor-bearing mice, colocalized with B cells[50]. They further describe the cross talk between MDSCs and B cells as requiring cell-cell contact and resulting in altered antibody production by B cells[50]. These findings are consistent with other studies, where MDSCs have also been documented to impair B cell responses[51,52].

1.8. Therapeutic Strategies Targeting MDSCs

In recent years there has been an insurgence of preclinical and clinical studies seeking to inhibit MDSC-driven tumor immunosuppression. MDSC inhibition is sometimes trialed as a monotherapeutic approach, but is often combined with radiation therapy, chemotherapy, surgery or immunotherapy[44]. Current preclinical strategies aim to

deplete MDSCs, inhibit their immunosuppressive potential, block migration to the site of the tumor or to directly modulate myelopoiesis itself[53].

Many therapeutic platforms are currently being investigated to mediate the MDSC-driven suppression in breast cancer patients. One such strategy suggests using oncolytic virotherapy in which the virus is modified to express tumor suppressor genes. Walker and colleagues have generated an oHSV-1 virus expressing the murine tumor suppressor 15-prostaglandin dehydrogenase (15-PGDH), which functions to reduce levels of MDSCs, ultimately leading to a reduction in the overall size of primary tumors and metastasis[54]. Other strategies for targeting MDSCs in TNBC include antibody-based therapies targeting cytokines known to drive MDSC accumulation. In one such study, Zhang and colleagues employed an anti-CCL5 antibody, resulting in increased T cell proliferation and improved management of disease in murine hosts[55].

Regardless of the approach employed, it is clear that MDSCs need to be considered when developing novel strategies for cancer therapy. There are 5 clear ways to target MDSC-mediated immunosuppression with therapeutic intervention: 1) Forcing MDSCs to complete differentiation into mature myeloid subtypes (such as monocytes, or DCs); 2) Inhibiting MDSC expansion from the precursor stage; 3) Preventing MDSC accumulation in peripheral organs; 4) Blocking MDSC function or soluble factors directly; and 5) Indirectly inhibiting MDSCs, by altering the prevalence, phenotype and function of other immune cell subsets in the TME.

To date, a limited number of clinical trials have examined whether or not MDSC inhibitors are functional in humans and whether they result in true clinical benefit in

patients. Current clinical approaches are now focused on combining depletion of MDSCs with other immune-based therapies in TNBC to assess the overall survival advantages[46]. Given the emerging importance and strong evidence of MDSC-mediated tumor resistance and relapse, it is clear that MDSCs will remain at the forefront of immune escape and therapeutic platforms to overcome these intrinsic resistance mechanisms.

1.9. Tumor-Infiltrating B Cells

While the impact of $CD8^+$ TILs and MDSCs has been extensively studied in various types of cancer including TNBC, it has become increasingly apparent that a more comprehensive overview of the immune landscape is necessary to develop effective cancer therapies and delineate prognostic biomarkers of disease. Current immunotherapies do not target B cells, despite their predominance in the TME and key role in the adaptive immune response. In TNBC, evidence suggests that tumor-infiltrating B cells (TIL-Bs) generate a robust humoral response to amplify antitumor immunity[56]. TIL-Bs are prominently detected within tertiary lymphoid structures (TLS), which correlate strongly with improved prognosis[57–60]. TLS predominantly contain B cells, $CD4^+$ T conventional cells, and $CD14^+$ myeloid cells, however, unlike normal lymphoid tissues, TLS in cancer patients do not always have well defined germinal centers (GCs)[61]. GCs are paramount for proper B cell development and function.

TIL-Bs have been correlated with enhanced overall survival[62], but findings in the literature suggest conflicting roles with TIL-Bs having both pro- and anti-tumorigenic functions. TIL-Bs have been identified as mediators of malignancy in several cancer types, with TIL-B depletion yielding positive outcomes[63]. Conversely, coordinated

antibody and T cell responses have been documented in cancer patients and TIL-Bs and TLS have been correlated with improved outcome[64–68]. Further, studies have reported that TIL-Bs and TLS are influenced by the TME and immunotherapy. In TNBC, TIL-Bs and TLS have been reported[56,69], but their phenotype, function and heterogeneity have not been thoroughly assessed.

1.10. Chemotherapy

The era of cancer chemotherapy began in the 1940s and its inception is directly tied to the use of chemical warfare during World War I[70]. Particularly, the use of mustard gas sparked the idea of using chemical agents to treat malignant conditions. While mustard gas itself was too volatile for laboratory experiments, researchers soon realized that they could exchange a nitrogen molecule for sulfur, creating the more stable alkylating agent, nitrogen mustard[71]. A year into the start of this research a German air raid in Italy resulted in more than 1000 people being exposed to mustard gas bombs. Autopsies of the victims showed profound lymphoid and myeloid suppression[72]. These findings quickly reached the medical community, which surmised that if mustard gas could stop the division of some types of somatic cells known for rapid division and proliferation, it could also potentially be repurposed to suppress the division of certain types of cancer cells[73]. In fact, while the discovery and first clinical trials using nitrogen mustards were crude, alkylating agents are still used in clinical practice to this day (such as the widely used drug cyclophosphamide) and are considered a standard first line therapy for many types of cancer. Following in the footsteps of primitive chemotherapy

discoveries, many other chemical agents were soon repurposed or synthesized to target rapidly proliferating cells for cytotoxic destruction.

From its initial inception through decades of clinical use, cancer chemotherapy has been most commonly prescribed for its anticancer benefits, the result of direct cytotoxicity, non-specifically targeting rapidly proliferating cells[74]. The notion that this toxicity was the sole mechanistic action of chemotherapies has led researchers and clinicians alike to the assumption that chemotherapies inevitably target not only rapidly dividing malignant cells, but also immune cells, resulting in immunosuppression[75]. This ideology has led to years of scientific research neglecting the possible (and now seemingly probable) reality that some chemotherapies may actually induce cell death in an immunological manner[76–79].

Researchers have recently begun identifying various chemotherapies (e.g. anthracyclines, oxaliplatin and cyclophosphamide) that are "inducers" of immunogenic cell death (ICD), as demonstrated through the use of dying cell vaccination experiments in mice[78,80]. Such inducers trigger a cycle of DC recruitment, activation, homing, maturation and release of danger-associated molecular patterns (DAMPs) that lead to T cell activation and ultimately ICD[81,82]. Experimental interventions that interfere with the ability of mouse tumor cells to release these DAMPs while being exposed to ICD-inducing chemotherapies nullifies their ability to vaccinate mice against a subsequent challenge with living cells of the same type[83]. As expected, chemotherapies that are unable to promote the release of one or more of these DAMPs fail to promote ICD and as such cannot be classified as inducers of ICD.

As studies continue to emerge expanding the list of ICD-inducing chemotherapies, it becomes more apparent that initial studies lacked focus on current clinical utility. Most experimental models rely upon the use of a single chemotherapeutic agent, whereas clinical regimens employ a cocktail of chemotherapies spanning different drug classes. This combination chemotherapy has proven vital to clinical success, especially in overcoming acquired drug resistance common with monotherapy approaches. Pittet and colleagues identified that a combination of clinically approved chemotherapies (oxaliplatin and cyclophosphamide) was able to elicit immunogenic phenotypes, foster $CD8^+$ T cell infiltration into tumors and delay cancer progression when studied in small animal models[84]. Interestingly, these findings were only apparent with the combined chemotherapeutics, but not when the drugs were administered independently of one another. Similarly, Zhang and colleagues focused their studies on a clinically approved agent commonly used for many types of cancer: 5-fluorouracil (5-FU)[85]. In their work, they have shown that a single cycle of 5-FU (three doses, 48 hr apart) promoted an antitumor immune response, with no increased response seen with repeated cycles. This work suggests that while selecting clinically used chemotherapies remains a priority for ease of translation and reference to current clinical guidelines, modelling immunotherapy studies after clinical schedules may in fact be detrimental to the ICD-inducing capabilities of chemotherapies.

1.11. Oncolytic Viruses

Since the early nineteenth century, viruses have attracted interest as potential agents for tumor destruction. Clinical case reports documenting regression of cancers

during naturally acquired virus infections sparked the idea of repurposing viruses for therapeutic benefit[86]. Early clinical trials were crude in design and focused on harvesting bodily fluids containing human or animal virus and using them to transmit infections to cancer patients. In most instances, the patient's immune system rapidly cleared the viral infection, and no impact was seen at the site of the tumor. However, some patients with compromised immune systems saw viral persistence and associated tumor regression[86]. As rodent models advanced and became more commonly used in preclinical development, so too did oncolytic virotherapy. However, it wasn't until 1991 that oncolytic viruses (OVs) gained traction, after Martuza and colleagues first demonstrated the use of genetically modified Herpes Simplex Virus-1 (HSV-1) as a suitable treatment for glioblastoma in mice[87]. Clinical documentation of naturally occurring OVs persists even to this day, with SARS-CoV-2 recently inducing remission of Hodgkin lymphoma in a 61 year old man[88].

Broadly defined, OVs are naturally occurring or engineered viruses that preferentially kill cancer cells. As with all therapeutic platforms, improvements in technology over the years have allowed for the advancement of virotherapy, allowing researchers to generate more potent, tumor-specific oncolytics. There are three primary mechanisms of action by which an OV can lead to tumor destruction – 1) traditional virus replication within a tumor, leading to direct oncolysis (as seen in Figure 1.2); 2) interference with tumor vasculature, compromising the growth of a tumor; and 3) virus-induced stimulation of the immune system to identify and engage antigens that were previously either unrecognizable or had been subjected to immune tolerance[89,90]. In the

development of effective OVs for cancer therapy, the third mechanism of OV-mediated killing is of most interest and relevance. Replicating virus within the tumor attracts immune cells into the TME, primes TAAs for activation and ultimately leads to increased immune stimulation for the development of anticancer immunity (Figure 1.5)[91].

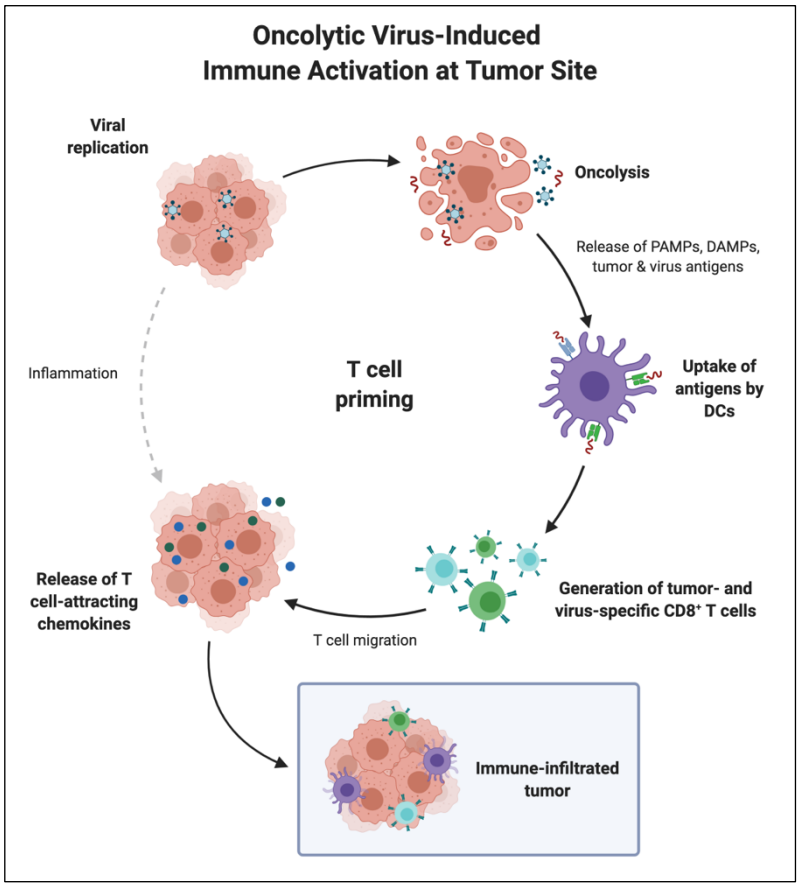

Fig. 1.5. Immune activation at the tumor site, as induced by oncolytic virotherapy. *Created using BioRender.com.

In theory, gain or loss of function mutations inherent in cancer cells allow OVs to preferentially target tumors while showing little to no toxicity in healthy cells[92], making them a favourable therapeutic option. Additionally, some OVs target breast cancer stem cells while exhibiting excellent clinical tolerability, even when used at high viral doses[93].

HSV OVs replicate in breast cancer cells irrespective of their subtype or receptor status, offering an overarching long-term solution to control metastatic and relapsing breast tumors. This treatment provides patients with efficacious therapy with fewer side effects, and a low probability of developing resistance as the immune system can effectively target multiple tumor antigens and pathways simultaneously. In 2015, the FDA approved an HSV OV (talimogene laherparepvec; T-Vec) for inoperable melanoma, showing the emerging immunotherapeutic potential of oncolytic HSV[94].

Despite preclinical and clinical studies showing that OVs are viable immunotherapeutic agents[93–96], tumors continue to evade immune recognition[16,25] limiting monotherapy efficacy. The ability to enhance inflammation in the TME and in turn induce ICD, can overcome these hurdles and lead to increased therapeutic potency. In our lab we have shown that some HSV OVs cause ICD and increased detection of TAAs[97,98]. Additionally, we have demonstrated the synergistic activity of OVs with certain ICD-inducing chemotherapies in transplantable tumour models[97–99]. As we continue to investigate the immune landscape of OV-treated tumors, it will be important to identify therapies that synergize with OVs to overcome immune tolerance and allow for immune-mediated killing.

1.12. Immune Checkpoint Blockade

While ICD-inducing chemotherapies and OVs have paved the way for modern-day immunotherapy as an emerging pillar of cancer treatment, it has become increasingly evident that complementary therapy will be required for prolonged overall survival[84]. To this point, researchers have employed immune checkpoint blockade (ICB), a form of

immunotherapy that uses antibodies to block inhibitory molecules on the surface of T cells. Seminal work utilizing ICB as a viable cancer immunotherapy has focused on two main inhibitory pathways: cytotoxic T lymphocyte antigen 4 (CTLA-4) and programmed death-1/programmed death-ligand 1 (PD-1/PD-L1).

The first immune checkpoint, CTLA-4, was discovered in 1987 by Brunet *et. al.*[100], but the function was not elucidated until 1995 when James Allison and his colleagues determined it to be a crucial immune checkpoint molecule with significant potential as an anticancer therapeutic target[101,102]. In parallel to this discovery and on the other side of the world, Dr. Tasuko Honjo and colleagues were running an assay to identify genes involved in programmed cell death when they discovered PD-1[103]. The identification of these two crucial checkpoints sent waves through the oncology community and preclinical studies rapidly began assessing the anticancer potential of blocking these inhibitory pathways.

The inhibitory receptor CTLA-4 is a key negative regulator of peripheral T cell responses and is expressed upon the activation of naïve T cells[104]. Primary work demonstrating that the blockage of CTLA-4 inhibitory receptor promotes antitumor immune responses in mouse tumour models[102] led to the development of an anti-CTLA-4 monoclonal antibody (ipilimumab) as a therapeutic agent for cancer, approved by the US Food and Drug Administration (FDA) in 2011 for the treatment of advanced melanoma[105,106]. Today, ipilimumab is approved for use in several cancer types and long-term follow-up shows that more than 20% of the patients enrolled in the first ipilimumab clinical trials are still alive, showing no evidence of disease[107,108]. With additional Phase II and III clinical trials currently underway in many forms of cancer, the therapeutic potential

of ipilimumab is indeed promising, but trial data shows that response rates vary greatly not only between cancer types, but also within patient groups of phenotypically identical cancers[106]. Initial studies suggest that although some patients show favourable responses and increased overall survival with administration of an anti-CTLA-4 monoclonal antibody, it may be better used as a complementary therapy rather than a standalone treatment.

PD-1 is a transmembrane protein receptor that functions in controlling T cell activation, T cell exhaustion, T cell tolerance and resolution of inflammation[106,109]. When T cells are repeatedly stimulated by TAAs, the level of PD-1 expression remains high and T cells undergo epigenetic modifications and changes in expression of transcription factors[106]. PD-1 has two ligands, PD-L1 and PD-L2, both of which are expressed on antigen-presenting cells as well as other hematopoietic and nonhematopoietic cells[110]. PD-L1, the more widely expressed of the two ligands, is induced by proinflammatory cytokines, serving as a negative feedback mechanism that downregulates effector T cell activity, protecting tumors from attack by the immune system[110–112]. Blockage of the PD-1/PD-L1 inhibitory pathway has led to astonishing clinical results with response rates as high as 50% in some forms of cancer[113,114]. In 2014 the FDA approved two PD-1 monoclonal antibodies (nivolumab and pembrolizumab) for use in patients with advanced refractory melanoma and over the next four years several other inhibitors of the PD-1/PD-L1 axis were approved worldwide with pembrolizumab, atezolizumab, durvalumab and avelumab showing significant improvements in many cancer types[108]. In particular, atezolizumab, a checkpoint inhibitor of the PD-L1 protein approved in 2016 for the

treatment of melanoma, lung cancer, bladder cancer had its clinical utility extended to include treatment of TNBC in March 2019[115,116].

1.13. Radiotherapy

While radiation therapy has long been a mainstay in cancer care, the not-so-well known counterpart, radiotherapy, has lived in its shadow with success in select cancer types. While standard radiation therapy uses external beams of radiation to treat an area of the body, radiotherapy is delivered internally through intravenous or intratumoral injections. In radiotherapy, a beta- or alpha-emitting radioisotope is attached via a chemical linker to the targeting moiety (usually an antibody). One of the most commonly known and efficacious radiotherapy platforms is the use of a prostate-specific membrane antigen (PSMA) targeting monoclonal antibody, radiolabeled with the beta-emitting radioisotope, lutetium-177 (Figure 1.6)[117]. In this therapeutic platform, patients with prostate cancer are administered the radiotherapy intravenously, and the specificity of the antibody allows for accumulation of the conjugate at the site of the tumor, which has high levels of PSMA. As Lutetium-177 only has a soft-tissue penetration depth of 1.7 mm, damage to surrounding tissue is minimal. This therapy is very effective in killing cancer cells that express PSMA, whether they be at the primary tumor mass or microscopic distant metastatic sites[117].

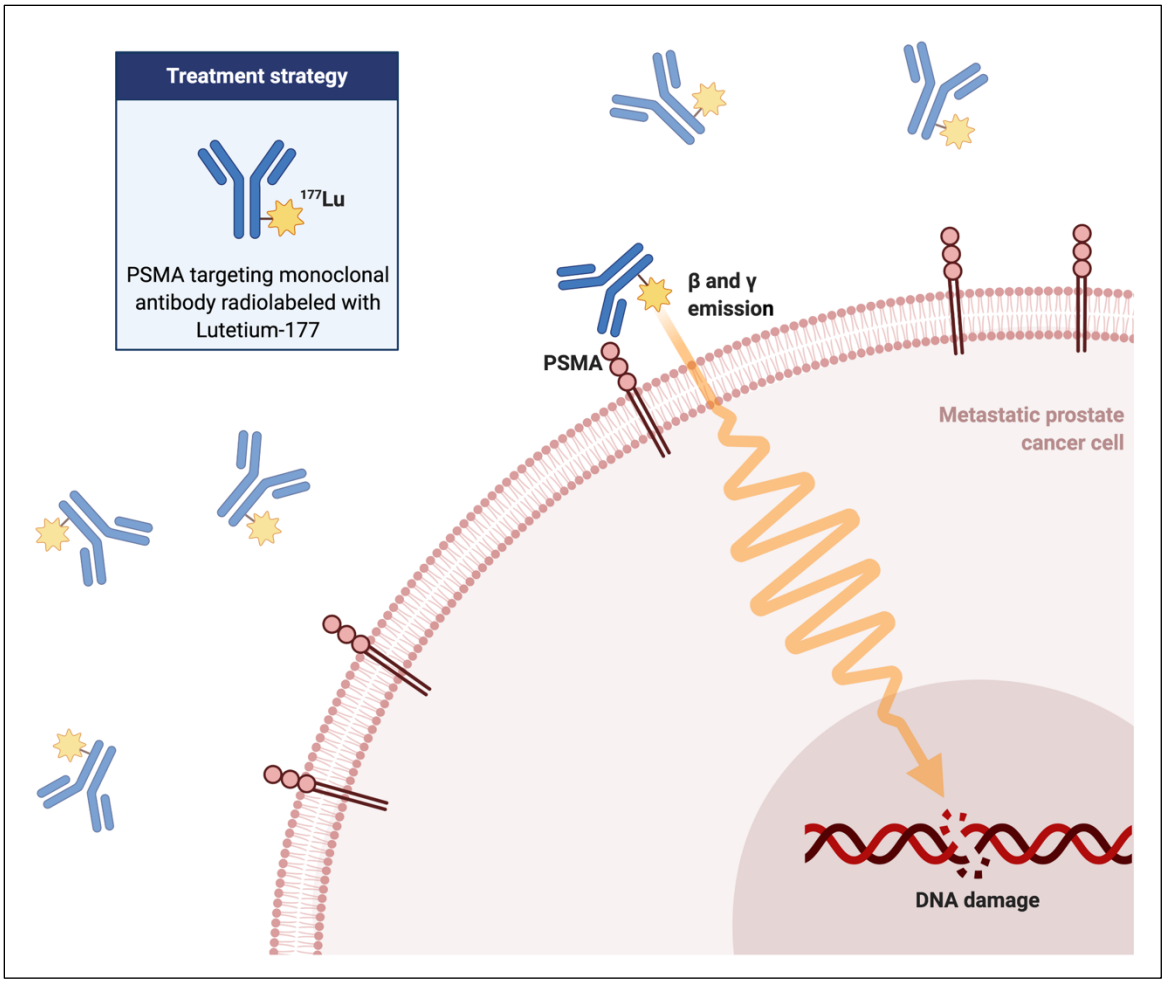

Fig. 1.6. Radiotherapy platform utilizing PSMA radiolabeled with Lutetium-177, for targeting prostate cancer. *Created using BioRender.com.

Radiotherapy has long been thought to induce a phenomenon called the abscopal effect. First proposed in 1953 by R. H. Mole[118], the term "abscopal" refers to effects of ionizing radiation at a distance from the irradiated volume, but within the same organism. Essentially what this means is that the anticancer properties and efficacy of radiotherapy could not only directly affect the tissue it comes in contact with, but also distant malignant cells within the body. In the last decade it has become increasingly evident that

the abscopal effect, while previously not well understood or characterized, may in fact be mediated by the immune system[119,120]. It is postulated that local irradiation of a tumour nodule may lead to ICD and in turn, priming of TAAs[121]. Abscopal effects of radiotherapy alone are often dampened by the immunosuppressive microenvironment of the tumour. However, treatment with immunotherapy allows for reinstatement of immunosurveillance and can potentiate radiotherapy treatment in metastatic disease[122].

1.14. Barriers to Immunotherapy

As the era of immunotherapy has surged to the forefront of oncology research, so too have the apparent barriers to efficacious treatment across widespread patient populations. While tumors grow and evolve, their increased proliferative kinetics result in nutrient depletion and an influx of transcription factors and proteins that are responsible for the induction of hypoxic conditions[123]. Hypoxia is known to drive immune escape and further promote tumor heterogeneity, a key factor in acquired resistant mechanisms[124]. With abnormal vasculature, uncontrolled proliferation and altered metabolic pathways, the TME is indeed an aberrant milieu, requiring unique and broad therapeutic approaches to actively target the full network of malignant changes.

Multi-pronged therapeutic platforms have existed for decades, since James F. Holland, Emil Freireich and Emil Frei first proposed in 1965 that cancer chemotherapy should follow the same strategic pipeline as antibiotic therapy and employ a combination of drugs, each with a different mechanism of action[70]. It is well established that cancer cells can mutate to become resistant to a single chemical agent[125]. Administration of multiple drugs from different classes concurrently, makes it more difficult for the tumor

to develop resistant mechanisms to the entire therapeutic regimen at once, allowing for successful treatment of disease by at least one arm of the therapeutic platform. Indeed, this combination therapy concept is still widely used in the clinic today, not only for chemotherapy regimens but also for combinatorial platforms across different types of therapy.

While the advent of immunotherapy has excited the cancer community and offered new prospective therapies with decreased toxicity profiles, monotherapy approaches are often unsuccessful and typically only result in durable responses in cancers with high mutational burden and high rates of cell turnover[126]. There remains a need to identify patients who will respond to therapy and overcome resistant mechanisms. To this end, advances in technology have been developed to better assess the TME, allowing for a more thorough analysis of the composition of a patient's individual cancer. Tumor heterogeneity, growth kinetics as well as genomic landscape can now be clearly delineated through the use of circulating tumor DNA, next-generation sequencing and histologic assessment.

As we move towards precision medicine and more personalized treatments for cancer patients, it is also important to simultaneously investigate the immunological synapse associated with individual diseases and correlate immune interactions with response to therapeutic outcomes. Indeed, in TNBC specifically we see widespread heterogeneity between different patients and also within individual tumors. This aggressive, highly heterogeneous cancer type is a prime candidate for combination therapy platforms. A phase III clinical trial has shown that chemotherapy works to

enhance the antitumor activity of ICB in metastatic TNBC patients[14]. However, this combination of chemotherapy and immunotherapy only confers a modest survival benefit. These results further highlight the need for additional strategies to treat TNBC and to mediate intrinsic resistance mechanisms. To this end, a more thorough analysis of the immune environment in TNBC patients beyond $CD8^+$ T cells is necessary.

In the work presented in this document, we have utilized a syngeneic TNBC tumor model to assess the underlying biology associated with the disease. Through different combination therapy platforms, we have investigated the immunological synapse and identified immune cell subsets that drive therapeutic efficacy.

1.15. Hypotheses and Objectives

TNBC accounts for 10 – 20% of all breast cancers[127], has a higher likelihood of brain and lung metastasis and has the poorest prognostic outcome of all breast cancer subtypes[128]. A phase III clinical trial has shown that chemotherapy works to enhance the antitumor activity of ICB in metastatic TNBC patients[14]. However, this combination of chemotherapy and immunotherapy only confers a modest survival benefit[14]. **These results further highlight the need for additional strategies to treat TNBC and to mediate intrinsic resistance mechanisms.** To this end, a more thorough analysis of the immune environment in TNBC patients beyond $CD8^+$ TILs is necessary to develop novel, effective therapies and delineate prognostic biomarkers of disease.

Our central hypothesis is that the combination of low dose chemotherapy and oncolytic HSV-1 or the use of internal radionuclide therapy can enhance tumor susceptibility to ICB and improve antitumor immunity.

The aims of this thesis were:

Aim 1: To develop a therapeutic platform to sensitize TNBC tumors to ICB.

Aim 2: To identify genes and signaling pathways driving efficacy of FEC + oHSV-1 therapy and radionuclide therapy.

Aim 3: To assess genes associated with MDSCs and whether they had pro- or antitumorigenic functions in our model.

Using the aggressive syngeneic TNBC tumor model, E0771, we established that naïve tumors lacked immune cell infiltration and were non-responsive to various types of therapies. In previous experiments done in our lab we have shown that oHSV-1 is capable of synergizing with certain ICD-inducing chemotherapies for increased detection of TAAs[97–99]. Building upon these studies, we focused on using a cocktail of chemotherapies routinely prescribed to breast cancer patients in the clinic (FEC) to assess synergistic effects when combined with oHSV-1 (**Chapter 3**). Not only did FEC + oHSV-1 therapy succeed in making otherwise resistant tumors susceptible to ICB therapy, but this therapeutic efficacy was driven by B cells and nullified in their absence. Further dissection of this phenomenon showed that in the absence of B cells we saw a rapid differentiation of immature myeloid cells to the granulocytic MDSC phenotype. This work strongly suggests that therapeutic efficacy in our model is reliant on alleviating tumor immunosuppression through the regulation of MDSCs and that B cells are required to achieve said effect.

In RNA sequencing studies performed on mice treated with FEC + oHSV-1 therapy, we reproducibly saw that S100A8 and S100A9 were two of the most commonly

upregulated genes with our therapy (**Chapter 4)**. A literature search shows conflicting reports of both pro- and antitumorigenic functions of these low molecular weight calcium binding proteins. Through our work and clinical data obtained from the TCGA database, we have shown that S100A8/A9 upregulation results in improved prognostic outcomes in breast cancer patients. Interestingly and relevant to our central hypothesis, S100A8/A9 are implicated in the regulation of tumor cell proliferation and metastasis and often secreted by MDSCs[129]. Indeed, blocking of the binding of S100A8/A9 to MDSCs reduces the overall levels of MDSCs in the blood of murine hosts[129].

In parallel to this work, we utilized a radiotherapy construct to again assess effects on the TME and the prognostic outcomes in mice bearing TNBC tumors (**Chapter 5**). Our radiotherapy regimen was able to sensitize tumors to ICB for enhanced overall survival and improved therapeutic outcome. Assessment of the immune cell levels after treatment revealed that once again, therapeutic efficacy correlated directly with decreased MDSC levels, further supporting our hypothesis.

Collectively in this thesis work I have developed two therapeutic platforms that can be used to sensitize TNBC tumors to ICB. I have identified an interesting association between B cells and enhanced therapeutic efficacy, which is in line with current impactful literature findings[64,65,130]. Additionally, I have shown the clinical relevance of MDSCs in breast cancer and their correlative potential to therapeutic outcomes.

References

1. Brenner, D. R. *et al.* Projected estimates of cancer in Canada in 2020. *CMAJ* (2020). doi:10.1503/cmaj.191292

2. Canadian Cancer Statistics Advisory Committee. Canadian Cancer Statistics 2019. *Canadian Cancer Society* (2019).

3. Ferlay, J. *et al.* Estimating the global cancer incidence and mortality in 2018: GLOBOCAN sources and methods. *International Journal of Cancer* (2019). doi:10.1002/ijc.31937

4. Shields, M. & Wilkins, K. An update on mammography use in Canada. *Health Rep.* (2009).

5. Wang, X. *et al.* Immunological therapy: A novel thriving area for triple-negative breast cancer treatment. *Cancer Letters* (2019). doi:10.1016/j.canlet.2018.10.042

6. Hanahan, D. & Weinberg, R. A. The hallmarks of cancer. *Cell* (2000). doi:10.1016/S0092-8674(00)81683-9

7. Hanahan, D. & Weinberg, R. A. Hallmarks of cancer: The next generation. *Cell* (2011). doi:10.1016/j.cell.2011.02.013

8. Ribatti, D. The concept of immune surveillance against tumors. The first theories. *Oncotarget* (2017). doi:10.18632/oncotarget.12739

9. Finn, O. J. A Believer's Overview of Cancer Immunosurveillance and Immunotherapy. *J. Immunol.* (2018). doi:10.4049/jimmunol.1701302

10. Awad, R. M., De Vlaeminck, Y., Maebe, J., Goyvaerts, C. & Breckpot, K. Turn Back the TIMe: Targeting Tumor Infiltrating Myeloid Cells to Revert Cancer Progression. *Frontiers in immunology* (2018). doi:10.3389/fimmu.2018.01977

11. Liu, M. & Guo, F. Recent updates on cancer immunotherapy. *Precis. Clin. Med.* (2018). doi:10.1093/pcmedi/pby011

12. Galluzzi, L. *et al.* Classification of current anticancer immunotherapies. *Oncotarget* (2014). doi:10.18632/oncotarget.2998

13. Schuster, M., Nechansky, A., Loibner, H. & Kircheis, R. Cancer immunotherapy. *Biotechnology Journal* (2006). doi:10.1002/biot.200500044

14. Schmid, P. *et al.* Atezolizumab and nab-paclitaxel in advanced triple-negative breast cancer. *N. Engl. J. Med.* (2018). doi:10.1056/NEJMoa1809615

15. Sambi, M., Bagheri, L. & Szewczuk, M. R. Current challenges in cancer immunotherapy: Multimodal approaches to improve efficacy and patient response rates. *Journal of Oncology* (2019). doi:10.1155/2019/4508794

16. Zitvogel, L., Tesniere, A. & Kroemer, G. Cancer despite immunosurveillance: Immunoselection and immunosubversion. *Nature Reviews Immunology* (2006). doi:10.1038/nri1936

17. Schreiber, R. D., Old, L. J. & Smyth, M. J. Cancer immunoediting: Integrating immunity's roles in cancer suppression and promotion. *Science* (2011). doi:10.1126/science.1203486

18. Shayakhmetov, D. M., Di Paolo, N. C. & Mossman, K. L. Recognition of virus infection and innate host responses to viral gene therapy vectors. *Molecular Therapy* (2010). doi:10.1038/mt.2010.124

19. Harris, T. J. & Drake, C. G. Primer on tumor immunology and cancer immunotherapy. *Journal for ImmunoTherapy of Cancer* (2013). doi:10.1186/2051-1426-1-12

20. Pardoll, D. M. The blockade of immune checkpoints in cancer immunotherapy.

Nature Reviews Cancer (2012). doi:10.1038/nrc3239

21. DeNardo, D. G. *et al.* Leukocyte complexity predicts breast cancer survival and functionally regulates response to chemotherapy. *Cancer Discov.* (2011). doi:10.1158/2159-8274.CD-10-0028
22. Kroemer, G., Senovilla, L., Galluzzi, L., André, F. & Zitvogel, L. Natural and therapy-induced immunosurveillance in breast cancer. *Nature Medicine* (2015). doi:10.1038/nm.3944
23. Mahmoud, S. M. A. *et al.* Tumor-infiltrating CD8+ lymphocytes predict clinical outcome in breast cancer. *J. Clin. Oncol.* (2011). doi:10.1200/JCO.2010.30.5037
24. Gajewski, T. F., Schreiber, H. & Fu, Y. X. Innate and adaptive immune cells in the tumor microenvironment. *Nature Immunology* (2013). doi:10.1038/ni.2703
25. Devaud, C., John, L. B., Westwood, J. A., Darcy, P. K. & Kershaw, M. H. Immune modulation of the tumor microenvironment for enhancing cancer immunotherapy. *Oncoimmunology* (2013). doi:10.4161/onci.25961
26. Myeloid Cell Origins, Differentiation, and Clinical Implications. in *Myeloid Cells in Health and Disease* (2016). doi:10.1128/microbiolspec.mchd-0031-2016
27. Patel, S. R., Hartwig, J. H. & Italiano, J. E. The biogenesis of platelets from megakaryocyte proplatelets. *Journal of Clinical Investigation* (2005). doi:10.1172/JCI26891
28. Velten, L. *et al.* Human haematopoietic stem cell lineage commitment is a continuous process. *Nat. Cell Biol.* (2017). doi:10.1038/ncb3493
29. Ioannou, M. *et al.* Crucial Role of Granulocytic Myeloid-Derived Suppressor Cells

in the Regulation of Central Nervous System Autoimmune Disease. *J. Immunol.* (2012). doi:10.4049/jimmunol.1101816

30. Meyera, C. *et al.* Chronic inflammation promotes myeloid-derived suppressor cell activation blocking antitumor immunity in transgenic mouse melanoma model. *Proc. Natl. Acad. Sci. U. S. A.* (2011). doi:10.1073/pnas.1108121108
31. Condamine, T. & Gabrilovich, D. I. Molecular mechanisms regulating myeloid-derived suppressor cell differentiation and function. *Trends in Immunology* (2011). doi:10.1016/j.it.2010.10.002
32. Ueda, Y., Kondo, M. & Kelsoe, G. Inflammation and the reciprocal production of granulocytes and lymphocytes in bone marrow. *J. Exp. Med.* (2005). doi:10.1084/jem.20041419
33. Jordan, K. R. *et al.* Immunosuppressive myeloid-derived suppressor cells are increased in splenocytes from cancer patients. *Cancer Immunol. Immunother.* (2017). doi:10.1007/s00262-016-1953-z
34. Bates, J. P., Derakhshandeh, R., Jones, L. & Webb, T. J. Mechanisms of immune evasion in breast cancer. *BMC Cancer* (2018). doi:10.1186/s12885-018-4441-3
35. Diaz-Montero, C. M. *et al.* Increased circulating myeloid-derived suppressor cells correlate with clinical cancer stage, metastatic tumor burden, and doxorubicin-cyclophosphamide chemotherapy. *Cancer Immunol. Immunother.* (2009). doi:10.1007/s00262-008-0523-4
36. Bergenfelz, C. *et al.* Systemic monocytic-MDSCs are generated from monocytes and correlate with disease progression in breast cancer patients. *PLoS One* (2015).

doi:10.1371/journal.pone.0127028

37. Loi, S. *et al.* Prognostic and predictive value of tumor-infiltrating lymphocytes in a phase III randomized adjuvant breast cancer trial in node-positive breast cancer comparing the addition of docetaxel to doxorubicin with doxorubicin-based chemotherapy: BIG 02-98. *J. Clin. Oncol.* (2013). doi:10.1200/JCO.2011.41.0902

38. Adams, S. *et al.* Prognostic value of tumor-infiltrating lymphocytes in triple-negative breast cancers from two phase III randomized adjuvant breast cancer trials: ECOG 2197 and ECOG 1199. *J. Clin. Oncol.* (2014). doi:10.1200/JCO.2013.55.0491

39. Denkert, C. *et al.* Tumour-infiltrating lymphocytes and prognosis in different subtypes of breast cancer: a pooled analysis of 3771 patients treated with neoadjuvant therapy. *Lancet Oncol.* (2018). doi:10.1016/S1470-2045(17)30904-X

40. Chen, W. C. *et al.* Interleukin-17-producing cell infiltration in the breast cancer tumour microenvironment is a poor prognostic factor. *Histopathology* (2013). doi:10.1111/his.12156

41. Cochaud, S. *et al.* IL-17A is produced by breast cancer TILs and promotes chemoresistance and proliferation through ERK1/2. *Sci. Rep.* (2013). doi:10.1038/srep03456

42. Culpepper, C., Tremblay, A., Bian, Z., Niu, S. & Liu, Y. IL-17A induced hematopoietic reprogramming produces both PMN and MDSC at the post-acute stage of inflammation. *J Immunol* **200**, 42 (2018).

43. Dawod, B. *et al.* Myeloid-derived suppressor cell depletion therapy targets IL-

17A-expressing mammary carcinomas. *Sci. Rep.* (2020). doi:10.1038/s41598-020-70231-7

44. Groth, C. *et al.* Immunosuppression mediated by myeloid-derived suppressor cells (MDSCs) during tumour progression. *British Journal of Cancer* (2019). doi:10.1038/s41416-018-0333-1

45. Weber, R. *et al.* Myeloid-derived suppressor cells hinder the anti-cancer activity of immune checkpoint inhibitors. *Frontiers in Immunology* (2018). doi:10.3389/fimmu.2018.01310

46. Markowitz, J., Wesolowski, R., Papenfuss, T., Brooks, T. R. & Carson, W. E. Myeloid-derived suppressor cells in breast cancer. *Breast Cancer Research and Treatment* (2013). doi:10.1007/s10549-013-2618-7

47. Park, Y. J. *et al.* Tumor microenvironmental conversion of natural killer cells into myeloid-derived suppressor cells. *Cancer Res.* (2013). doi:10.1158/0008-5472.CAN-13-0545

48. Kamran, N. *et al.* Melanoma induced immunosuppression is mediated by hematopoietic dysregulation. *Oncoimmunology* (2018). doi:10.1080/2162402X.2017.1408750

49. Sarvaria, A., Madrigal, J. A. & Saudemont, A. B cell regulation in cancer and anti-tumor immunity. *Cellular and Molecular Immunology* (2017). doi:10.1038/cmi.2017.35

50. Xu, X. *et al.* Myeloid-derived suppressor cells promote B-cell production of IgA in a TNFR2-dependent manner. *Cell. Mol. Immunol.* (2017).

doi:10.1038/cmi.2015.103

51. Wang, Y. *et al.* Myeloid-Derived Suppressor Cells Impair B Cell Responses in Lung Cancer through IL-7 and STAT5. *J. Immunol.* (2018). doi:10.4049/jimmunol.1701069

52. Baert, T. *et al.* Myeloid derived suppressor cells: Key drivers of immunosuppression in ovarian cancer. *Front. Immunol.* (2019). doi:10.3389/fimmu.2019.01273

53. Fleming, V. *et al.* Targeting myeloid-derived suppressor cells to bypass tumor-induced immunosuppression. *Frontiers in Immunology* (2018). doi:10.3389/fimmu.2018.00398

54. Walker, J. D., Sehgal, I. & Kousoulas, K. G. Oncolytic Herpes Simplex Virus 1 Encoding 15-Prostaglandin Dehydrogenase Mitigates Immune Suppression and Reduces Ectopic Primary and Metastatic Breast Cancer in Mice. *J. Virol.* (2011). doi:10.1128/jvi.00098-11

55. Zhang, Y. *et al.* A novel role of hematopoietic CCL5 in promoting triple-negative mammary tumor progression by regulating generation of myeloid-derived suppressor cells. *Cell Res.* (2013). doi:10.1038/cr.2012.178

56. Garaud, S. *et al.* Tumor-infiltrating B cells signal functional humoral immune responses in breast cancer. *JCI Insight* (2019). doi:10.1172/jci.insight.129641

57. Germain, C., Gnjatic, S. & Dieu-Nosjean, M. C. Tertiary lymphoid structure-associated B cells are key players in anti-tumor immunity. *Frontiers in Immunology* (2015). doi:10.3389/fimmu.2015.00067

58. Dieu-Nosjean, M. C. *et al.* Tertiary lymphoid structures, drivers of the anti-tumor responses in human cancers. *Immunol. Rev.* (2016). doi:10.1111/imr.12405

59. Seow, D. Y. Bin *et al.* Tertiary lymphoid structures and associated plasma cells play an important role in the biology of triple-negative breast cancers. *Breast Cancer Res. Treat.* (2020). doi:10.1007/s10549-020-05548-y

60. Jézéquel, P. *et al.* Identification of three subtypes of triple-negative breast cancer with potential therapeutic implications. *Breast Cancer Res.* (2019). doi:10.1186/s13058-019-1148-6

61. Engelhard, V. H. *et al.* Immune Cell Infiltration and Tertiary Lymphoid Structures as Determinants of Antitumor Immunity. *J. Immunol.* (2018). doi:10.4049/jimmunol.1701269

62. Tsou, P., Katayama, H., Ostrin, E. J. & Hanash, S. M. The emerging role of b cells in tumor immunity. *Cancer Research* (2016). doi:10.1158/0008-5472.CAN-16-0431

63. Liudahl, S. M. & Coussens, L. M. B cells as biomarkers: Predicting immune checkpoint therapy adverse events. *Journal of Clinical Investigation* (2018). doi:10.1172/JCI99036

64. Petitprez, F. *et al.* B cells are associated with survival and immunotherapy response in sarcoma. *Nature* (2020). doi:10.1038/s41586-019-1906-8

65. Cabrita, R. *et al.* Tertiary lymphoid structures improve immunotherapy and survival in melanoma. *Nature* (2020). doi:10.1038/s41586-019-1914-8

66. Bruno, T. C. New predictors for immunotherapy responses sharpen our view of the

tumour microenvironment. *Nature* (2020). doi:10.1038/d41586-019-03943-0

67. Helmink, B. A. *et al.* B cells and tertiary lymphoid structures promote immunotherapy response. *Nature* (2020). doi:10.1038/s41586-019-1922-8

68. Gnjatic, S. *et al.* Survey of naturally occurring CD4+ T cell responses against NY-ESO-1 in cancer patients: Correlation with antibody responses. *Proc. Natl. Acad. Sci. U. S. A.* (2003). doi:10.1073/pnas.1133324100

69. Hollern, D. P. *et al.* B Cells and T Follicular Helper Cells Mediate Response to Checkpoint Inhibitors in High Mutation Burden Mouse Models of Breast Cancer. *Cell* (2019). doi:10.1016/j.cell.2019.10.028

70. DeVita, V. T. & Chu, E. A history of cancer chemotherapy. *Cancer Research* (2008). doi:10.1158/0008-5472.CAN-07-6611

71. Medical Odysseys: The Different and Sometimes Unexpected Pathways to Twentieth-Century Medical Discoveries. *Ann. Intern. Med.* (1991). doi:10.7326/0003-4819-115-5-413_5

72. Hess, J. A. & Khasawneh, M. K. Cancer metabolism and oxidative stress: Insights into carcinogenesis and chemotherapy via the non-dihydrofolate reductase effects of methotrexate. *BBA Clinical* (2015). doi:10.1016/j.bbacli.2015.01.006

73. Laughing gas, Viagra, and Lipitor: the human stories behind the drugs we use. *Choice Rev. Online* (2007). doi:10.5860/choice.44-3904

74. Cheok, C. F. Protecting normal cells from the cytotoxicity of chemotherapy. *Cell Cycle* (2012). doi:10.4161/cc.20961

75. Rasmussen, L. & Arvin, A. Chemotherapy-induced immunosuppression.

Environmental Health Perspectives (1982). doi:10.2307/3429163

76. Bracci, L., Schiavoni, G., Sistigu, A. & Belardelli, F. Immune-based mechanisms of cytotoxic chemotherapy: Implications for the design of novel and rationale-based combined treatments against cancer. *Cell Death and Differentiation* (2014). doi:10.1038/cdd.2013.67

77. Vacchelli, E. *et al.* Trial watch: Chemotherapy with immunogenic cell death inducers. *OncoImmunology* (2014). doi:10.4161/onci.27878

78. Casares, N. *et al.* Caspase-dependent immunogenicity of doxorubicin-induced tumor cell death. *J. Exp. Med.* (2005). doi:10.1084/jem.20050915

79. Landreneau, J. P. *et al.* Immunological Mechanisms of Low and Ultra-Low Dose Cancer Chemotherapy. *Cancer Microenviron.* (2015). doi:10.1007/s12307-013-0141-3

80. Dudek, A. M., Garg, A. D., Krysko, D. V., De Ruysscher, D. & Agostinis, P. Inducers of immunogenic cancer cell death. *Cytokine and Growth Factor Reviews* (2013). doi:10.1016/j.cytogfr.2013.01.005

81. Kroemer, G., Galluzzi, L., Kepp, O. & Zitvogel, L. Immunogenic Cell Death in Cancer Therapy. *Annu. Rev. Immunol.* (2013). doi:10.1146/annurev-immunol-032712-100008

82. Galluzzi, L., Buqué, A., Kepp, O., Zitvogel, L. & Kroemer, G. Immunogenic cell death in cancer and infectious disease. *Nature Reviews Immunology* (2017). doi:10.1038/nri.2016.107

83. Apetoh, L. *et al.* Toll-like receptor 4-dependent contribution of the immune system

to anticancer chemotherapy and radiotherapy. *Nat. Med.* (2007). doi:10.1038/nm1622

84. Pfirschke, C. *et al.* Immunogenic Chemotherapy Sensitizes Tumors to Checkpoint Blockade Therapy. *Immunity* (2016). doi:10.1016/j.immuni.2015.11.024

85. Wu, Y. *et al.* Repeated cycles of 5-fluorouracil chemotherapy impaired anti-tumor functions of cytotoxic T cells in a CT26 tumor-bearing mouse model. *BMC Immunol.* (2016). doi:10.1186/s12865-016-0167-7

86. Kelly, E. & Russell, S. J. History of oncolytic viruses: Genesis to genetic engineering. *Molecular Therapy* (2007). doi:10.1038/sj.mt.6300108

87. Martuza, R. L., Malick, A., Markert, J. M., Ruffner, K. L. & Coen, D. M. Experimental therapy of human glioma by means of a genetically engineered virus mutant. *Science (80-.).* (1991). doi:10.1126/science.1851332

88. Challenor, S. & Tucker, D. SARS-CoV-2-induced remission of Hodgkin lymphoma. *Br. J. Haematol.* (2021). doi:10.1111/bjh.17116

89. Prestwich, R. J. *et al.* The case of oncolytic viruses versus the immune system: waiting on the judgment of Solomon. *Human gene therapy* (2009). doi:10.1089/hum.2009.135

90. Donahue, J. M., Mullen, J. T. & Tanabe, K. K. Viral oncolysis. *Surgical Oncology Clinics of North America* (2002). doi:10.1016/S1055-3207(02)00025-X

91. Workenhe, S. T. & Mossman, K. L. Oncolytic virotherapy and immunogenic cancer cell death: Sharpening the sword for improved cancer treatment strategies. *Molecular Therapy* (2014). doi:10.1038/mt.2013.220

92. Ilkow, C. S., Swift, S. L., Bell, J. C. & Diallo, J. S. From Scourge to Cure: Tumour-Selective Viral Pathogenesis as a New Strategy against Cancer. *PLoS Pathogens* (2014). doi:10.1371/journal.ppat.1003836

93. Heo, J. *et al.* Randomized dose-finding clinical trial of oncolytic immunotherapeutic vaccinia JX-594 in liver cancer. *Nat. Med.* (2013). doi:10.1038/nm.3089

94. Andtbacka, R. H. I. *et al.* Talimogene laherparepvec improves durable response rate in patients with advanced melanoma. *J. Clin. Oncol.* (2015). doi:10.1200/JCO.2014.58.3377

95. Willmon, C. L. *et al.* Expression of IFN-β enhances both efficacy and safety of oncolytic vesicular stomatitis virus for therapy of mesothelioma. *Cancer Res.* (2009). doi:10.1158/0008-5472.CAN-09-1013

96. Kottke, T. *et al.* Broad antigenic coverage induced by vaccination with virus-based cDNA libraries cures established tumors. *Nat. Med.* (2011). doi:10.1038/nm.2390

97. Workenhe, S. T. *et al.* Immunogenic HSV-mediated Oncolysis shapes the antitumor immune response and contributes to therapeutic efficacy. *Mol. Ther.* (2014). doi:10.1038/mt.2013.238

98. Workenhe, S. T., Pol, J. G., Lichty, B. D., Cummings, D. T. & Mossman, K. L. Combining oncolytic HSV-1 with immunogenic cell death-inducing drug mitoxantrone breaks cancer immune tolerance and improves therapeutic efficacy. *Cancer Immunol. Res.* (2013). doi:10.1158/2326-6066.CIR-13-0059-T

99. Workenhe, S. T. *et al.* De novo necroptosis creates an inflammatory environment

mediating tumor susceptibility to immune checkpoint inhibitors. *Commun. Biol.* (2020). doi:10.1038/s42003-020-01362-w

100. Brunet, J. F. *et al.* A new member of the immunoglobulin superfamily-CTLA-4. *Nature* (1988). doi:10.1038/328267a0

101. Krummel, M. F. & Allison, J. P. CD28 and CTLA-4 have opposing effects on the response of T ceils to stimulation. *J. Exp. Med.* (1995). doi:10.1084/jem.182.2.459

102. Leach, D. R., Krummel, M. F. & Allison, J. P. Enhancement of antitumor immunity by CTLA-4 blockade. *Science (80-.).* (1996). doi:10.1126/science.271.5256.1734

103. Ishida, Y., Agata, Y., Shibahara, K. & Honjo, T. Induced expression of PD-1, a novel member of the immunoglobulin gene superfamily, upon programmed cell death. *EMBO J.* (1992). doi:10.1002/j.1460-2075.1992.tb05481.x

104. Alegre, M. L. *et al.* Regulation of Surface and Intracellular Expression of CTLA4 on Mouse T Cells. *J. Immunol.* (1996).

105. Decker, W. K. *et al.* Cancer immunotherapy: Historical perspective of a clinical revolution and emerging preclinical animal models. *Frontiers in Immunology* (2017). doi:10.3389/fimmu.2017.00829

106. Baumeister, S. H., Freeman, G. J., Dranoff, G. & Sharpe, A. H. Coinhibitory Pathways in Immunotherapy for Cancer. *Annu. Rev. Immunol.* (2016). doi:10.1146/annurev-immunol-032414-112049

107. Oiseth, S. J. & Aziz, M. S. Cancer immunotherapy: a brief review of the history, possibilities, and challenges ahead. *J. Cancer Metastasis Treat.* (2017).

doi:10.20517/2394-4722.2017.41

108. Levitan, D. Combination PARP/PD-1 Inhibition Shows Promise in Phase I Trial of Advanced Solid Tumors. *ASCO-SITC Dly. News* (2018).

109. Okazaki, T., Chikuma, S., Iwai, Y., Fagarasan, S. & Honjo, T. A rheostat for immune responses: The unique properties of PD-1 and their advantages for clinical application. *Nature Immunology* (2013). doi:10.1038/ni.2762

110. Keir, M. E. *et al.* Tissue expression of PD-L1 mediates peripheral T cell tolerance. *J. Exp. Med.* (2006). doi:10.1084/jem.20051776

111. Taube, J. M. *et al.* Differential expression of immune-regulatory genes associated with PD-L1 display in melanoma: Implications for PD-1 pathway blockade. *Clin. Cancer Res.* (2015). doi:10.1158/1078-0432.CCR-15-0244

112. Taube, J. M. *et al.* Colocalization of inflammatory response with B7-H1 expression in human melanocytic lesions supports an adaptive resistance mechanism of immune escape. *Sci. Transl. Med.* (2012). doi:10.1126/scitranslmed.3003689

113. Brahmer, J. R. *et al.* Safety and Activity of Anti–PD-L1 Antibody in Patients with Advanced Cancer. *N. Engl. J. Med.* (2012). doi:10.1056/nejmoa1200694

114. Topalian, S. & Hodi, F. Safety, activity, and immune correlates of anti–PD-1 antibody in cancer. *N. Engl. J. Med.* (2012).

115. Targeted Oncology. A Brief History of Immunotherapy. *Targeted Oncology* (2014).

116. Powles, T. *et al.* Inhibition of PD-L1 by MPDL3280A and clinical activity in pts with metastatic urothelial bladder cancer (UBC). *J. Clin. Oncol.* (2014).

doi:10.1200/jco.2014.32.15_suppl.5011

117. Emmett, L. *et al.* Lutetium 177 PSMA radionuclide therapy for men with prostate cancer: a review of the current literature and discussion of practical aspects of therapy. *Journal of Medical Radiation Sciences* (2017). doi:10.1002/jmrs.227

118. MOLE, R. H. Whole body irradiation; radiobiology or medicine? *Br. J. Radiol.* (1953). doi:10.1259/0007-1285-26-305-234

119. Rodriguez-Ruiz, M. E. *et al.* Abscopal effects of radiotherapy are enhanced by combined immunostimulatory mAbs and are dependent on CD8 T cells and crosspriming. *Cancer Res.* (2016). doi:10.1158/0008-5472.CAN-16-0549

120. Demaria, S. *et al.* Immune-mediated inhibition of metastases after treatment with local radiation and CTLA-4 blockade in a mouse model of breast cancer. *Clin. Cancer Res.* (2005).

121. Galluzzi, L., Kepp, O. & Kroemer, G. Immunogenic cell death in radiation therapy. *Oncoimmunology* (2013). doi:10.4161/onci.26536

122. Pitroda, S. P., Chmura, S. J. & Weichselbaum, R. R. Integration of radiotherapy and immunotherapy for treatment of oligometastases. *The Lancet Oncology* (2019). doi:10.1016/S1470-2045(19)30157-3

123. Vito, A., El-Sayes, N. & Mossman, K. Hypoxia-Driven Immune Escape in the Tumor Microenvironment. *Cells* (2020). doi:10.3390/cells9040992

124. Lim, Z. F. & Ma, P. C. Emerging insights of tumor heterogeneity and drug resistance mechanisms in lung cancer targeted therapy. *Journal of Hematology and Oncology* (2019). doi:10.1186/s13045-019-0818-2

125. Riganti, C. & Contino, M. New strategies to overcome resistance to chemotherapy and immune system in cancer. *International Journal of Molecular Sciences* (2019). doi:10.3390/ijms20194783

126. Berland, L. *et al.* Current views on tumor mutational burden in patients with nonsmall cell lung cancer treated by immune checkpoint inhibitors. *Journal of Thoracic Disease* (2019). doi:10.21037/jtd.2018.11.102

127. Dawson, S. J., Provenzano, E. & Caldas, C. Triple negative breast cancers: Clinical and prognostic implications. *Eur. J. Cancer* (2009). doi:10.1016/S0959-8049(09)70013-9

128. Lin, N. U. *et al.* Clinicopathologic features, patterns of recurrence, and survival among women with triple-negative breast cancer in the National Comprehensive Cancer Network. *Cancer* (2012). doi:10.1002/cncr.27581

129. Zhao, F. *et al.* S100A9 a new marker for monocytic human myeloid-derived suppressor cells. *Immunology* (2012). doi:10.1111/j.1365-2567.2012.03566.x

130. Roerink, S. F. *et al.* Intra-tumour diversification in colorectal cancer at the single-cell level. *Nature* (2018). doi:10.1038/s41586-018-0024-3

CHAPTER TWO: HYPOXIA-DRIVEN IMMUNE ESCAPE IN THE TUMOR MICROENVIRONMENT

Preamble

This is a pre-copyedited, author-produced version of an article accepted for publication in Cells following peer review. The version of record **Vito A**, El-Sayes N, Mossman K. Hypoxia-driven immune escape in the tumor microenvironment. *Cells*, 9(4):992, 2020 is available online at: https://www.mdpi.com/2073-4409/9/4/992, DOI: 10.3390/cells9040992.

AV conceived the idea, prepared the manuscript and created the figures. NES prepared the manuscript and created the figures. KM supervised and edited the manuscript.

In this review, we explore the role hypoxia plays in driving immune escape and altering the TME. More specifically, we discuss the way hypoxic conditions effect various immune cell phenotypes as well as conflicting reports as to whether or not hypoxia shifts cell death towards that of an immunogenic nature. Next, we explore hypoxia-mediated therapeutic resistance and how immunotherapies can be used to combat hypoxia-driven suppression and immune escape. This review contributes to the work included in this thesis as it helps to better understand the ever-shifting TME and the factors inherent within a tumor that need to be overcome to achieve successful treatment with immunotherapy platforms.

Permission of re-use of this material is granted by the Creative Commons Attribution License (https://creativecommons.org/licenses/by/4.0/). The only changes made to the document are to the figure numbers, which have been renumbered to fit within the structure of this dissertation.

Hypoxia-driven immune escape in the tumor microenvironment

Vito, A[1†], El-Sayes, N[1†] and Mossman, K M[2*]

[1]Department of Biochemistry and Biomedical Sciences, McMaster Immunology Research Centre, McMaster University, Hamilton, ON, Canada

[2]Department of Pathology and Molecular Medicine, McMaster Immunology Research Centre, McMaster University, Hamilton, ON, Canada

[†]The authors contributed equally to this publication.

[*]Corresponding Author: mossk@mcmaster.ca

Abstract

The tumor microenvironment is a complex ecosystem comprised of many different cell types, abnormal vasculature and immunosuppressive cytokines. The irregular growth kinetics with which tumors grow leads to increased oxygen consumption and in turn, hypoxic conditions. Hypoxia has been associated with poor clinical outcome, increased tumor heterogeneity, emergence of resistant clones and evasion of immune detection. Additionally, hypoxia-driven cell death pathways have traditionally been thought of as tolerogenic processes. However, as researchers working in the field of immunotherapy continue to investigate and unveil new types of immunogenic cell death (ICD), it has become clear that in some instances, hypoxia may actually induce ICD within a tumor. In this review we will discuss hypoxia-driven immune escape that drives poor prognostic outcomes, the ability of hypoxia to induce ICD and potential therapeutic targets amongst hypoxia pathways.

Keywords: hypoxia; tumor microenvironment; immunogenic cell death; therapeutics

2.1. Introduction

Cancer is characterized by uncontrolled cell growth and rapid proliferation. The enhanced cellular kinetics with which cancer cells divide and grow inevitably causes nutrient depletion, as well as an influx of transcription factors and proteins responsible for the induction of hypoxia[89]. The increased proliferative capacity of malignant cells requires constant uptake of oxygen, which is a limiting factor in an oxygen-deprived environment. In response to low oxygen levels in tumors, transcriptional responses upregulate hypoxia-inducible factors (HIFs), transcriptional factors that control the expression of many angiogenic, metabolic and cell cycle genes[90]. While malignant cells are able to continue to grow and even thrive in the resultant hypoxic microenvironment, it creates inhospitable conditions for immune cells and dampens the response of key regulatory pathways, resulting in immunosuppression[91]. Interestingly, while it is well established in the literature that hypoxia contributes to a diminishing immune response[92–94], it has also been shown to simultaneously play an immunostimulatory role, as the consequential pro-inflammatory environment lends to cells dying in an immunogenic manner[95]. This paper discusses the complex and opposing roles of hypoxia signaling in driving immune escape, promoting tumor growth and metastatic potential, while also enhancing certain immunogenic features of the tumor microenvironment (TME).

The ability of the immune system to recognize malignant cells as foreign entities and clear them from the body has been the springboard for a wave of innovative immunotherapies that have revolutionized the way we think about treating cancer patients. As we focus on the development of new and improved therapies that can harness

the potential of the immune system to detect and kill tumors, we also begin to better understand the multi-faceted biology and interactions associated with the TME. The TME is composed of immune cells, endothelial cells, fibroblasts, extracellular matrix and various signaling molecules such as chemokines[96]. The push and pull between pro- and anti-tumorigenic signaling pathways create a challenging environment to study, treat and fully understand. Add to this the individual characteristics of different cancer phenotypes and the goal of identifying overarching, unifying concepts that will apply to many cancers becomes even more difficult. Hypoxia has been shown to be universally associated with many tumor types as the natural metabolic profile of an evolving tumor is characterized by critical oxygen depletion, extracellular acidosis, elevated levels of adenosine and lactate and deprivation of essential nutrients[89]. Additionally, hypoxia contributes to intratumoral heterogeneity, metastatic progression, genetic instability, angiogenesis and the evolution of therapy-resistant clones[89,96]. For this reason, it is apparent why so many researchers have sought to target hypoxia pathways to mitigate immunosuppression and improve therapeutic outcomes.

2.2. Hypoxia Signaling and Metabolism

2.2.1. HIF signaling pathways. Hypoxia signaling in the TME involves complex pathways and processes. At the core, the cellular response to hypoxia is mediated by two master regulators that comprise a heterodimeric complex. This complex, formed by a constitutively expressed nuclear HIF-1β and a cytoplasmic oxygen-dependent HIF-α (HIF-1α, HIF-2α and HIF-3α), is further stabilized by a group of oxygen- and iron-dependent enzymes known as HIF-prolyl hydroxylase domain enzymes (PHD1-3)[97].

Under normative conditions, PHDs hydroxylate two prolyl residues of the HIF-α subunit, initiating binding of the Von Hippel-Lindau tumor-suppressor protein (pVHL) and subsequent ubiquitination and proteasomal degradation. However, under hypoxic conditions, PHDs are suppressed, and HIF-α subunits translocate into the nucleus to bind with HIF-1β. The heterodimeric HIF-α : HIF-1β transcription factor complex then locates to the hypoxia-responsive elements (HREs) of its target genes, resulting in their transcriptional upregulation (Figure 2.1).

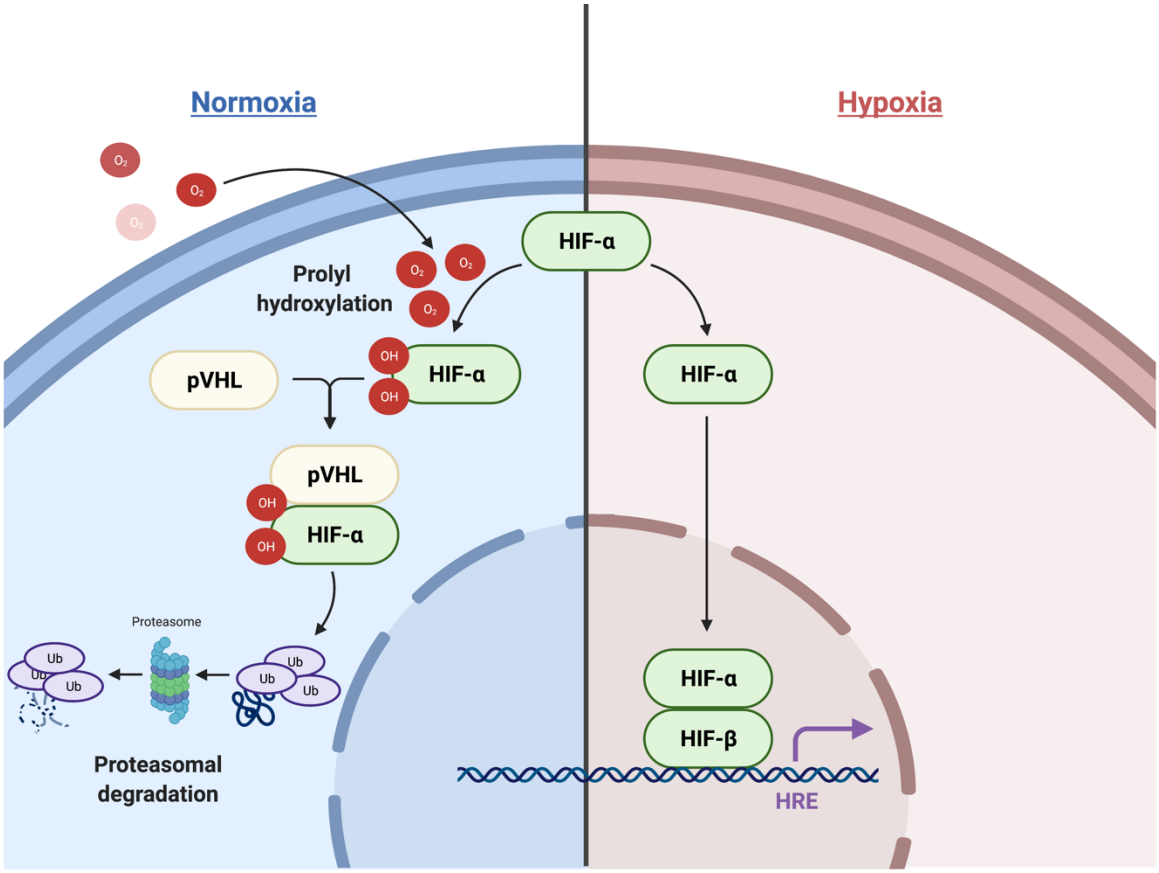

Fig. 2.1. HIF signaling pathway. *Created using BioRender.com.

There are three HIF-α subunits: HIF-1α, HIF-2α and HIF-3α. Of the three subunits, HIF-1α and HIF-2α are the most well studied and share 48% of their amino

acid sequence, with similar protein structures[98]. Interestingly, even with their extreme similarities, these two subunits are nonredundant to one another and have both overlapping and distinct target genes and mechanisms of regulation (Figure 2.2). In one study, Holmquist-Mengelbier et. al. demonstrated that the difference between the two subunits lies not only in the genes in which they transcribe, but also in the conditions under which they are stabilized[99]. They propose a temporal shift in HIF utilization, where HIF-1α appears to be most active during the acute phase of hypoxic adaptation and HIF-2α dominates during later, chronic phases of hypoxia. Further to the genetic differences at the transcriptional level between the two subunits, HIF-2α has been identified as the endothelial Per-Arnt-SIM (EPAS1) domain, an endothelium-specific HIF-α isoform suggested to have a more specialized function. Peng and colleagues have shown that EPAS1 plays an important role in controlling vascular remodeling and that the protein level of EPAS1 is regulated by oxygen tension, where hypoxia induces stabilization of the protein[100]. Additionally, Bangoura et. al. nicely demonstrated that EPAS1 overexpression is directly correlated with tumor size, vascular endothelial growth factor (VEGF) expression and initiation of angiogenesis[101].

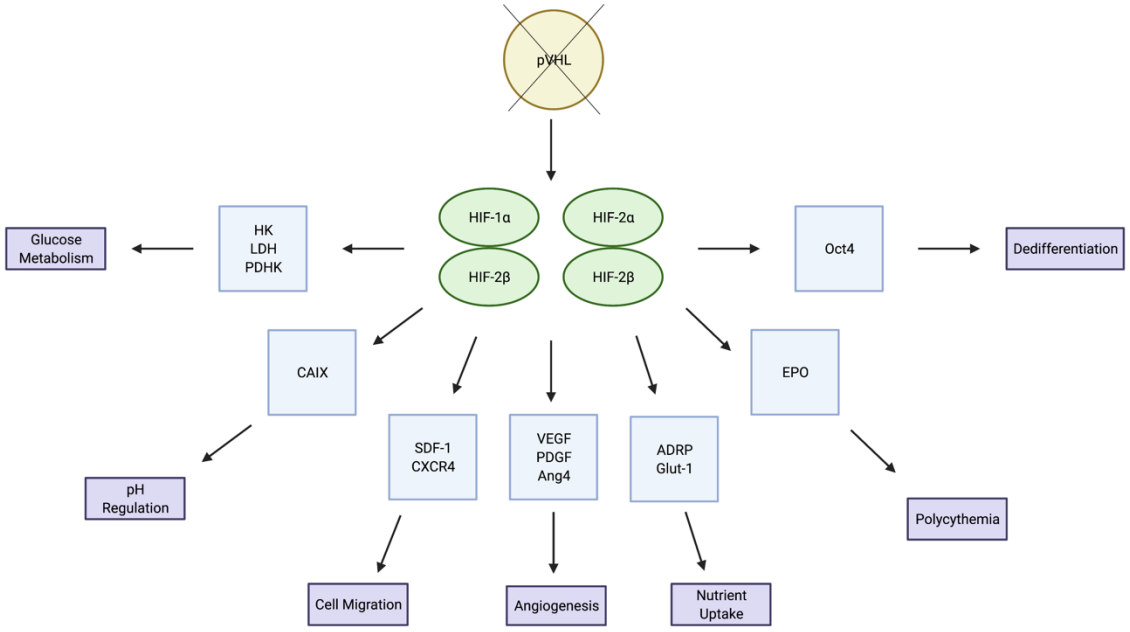

Fig. 2.2. Overlapping and distinict target genes and pathways for HIF-1α and HIF-2α. *Created using BioRender.com.

2.2.2. Metabolic changes in the TME under hypoxic conditions. It is well established that a hypoxic TME is characterized by increased concentrations of lactic acid, due to the "Warburg effect" – the metabolic shift occurring in highly proliferating cells that convert glucose to lactate, even in the presence of oxygen (aerobic glycolysis). During this process, cancer cells predominantly obtain their energy through the glycolytic pathway, rather than the tricarboxylic acid (TCA) cycle (Figure 2.3). This phenomenon seems inefficient at first glance, due to the fact that glycolysis only produces 2 ATP per molecule of glucose, whereas the TCA cycle is able to produce 36 ATP. However, the glycolytic pathway has significantly faster kinetics, meaning it can produce a comparable amount of ATP during the same amount of time[102]. This metabolic reprogramming conserves nutrients for synthesis of nucleic acids, lipids and amino acids to support

cellular growth, rather than being oxidized in the mitochondria for maximal output of ATP[103–106]. Further to this, a high rate of glycolysis leads to increased lactate production, which ultimately results in TME acidosis, altering the tumor stroma and increasing invasive potential.

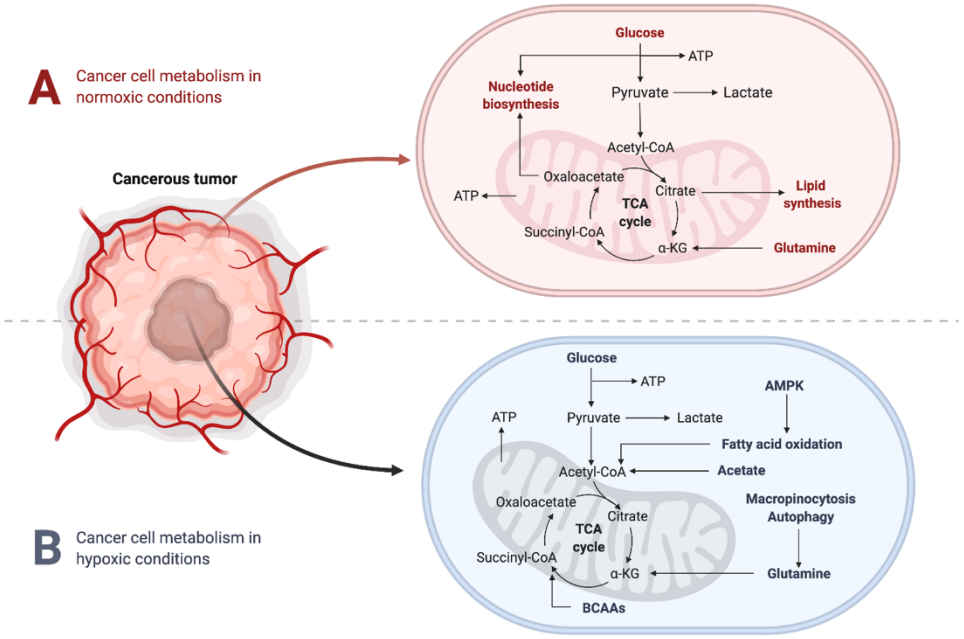

Fig. 2.3. Cancer cell metabolism under hypoxic and normoxic conditions. *Created using BioRender.com.

Studies have shown that oxygen can act as a direct regulator of PHD activity and that CO_2 production during mitochondrial respiration through the TCA cycle can also suppress HIF activity[107]. While the exact mechanism for HIF suppression is not well elucidated, many studies suggest that acidification inhibits synthesis of the mammalian target of rapamycin (mTOR), a protein kinase that is a core regulator of cellular processes[108]. Indeed, hypoxia inhibits downstream signaling and mRNA translation initiation of mTOR, resulting in tumor progression and hypoxia tolerance in advanced

tumor settings. Prolonged hypoxic exposure can also lead to endoplasmic reticulum (ER) stress, which activates the unfolded protein responses (UPR). Similar to mTOR signaling, this hypoxia-induced cascade results in several downstream effector pathways that function together to promote hypoxia tolerance. Ultimately, hypoxia-mediated signaling through mTOR and the UPR can have profound influences on gene expression and cellular behavior[97].

2.3. Hypoxia and the Immune System

In hypoxic regions in the TME cancer cells are able to adapt and support cellular growth and proliferation through the production of metabolic intermediates that can act as precursors for biosynthetic pathways. However, these oxygen-deprived conditions have been shown to reduce activation levels of tumor infiltrating lymphocytes (TILs), resulting in immunosuppression and evasion of immune detection[91]. Long proposed as a viable pathway to target for immunostimulatory therapies, many researchers have developed therapeutic pathways for blocking hypoxia-associated transcription factors. In particular, upregulation of HIF-1α has been heavily implicated in cancer biology[109] and is shown to affect varying aspects of the anti-tumor immune response, including the differentiation and function of immune cells within the TME[89]. There are many different immune cell populations that are key to mounting an effective anti-tumor immune response. Disruption of any of these cellular populations can shift or diminish the immune response, allowing tumors to evade detection and escape immune-mediated killing. In this section we will review some key immune populations and how their functions are altered under hypoxic conditions (Table 2.1).

2.3.1. Dendritic Cells. Dendritic cells (DCs) represent a heterogenous population of immune cells that infiltrate the TME to process and present antigens to naïve T cells. While DCs are only one of many antigen-presenting cell types, they are a key link between the innate and acquired immune response, as they are involved in the initiation of both stages of immunity. While DC maturation is unaffected in hypoxic conditions, their differentiation and function are heavily altered. Giovarelli and colleagues have shown that hypoxia inhibits antigen uptake by DCs, changes the DC chemokine expression profile and has profound effects on DC differentiation, adaptation and activation in inflamed tissues such as tumors[110]. This is corroborated by another report demonstrating hypoxia-induced downregulation of a variety of DC differentiation and activation markers, including CD40, CD80 and MHC class II[111]. DCs are also key components of the immunostimulatory cascade and an integral part of generating an immunogenic cell death (ICD)-mediated anti-tumor immune response[38]. For this reason, environmental factors influencing DC function may also change the natural "immunogenicity" of a tumor and in turn, shift the mechanism of cell killing to be tolerogenic in nature.

2.3.2. Macrophages. Macrophages represent key regulators of the complex relationship between the immune system and cancer. In particular, increased levels of tumor-associated macrophages (TAMs) has been implicated in immunosuppression, neovascularization, metastasis and poor responses to cancer therapies[112]. In contrast to these pro-tumorigenic functions, macrophages may also be essential mediators in immune defense, contributing to an effective anti-tumor immune response. These polarizing

functions of a singular cell type can be attributed to the fact that macrophages have high levels of plasticity and as such, their differentiation relies heavily on the microenvironment in which they are found[113]. There are two main types of tissue macrophages: classical M1 and the alternative M2 phenotype. In general, macrophage responses are shaped by the type, each with their own unique actions. Macrophages that are able to function as effector molecules for pathogen recognition and killing are generally M1-like, characterized by the generation of reactive oxygen species (ROS) and nitric oxide (NO), as well as the expression of high amounts of IL-2 and low levels of IL-10[114]. Alternatively, cytokines such as IL-4, IL-13 and IL-10 can induce macrophages to effectively execute anti-inflammatory, pro-tumorigenic and pro-angiogenic (M2-like) features[114]. Upon assessment of TAMs found specifically in hypoxic niches within the tumor, researchers have found an aggressive M2 phenotype capable of mediating resistance to many anticancer therapies[115]. Similarly, clinical studies of the histological localization of TAMs have demonstrated a clear correlation between TAM infiltration in hypoxic/necrotic tumor niches and worse prognostic outcomes[116].

2.3.3. B Cells. The humoral immune response relies on the production of antibodies by B lymphocytes and their progeny, plasma cells. While B cells are primarily known for their crucial role in antibody production, they also stimulate the release of a variety of cytokines and contribute to immunomodulatory responses[117,118]. Defects in the B cell development process can lead to immunodeficiency, autoimmunity or malignancy. While not fully understood or well characterized, the significance of hypoxia-mediated channels, and specifically HIF-1α, to B cell developmental and signaling pathways is well

established in the literature[119,120]. Studies have shown that HIF-1α is required for hypoxia-induced cell cycle arrest and the absence of HIF-1α in lymphoid tissues of chimeric mice causes disruption of B cell development[121]. HIF-1α also plays a key role in controlling B cell protective activity in autoimmune diseases and in driving IL-10 production[122].

Germinal centers (GCs) are well established and studied as the main sites where antigen-activated B cells expand and undergo hypermutation and selection[123]. This process plays a key role in the presentation of antigens on follicular DCs and associated responses to immunotherapy treatments. A recent study published by Jellusova et al. demonstrated that GC B cells increase glycolysis through HIF during metabolic adaptation to hypoxic conditions[124]. They further identified a metabolic sensor, glycogen synthase kinase 3 (Gsk3), as being required for the generation and maintenance of GC B cells, which require high glycolytic activity to support growth and proliferation in a hypoxic TME[124]. Caro-Maldonado and colleagues have shown that B cell-specific deletion of the glucose transporter Glut1 resulted in decreased B cell proliferation and impaired antibody production[125], further highlighting the need for increased glycolysis to maintain B cell activity in hypoxic microenvironments. In the context of malignant conditions, tumor-associated B cells have been identified as key drivers of the sustained inflammation necessary for therapeutic efficacy[126]. This emphasizes the importance for HIF-1α-B cell interactions in the TME. Overall, as the significance of B cells in mediating responses to immunotherapies gains increasing prominence in the literature, so

too does the need to better understand the relationship between hypoxia factors and B cell developmental processes and functions.

2.3.4. T Cells. T cells are a type of lymphocyte that develop in the thymus gland and play a central role in the adaptive immune response. During the maturation process, T cells differentiate into $CD4^+$ helper T cells and $CD8^+$ cytotoxic T cells. Stimulation of $CD4^+$ T cells in the TME causes further cell differentiation into the different subpopulations Th1, Th2, Th17 or Treg (regulatory T cells)[127]. The function of T cells in humoral immunity includes critical interactions between B cells and activated extrafollicular $CD4^+$ T cells. Well established as a mainstay of GC architecture, hypoxia drives response mechanisms and T cell function in response to the generation of antibodies. In particular, depletion of HIF-1α from $CD4^+$ T cells has been shown to reduce frequencies of antigen-specific GC B cells, follicular T helper (Tfh) cells and antigen-specific antibodies[128].

In a resting state, naïve T cells require low amounts of glucose, amino acids and fatty acids to sustain basic energy requirements. However, activated T cells require markedly increased energy to fuel the synthesis of macromolecules, intracellular mediators and effector cytokines. This increased energy consumption requires metabolic reprogramming in which active T cells increase glucose and glutamine catabolism for nucleotide and lipid synthesis, while oxidative phosphorylation is maintained for production of ATP[129]. Additionally, T cell receptor (TCR)-CD28 co-stimulation triggers the shift from naïve to effector T (Teff) cells partially through the mTOR pathway and activation of HIF-1α. This promotes glycolytic gene expression and post-translational modification that is an essential driver of aerobic glycolysis and amino acid metabolism

in Teff cells[130]. Glycolic inadequacies during metabolic reprogramming can result in T cell anergy or the shunting of potential Teff cells to the Treg lineage[131].

Hypoxic TMEs and HIF-1α can directly affect the frequency of $CD8^+$ T cells in the TME, leading to immunosuppression due to a lack of cytotoxic cells. Additionally, high lactate levels in the TME have been shown to suppress the mTOR pathway, inhibiting glycolysis and resulting in impaired T cell function[132]. Glycolysis inhibition is also associated with an increased expression of the inhibitory receptor programmed death-1 (PD-1), which is correlated with T cell exhaustion and non-responsiveness, aiding in tumor immune escape[133]. Interestingly, hypoxia can also contribute to an immunostimulatory function as T cells that survive in hypoxic niches have actually been shown to display increased cytolytic activity[134]. HIF-1α has been shown to play a role in memory $CD8^+$ T cells, which persist beyond the initial immune response, outlasting their terminally differentiated effector counterparts. Similar to naïve T cells, memory $CD8^+$ cells are quiescent in nature. They can however traffic to a diverse range of tissues and mount a rapid response against future antigenic re-challenge. This increase in functional kinetics is characterized by an immediate metabolic transition towards a reliance on aerobic glycolysis, dependent on the phosphatidylinositol-3-kinase/protein kinase B (PI3K/Akt) signaling pathway. Interestingly, Sukumar and colleagues have shown that while inhibition of glycolysis (and in turn, inhibition of HIF-1α expression) led to shortened effector function, it concomitantly enhanced the generation of memory cells and antitumor functionality[135].

2.3.5. Natural Killer (NK) Cells. NK cells are a class of cytotoxic innate lymphoid cells with potent anti-tumor activity. They possess a broad array of receptors that can recognize ligands induced by tumor formation, cellular stress and DNA damage[136]. Through these receptor recognitions, NK cells are able to direct their lytic machinery to target and eliminate malignant cells in the body. NK cells also release many pro-inflammatory cytokines and chemokines that can aid in amplifying an anti-tumor immune response[136]. In hypoxic niches, NK cells undergo significant metabolic reprogramming that alters their phenotypic and functional responses. Balsamo et. al. have shown that hypoxia can down-regulate expression and function of most NK cell receptors that are directly responsible for exerting cytolytic activity against tumor cells[137]. In an interesting study, Krzywinska and colleagues demonstrated that HIF-1α depletion impairs NK cell function and tumor growth. This finding was in direct correlation with decreased levels of VEGF, identifying NK cells as an inhibitor of angiogenesis in response to hypoxic conditions[138]. Further data has illustrated that activation of the PI3K/mTOR signaling pathway is critical for HIF-1α upregulation in NK cells, providing a molecular basis for reduced NK cell functions[139].

2.3.6. Myeloid-Derived Suppressor Cells (MDSCs). One of the most well-studied yet poorly understood immune populations is that of MDSCs. MDSCs are bone marrow-derived myeloid progenitors and one of the largest contributors to immunosuppression in the TME. As well as directly suppressing T cells, NK cells and DCs, they also aid in evasion of immune detection. MDSCs normally differentiate into granulocytes, macrophages or DCs[140], but in abnormal pathological conditions such as cancer they have been shown to maintain their undifferentiated state and rapidly undergo expansion[141].

Corzo et. al. detailed the role of hypoxia pathways in MDSCs and showed that HIF-1α is responsible for MDSC differentiation and function in the TME[142]. Additionally, hypoxia can enhance MDSC migration to the tumor site directly via HIF-1α-mediated chemokine production[143]. Chiu and colleagues eloquently demonstrated hypoxia as a central driver of MDSC accumulation in tumors through their secretion of various chemokines such as CCL26[144]. In a follow-up study, Chiu and colleagues further showed that knockdown of CCL26 profoundly reduces MDSC recruitment, angiogenesis and tumor growth[145]. Hypoxia also aids in MDSC-driven metastasis by influencing the seeding of MDSCs in the pre-metastatic niche through secretion of lysyl oxidase[146]. This process is a key component of in the development of metastatic lesions. This highlights the detrimental effects hypoxia can have in promoting these highly immunosuppressive, pro-tumorigenic cell types.

Table 2.1. Changes in immune cell phenotypes and secretome during hypoxia.

Cell Type	Changes in Function and Secretome	References
DCs	↓ Antigen uptake	110,111
	↓ CD1a, CD40, CD80, CD83, CD86, MHC class II	
Macrophages	↓ M1 phenotype	114–116
	↑ M2 phenotype	
	↓ IL-2	
	↑ IL-4, IL-10, IL-13	
B cells	↑ Development	121,122
	↑ IL-10	
T cells	↓ Cytotoxic function	128,131,135
	↑ Anergy	
	↑ Treg expansion	
	↑ Memory function	
	↑ Antibody production	
	↑ PD-1	
NK cells	↓ Cytolytic activity	138,139
	↑ VEGF	
MDSCs	↑ Differentiation and function	142,143,146
	↑ Recruitment to tumor site	
	↑ Extracellular remodeling	

2.4. Hypoxia and Immunogenic Cell Death

Since the initial descriptions of cell death dating back to the mid-19th century[147], researchers have abandoned the singular postulation that cell death is a uniform, regulated process that serves only in the maintenance of homeostatic conditions and goes undetected by the immune system. Instead, as new, unique forms of cell death have been identified and described in the literature, researchers have begun to delve deeper into the

associated biology of each type and in particular, the quantifiable functional features of them[148–150]. A good example of this paradigm shift in classification is the streamlined and well-studied process of apoptosis. Though apoptosis has historically been thought to be an "immune-quiet" form of cell death, more investigation in recent years has shown that apoptotic cells can in fact be detected by the immune system and elicit an antigen-specific adaptive immune response[34,37,151,152].

ICD is a form of cell death characterized by the chronic release of damage-associated molecular patterns (DAMPs) in the TME[37,153]. Hallmarks of classic ICD include the release of immunomodulatory molecules such as high mobility group box 1 (HMGB1) and adenosine triphosphate (ATP) and surface expression of calreticulin (CR). The quantity of these DAMPs in the TME correlates closely with the "immunogenicity" of a tumor and in turn, its ability to kill cells through *bona fide* ICD. Currently, the gold-standard strategy used to evaluate the ability of a specific stimulus to cause true ICD relies on vaccination assays[37,147]. In brief, cancer cells are exposed *in vitro* to the stimulus and dying cells are inoculated subcutaneously into the flank of immunocompetent mice, prior to tumor implantation with live cells of the same type. Mice are monitored for tumor growth and the number of mice that do not develop tumors is a direct reflection of the degree of immunogenicity of cell death induced by the chosen stimulus[147].

CR, a resident chaperon protein predominantly located in the endoplasmic reticulum (ER), is of particular interest when it comes to hypoxia. Han and colleagues recently showed that hypoxia induces cell surface exposure of CR in human and murine breast cancer cell lines, in an ER stress-dependent manner[95]. In line with these findings,

Olin and colleagues hypothesized that reducing oxygen tension when culturing tumor cells would increase the efficacy of tumor cell lysate vaccines[154]. Indeed, upon vaccinating mice bearing orthotopic glioma and breast carcinoma with lysates cultured in 5% O_2 (as opposed to the regular level of 20%), mice survived significantly longer, displayed enhanced antigen-specific T cell activation and increased cross-presentation of exogenous antigens. To our knowledge, this is the first paper to eloquently demonstrate the use of tissue culture oxygen levels as an "immunologic switch" to dictate the cellular and humoral immune responses elicited by tumor cell lysates[154]. As a follow-up to their initial studies, Olin et. al. further investigated the effects of physiological oxygen levels in the development of tumor vaccines, this time assessing DCs as a viable vaccination platform. They showed that gene expression patterns in primary glioma cultures established at 5% O_2 more closely resembled patient tumors *in situ* and known immunogenic antigens were more highly expressed. Furthermore, DCs treated with tumor lysates generated from primary tumor cells cultured in 5% O_2 showed improved antigen-presentation capabilities and increased $CD8^+$ T cell tumoricidal activity[155]. In these novel reports, Olin and colleagues have inadvertently demonstrated that physiological oxygen levels induce ICD, as shown through the gold-standard vaccination assay.

Photodynamic therapy (PDT) has also been demonstrated to kill cancer cells through the manipulation of oxygen levels to generate ROS, which induces ER-stress-mediated anti-tumor immunity and even the killing of distant metastatic lesions[156–158]. Conversely, many studies have shown low levels of oxygen in the TME to be a deterrent to efficacious outcomes with PDT[159,160]. In an effort to switch the effects of a hypoxic

TME on PDT, Chen and colleagues developed a hybrid protein oxygen nanocarrier with chlorine e6 (a photosensitizer with anti-tumor activity) encapsulated (C@HPOC) for oxygen self-sufficient PDT. C@HPOC relieved tumor hypoxia, showed increased efficiency over PDT alone and increased infiltration of tumor-infiltrating $CD8^+$ T cells. Additionally, in 4T1 murine breast tumor cells, C@HPOC-mediated PDT successfully enhanced ICD through the increased exposure of CR as well as secretion of HMGB1 and ATP[161].

Hypoxia can interfere with a variety of homeostatic regulators within cells, including the UPR and autophagy. Autophagy is of particular interest as it contributes to the expression of ICD-associated damage-associated molecular patterns (DAMPs), such as CR[162,163]. The role of hypoxia in regulating the UPR and autophagy is quite controversial, with several reports indicating that hypoxia can inhibit or induce autophagy. Indeed, some reports find that hypoxia can induce autophagy in an mTOR-independent manner[164,165]. This supports the notion that hypoxia may potentiate ICD through autophagy-mediated release of DAMPs, DC maturation and the subsequent release of tumor-associated antigens[162]. On the other hand, some reports show that hypoxia prevents autophagy through inhibition of the mTOR pathway[166,167]. One study performed by Li et. al. demonstrates enhanced CR expression upon inhibition of late-stage autophagy[168]. It will be important for future studies to elucidate the effects of hypoxia on autophagy within the TME and identify potential immunostimulatory effects that can be exploited for use as immunotherapies.

While hypoxia is generally associated with worse prognostic outcomes, selective studies have also shown that oxygen deprived TMEs create the inflammatory setting conducive to cells dying via ICD. This finding, while not extensively studied in the literature, highlights the complexity of hypoxia-mediated changes in the TME and the importance of addressing the opposing pro- and anti-tumorigenic nature of hypoxia-driven pathways.

2.5. Hypoxia-Mediated Therapeutic Resistance

As seen with chemotherapy, resistance to immunotherapy can arise in many forms of cancer. Primary resistance can be seen in patients that do not respond to treatment, indicating the inability to generate a robust anti-tumor immune response. However, even when patients respond to therapy, acquired resistance can occur, in which patients relapse after a period of tumor regression. Both primary and acquired resistance can occur as a result of tumor cell intrinsic and extrinsic factors, as described by Sharma et. al.[169] Examples of tumor cell intrinsic factors include the ability of some cancer cells to alter pathways involved in antigen presentation, thereby preventing the initial priming of an anti-tumor response. The most straightforward example of tumor cell extrinsic factors comes in the form of immunosuppressive cells within the TME, including Tregs and MDSCs, which were discussed previously. In this section, we will discuss the role of hypoxia in mediating both primary and acquired forms of resistance to cancer immunotherapy, which can be either intrinsic or extrinsic to the cancer cells.

2.5.1. Hypoxia-mediated primary resistance. As described above, one of the most prominent mechanisms of primary resistance to immunotherapy is the alteration of

antigen presentation pathways. Indeed, downregulation of MHC class I (MHC-I) expression and other antigen presentation machinery is a common strategy developed by malignant cells to avoid detection by the immune system[170–172]. Several reports have demonstrated how hypoxia can mediate the downregulation of MHC-I in malignant cells[173–175]. In one such report, Marjit and colleagues show that the combination of hypoxia and glucose deprivation prevents interferon gamma (IFNγ)-mediated upregulation of MHC-I in B16F10 and TC1 murine cancer cells[176]. This is a result of disrupted IFNγ-mediated phosphorylation of signal transducer and activator of transcription 1 (STAT1), thereby preventing the transcription of its target molecules, including MHC-I and transporter associated with antigen processing 1 (TAP1). Furthermore, PI3K was highly activated under hypoxic/glucose-deprived conditions, and inhibition of PI3K using small molecule inhibitors restored antigen presentation and $CD8^+$ T cell recognition of both B16F10 and TC1 cell lines[176]. Similar studies have demonstrated how hypoxia causes the downregulation of MHC-I, TAP1/2 and LMP7 in human renal carcinoma cells in a HIF-dependent manner[173]. Another well-known mechanism of primary resistance to immunotherapy is the upregulation of immune checkpoint molecules on tumor cells. One such immunosuppressive molecule, programmed death-ligand 1 (PD-L1), binds to the inhibitory programmed death 1 (PD-1) receptor on T cells and inhibits their activation and cytotoxic functions[177]. Interestingly, PD-L1 is now considered to be a target gene of HIF-1α and HIF-2α, indicating a crucial role of intratumoral hypoxia in the regulation of this immunosuppressive ligand[178–181]. One study demonstrated that PD-L1 levels decreased in 786-O human renal carcinoma

cells upon HIF-2α siRNA knockdown. Furthermore, PD-L1 expression was highly upregulated in cells with HIF-2α overexpression[182]. This observation, however, is not limited to cancer cells within the TME. A study spearheaded by Noman et. al. found that hypoxia significantly increases PD-L1 expression on MDSCs, macrophages, DCs and tumor cells in the TME[179]. This upregulation was shown to be dependent on HIF-1α, but not HIF-2α[179]. The discrepancies between studies indicate that the roles of HIF-1α and HIF-2α in mediating PD-L1 expression may depend on the cell type and type/location of the tumor. Future research should focus on delineating the role of these transcription factors in regulating PD-L1 expression in different tumor models. Another immune checkpoint molecule, cytotoxic T-lymphocyte-associated protein 4 (CTLA-4), is expressed on activated T cells and inhibits T cell activation when bound to its ligand, CD86, on antigen-presenting cells (APCs) such as DCs[183,184]. Similar to PD-L1, hypoxia has been shown to upregulate the expression of CD86 on DCs in a HIF-1α-dependent manner[185]. As mentioned previously, it is well known that hypoxia can shift the metabolic state within a tumor. Several reports have shown that cancer cells can adapt their metabolism to thrive under hypoxic conditions, allowing cancer cells to metabolically outcompete tumor-infiltrating T cells for glucose, resulting in the inhibition of T cell activity and increased cancer progression[186,187]. Indeed, the metabolic stress in the TME can negatively impact the immune functions of several immune cells in the tumor, including T cells, macrophages and MDSCs[97]. These studies imply that the HIF transcription factors may be suitable therapeutic targets for preventing

immunosuppression in the TME, a concept that will be further discussed later in this review.

2.5.2. Hypoxia-mediated acquired resistance. Resistance to immunotherapy can still arise in patients that briefly respond to therapy. This form of acquired resistance can often be attributed to tumor heterogeneity. In the case of immunotherapy, response against specific antigens exerts selective pressure towards antigen-loss cancer cells over time, a concept termed antigen escape[188]. This phenomenon has been observed in patients with triple-negative breast cancer (TNBC) during neoadjuvant chemotherapy (NAC), in which TNBC persisted after treatment in half of the patients. Upon further analysis using single-cell DNA and RNA sequencing, the data indicated that the resistant clones were pre-existing and adaptively selected by NAC[189]. Similar findings were seen in patients with stage IV melanoma treated with adoptive T-cell transfer[190], and even in murine models harboring B16 melanoma tumors[191]. As with other forms of resistance, there is accumulating evidence that hypoxia can potentiate intratumoral heterogeneity. The expression of genes involved in mismatch repair and homologous recombination are downregulated under hypoxic conditions[192–194]. This, in turn, can drive genomic instability and mutagenesis which can increase the probability of creating resistant clones[195–197]. Aside from generating resistant clones in the primary tumor, genomic instability can also result in the formation of metastasis. HIF-1α is heavily associated with metastasis formation and has been shown to drive several steps of metastasis, including epithelial-mesenchymal transition (EMT), invasion and extravasation[198]. One report investigating the invasion and metastasis of esophageal carcinoma Eca109 cells shows

that HIF-1α inhibits the tumor suppressor E-cadherin and upregulates the expression of matrix metalloproteinase-2 (MMP-2), a protein involved in enabling the migration of cells from the primary tumor to sites of metastasis[199]. Another, similar study performed by Zhao et. al. finds that the actin-binding protein LIM and SH3 domain protein 1 (LASP1) is upregulated by HIF-1α and is critical for metastasis formation of several human pancreatic cancer cell lines[199]. Angiogenesis is also essential for the dissemination and establishment of tumor metastases, since the ability of metastatic clusters to access blood vessels allows for their migration[200,201]. One of the key roles of HIF-1α includes its regulation of angiogenic factors such as vascular endothelial growth factor (VEGF). HIF-1α has been shown to drive VEGF-mediated angiogenesis within the TME in a variety of cancers, including ovarian, pancreatic and breast cancers[202–205]. Furthermore, HIF-1α-mediated proangiogenic signaling is not limited to cancer cells, and can occur in other cell types within the TME, including cancer-associated fibroblasts (CAFs)[206].

Based on the studies highlighted in this section, hypoxia and HIF transcription factors heavily contribute to different forms of resistance to immunotherapy (Figure 2.4). This is in line with studies that correlate high HIF expression with poor prognostic outcomes in several cancers[207–209]. Altogether, selective targeting of HIF in tumors is an attractive therapeutic approach that may bolster immunotherapeutic agents and prevent hypoxia-mediated resistance to immunotherapy.

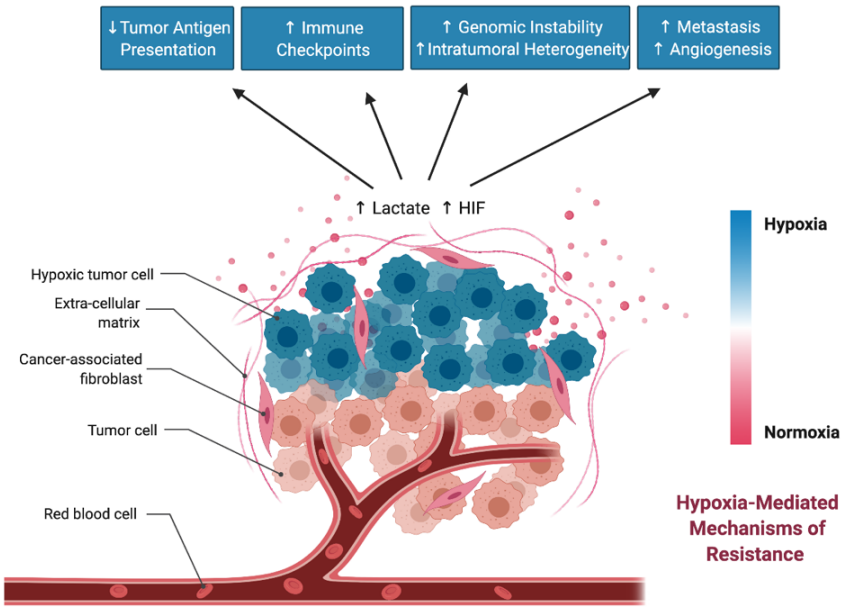

Fig. 2.4. Hypoxia-mediated changes in the TME that can drive resistance to immunotherapy. *Created using BioRender.com.

2.6. Hypoxia-Targeted Immunotherapies

2.6.1. Strategies for targeting hypoxia-induced pathways. The concept of targeting hypoxia-induced pathways as a cancer therapy is well-established [210–214]. Indeed, several candidates for HIF inhibitors are currently being tested in phase I and phase II clinical trials as cancer therapeutics[215]. Most hypoxia-targeting therapies however, are focused on disrupting metabolism and angiogenesis in the tumor to suppress tumor progression and the formation of metastasis[216,217]. Unfortunately, HIF inhibitors have poor selectivity, and so therapies often involve inhibition of downstream pathways or the use of hypoxia-activated prodrugs. In this section of the review, we will discuss the potential of targeting hypoxia-mediated pathways to potentiate cancer immunotherapy. As discussed previously, hypoxia has been shown to mediate many forms of resistance to

immunotherapy. This provides good rationale for combinatorial approaches for immunotherapy and inhibition of HIF pathways.

Hypoxia can play an important role in the regulation of immunosuppressive molecules and the activation of immunosuppressive cells such as Tregs and MDSCs. Therefore, reducing hypoxia in the tumor may prevent suppression of an anti-tumor immune response. Indeed, a few promising pre-clinical studies support the potential for combinatorial therapies involving immunotherapy and hypoxia-based therapies. One such study includes the use of the hypoxia-activated prodrug, TH-302. This study demonstrates that TH-302 reduces hypoxia in a murine prostate tumor model, and can cure up to 80% of tumor-bearing mice when combined with immune checkpoint inhibitors[215]. Furthermore, the combination reduced MDSC density in the tumor by 50%[215]. Another example published in Nature Communications describes the HIF-1-mediated expression of ectoenzyme, ectonucleoside triphosphate diphosphohydrolase 2 (ENTPD2), which promotes the maintenance of MDSCs in a murine hepatocellular carcinoma model[215]. The combination of ENTPD2 inhibitors and immune checkpoint inhibitors significantly increased the infiltration of T cells into the tumor and prolonged survival of tumor-bearing mice, when compared to using immune checkpoint inhibitors alone[215]. Another group reduced intratumoral hypoxia using the type II diabetes drug, Metformin, and found that combination with PD-1 blockade improved anti-tumor T cell function and tumor clearance in B16 and MC38 murine tumor models[215].

Inhibition of HIF transcription factors can also be achieved by targeting the PI3K/AKT/mTOR pathways[218–220]. Molecular regulators of mTOR, such as Tuberous

sclerosis complex 2 (TSC2) have been implicated in HIF-1α. TSC2 knockouts resulted in increased HIF-1α accumulation and the upregulation of HIF-induced genes such as VEGF. Interestingly, the mTOR inhibitor, rapamycin, reduced HIF-1α levels in TSC2 knockouts, although only partially reducing VEGF levels[219]. Other studies have found that the PI3K/AKT/mTOR pathways play a role in the regulation of PD-L1 in several murine cancer models, including non-small cell lung cancer[221], colorectal cancer[222], pancreatic cancer[223] and breast cancer[224]. Furthermore, both rapamycin and the AKT inhibitor, MK-2206, inhibit the expression of PD-L1 in breast cancer cells[224], although it is unclear if this regulation occurs in a HIF-dependent manner. Other strategies include targeting factors downstream of HIF-1α, such as VEGF, to reduce immunosuppression and sensitize cells to immunotherapy[225]. One study in PNAS demonstrated that low doses of anti-VEGF2 antibody polarizes TAMs from their immunosuppressive M2 phenotype into an immunostimulatory M1 phenotype. This results in improved tumor infiltration of $CD8^+$ and $CD4^+$ T cells[226]

2.6.2. Considerations for targeting hypoxia-induced pathways. While targeting hypoxia-induced pathways in combination with immunotherapies is an attractive approach, it should be carefully considered, as some immunotherapies may benefit from the hypoxic conditions within the TME. Oncolytic viruses are gaining traction as a promising form of immunotherapy, with an FDA-approved oncolytic Herpes Simplex Virus-1 (HSV-1) already available as a first-line treatment for melanoma in North America. One study demonstrates that oncolytic HSV-1 replicates more efficiently in hypoxic tumors, and that oxygenation of subcutaneous tumors in mice results in reduced replication in the

tumor[227]. This study is corroborated by a similar finding in which hypoxic conditions promoted the replication of oncolytic HSV-1 in otherwise resistant breast cancer cells[228]. Interestingly, the effect of hypoxia on therapeutic efficacy with oncolytic virotherapy depends on the virus. For example, oncolytic adenovirus replication is hampered under hypoxic conditions, while oncolytic HSV-1 replication is enhanced under hypoxic conditions. Oncolytic Vaccinia virus demonstrates improved cytotoxicity in hypoxic cancer cells, but has no increase in transgene expression[229]. [229]. Some studies have also demonstrated that inhibition of the mTOR pathway can also be detrimental for immunotherapy. Rapamycin and other mTOR inhibitors may have immunosuppressive effects on a variety of immune cells. This includes reduced activation and antigen presentation by dendritic cells[230–232], reduced $CD8^+$ T cell infiltration into the tumor[233], and increased Treg expansion[234,235].

Therefore, pre-clinical data provides promising evidence for the potential of targeting hypoxia-induced pathways in combination with immunotherapy, however such combinations must be carefully considered. It is pertinent that future research focuses on the effects of targeting hypoxia when combined with different forms of immunotherapy. While there is potential for reducing hypoxia-mediated resistance to immunotherapy, some therapies may be hampered in oxygenated tumors, resulting in reduced therapeutic efficacy.

2.7. Conclusions

The TME is a complex network composed of immune cells, endothelial cells, fibroblasts, extracellular matrix and various signaling molecules. While scientific

literature and clinical studies predominantly address the immunosuppressive nature of hypoxia-driven pathways, they often fail to acknowledge the potential of the resultant inflammatory microenvironment to promote cells dying via *bona fide* ICD. In this review, we have objectively assessed the role of hypoxia in both pro- and anti-tumorigenic pathways and identified ways in which hypoxia-mediated therapeutic resistance may be overcome. Furthermore, we have highlighted current strategies for targeting hypoxia with immunotherapy treatments. Development of future immunotherapy platforms targeting hypoxia signaling pathways should take into consideration not only the immunosuppressive nature of hypoxia, but also the potential to increase ICD through hypoxia-mediated inflammation.

Acknowledgments

Research in the Mossman lab is funded by the Canadian Cancer Society Research Institute, the Canadian Institutes for Health Research and the Terry Fox Research Institute. AV holds a Vanier Canada Graduate Scholarship while NE-S holds an Ontario Graduate Scholarship.

Author Contributions

AV and NE-S conceived of and wrote the review. KM reviewed and edited the review.

Conflict of Interest

The authors declare no conflict of interest.

References

1. Multhoff, G.; Vaupel, P. Hypoxia compromises anti-cancer immune responses. In *Advances in Experimental Medicine and Biology*; Springer: Berlin, Germany, 2020; Volume 1232, pp. 131–143.
2. Krock, B.L.; Skuli, N.; Simon, M.C. Hypoxia-Induced Angiogenesis: Good and Evil. *Genes Cancer* **2011**, *2*, 1117–1133.
3. Chen, L.; Endler, A.; Shibasaki, F. Hypoxia and angiogenesis: Regulation of hypoxia-inducible factors via novel binding factors. *Exp. Mol. Med.* **2009**, *41*, 849–857.
4. Engel, C.; Brügmann, G.; Lambing, S.; Mühlenbeck, L.H.; Marx, S.; Hagen, C.; Horv, D.; Goldeck, M.; Ludwig, J.; Herzne, A.M.; et al. RIG-I Resists Hypoxia-Induced Immunosuppression and Dedifferentiation. *Cancer Immunol. Res.* **2017**, *5*, 455–467.
5. Zhao, T.; Ren, H.; Jia, L.; Chen, J.; Xin, W.; Yan, F.; Li, J.; Wang, X.; Gao, S.; Qian, D.; et al. Inhibition of HIF-1α by PX-478 enhances the anti-tumor effect of gemcitabine by inducing immunogenic cell death in pancreatic ductal adenocarcinoma. *Oncotarget* **2015**, *6*, 2250–2262.
6. Hatfield, S.; Veszeleiova, K.; Steingold, J.; Sethuraman, J.; Sitkovsky, M. Mechanistic justifications of systemic therapeutic oxygenation of tumors to weaken the hypoxia inducible factor 1α-mediated immunosuppression. *Adv. Exp. Med. Biol.* **2019**, *1136*, 113–121.
7. Han, Y.K.; Park, G.Y.; Bae, M.J.I.; Kim, J.S.; Jo, W.S.; Lee, C.G. Hypoxia induces immunogenic cell death of cancer cells by enhancing the exposure of cell

surface calreticulin in an endoplasmic reticulum stress-dependent manner. *Oncol. Lett.* **2019**, *18*, 6269–6274.

8. Tamura, R.; Tanaka, T.; Akasaki, Y.; Murayama, Y.; Yoshida, K.; Sasaki, H. The role of vascular endothelial growth factor in the hypoxic and immunosuppressive tumor microenvironment: Perspectives for therapeutic implications. *Med. Oncol.* **2020**, *37*, 2.
9. Sormendi, S.; Wielockx, B. Hypoxia pathway proteins as central mediators of metabolism in the tumor cells and their microenvironment. *Front. Immunol.* **2018**, *9*, 40.
10. Koh, M.Y.; Powis, G. Passing the baton: The HIF switch. *Trends Biochem. Sci.* **2012**, *37*, 364–372.
11. Holmquist-Mengelbier, L.; Fredlund, E.; Löfstedt, T.; Noguera, R.; Navarro, S.; Nilsson, H.; Pietras, A.; Vallon-Christersson, J.; Borg, Å.; Gradin, K.; et al. Recruitment of HIF-1α and HIF-2α to common target genes is differentially regulated in neuroblastoma: HIF-2α promotes an aggressive phenotype. *Cancer Cell* **2006**, *10*, 413–423.
12. Peng, J.; Zhang, L.; Drysdale, L.; Fong, G.H. The transcription factor EPAS-1/hypoxia-inducible factor 2α plays an important role in vascular remodeling. *Proc. Natl. Acad. Sci. USA* **2000**, *97*, 8386–8391.
13. Bangoura, G.; Yang, L.Y.; Huang, G.W.; Wang, W. Expression of HIF-2α/EPAS1 in hepatocellular carcinoma. *World J. Gastroenterol.* **2004**, *10*, 525–530.

14. Shestov, A.A.; Liu, X.; Ser, Z.; Cluntun, A.A.; Hung, Y.P.; Huang, L.; Kim, D.; Le, A.; Yellen, G.; Albeck, J.G.; et al. Quantitative determinants of aerobic glycolysis identify flux through the enzyme GAPDH as a limiting step. *Elife* **2014**, *3*, 1–18.
15. DeBerardinis, R.J.; Lum, J.J.; Hatzivassiliou, G.; Thompson, C.B. The Biology of Cancer: Metabolic Reprogramming Fuels Cell Growth and Proliferation. *Cell Metab.* **2008**, *7*, 11–20.
16. Levine, A.J.; Puzio-Kuter, A.M. The control of the metabolic switch in cancers by oncogenes and tumor suppressor genes. *Science* **2010**, *330*, 1340–1344.
17. Cairns, R.A.; Harris, I.S.; Mak, T.W. Regulation of cancer cell metabolism. *Nat. Rev. Cancer* **2011**, *11*, 85–95.
18. Koppenol, W.H.; Bounds, P.L.; Dang, C.V. Otto Warburg's contributions to current concepts of cancer metabolism. *Nat. Rev. Cancer* **2011**, *11*, 325–337.
19. Wielockx, B.; Meneses, A. PHD2: From hypoxia regulation to disease progression. *Hypoxia* **2016**, 53.
20. Selfridge, A.C.; Cavadas, M.A.S.; Scholz, C.C.; Campbell, E.L.; Welch, L.C.; Lecuona, E.; Colgan, S.P.; Barrett, K.E.; Sporn, P.H.S.; Sznajder, J.I.; et al. Hypercapnia suppresses the HIF-dependent adaptive response to hypoxia. *J. Biol. Chem.* **2016**, *291*, 11800–11808.
21. Pezzuto, A.; Carico, E. Role of HIF-1 in Cancer Progression: Novel Insights. A Review. *Curr. Mol. Med.* **2018**, *18*, 343–351.

22. Elia, A.R.; Cappello, P.; Puppo, M.; Fraone, T.; Vanni, C.; Eva, A.; Musso, T.; Novelli, F.; Varesio, L.; Giovarelli, M. Human dendritic cells differentiated in hypoxia down-modulate antigen uptake and change their chemokine expression profile. *J. Leukoc. Biol.* **2008**, *84*, 1472–1482.

23. Mancino, A.; Schioppa, T.; Larghi, P.; Pasqualini, F.; Nebuloni, M.; Chen, I.H.; Sozzani, S.; Austyn, J.M.; Mantovani, A.; Sica, A. Divergent effects of hypoxia on dendritic cell functions. *Blood* **2008**, *112*, 3723–3734.

24. Galluzzi, L.; Buqué, A.; Kepp, O.; Zitvogel, L.; Kroemer, G. Immunogenic cell death in cancer and infectious disease. *Nat. Rev. Immunol.* **2017**, *17*, 97–111.

25. Ostuni, R.; Kratochvill, F.; Murray, P.J.; Natoli, G. Macrophages and cancer: From mechanisms to therapeutic implications. *Trends Immunol.* **2015**, *36*, 229–239.

26. Sica, A.; Mantovani, A. Macrophage plasticity and polarization: In vivo veritas. *J. Clin. Investig.* **2012**, *122*, 787–795.

27. Henze, A.T.; Mazzone, M. The impact of hypoxia on tumor-associated macrophages. *J. Clin. Investig.* **2016**, *126*, 3672–3679.

28. Hughes, R.; Qian, B.Z.; Rowan, C.; Muthana, M.; Keklikoglou, I.; Olson, O.C.; Tazzyman, S.; Danson, S.; Addison, C.; Clemons, M.; et al. Perivascular M2 macrophages stimulate tumor relapse after chemotherapy. *Cancer Res.* **2015**, *75*, 3479–3491.

29. Ohno, S.; Ohno, Y.; Suzuki, N.; Kamei, T.; Koike, K.; Inagawa, H.; Kohchi, C.; Soma, G.I.; Inoue, M. Correlation of histological localization of tumor-associated

macrophages with clinicopathological features in endometrial cancer. *Anticancer Res.* **2004**, *24*, 3335–3342.

30. Hoffman, W.; Lakkis, F.G.; Chalasani, G. B cells, antibodies, and more. *Clin. J. Am. Soc. Nephrol.* **2016**, *11*, 137–154.
31. Mauri, C.; Bosma, A. Immune Regulatory Function of B Cells. *Annu. Rev. Immunol.* **2012**, *30*, 221–241.
32. Krzywinska, E.; Stockmann, C. Hypoxia, metabolism and immune cell function. *Biomedicines* **2018**, *6*, 56.
33. Kojima, H.; Gu, H.; Nomura, S.; Caldwell, C.C.; Kobata, T.; Carmeliet, P.; Semenza, G.L.; Sitkovsky, M.V. Abnormal B lymphocyte development and autoimmunity in hypoxia-inducible factor 1α-deficient chimeric mice. *Proc. Natl. Acad. Sci. USA* **2002**, *99*, 2170–2174.
34. Goda, N.; Ryan, H.E.; Khadivi, B.; McNulty, W.; Rickert, R.C.; Johnson, R.S. Hypoxia-Inducible Factor 1 Is Essential for Cell Cycle Arrest during Hypoxia. *Mol. Cell. Biol.* **2003**, *23*, 359–369.
35. Meng, X.; Grötsch, B.; Luo, Y.; Knaup, K.X.; Wiesener, M.S.; Chen, X.X.; Jantsch, J.; Fillatreau, S.; Schett, G.; Bozec, A. Hypoxia-inducible factor-1α is a critical transcription factor for IL-10-producing B cells in autoimmune disease. *Nat. Commun.* **2018**, *9*.
36. Zhang, Y.; Garcia-Ibanez, L.; Toellner, K.M. Regulation of germinal center B-cell differentiation. *Immunol. Rev.* **2016**, *270*, 8–19.

37. Jellusova, J.; Cato, M.H.; Apgar, J.R.; Ramezani-Rad, P.; Leung, C.R.; Chen, C.; Richardson, A.D.; Conner, E.M.; Benschop, R.J.; Woodgett, J.R.; et al. Gsk3 is a metabolic checkpoint regulator in B cells. *Nat. Immunol.* **2017**, *18*, 303–312.

38. Caro-Maldonado, A.; Wang, R.; Nichols, A.G.; Kuraoka, M.; Milasta, S.; Sun, L.D.; Gavin, A.L.; Abel, E.D.; Kelsoe, G.; Green, D.R.; et al. Metabolic Reprogramming Is Required for Antibody Production That Is Suppressed in Anergic but Exaggerated in Chronically BAFF-Exposed B Cells. *J. Immunol.* **2014**, *192*, 3626–3636.

39. Griss, J.; Bauer, W.; Wagner, C.; Simon, M.; Chen, M.; Grabmeier-Pfistershammer, K.; Maurer-Granofszky, M.; Roka, F.; Penz, T.; Bock, C.; et al. B cells sustain inflammation and predict response to immune checkpoint blockade in human melanoma. *Nat. Commun.* **2019**, *10*.

40. Masopust, D.; Schenkel, J.M. The integration of T cell migration, differentiation and function. *Nat. Rev. Immunol.* **2013**, *13*, 309–320.

41. Cho, S.H.; Raybuck, A.L.; Blagih, J.; Kemboi, E.; Haase, V.H.; Jones, R.G.; Boothby, M.R. Hypoxia-inducible factors in CD4+ T cells promote metabolism, switch cytokine secretion, and T cell help in humoral immunity. *Proc. Natl. Acad. Sci. USA* **2019**, *116*, 8975–8984.

42. Tao, J.H.; Barbi, J.; Pan, F. Hypoxia-inducible factors in T lymphocyte differentiation and function. A review in the theme: Cellular responses to hypoxia. *Am. J. Physiol. - Cell Physiol.* **2015**, *309*, C580–C589.

43. Waickman, A.T.; Powell, J.D. mTOR, metabolism, and the regulation of T-cell differentiation and function. *Immunol. Rev.* **2012**, *249*, 43–58.

44. Frauwirth, K.A.; Thompson, C.B. Regulation of T Lymphocyte Metabolism. *J. Immunol.* **2004**, *172*, 4661–4665.

45. Chen, J.L.Y.; Lucas, J.E.; Schroeder, T.; Mori, S.; Wu, J.; Nevins, J.; Dewhirst, M.; West, M.; Chi, J.T. The genomic analysis of lactic acidosis and acidosis response in human cancers. *PLoS Genet.* **2008**, *4*, e100293.

46. Pauken, K.E.; Wherry, E.J. Overcoming T cell exhaustion in infection and cancer. *Trends Immunol.* **2015**, *36*, 265–276.

47. Caldwell, C.C.; Kojima, H.; Lukashev, D.; Armstrong, J.; Farber, M.; Apasov, S.G.; Sitkovsky, M.V. Differential Effects of Physiologically Relevant Hypoxic Conditions on T Lymphocyte Development and Effector Functions. *J. Immunol.* **2001**, *167*, 6140–6149.

48. Sukumar, M.; Liu, J.; Ji, Y.; Subramanian, M.; Crompton, J.G.; Yu, Z.; Roychoudhuri, R.; Palmer, D.C.; Muranski, P.; Karoly, E.D.; et al. Inhibiting glycolytic metabolism enhances CD8+ T cell memory and antitumor function. *J. Clin. Investig.* **2013**, *123*, 4479–4488.

49. Parodi, M.; Raggi, F.; Cangelosi, D.; Manzini, C.; Balsamo, M.; Blengio, F.; Eva, A.; Varesio, L.; Pietra, G.; Moretta, L.; et al. Hypoxia modifies the transcriptome of human NK cells, modulates their immunoregulatory profile, and influences NK cell subset migration. *Front. Immunol.* **2018**, *9*.

50. Balsamo, M.; Manzini, C.; Pietra, G.; Raggi, F.; Blengio, F.; Mingari, M.C.; Varesio, L.; Moretta, L.; Bosco, M.C.; Vitale, M. Hypoxia downregulates the expression of activating receptors involved in NK-cell-mediated target cell killing without affecting ADCC. *Eur. J. Immunol.* **2013**, *43*, 2756–2764.

51. Krzywinska, E.; Kantari-Mimoun, C.; Kerdiles, Y.; Sobecki, M.; Isagawa, T.; Gotthardt, D.; Castells, M.; Haubold, J.; Millien, C.; Viel, T.; et al. Loss of HIF-1α in natural killer cells inhibits tumour growth by stimulating non-productive angiogenesis. *Nat. Commun.* **2017**, *8*.

52. Cluff, E.R.; Nolan, J.; Collins, C.; Varadaraj, A.; Rajasekaran, N. Hypoxia-Inducible Factor-1α is upregulated in Natural Killer cells by Interleukin-2 and hypoxia via PI3K/mTOR signaling pathway. *J. Immunol.* **2019**, *202*, 194.37.

53. Gabrilovich, D.I.; Nagaraj, S. Myeloid-derived suppressor cells as regulators of the immune system. *Nat. Rev. Immunol.* **2009**, *9*, 162–174.

54. Murdoch, C.; Muthana, M.; Coffelt, S.B.; Lewis, C.E. The role of myeloid cells in the promotion of tumour angiogenesis. *Nat. Rev. Cancer* **2008**, *8*, 618–631.

55. Corzo, C.A.; Condamine, T.; Lu, L.; Cotter, M.J.; Youn, J.I.; Cheng, P.; Cho, H.I.; Celis, E.; Quiceno, D.G.; Padhya, T.; et al. HIF-1α regulates function and differentiation of myeloid-derived suppressor cells in the tumor microenvironment. *J. Exp. Med.* **2010**, *207*, 2439–2453.

56. Ye, X.Z.; Yu, S.C.; Bian, X.W. Contribution of myeloid-derived suppressor cells to tumor-induced immune suppression, angiogenesis, invasion and metastasis. *J. Genet. Genomics* **2010**, *37*, 423–430.

57. Chiu, D.K.C.; Tse, A.P.W.; Xu, I.M.J.; Di Cui, J.; Lai, R.K.H.; Li, L.L.; Koh, H.Y.; Tsang, F.H.C.; Wei, L.L.; Wong, C.M.; et al. Hypoxia inducible factor HIF-1 promotes myeloid-derived suppressor cells accumulation through ENTPD2/CD39L1 in hepatocellular carcinoma. *Nat. Commun.* **2017**, *8*, 1–12.

58. Chiu, D.K.C.; Xu, I.M.J.; Lai, R.K.H.; Tse, A.P.W.; Wei, L.L.; Koh, H.Y.; Li, L.L.; Lee, D.; Lo, R.C.L.; Wong, C.M.; et al. Hypoxia induces myeloid-derived suppressor cell recruitment to hepatocellular carcinoma through chemokine (C-C motif) ligand 26. *Hepatology* **2016**, *64*, 797–813.

59. Erler, J.T.; Bennewith, K.L.; Nicolau, M.; Dornhöfer, N.; Kong, C.; Le, Q.T.; Chi, J.T.A.; Jeffrey, S.S.; Giaccia, A.J. Lysyl oxidase is essential for hypoxia-induced metastasis. *Nature* **2006**, *440*, 1222–1226.

60. Kepp, O.; Tartour, E.; Vitale, I.; Vacchelli, E.; Adjemian, S.; Agostinis, P.; Apetoh, L.; Aranda, F.; Barnaba, V.; Bloy, N.; et al. Consensus guidelines for the detection of immunogenic cell death. *Oncoimmunology* **2014**, *3*, e955691.

61. Galluzzi, L.; Vitale, I.; Abrams, J.M.; Alnemri, E.S.; Baehrecke, E.H.; Blagosklonny, M.V.; Dawson, T.M.; Dawson, V.L.; El-Deiry, W.S.; Fulda, S.; et al. Molecular definitions of cell death subroutines: Recommendations of the Nomenclature Committee on Cell Death 2012. *Cell Death Differ.* **2012**, *19*, 107–120.

62. Klionsky, D.J.; Abeliovich, H.; Agostinis, P.; Agrawal, D.K.; Aliev, G.; Askew, D.S.; Baba, M.; Baehrecke, E.H.; Bahr, B.A.; Ballabio, A.; et al. Guidelines for

the use and interpretation of assays for monitoring autophagy in higher eukaryotes. *Autophagy* **2008**, *4*, 151–175.

63. Tait, S.W.G.; Green, D.R. Mitochondria and cell death: Outer membrane permeabilization and beyond. *Nat. Rev. Mol. Cell Biol.* **2010**, *11*, 621–632.
64. Kroemer, G.; Galluzzi, L.; Kepp, O.; Zitvogel, L. Immunogenic Cell Death in Cancer Therapy. *Annu. Rev. Immunol.* **2013**, *31*, 51–72.
65. Krysko, D.V.; Garg, A.D.; Kaczmarek, A.; Krysko, O.; Agostinis, P.; Vandenabeele, P. Immunogenic cell death and DAMPs in cancer therapy. *Nat. Rev. Cancer* **2012**, *12*, 860–875.
66. Casares, N.; Pequignot, M.O.; Tesniere, A.; Ghiringhelli, F.; Roux, S.; Chaput, N.; Schmitt, E.; Hamai, A.; Hervas-Stubbs, S.; Obeid, M.; et al. Caspase-dependent immunogenicity of doxorubicin-induced tumor cell death. *J. Exp. Med.* **2005**, *202*, 1691–1701.
67. Cirone, M.; Renzo, L.D.; Lotti, L.V.; Conte, V.; Trivedi, P.; Santarelli, R.; Gonnella, R.; Frati, L.; Faggioni, A. Activation of dendritic cells by tumor cell death. *Oncoimmunology* **2012**, *1*, 1218–1219.
68. Zhou, J.; Wang, G.; Chen, Y.; Wang, H.; Hua, Y.; Cai, Z. Immunogenic cell death in cancer therapy: Present and emerging inducers. *J. Cell. Mol. Med.* **2019**, *23*, 4854–4865.
69. Olin, M.R.; Andersen, B.M.; Zellmer, D.M.; Grogan, P.T.; Popescu, F.E.; Xiong, Z.; Forster, C.L.; Seiler, C.; SantaCruz, K.S.; Chen, W.; et al. Superior efficacy of

tumor cell vaccines grown in physiologic oxygen. *Clin. Cancer Res.* **2010**, *16*, 4800–4808.

70. Olin, M.R.; Andersen, B.M.; Litterman, A.J.; Grogan, P.T.; Sarver, A.L.; Robertson, P.T.; Liang, X.; Chen, W.; Parney, I.F.; Hunt, M.A.; et al. Oxygen is a master regulator of the immunogenicity of primary human glioma cells. *Cancer Res.* **2011**, *71*, 6583–6589.
71. Garg, A.D.; Krysko, D.V.; Verfaillie, T.; Kaczmarek, A.; Ferreira, G.B.; Marysael, T.; Rubio, N.; Firczuk, M.; Mathieu, C.; Roebroek, A.J.M.; et al. A novel pathway combining calreticulin exposure and ATP secretion in immunogenic cancer cell death. *EMBO J.* **2012**, *31*, 1062–1079.
72. Garg, A.D.; Krysko, D.V.; Vandenabeele, P.; Agostinis, P. Hypericin-based photodynamic therapy induces surface exposure of damage-associated molecular patterns like HSP70 and calreticulin. *Cancer Immunol. Immunother.* **2012**, *61*, 215–221.
73. Galluzzi, L.; Kepp, O.; Kroemer, G. Enlightening the impact of immunogenic cell death in photodynamic cancer therapy. *EMBO J.* **2012**, *31*, 1055–1057.
74. Lucky, S.S.; Soo, K.C.; Zhang, Y. Nanoparticles in photodynamic therapy. *Chem. Rev.* **2015**, *115*, 1990–2042.
75. Chouaib, S.; Noman, M.Z.; Kosmatopoulos, K.; Curran, M.A. Hypoxic stress: Obstacles and opportunities for innovative immunotherapy of cancer. *Oncogene* **2017**, *36*, 439–445.

76. Chen, Z.; Liu, L.; Liang, R.; Luo, Z.; He, H.; Wu, Z.; Tian, H.; Zheng, M.; Ma, Y.; Cai, L. Bioinspired hybrid protein oxygen nanocarrier amplified photodynamic therapy for eliciting anti-tumor immunity and abscopal effect. *ACS Nano* **2018**, *12*, 8633–8645.

77. Hou, W.; Zhang, Q.; Yan, Z.; Chen, R.; Zeh, H.J.; Kang, R.; Lotze, M.T.; Tang, D. Strange attractors: DAMPs and autophagy link tumor cell death and immunity. *Cell Death Dis.* **2013**, *4*, e966.

78. Garg, A.D.; Dudek, A.M.; Agostinis, P. Calreticulin surface exposure is abrogated in cells lacking, chaperone-mediated autophagy-essential gene, LAMP2A. *Cell Death Dis.* **2013**, *4*, e826.

79. Papandreou, I.; Lim, A.L.; Laderoute, K.; Denko, N.C. Hypoxia signals autophagy in tumor cells via AMPK activity, independent of HIF-1, BNIP3, and BNIP3L. *Cell Death Differ.* **2008**, *15*, 1572–1581.

80. Bellot, G.; Garcia-Medina, R.; Gounon, P.; Chiche, J.; Roux, D.; Pouyssegur, J.; Mazure, N.M. Hypoxia-Induced Autophagy Is Mediated through Hypoxia-Inducible Factor Induction of BNIP3 and BNIP3L via Their BH3 Domains. *Mol. Cell. Biol.* **2009**, *29*, 2570–2581.

81. Li, Y.; Wang, Y.; Kim, E.; Beemiller, P.; Wang, C.Y.; Swanson, J.; You, M.; Guan, K.L. Bnip3 mediates the hypoxia-induced inhibition on mammalian target of rapamycin by interacting with Rheb. *J. Biol. Chem.* **2007**, *282*, 35803–35813.

82. Cam, H.; Easton, J.B.; High, A.; Houghton, P.J. mTORC1 signaling under hypoxic conditions is controlled by atm-dependent phosphorylation of HIF-1α. *Mol. Cell* **2010**, *40*, 509–520.

83. Li, D.D.; Xie, B.; Wu, X.J.; Li, J.J.; Ding, Y.; Wen, X.Z.; Zhang, X.; Zhu, S.G.; Liu, W.; Zhang, X.S.; et al. Late-stage inhibition of autophagy enhances calreticulin surface exposure. *Oncotarget* **2016**, *7*, 80842–80854.

84. Sharma, P.; Hu-Lieskovan, S.; Wargo, J.A.; Ribas, A. Primary, Adaptive, and Acquired Resistance to Cancer Immunotherapy. *Cell* **2017**, *168*, 707–723.

85. Garrido, F.; Aptsiauri, N.; Doorduijn, E.M.; Garcia Lora, A.M.; van Hall, T. The urgent need to recover MHC class I in cancers for effective immunotherapy. *Curr. Opin. Immunol.* **2016**, *39*, 44–51.

86. Garrido, F.; Algarra, I. MHC antigens and tumor escape from immune surveillance. *Adv. Cancer Res.* **2001**, *83*, 117–158.

87. Seliger, B.; Cabrera, T.; Garrido, F.; Ferrone, S. HLA class I antigen abnormalities and immune escape by malignant cells. *Semin. Cancer Biol.* **2002**, *12*, 3–13.

88. Sethumadhavan, S.; Silva, M.; Philbrook, P.; Nguyen, T.; Hatfield, S.M.; Ohta, A.; Sitkovsky, M.V. Hypoxia and hypoxia-inducible factor (HIF) downregulate antigen-presenting MHC class I molecules limiting tumor cell recognition by T cells. *PLoS ONE* **2017**, *12*, e0187314.

89. Murthy, A.; Gerber, S.A.; Koch, C.J.; Lord, E.M. Intratumoral Hypoxia Reduces IFN-γ–Mediated Immunity and MHC Class I Induction in a Preclinical Tumor Model. *ImmunoHorizons* **2019**, *3*, 149–160.

90. Siemens, D.R.; Hu, N.; Sheikhi, A.K.; Chung, E.; Frederiksen, L.J.; Pross, H.; Graham, C.H. Hypoxia increases tumor cell shedding of MHC class I chain-related molecule: Role of nitric oxide. *Cancer Res.* **2008**, *68*, 4746–4753.

91. Marijt, K.A.; Sluijter, M.; Blijleven, L.; Tolmeijer, S.H.; Scheeren, F.A.; Van Der Burg, S.H.; Van Hall, T. Metabolic stress in cancer cells induces immune escape through a PI3K-dependent blockade of IFNγreceptor signaling. *J. Immunother. Cancer* **2019**, *7*, 152.

92. Qin, W.; Hu, L.; Zhang, X.; Jiang, S.; Li, J.; Zhang, Z.; Wang, X. The Diverse Function of PD-1/PD-L Pathway Beyond Cancer. *Front. Immunol.* **2019**, *10*, 152.

93. Tawadros, A.I.F.; Khalafalla, M.M.M. Expression of programmed death-ligand 1 and hypoxia-inducible factor-1α proteins in endometrial carcinoma. *J. Cancer Res. Ther.* **2018**, *14*, S1063–S1069.

94. Noman, M.Z.; Desantis, G.; Janji, B.; Hasmim, M.; Karray, S.; Dessen, P.; Bronte, V.; Chouaib, S. PD-L1 is a novel direct target of HIF-1α, and its blockade under hypoxia enhanced: MDSC-mediated T cell activation. *J. Exp. Med.* **2014**, *211*, 781–790.

95. Cubillos-Zapata, C.; Avendaño-Ortiz, J.; Hernandez-Jimenez, E.; Toledano, V.; Casas-Martin, J.; Varela-Serrano, A.; Torres, M.; Almendros, I.; Casitas, R.;

Fernández-Navarro, I.; et al. Hypoxia-induced PD-L1/PD-1 crosstalk impairs T-cell function in sleep apnoea. *Eur. Respir. J.* **2017**, *50*.

96. Jiang, X.; Wang, J.; Deng, X.; Xiong, F.; Ge, J.; Xiang, B.; Wu, X.; Ma, J.; Zhou, M.; Li, X.; et al. Role of the tumor microenvironment in PD-L1/PD-1-mediated tumor immune escape. *Mol. Cancer* **2019**, *18*, 1–17.
97. Messai, Y.; Gad, S.; Noman, M.Z.; Le Teuff, G.; Couve, S.; Janji, B.; Kammerer, S.F.; Rioux-Leclerc, N.; Hasmim, M.; Ferlicot, S.; et al. Renal Cell Carcinoma Programmed Death-ligand 1, a New Direct Target of Hypoxia-inducible Factor-2 Alpha, is Regulated by von Hippel–Lindau Gene Mutation Status. *Eur. Urol.* **2016**, *70*, 623–632.
98. Sansom, D.M. CD28, CTLA-4 and their ligands: Who does what and to whom? *Immunology* **2000**, *101*, 169–177.
99. Rowshanravan, B.; Halliday, N.; Sansom, D.M. CTLA-4: A moving target in immunotherapy. *Blood* **2018**, *131*, 58–67.
100. Köhler, T.; Reizis, B.; Johnson, R.S.; Weighardt, H.; Förster, I. Influence of hypoxia-inducible factor 1α on dendritic cell differentiation and migration. *Eur. J. Immunol.* **2012**, *42*, 1226–1236.
101. Ho, P.-C.; Bihuniak, J.D.; Macintyre, A.N.; Staron, M.; Liu, X.; Amezquita, R.; Tsui, Y.-C.; Cui, G.; Micevic, G.; Perales, J.C.; et al. Phosphoenolpyruvate Is a Metabolic Checkpoint of Anti-tumor T Cell Responses. *Cell* **2015**, *162*, 1217–1228.

102. Chang, C.-H.; Qiu, J.; Buck, M.D.; Noguchi, T.; Curtis, J.D.; Chen, Q.; Gindin, M.; Gubin, M.M.; van der Windt, G.J.; Tonc, E.; et al. Metabolic competition in the tumor microenvironment is a driver of cancer progression Graphical Abstract HHS Public Access. *Cell* **2015**, *162*, 1229–1241.

103. Vyas, M.; Müller, R.; Pogge von Strandmann, E. Antigen Loss Variants: Catching Hold of Escaping Foes. *Front. Immunol.* **2017**, *8*, 175.

104. Kim, C.; Gao, R.; Sei, E.; Brandt, R.; Hartman, J.; Hatschek, T.; Crosetto, N.; Foukakis, T.; Navin, N.E. Chemoresistance Evolution in Triple-Negative Breast Cancer Delineated by Single-Cell Sequencing. *Cell* **2018**, *173*, 879–893.e13.

105. Verdegaal, E.M.E.; de Miranda, N.F.C.C.; Visser, M.; Harryvan, T.; van Buuren, M.M.; Andersen, R.S.; Hadrup, S.R.; van der Minne, C.E.; Schotte, R.; Spits, H.; et al. Neoantigen landscape dynamics during human melanoma–T cell interactions. *Nature* **2016**, *536*, 91–95.

106. Sanchez-Perez, L.; Kottke, T.; Diaz, R.M.; Ahmed, A.; Thompson, J.; Chong, H.; Melcher, A.; Holmen, S.; Daniels, G.; Vile, R.G. Potent Selection of Antigen Loss Variants of B16 Melanoma following Inflammatory Killing of Melanocytes In vivo. *Cancer Res.* **2005**, *65*, 2009–2017.

107. Rodríguez-Jiménez, F.J.; Moreno-Manzano, V.; Lucas-Dominguez, R.; Sánchez-Puelles, J.-M. Hypoxia Causes Downregulation of Mismatch Repair System and Genomic Instability in Stem Cells. *Stem Cells* **2008**, *26*, 2052–2062.

108. Cowman, S.; Pizer, B.; See, V. Downregulation of both mismatch repair and non-homologous end-joining pathways in hypoxic brain tumour cell lines. *bioRxiv Cancer Biol.* **2020**.

109. Mihaylova, V.T.; Bindra, R.S.; Yuan, J.; Campisi, D.; Narayanan, L.; Jensen, R.; Giordano, F.; Johnson, R.S.; Rockwell, S.; Glazer, P.M. Decreased Expression of the DNA Mismatch Repair Gene Mlh1 under Hypoxic Stress in Mammalian Cells. *Mol. Cell. Biol.* **2003**, *23*, 3265–3273.

110. Kondo, A.; Safaei, R.; Mishima, M.; Niedner, H.; Lin, X.; Howell, S.B. Hypoxia-induced enrichment and mutagenesis of cells that have lost DNA mismatch repair. *Cancer Res.* **2001**, *61*, 7603–7607.

111. Luoto, K.R.; Kumareswaran, R.; Bristow, R.G. Tumor hypoxia as a driving force in genetic instability. *Genome Integr.* **2013**, *4*, 5.

112. Kumareswaran, R.; Ludkovski, O.; Meng, A.; Sykes, J.; Pintilie, M.; Bristow, R.G. Chronic hypoxia compromises repair of DNA double-strand breaks to drive genetic instability. *J. Cell Sci.* **2012**, *125*, 189–199.

113. Liu, Z.J.; Semenza, G.L.; Zhang, H. feng Hypoxia-inducible factor 1 and breast cancer metastasis. *J. Zhejiang Univ. Sci. B* **2015**, *16*, 32–43.

114. Jing, S.W.; Wang, Y.D.; Kuroda, M.; Su, J.W.; Sun, G.G.; Liu, Q.; Cheng, Y.J.; Yang, C.R. HIF-1α contributes to hypoxia-induced invasion and metastasis of esophageal carcinoma via inibiting E-cadherin and promoting MMP-2 expression. *Acta Med. Okayama* **2012**, *66*, 399–407.

115. Folkman, J. Role of angiogenesis in tumor growth and metastasis. *Semin. Oncol.* **2002**, *29*, 15–18.

116. Bielenberg, D.R.; Zetter, B.R. The Contribution of Angiogenesis to the Process of Metastasis. *Cancer J. (USA)* **2015**, *21*, 267–273.

117. Büchler, P.; Reber, H.A.; Büchler, M.; Shrinkante, S.; Büchler, M.W.; Friess, H.; Semenza, G.L.; Hines, O.J. Hypoxia-inducible factor 1 regulates vascular endothelial growth factor expression in human pancreatic cancer. *Pancreas* **2003**, *26*, 56–64.

118. Sivridis, E.; Giatromanolaki, A.; Gatter, K.C.; Harris, A.L.; Koukourakis, M.I. Association of hypoxia-inducible factors 1α and 2α with activated angiogenic pathways and prognosis in patients with endometrial carcinoma. *Cancer* **2002**, *95*, 1055–1063.

119. Oladipupo, S.; Hu, S.; Kovalski, J.; Yao, J.; Santeford, A.; Sohn, R.E.; Shohet, R.; Maslov, K.; Wang, L.V.; Arbeit, J.M. VEGF is essential for hypoxia-inducible factor-mediated neovascularization but dispensable for endothelial sprouting. *Proc. Natl. Acad. Sci. USA* **2011**, *108*, 13264–13269.

120. Skinner, H.D.; Zheng, J.Z.; Fang, J.; Agani, F.; Jiang, B.H. Vascular endothelial growth factor transcriptional activation is mediated by hypoxia-inducible factor 1α, HDM2, and p70S6K1 in response to phosphatidylinositol 3-kinase/AKT signaling. *J. Biol. Chem.* **2004**, *279*, 45643–45651.

121. De Francesco, E.M.; Lappano, R.; Santolla, M.F.; Marsico, S.; Caruso, A.; Maggiolini, M. HIF-1α/GPER signaling mediates the expression of VEGF

induced by hypoxia in breast cancer associated fibroblasts (CAFs). *Breast Cancer Res.* **2013**, *15*, R64.

122. Han, S.; Huang, T.; Li, W.; Liu, S.; Yang, W.; Shi, Q.; Li, H.; Ren, J.; Hou, F. Association between Hypoxia-Inducible Factor-2α (HIF-2α) Expression and Colorectal Cancer and Its Prognostic Role: A Systematic Analysis. *Cell. Physiol. Biochem.* **2018**, *48*, 516–527.
123. Wierzbicki, P.M.; Klacz, J.; Kotulak-Chrzaszcz, A.; Wronska, A.; Stanislawowski, M.; Rybarczyk, A.; Ludziejewska, A.; Kmiec, Z.; Matuszewski, M. Prognostic significance of VHL, HIF1A, HIF2A, VEGFA and p53 expression in patients with clear-cell renal cell carcinoma treated with sunitinib as first-line treatment. *Int. J. Oncol.* **2019**, *55*, 371–390.
124. Baba, Y.; Nosho, K.; Shima, K.; Irahara, N.; Chan, A.T.; Meyerhardt, J.A.; Chung, D.C.; Giovannucci, E.L.; Fuchs, C.S.; Ogino, S. HIF1A overexpression is associated with poor prognosis in a cohort of 731 colorectal cancers. *Am. J. Pathol.* **2010**, *176*, 2292–2301.
125. Burroughs, S.K.; Kaluz, S.; Wang, D.; Wang, K.; Van Meir, E.G.; Wang, B. Hypoxia inducible factor pathway inhibitors as anticancer therapeutics. *Future Med. Chem.* **2013**, *5*, 553–572.
126. Wigerup, C.; Påhlman, S.; Bexell, D. Therapeutic targeting of hypoxia and hypoxia-inducible factors in cancer. *Pharmacol. Ther.* **2016**, *164*, 152–169.
127. Onnis, B.; Rapisarda, A.; Melillo, G. Development of HIF-1 inhibitors for cancer therapy. *J. Cell. Mol. Med.* **2009**, *13*, 2780–2786.

128. Li, Y.; Patel, S.P.; Roszik, J.; Qin, Y. Hypoxia-driven immunosuppressive metabolites in the tumor microenvironment: New approaches for combinational immunotherapy. *Front. Immunol.* **2018**, *9*, 1.

129. Yu, T.; Tang, B.; Sun, X. Development of Inhibitors Targeting Hypoxia-Inducible Factor 1 and 2 for Cancer Therapy. *Yonsei Med. J.* **2017**, *58*, 489–496.

130. Fallah, J.; Rini, B.I. HIF Inhibitors: Status of Current Clinical Development. *Curr. Oncol. Rep.* **2019**, *21*, 1–10.

131. Carbajo-Pescador, S.; Ordoñez, R.; Benet, M.; Jover, R.; García-Palomo, A.; Mauriz, J.L.; González-Gallego, J. Inhibition of VEGF expression through blockade of Hif1α and STAT3 signalling mediates the anti-angiogenic effect of melatonin in HepG2 liver cancer cells. *Br. J. Cancer* **2013**, *109*, 83–91.

132. Ban, H.S.; Kim, B.K.; Lee, H.; Kim, H.M.; Harmalkar, D.; Nam, M.; Park, S.K.; Lee, K.; Park, J.T.; Kim, I.; et al. The novel hypoxia-inducible factor-1α inhibitor IDF-11774 regulates cancer metabolism, thereby suppressing tumor growth. *Cell Death Dis.* **2017**, *8*, e2843.

133. Laughner, E.; Taghavi, P.; Chiles, K.; Mahon, P.C.; Semenza, G.L. HER2 (neu) Signaling Increases the Rate of Hypoxia-Inducible Factor 1 (HIF-1) Synthesis: Novel Mechanism for HIF-1-Mediated Vascular Endothelial Growth Factor Expression. *Mol. Cell. Biol.* **2001**, *21*, 3995–4004.

134. Brugarolas, J.B.; Vazquez, F.; Reddy, A.; Sellers, W.R.; Kaelin, W.G. TSC2 regulates VEGF through mTOR-dependent and -independent pathways. *Cancer Cell* **2003**, *4*, 147–158.

135. Hudson, C.C.; Liu, M.; Chiang, G.G.; Otterness, D.M.; Loomis, D.C.; Kaper, F.; Giaccia, A.J.; Abraham, R.T. Regulation of Hypoxia-Inducible Factor 1 Expression and Function by the Mammalian Target of Rapamycin. *Mol. Cell. Biol.* **2002**, *22*, 7004–7014.

136. Lastwika, K.J.; Wilson, W.; Li, Q.K.; Norris, J.; Xu, H.; Ghazarian, S.R.; Kitagawa, H.; Kawabata, S.; Taube, J.M.; Yao, S.; et al. Control of PD-L1 expression by oncogenic activation of the AKT-mTOR pathway in non-small cell lung cancer. *Cancer Res.* **2016**, *76*, 227–238.

137. Song, M.; Chen, D.; Lu, B.; Wang, C.; Zhang, J.; Huang, L.; Wang, X.; Timmons, C.L.; Hu, J.; Liu, B.; et al. PTEN Loss Increases PD-L1 Protein Expression and Affects the Correlation between PD-L1 Expression and Clinical Parameters in Colorectal Cancer. *PLoS ONE* **2013**, *8*, e65821.

138. Zhao, L.; Li, C.; Liu, F.; Zhao, Y.; Liu, J.; Hua, Y.; Liu, J.; Huang, J.; Ge, C. A blockade of PD-L1 produced antitumor and antimetastatic effects in an orthotopic mouse pancreatic cancer model via the PI3K/Akt/mTOR signaling pathway. *Onco. Targets. Ther.* **2017**, *10*, 2115–2126.

139. Mittendorf, E.A.; Philips, A.V.; Meric-Bernstam, F.; Qiao, N.; Wu, Y.; Harrington, S.; Su, X.; Wang, Y.; Gonzalez-Angulo, A.M.; Akcakanat, A.; et al. PD-L1 expression in triple-negative breast cancer. *Cancer Immunol. Res.* **2014**, *2*, 361–370.

140. Zhang, X.; Wang, Y.; Fan, J.; Chen, W.; Luan, J.; Mei, X.; Wang, S.; Li, Y.; Ye, L.; Li, S.; et al. Blocking CD47 efficiently potentiated therapeutic effects of anti-

angiogenic therapy in non-small cell lung cancer. *J. Immunother. Cancer* **2019**, *7*, 346.

141. Huang, Y.; Yuan, J.; Righi, E.; Kamoun, W.S.; Ancukiewicz, M.; Nezivar, J.; Santosuosso, M.; Martin, J.D.; Martin, M.R.; Vianello, F.; et al. Vascular normalizing doses of antiangiogenic treatment reprogram the immunosuppressive tumor microenvironment and enhance immunotherapy. *Proc. Natl. Acad. Sci. USA* **2012**, *109*, 17561–17566.
142. Aghi, M.K.; Liu, T.C.; Rabkin, S.; Martuza, R.L. Hypoxia enhances the replication of oncolytic herpes simplex virus. *Mol. Ther.* **2009**, *17*, 51–56.
143. Pin, R.H.; Reinblatt, M.; Fong, Y. Employing tumor hypoxia to enhance oncolytic viral therapy in breast cancer. *Surgery* **2004**, *136*, 199–204.
144. Guo, Z.S. The impact of hypoxia on oncolytic virotherapy. *Virus Adapt. Treat.* **2011**, *3*, 71.
145. Hackstein, H.; Taner, T.; Logar, A.J.; Thomson, A.W. Rapamycin inhibits macropinocytosis and mannose receptor-mediated endocytosis by bone marrow-derived dendritic cells. *Blood* **2002**, *100*, 1084–1087.
146. Hackstein, H.; Taner, T.; Zahorchak, A.F.; Morelli, A.E.; Logar, A.J.; Gessner, A.; Thomson, A.W. Rapamycin inhibits IL-4-induced dendritic cell maturation in vitro and dendritic cell mobilization and function in vivo. *Blood* **2003**, *101*, 4457–4463.
147. Thomson, A.W.; Turnquist, H.R.; Raimondi, G. Immunoregulatory functions of mTOR inhibition. *Nat. Rev. Immunol.* **2009**, *9*, 324–337.

148. Chaoul, N.; Fayolle, C.; Desrues, B.; Oberkampf, M.; Tang, A.; Ladant, D.; Leclerc, C. Rapamycin impairs antitumor CD8p T-cell responses and vaccine-induced tumor eradication. *Cancer Res.* **2015**, *75*, 3279–3291.

149. Battaglia, M.; Stabilini, A.; Roncarolo, M.G. Rapamycin selectively expands CD4+CD25+FoxP3 + regulatory T cells. *Blood* **2005**, *105*, 4743–4748.

150. Battaglia, M.; Stabilini, A.; Migliavacca, B.; Horejs-Hoeck, J.; Kaupper, T.; Roncarolo, M.-G. Rapamycin Promotes Expansion of Functional CD4 + CD25 + FOXP3 + Regulatory T Cells of Both Healthy Subjects and Type 1 Diabetic Patients. *J. Immunol.* **2006**, *177*, 8338–8347.

CHAPTER THREE: B CELL INVOLVEMENT RENDERS TRIPLE NEGATIVE BREAST CANCER SENSITIVE TO IMMUNE CHECKPOINT BLOCKADE THROUGH DOWNREGULATION OF MYELOID-DERIVED SUPPRESSOR CELLS

Preamble

This is an author-produced version of an article currently under revision with Communications Biology. The version of record **Vito A**, Salem O, El-Sayes N, Portillo AL, Ashkar A, Milne A, Harrington D, Nelson B, Wan Y, Workenhe S, Mossman KL. B cell involvement renders triple negative breast cancer sensitive to immune checkpoint blockade through downregulation of myeloid-derived suppressor cells.

AV conceived and designed the project, acquired and analyzed the data, interpreted the results and wrote the manuscript. OS acquired and analyzed the data and revised the manuscript. NES acquired and analyzed the data and revised the manuscript. ALP acquired and analyzed the data. KM acquired data. DH acquired data. BN supervised the study and revised the manuscript. AA supervised the study and revised the manuscript. YW supervised the study and revised the manuscript. SW supervised the study and revised the manuscript. KLM supervised the study, interpreted the results and revised the manuscript.

Our literature review showed a lack of understanding of the immune landscape of TNBC tumors and poor clinical response rates to ICB therapy. Hence, the aim of this work was to develop a therapeutic platform to sensitize TNBC tumors to ICB and to investigate what factors in the TME contributed to therapeutic efficacy. We used in vivo

survival studies to assess the effect of our combination therapies and flow cytometry to analyze the changes of key immune cell populations. IHC was used to investigate the levels of infiltrating immune cells, which was further characterized by immune analysis flow cytometry studies. RNA sequencing studies identified key pathways responsible for therapeutic efficacy, which was substantiated by in vivo depletion studies. Overall, this work developed a combined chemotherapy and oncolytic virotherapy model to sensitize tumors to ICB. It additionally assessed relevant pathways and cellular populations as being drivers of therapeutic efficacy and tumor immunosuppression.

B cell involvement renders triple negative breast cancer sensitive to immune checkpoint blockade through downregulation of myeloid-derived suppressor cells

Alyssa Vito[1,2], Omar Salem[1,2], Nader El-Sayes[1,2], Ana L. Portillo[1,2], Ali Ashkar[1,2], Katy Milne[3], Danielle Harrington[3], Brad Nelson[4], Yonghong Wan[1,2], Samuel Workenhe[5] and Karen Mossman[1,2*]

[1]McMaster Immunology Research Centre, McMaster University, Hamilton, ON, Canada.

[2]Department of Medicine, McMaster Immunology Research Centre, McMaster University, Hamilton, Ontario, L8S 4K1, Canada.

[3]Trev and Joyce Deeley Research Centre, British Columbia Cancer Agency, Victoria, Canada.

[4]Trev and Joyce Deeley Research Centre, British Columbia Cancer Agency, Victoria, Canada; Department of Biochemistry and Microbiology, University of Victoria, Victoria, British Columbia, Canada; Department of Medical Genetics, University of British Columbia, Vancouver, British Columbia, Canada.

[5]Department of Pathobiology, Ontario Veterinary College, University of Guelph, Guelph, Ontario, N1G 2W1, Canada.

*Corresponding author. Email: mossk@mcmaster.ca

Abstract

Triple negative breast cancer (TNBC) holds a dismal clinical outcome and as such, patients routinely undergo aggressive, highly toxic treatment regimens. Clinical trials for TNBC employing immune checkpoint blockade (CP) in combination with chemotherapy have shown modest prognostic benefit, but the percentage of patients that respond to treatment is low, and patients often succumb to relapsed disease. We have developed a combination immunotherapy platform utilizing low dose chemotherapy (FEC) combined with oncolytic virotherapy (oHSV-1) in an E0771 murine TNBC tumor model. This combination increased tumor-infiltrating lymphocytes, in otherwise immune-bare tumors, allowing 60% of mice to achieve durable tumor regression when treated with CP. Whole-tumor RNA sequencing was performed, and differential gene expression identified that FEC + oHSV-1 therapy upregulates many genes associated with B cell receptor signaling pathways. In vivo studies in which mice were depleted of circulating B cells resulted in loss of therapeutic efficacy and expansion of myeloid-derived suppressor cells (MDSCs). Additionally, RNA sequencing data revealed genes involved in the maturation and migration of MDSCs that were suppressed by FEC + oHSV-1 therapy, suggesting that B cells can act as regulators of MDSCs, a key population of cells that drive immune escape and mediate therapeutic resistance.

3.1. Introduction

Triple negative breast cancer (TNBC) is an aggressive disease with dismal clinical outcome due to limited therapeutic options[1,2]. Immune checkpoint blockade (CP), which limits inhibitory pathways on $CD8^+$ and $CD4^+$ tumor-infiltrating lymphocytes (TILs), has demonstrated unparalleled clinical success in a wide variety of cancer types. Antibodies blocking the PD1: PDL1 inhibitory axis aim to target PD1 on T cells and PDL1 on tumor cells. However, only ~9% of patients with advanced TNBC express PDL1 on tumor cells[3]. Recently approved therapies for TNBC are limited (PARPi, atezolizumab and sacituzumab-govitecan) and only benefit 10-20% of patients treated[3]. For this reason, a deeper understanding of the immune landscape in TNBC tumors is required to develop novel, effective therapies and delineate prognostic biomarkers of disease.

Many clinical trials are currently underway using CP as a standalone, adjuvant or neoadjuvant therapy for various tumor types[4]. However, the percentage of patients that respond to CP as a monotherapy is low and is generally limited to cancers with a favourable mutational landscape and high rates of cell turnover, such as melanoma and non-small cell lung cancer. In contrast, most breast lesions establish a highly suppressive tumor microenvironment (TME) with high levels of myeloid-derived suppressor cells (MDSCs), which has been shown to directly correlate with disease stage and overall tumor burden[5,6]. Additionally, clinical studies have shown the extent of immune cell infiltration and activation in breast tumors to be a key indicator of long-term survival and a predictor of therapeutic efficacy[7–10]. The use of therapies that can decrease MDSCs,

increase TILs and induce potent immunogenic cell death (ICD) may allow immunogenically cold breast tumors to better respond to CP.

A phase III clinical trial has shown that chemotherapy works to enhance the antitumor activity of CP in metastatic TNBC patients[3]. However, this combination of chemotherapy and immunotherapy only confers a modest overall survival benefit[3]. These results further highlight the need for additional strategies to treat TNBC and to mediate intrinsic resistance mechanisms. To this end, a more thorough analysis of the immune environment in TNBC patients beyond $CD8^+$ TILs is necessary.

Oncolytic viruses (OVs) have risen as an interesting therapeutic option with widespread clinical application and safe toxicity profiles due to their ability to preferentially target cancer cells over normal healthy cells. We have developed herpesvirus-based OVs that target multiple tumor types [11–14] and identified a strong correlation between OV-mediated ICD and antitumor immunity [14–19]. Moreover, oncolytic HSV-1s, such as oHSV-1 dICP0 [14], synergize with low dose chemotherapy to overcome immune tolerance [14,16–18]. Our early studies used mitoxantrone, a well-characterized "immunogenic" agent [18,20–22]. However, mitoxantrone is not normally used for breast cancer therapy, decreasing the translational value of our findings. Using a chemotherapy cocktail that is routinely used for TNBC patients will allow for ease of translation and biological analysis of current clinical applications.

Additional to the need for improved therapeutic approaches for TNBC patients is the simultaneous need to better understand the foundational biology that allows some patients to respond to treatment while their phenotypically identical counterparts do not.

Here, we focused on the development of clinically relevant therapies that can be used to induce the inflamed microenvironment needed for tumors to respond to CP. We have used our therapeutic platform as a mechanism to study and better understand the complex biological processes that mediate therapeutic responses, as well as the interactions of key immune cell populations within the TME. This approach facilitates translation of findings to the clinic to improve immunotherapy responses in solid tumors.

3.2. Results

FEC + oHSV-1 improves survival outcome in TNBC tumor-bearing mice

While chemotherapies are often given in dose-dense cytotoxic regimens, many studies have described the immunostimulatory properties of various chemotherapeutics through the use of low dose intervention[23–26]. Based on current clinical practice, two of the most commonly used chemotherapy cocktails for breast cancer patients are FEC (5-fluorouracil, epirubicin and cyclophosphamide) and AC (doxorubicin and cyclophosphamide)[27]. In an effort to reverse translate these regimens from the clinic into murine models, we performed optimization studies to find dosing levels and schedules that showed no acute cytotoxicity to murine hosts, as determined through close monitoring of body weights and scoring (Figure S3.1). In an effort to mimic clinical dosing, the individual ratios of the drugs to one another were the same as commonly prescribed in the clinic. The therapeutic potential of each regimen was evaluated in combination with oHSV-1 (Figure 3.1A) using the E0771 TNBC syngeneic murine model. While no monotherapy showed efficacy, the addition of oHSV-1 to the clinical FEC regimen (FEC + oHSV-1) delayed tumor growth in some mice (Figure 3.1B) and

significantly extended survival, with 10% of mice resulting in durable tumor regression (Figure 3.1C). Since epirubicin and doxorubicin are chemical analogues of one another, the main difference between these two regimens is in the addition of 5-fluorouracil to the FEC regimen. Indeed, a single dose of 5-fluorouracil alone has been shown to promote an antitumor immune response[28].

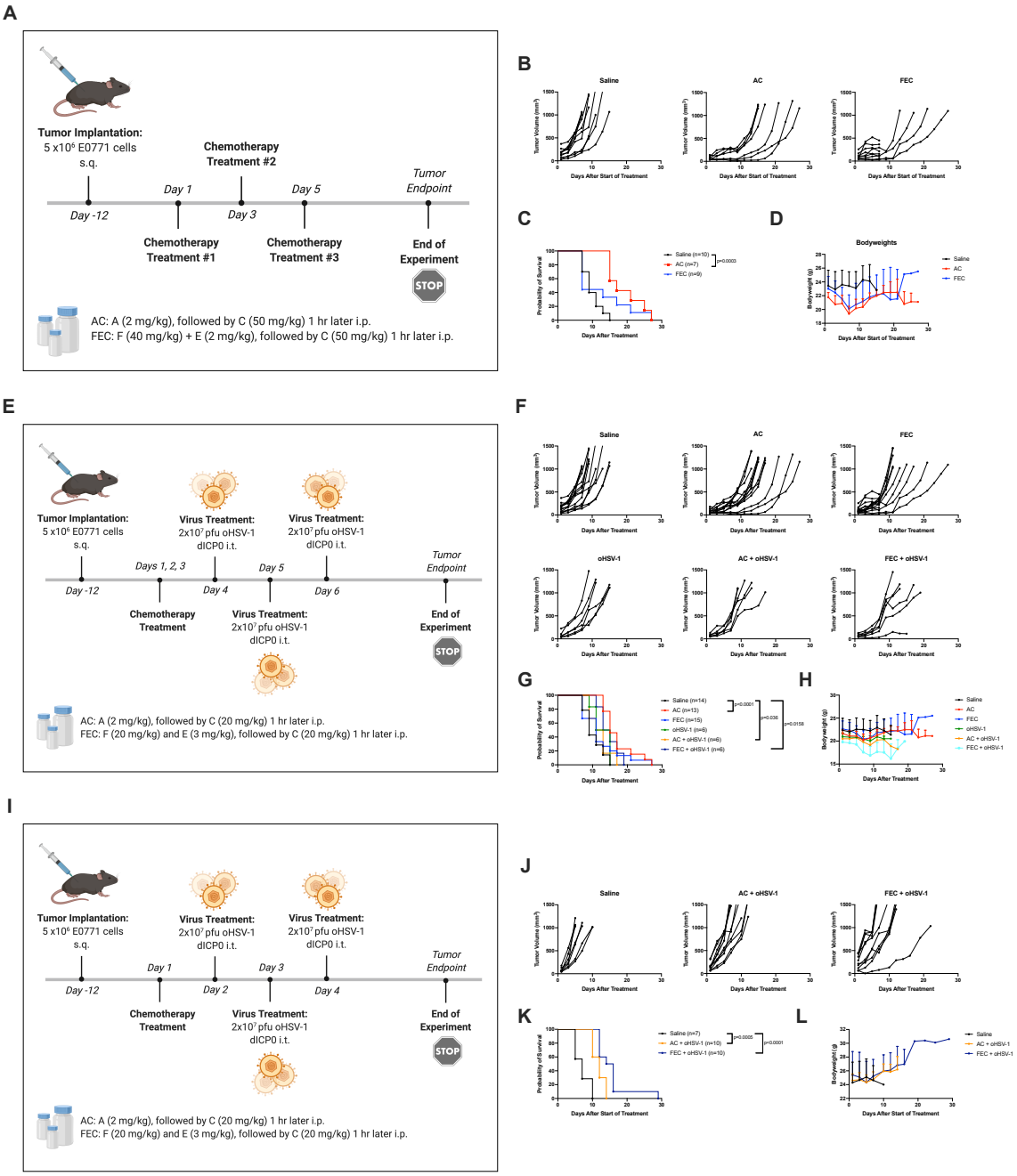

Fig. S3.1. Preliminary dose optimization studies for AC and FEC chemotherapy regimens

(**A**)(**E**)(**I**) C57/Bl6 mice bearing E0771 tumors were treated with saline, AC, FEC, oHSV-1, AC + oHSV-1 or FEC + oHSV-1. Each treatment schedule outlines a separate,

successive experiment. *Created using BioRender.com. (**B**)(**F**)(**J**) Tumor volumes were measured every 2-3 days from the start of treatment until mice reached endpoint. Each line represents an individual mouse within the group. (**C**)(**G**)(**K**) Kaplan-Meier survival curves of each group. (**D**)(**H**)(**L**) Average bodyweights for all groups. *Mantel-Cox test was used for statistical analyses. Error bars are representative of the standard deviation. Note: Survival statistics are not an accurate measure of therapeutic efficacy for experiments 1 and 2 (C and G), as many mice were sacrificed due to extreme weight loss, rather than a lack of therapeutic efficacy.

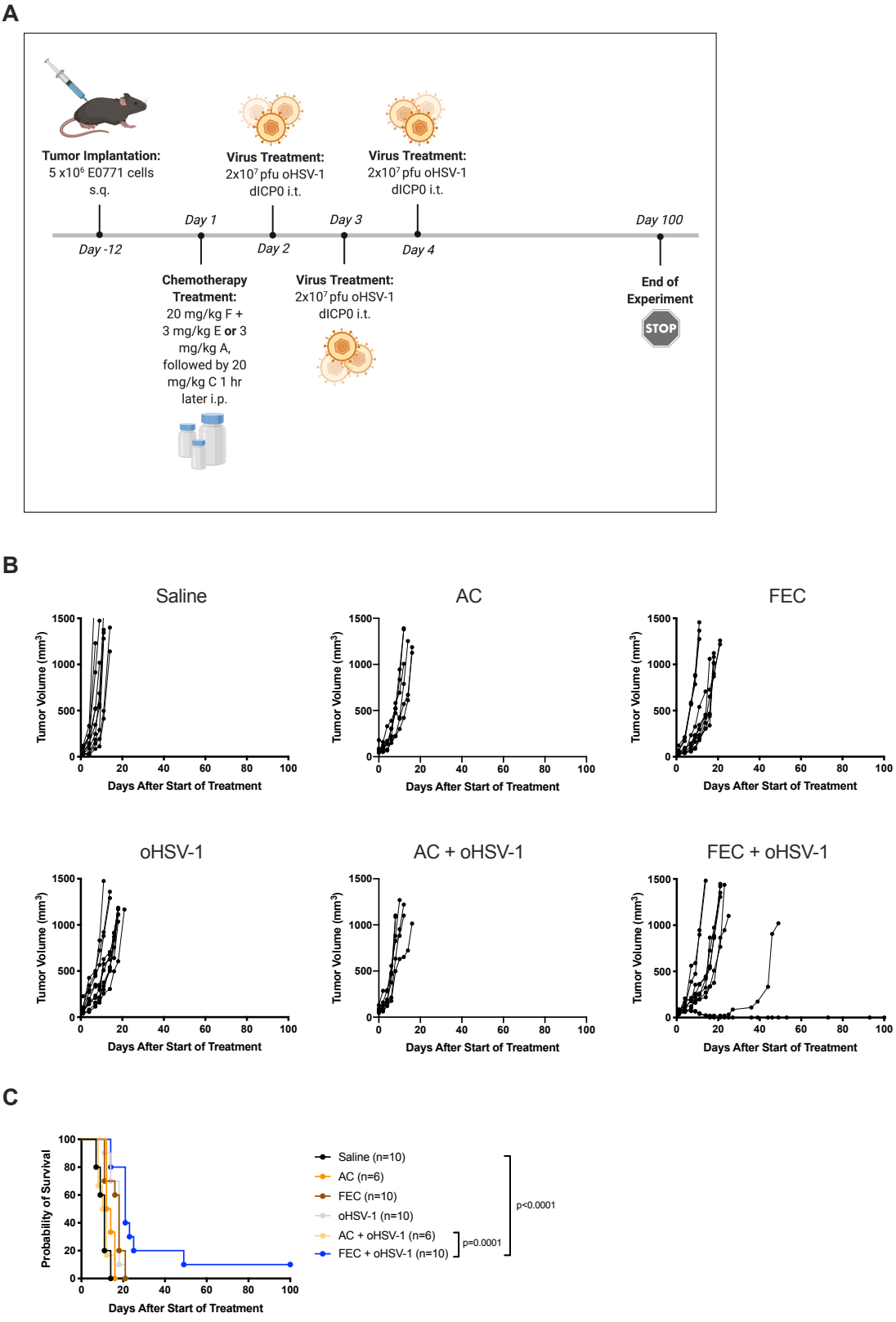
A
Tumor Implantation:
5 x10⁶ E0771 cells
s.q.
Virus Treatment:
2x10⁷ pfu oHSV-1
dICP0 i.t.
Virus Treatment:
2x10⁷ pfu oHSV-1
dICP0 i.t.
Day -12
Day 1
Day 2
Day 3
Day 4
Day 100
Chemotherapy Treatment:
20 mg/kg F +
3 mg/kg E or 3 mg/kg A,
followed by 20 mg/kg C 1 hr later i.p.
Virus Treatment:
2x10⁷ pfu oHSV-1
dICP0 i.t.
End of Experiment
STOP
B
Saline
AC
FEC
oHSV-1
AC + oHSV-1
FEC + oHSV-1
Tumor Volume (mm³)
Days After Start of Treatment
C
Probability of Survival
Days After Start of Treatment
Saline (n=10)
AC (n=6)
FEC (n=10)
oHSV-1 (n=10)
AC + oHSV-1 (n=6)
FEC + oHSV-1 (n=10)
p=0.0001
p<0.0001

Fig. 3.1. FEC + oHSV-1 slows tumor growth and decreases tumor kinetics and results in tumor regression in 10% of mice.

(**A**) C57/Bl6 mice bearing E0771 tumors were treated with saline, chemotherapy (FEC or AC), oncolytic virus (oHSV-1 dICP0) or chemotherapy + oncolytic virus. *Created using BioRender.com. (**B**) Tumor volumes were measured every 2-3 days from the start of treatment until mice reached endpoint. Each line represents an individual mouse within the group. (**C**) Kaplan- Meier survival curves of each group. *Mantel-Cox test was used for statistical analyses.

FEC + oHSV-1 sensitizes tumors to checkpoint blockade therapy

Although TNBC tumors were previously thought to be immunologically cold, recent clinical studies have shown that they do indeed express various immunogenic markers, such as PD-L1[29]. However, the expression of these markers is low and it is not diffuse throughout the tumor, but rather clumped in focal areas limited to a small proportion of cancer cells[30]. Further, clinical trials have reported both the efficiency and necessity of combined therapeutic modalities (e.g. immunotherapy and chemotherapy), as TNBC patients often have low, short-lived responses to CP on its own[31]. Based on our preliminary studies, we hypothesized that FEC + oHSV-1 is capable of sensitizing tumors to CP by turning an immune-cold tumor into an immunogenic one. Survival studies were performed with the addition of dual CP targeting the non-redundant pathways of cytotoxic T-lymphocyte antigen 4 and programmed death ligand-1 (with anti-CTLA4 and anti-PD-L1 antibodies, respectively). While neither CP alone, or in combination with FEC or oHSV-1, showed therapeutic efficacy, the combination of FEC + oHSV-1 + CP

resulted in greatly improved responses with 60% of mice achieving durable tumor regression (Figure 3.2A-C). Furthermore, mice that showed durable regression of tumors subsequently rejected the parental (E0771) tumor cells when re-challenged, suggesting that responding mice generated immune memory against the tumor (Figure 3.2D). Interestingly, when this triple combination therapy was tried with singular administration of CP (anti-CTLA4 mAb or anti-PD-L1 mAb) no therapeutic efficacy was seen (Figure S3.2), suggesting that targeting both pathways simultaneously is beneficial in overcoming resistance mechanisms in this aggressive tumor model.

To identify pathways essential for therapeutic efficacy, cytokine analysis was performed on tumor lysates obtained from mice treated with either saline or FEC + oHSV-1 + CP (Figure 3.3; full dataset shown in Figure S3.3). Mice treated with FEC + oHSV-1 + CP had significantly changed expression levels of cytokines related to myeloid cell differentiation and chemotaxis, macrophage activation and inflammatory pathways.

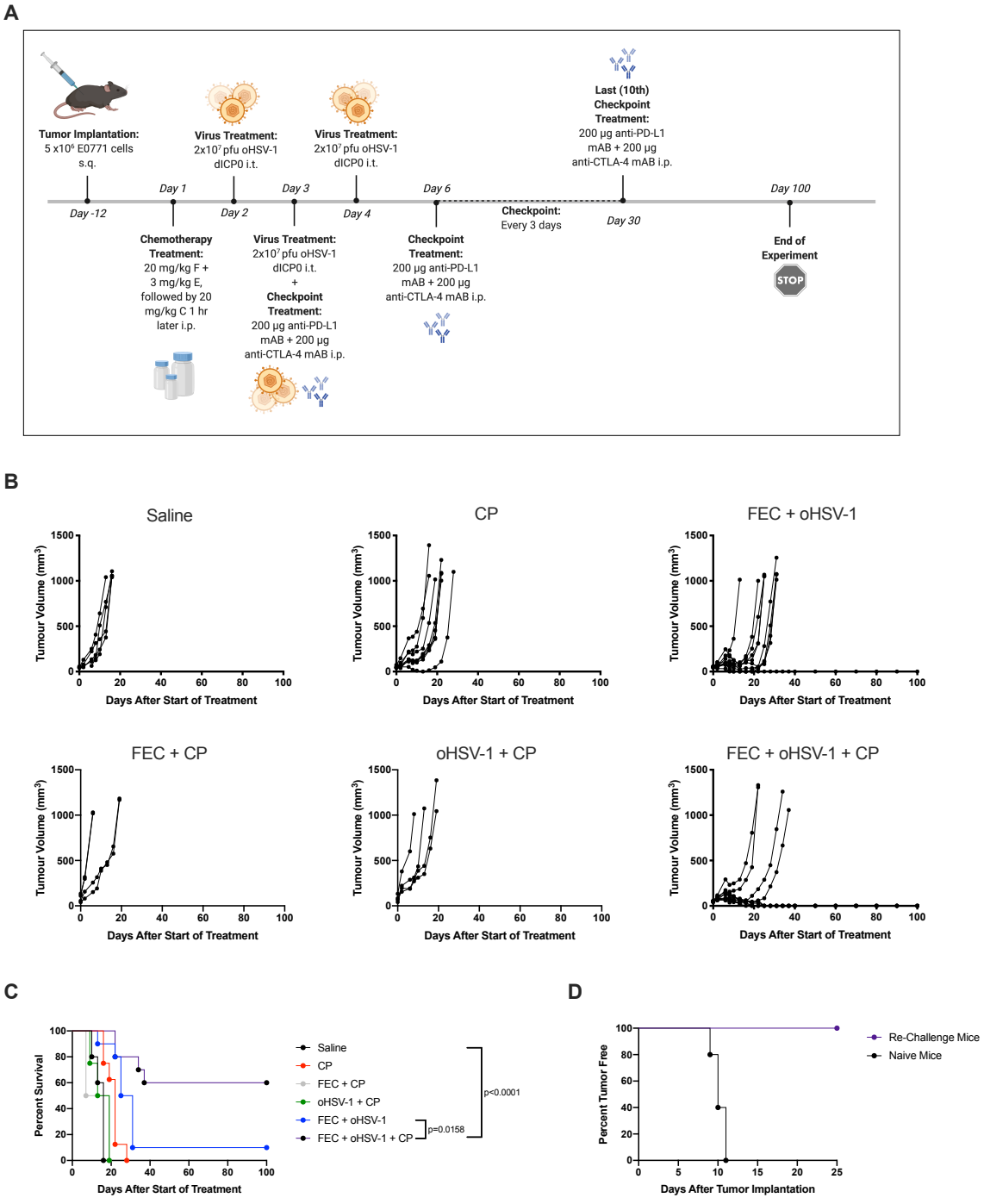

Fig. 3.2. FEC + oHSV-1 + CP decreases tumor kinetics and results in durable tumor regression in 60% of mice.

(**A**) C57/Bl6 mice bearing E0771 tumors were treated with saline, CP (anti-CTLA4 and anti-PD-L1), FEC + CP, oHSV-1 + CP, FEC + oHSV-1 or FEC + oHSV-1 + CP. *Created using BioRender.com. (**B**) Tumor volumes were measured every 2-3 days from the start of treatment until mice reached endpoint. Each line represents an individual mouse within the group. (**C**) Kaplan- Meier survival curves of each group. (**D**) Mice who achieved durable tumor regression with FEC + oHSV-1 + CP therapy were subsequently re-challenged with E0771 cells on day 63 days. Naïve mice of similar age were used as a control for tumor implantation and growth. *Mantel-Cox test was used for statistical analyses.

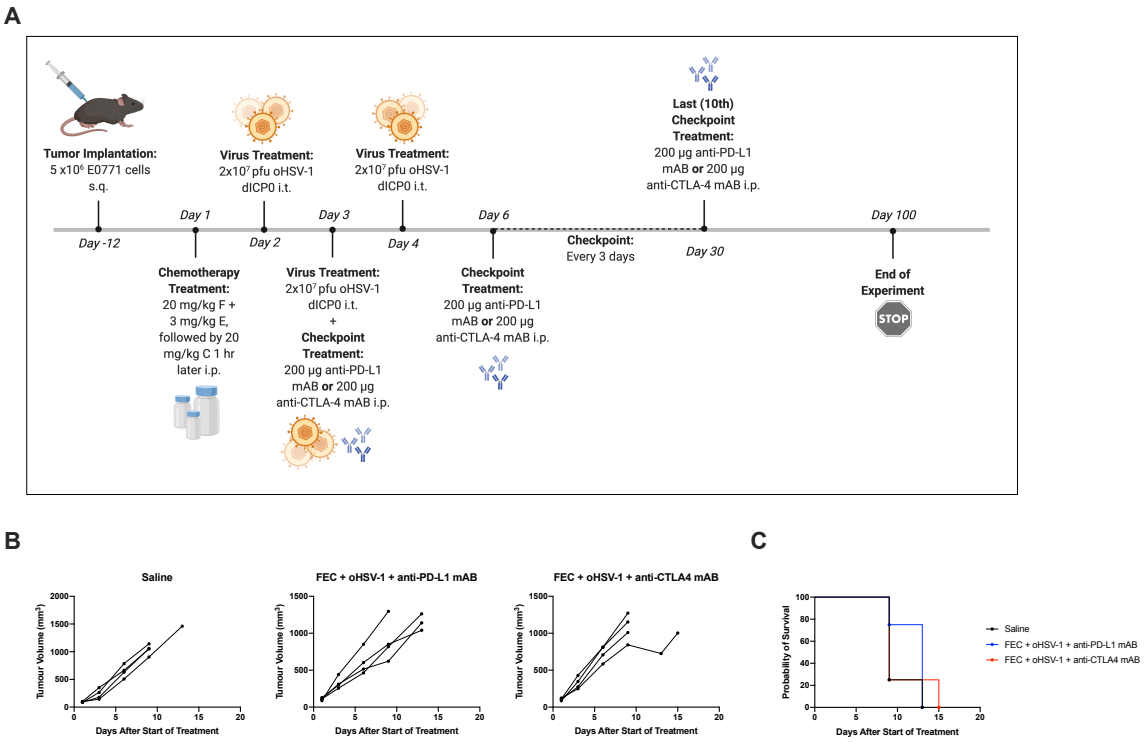

Fig. S3.2. Administration of singular checkpoint antibodies shows no therapeutic efficacy

(**A**) C57/Bl6 mice bearing E0771 tumors were treated with saline or FEC + oHSV-1 + CP (anti-CTLA4 or anti-PD-L1). *Created using BioRender.com. (**B**) Tumor volumes were measured every 2-3 days from the start of treatment until mice reached endpoint (tumor volume = 1000 mm^3). Each line represents an individual mouse within the group. (**C**) Kaplan-Meier survival curves of each group. *Mantel-Cox test was used for statistical analyses.

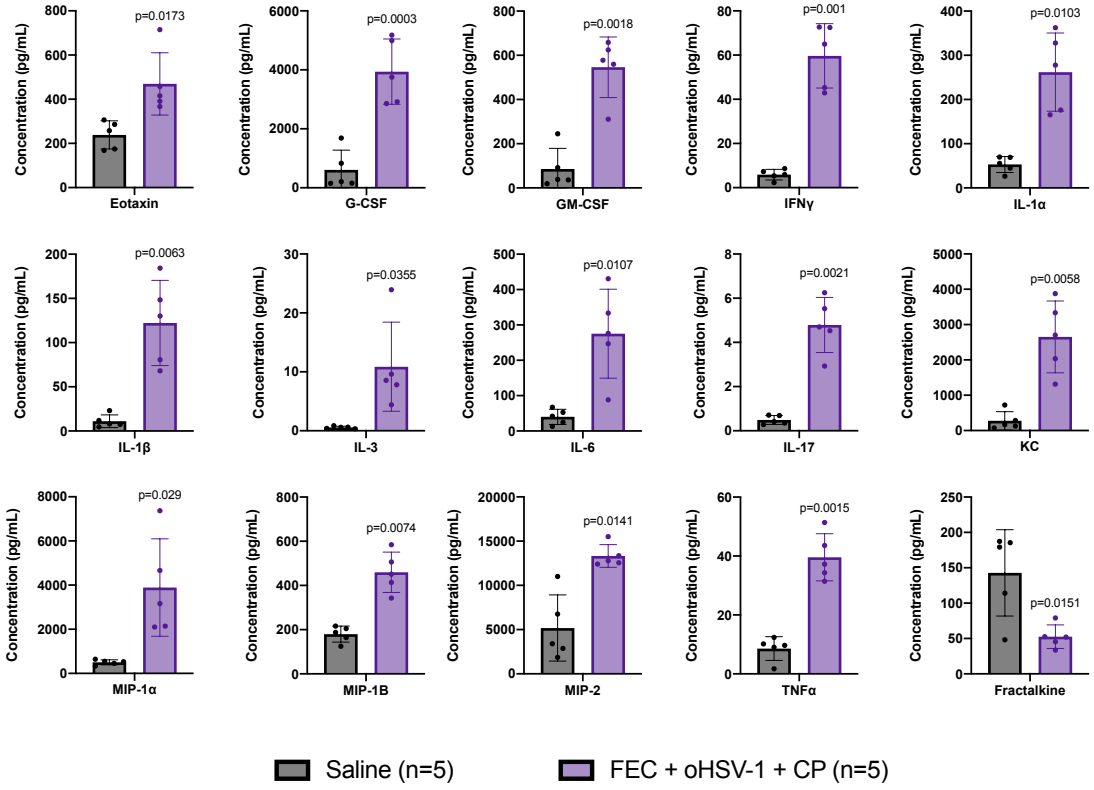

Fig 3.3. Cytokine analysis shows that treatment with FEC + oHSV-1 + CP significantly alters the expression of a variety of cytokines.

C57/Bl6 mice bearing E0771 tumors were treated with saline or FEC + oHSV-1 + CP. Mice were sacrificed on day 10 treatment and tumors flash frozen. Tumor lysates were

made and sent for cytokines expression analysis. All values are reported as a concentration (pg/mL). Two-tailed paired t test was used for statistical analyses. Error bars are representative of the standard deviation.

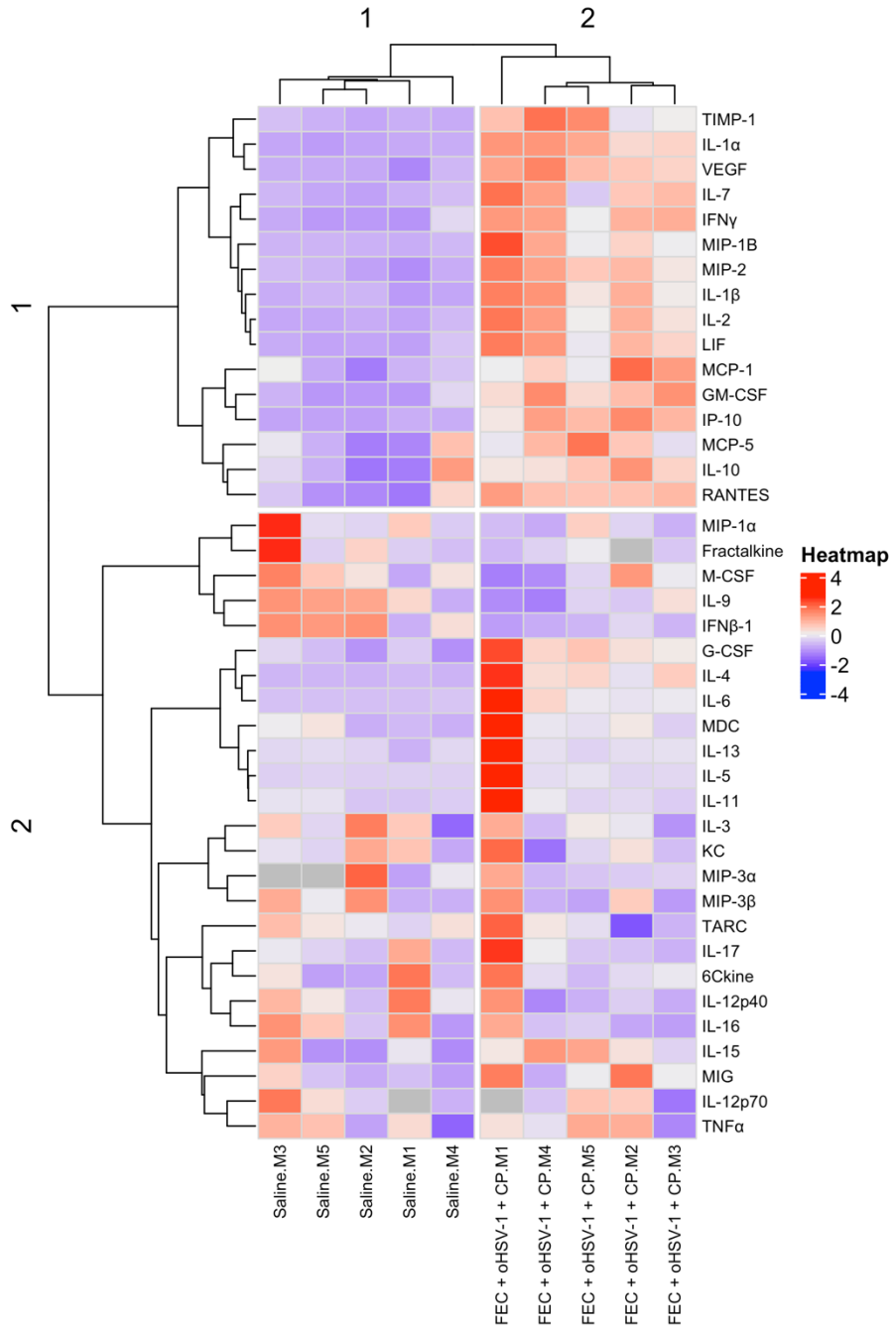

Figure S3.3. FEC + oHSV + CP significantly changes the expression of many cytokines in tumor-bearing mice

E0771 tumors were grown in C57/Bl6 mice. Mice were sacrificed on day 10 and tumors flash frozen. Tumor lysates were made and sent for cytokines expression analysis. Heat map showing the differential expression levels (concentration, pg/mL) of a panel of cytokines. All values are reported as a concentration (pg/mL).

Immunogenic therapy induces TILs into otherwise immune-bare tumors

To investigate the immune landscape of untreated and treated E0771 tumors, histologic assessment was performed. Tumors were harvested on days 7 and 10 from mice treated with saline, FEC, oHSV-1, FEC + oHSV-1 or FEC + oHSV-1 + CP (Figure 4A-B). Analysis of whole tumor sections harvested on day 7 and stained with hematoxylin and eosin (H&E) (Figure S3.4A) shows that saline and FEC treated mice have large, densely packed tumors with many cells actively undergoing cellular division. Conversely, mice treated with oHSV-1, FEC + oHSV-1 and FEC + oHSV-1 + CP present with shrinking cellular structures and large areas of necrosis, likely due to direct viral oncolysis from intratumoral administration of the virus. When these same groups are again analyzed on day 10 (Figure S3.4B) it is clear that saline and FEC treated mice have continued to progress towards tumor endpoint with highly vascularized tumors undergoing extensive angiogenesis, displayed by the appearance of many new microvessels and infiltrating vasculature. oHSV-1 treated mice still have areas of necrosis in the center, but the remaining tumor tissue has begun to progress towards tumor endpoint, with large tumors that are densely packed with viable cells. Interestingly, FEC + oHSV-1 treated tumors now present two distinct populations within mice, with 80% of tumors shifting towards an untreated phenotype with increased proliferation and density,

similar in appearance to saline and FEC treated tumors. The remaining 20% of tumors show increased areas of necrosis and decreased overall tumor size. As expected from survival outcomes, tumors harvested from mice that were treated with FEC + oHSV-1 + CP present with increased necrosis and very small tumors (Figure S3.4C).

Tumors were further stained with antibodies for CD3, CD4 and CD8α to assess the level of immune cell infiltration across the treatment groups (Figure 3.4A-B). As expected, saline and FEC treated mice presented with immune-bare tumors with almost no immune cells present in the tumor bulk or surrounding connective tissue. Tumors treated with oHSV-1, FEC + oHSV-1 or FEC + oHSV-1 + CP, however, show increased levels of T cell infiltration throughout the remaining viable tumor tissue. Quantification of these stains (Figure 3.4C) reveals that tumors treated with oHSV-1, FEC + oHSV-1 or FEC + oHSV-1 + CP have statistically significant recruitment of immune cells into the tumor, as compared to saline treated tumors. Clinical studies have shown the ratio of $CD8^+$ T cells to $FOXP3^+$ regulatory T cells to be a significant indicator of prognostic outcome in TNBC patients [32,33]. For this reason, all tumor slices stained for CD8α were co-stained for FOXP3 expression and the ratio between the two was assessed within individual mice (Figure 3.4C). As shown, mice treated with oHSV-1, FEC + oHSV-1 or FEC + oHSV-1 + CP had statistically significant increases in their ratio of $CD8\alpha^+/FOXP3^+$ infiltrates at day 7, but only with the combination therapies (FEC + oHSV-1 and FEC + oHSV-1 + CP) is this increase sustained out to day 10. This observation suggests that while oncolytic virotherapy is able to prime the tumor

microenvironment, additional therapeutic intervention may be required for durable response to immunotherapy treatments.

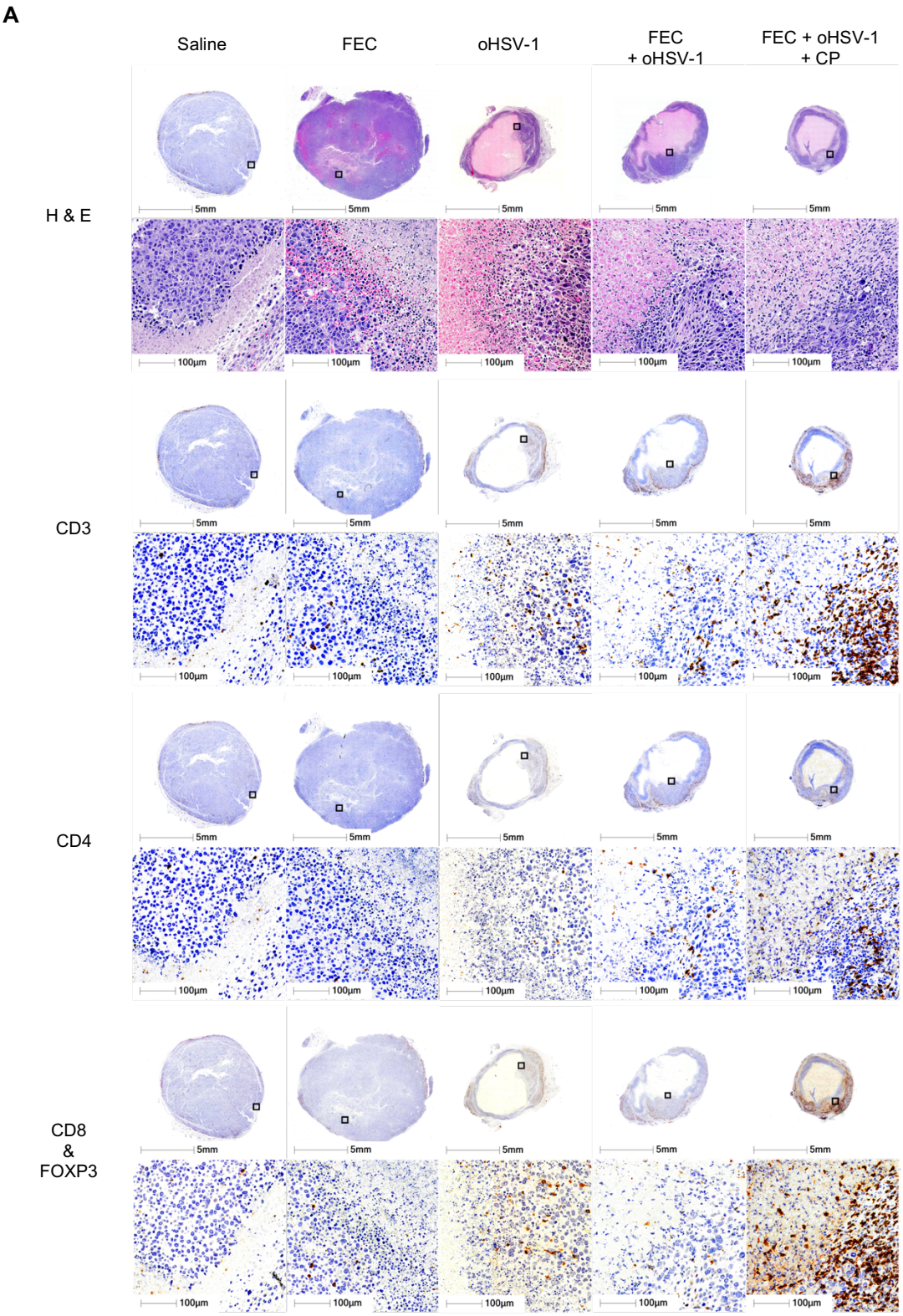
A
Saline
FEC
oHSV-1
FEC + oHSV-1
FEC + oHSV-1 + CP
H & E
CD3
CD4
CD8 & FOXP3
5mm
100µm

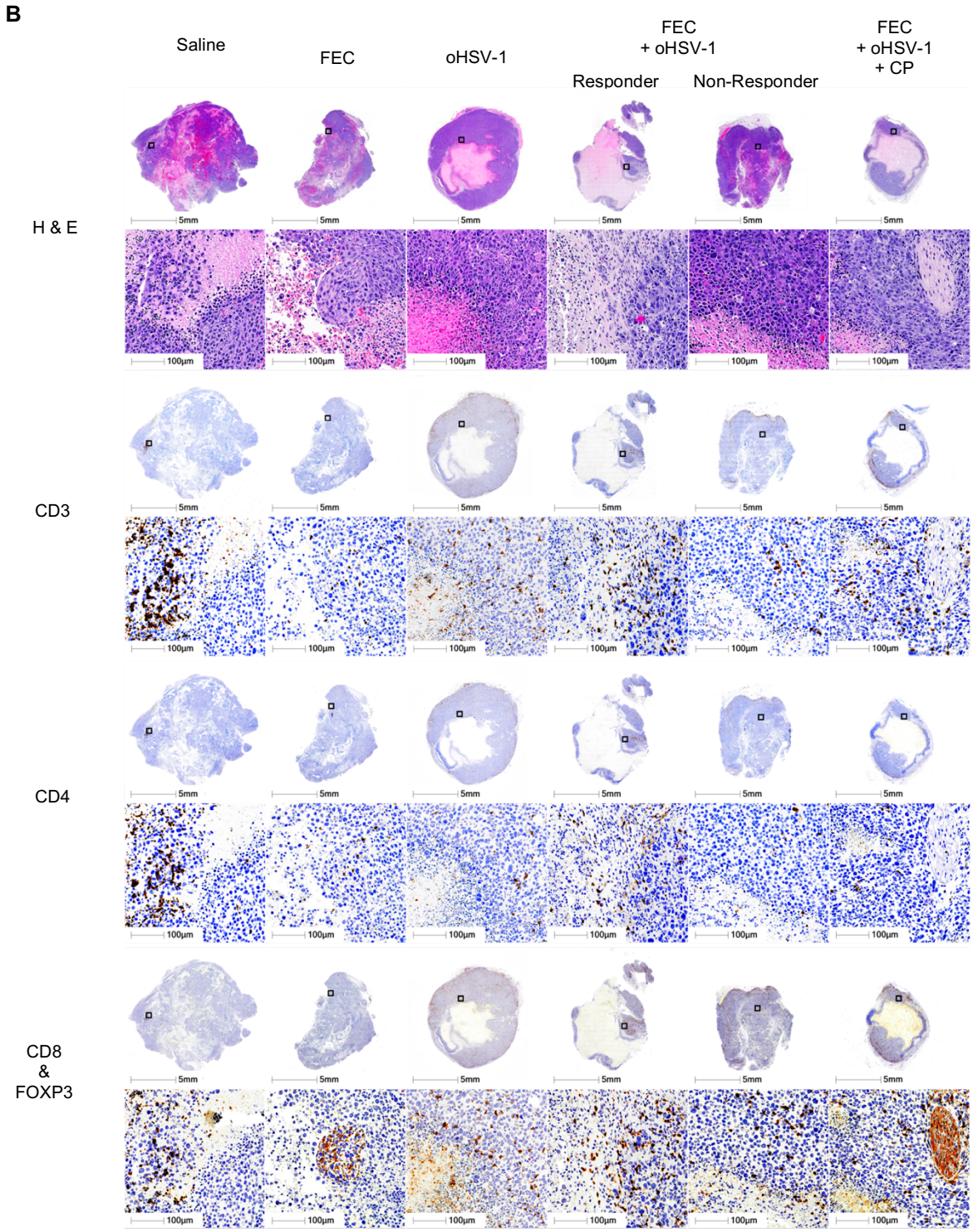
B
Saline
FEC
oHSV-1
FEC + oHSV-1
Responder
Non-Responder
FEC + oHSV-1 + CP
H & E
CD3
CD4
CD8 & FOXP3
5mm
100µm

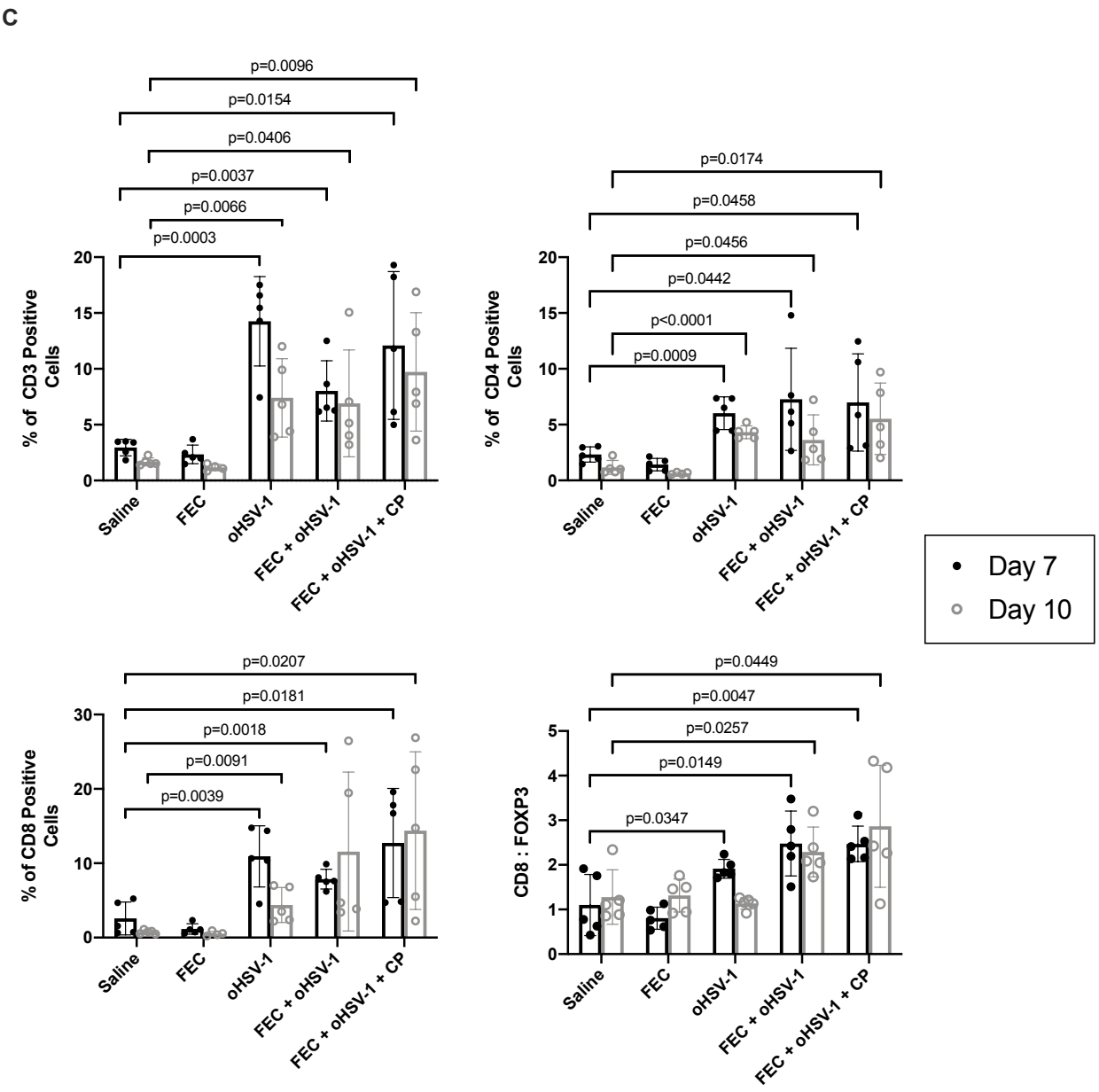

Fig. 3.4. Immunohistochemistry analysis shows that oHSV-1, FEC + oHSV-1 and FEC + oHSV-1 + CP treatments induce TILs.

C57/Bl6 mice bearing E0771 tumors were treated with saline, FEC, oHSV-1, FEC + oHSV-1 or FEC + oHSV-1 + CP and tumors were harvested on days 7 and 10 (n=5 per

group). Tumors were sectioned and stained with H&E for pathological analysis. Sections were then further stained with antibodies for CD3, CD4, CD8α and FOXP3. (**A**) Representative images for tumors harvested on day 7. Each image shows a whole section of an individual tumor. (**B**) Representative images for tumors harvested on day 10. Each image shows a whole section of an individual tumor. (**C**) Whole tumor sections were scanned and quantified using HALO quantification software. Each symbol represents an individual mouse within that group. Two-tailed paired t test was used for statistical analyses. Error bars are representative of the standard deviation.

A

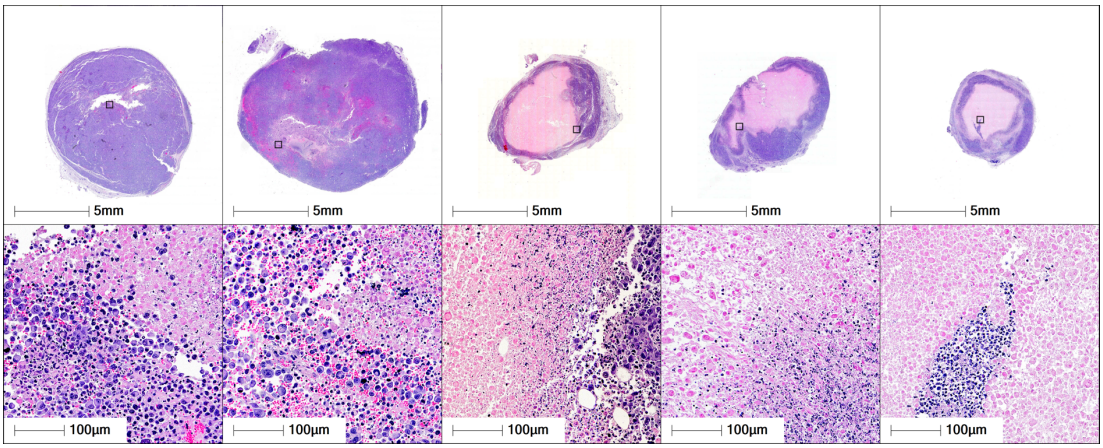
5mm
100µm

B

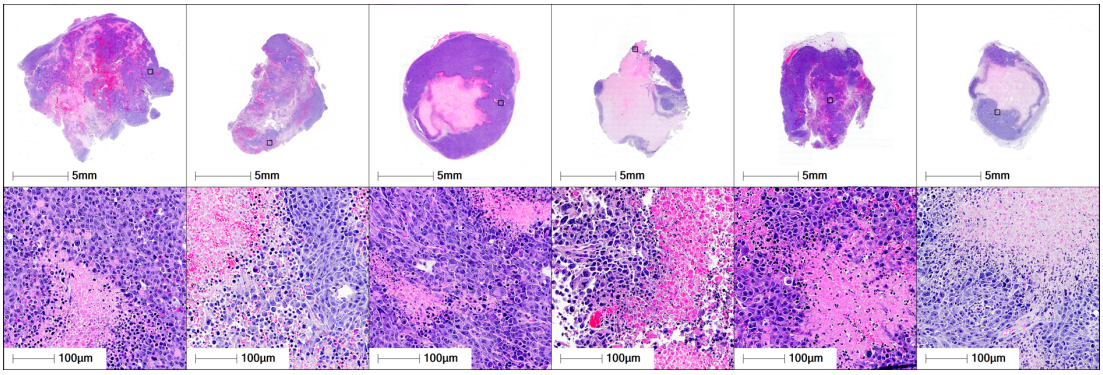
5mm
100µm

C

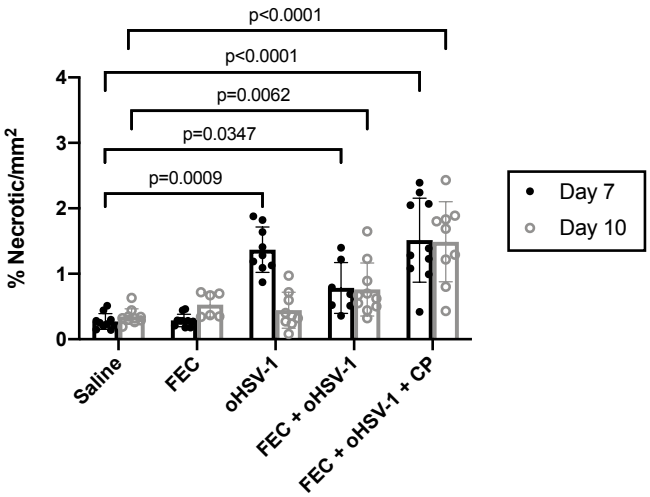
p<0.0001
p<0.0001
p=0.0062
p=0.0347
p=0.0009
% Necrotic/mm2
0
1
2
3
4
Saline
FEC
oHSV-1
FEC + oHSV-1
FEC + oHSV-1 + CP
Day 7
Day 10

Fig. S3.4. H&E staining reveals increased necrotic tissue in FEC + oHSV-1 + CP treated mice

C57/Bl6 mice bearing E0771 tumors were treated with saline, FEC, oHSV-1, FEC + oHSV-1 or FEC + oHSV-1 + CP and tumors were harvested on days 7 and 10. Tumors were sectioned and stained with H&E for pathological analysis. (**A**) Representative images for tumors harvested on day 7. Each image shows a whole section of an individual tumor. (**B**) Representative images for tumors harvested on day 10. Each image shows a whole section of an individual tumor. (**C**) Whole tumor sections were scanned, and viable and necrotic cells were quantified using HALO quantification software. Each symbol represents an individual mouse within that group. Two-tailed paired t test was used for statistical analyses. Error bars are representative of the standard deviation.

FEC + oHSV-1 induces a B cell signature in whole tumor RNA sequencing

Immunohistochemistry (IHC) clearly demonstrates that treatment with oHSV-1 creates an initial influx of T cells into the TME. However, IHC is unable to determine the functionality and activation state of these T cells and more specifically, whether they are capable of contributing to a robust antitumor immune response. The therapeutic efficacy of oHSV-1 as a monotherapy (as shown in Figure 3.1C) shows that it is insufficient to limit tumor progression. To begin to understand how the addition of FEC mechanistically alters therapeutic responses to oHSV-1 treatment, we performed RNA sequencing analysis. Tumors were treated with saline, FEC, oHSV-1 or FEC + oHSV-1 and harvested on day 5. Principal component analysis (PCA) shows that while saline and FEC treated tumors cluster closely together, both oHSV-1 and FEC + oHSV-1 show distinct

clustering patterns (Figure 3.5A). Interestingly, within the FEC + oHSV-1 group we see two separate clusters of mice; one that has a similar expression profile to saline and FEC treated mice (thought to be non-responders to treatment) and one that clusters distinctly (thought to be responders to treatment), consistent with previous data that FEC + oHSV-1 therapy results in a dichotomous response.

Pathway enrichment analysis identified many immune pathways and processes that were upregulated with FEC + oHSV-1 therapy (as compared to saline, Figure 3.5B). Assessment of the differentially expressed gene pool (Figure 3.5C) reveals that mice treated with FEC show very similar genomic profiles to those treated with saline alone. However, treatment with either oHSV-1 or FEC + oHSV-1 shows a very different gene signature. Deeper analysis of these differentially expressed genes reveals that both oHSV-1 and FEC + oHSV-1 treatments upregulate many genes associated with the B cell lineage (Figure 3.5D, Table S3.1), including *Ifitm1*, *Il1b*, *CD24a*, *CXCL12*, *FGF7* and *Nrg1*.

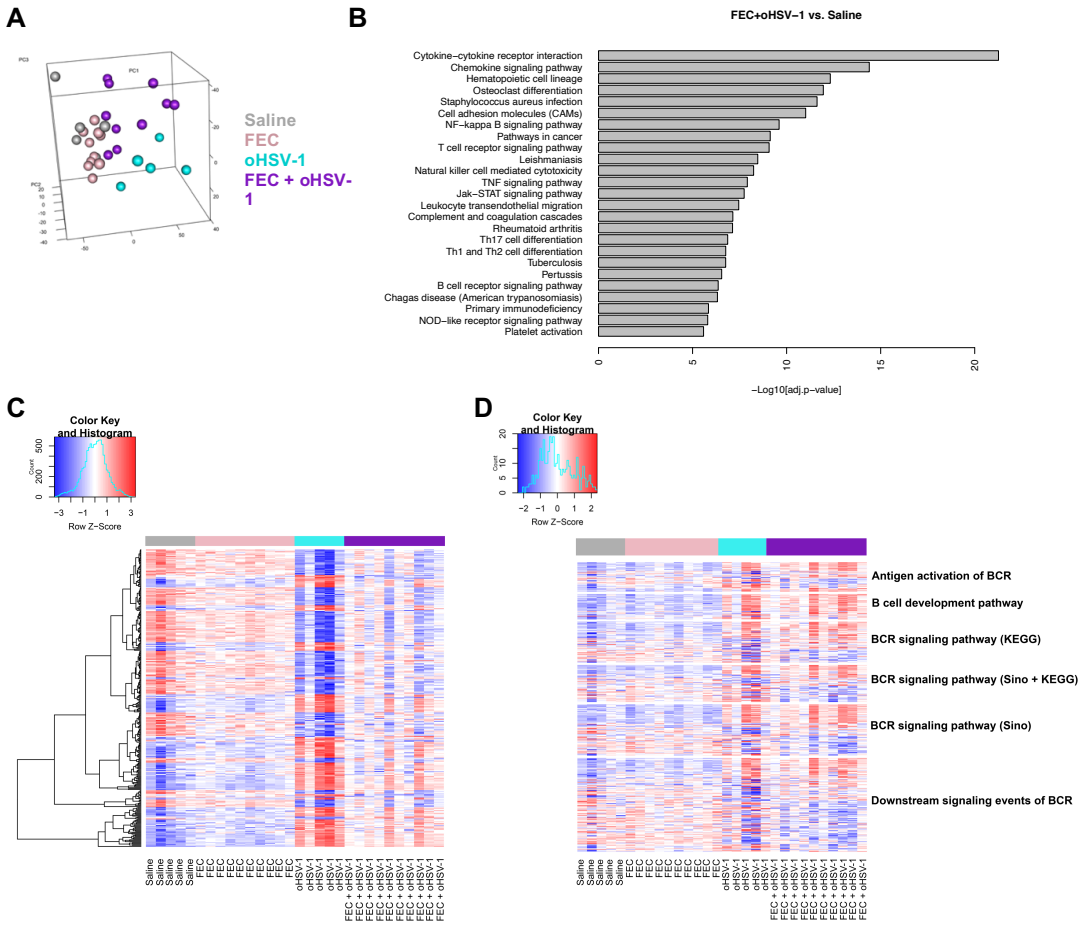

Fig. 3.5. FEC + oHSV-1 induces significant upregulation in RNA transcriptomes associated with immune processes and pathways and more specifically, B cell receptor signaling pathways.

(**A**) 3-D cluster plot showing the RNA expression correlations between mice treated with saline (grey; n=5), FEC (pink; n=10), oHSV-1 (teal; n=5) and FEC + oHSV-1 (purple; n=10). (**B**) Bar plot illustrating the results of pathway enrichment analysis performed on samples from mice treated with FEC + oHSV-1, compared to those treated with saline alone. (**C**) Heat map showing the normalized expression values of genes across all

samples. (**D**) Heat map showing the normalized expression values of genes associated with B cell receptor pathways. *BCR = B Cell Receptor.

Table S3.1. Differentially expressed genes associated with B cell pathways. *F = FEC, O = oHSV-1, S = Saline, BCR = B cell receptor, KEGG = Kyoto Encyclopedia of Genes and Genomes, Sino = Sino Biological

Gene	F + O vs. S	F + O vs. F	F + O vs. O	F vs. S	O vs. S	Function/Pathway
Ifitm1	18.18	8.92			37.14	BCR signaling pathway (KEGG)
Il1b	9.42	4.59			19.98	BCR signaling pathway (Sino)
Cd24a	7.77	5.30			15.22	B cell development pathway
Cxcl12	7.06	4.04			10.39	BCR signaling pathway (Sino)
Nrg1	5.55	3.70			6.72	Downstream signaling events of BCR
Fgf7	4.21	3.47			8.09	Downstream signaling events of BCR
Slamf6	3.95	3.62			3.56	BCR signaling pathway (Sino)
Il21r	3.41	2.75			3.48	B cell development pathway
Cd22	3.30	2.70			2.17	BCR signaling pathway (Sino + KEGG) Downstream signaling events of BCR Antigen activation of BCR B cell development pathway
Cd3g	3.29	3.41			3.94	BCR signaling pathway (Sino)
Rac2	3.29	3.10			3.46	BCR signaling pathway (Sino + KEGG)
Fcgr2b	3.25	2.48			3.44	BCR signaling pathway (Sino + KEGG)
Dok3	3.22	2.36			3.78	BCR signaling pathway (Sino)
Cd28	3.13	3.04			3.14	BCR signaling pathway (Sino) Downstream signaling events of BCR
Cd27	2.91	3.21			2.37	B cell development pathway
Creb3l1	2.91	2.65			2.66	BCR signaling pathway (Sino)
Cd3e	2.88	4.09			2.85	BCR signaling pathway (Sino) B cell development pathway
Ptprcap	2.81	2.98			3.70	BCR signaling pathway (Sino)

Cxcr4	2.81	2.47			3.50	B cell development pathway
Itk	2.81	2.41			2.48	Antigen activation of BCR
Btk	2.72	2.39			2.34	BCR signaling pathway (Sino) Antigen activation of BCR
Zap70	2.67	3.69				BCR signaling pathway (Sino)
Foxo1	2.66	2.25			3.32	BCR signaling pathway (KEGG) Downstream signaling events of BCR
Mef2c	2.63	2.88				BCR signaling pathway (Sino + KEGG)
Dclk1	2.61	2.69			2.37	BCR signaling pathway (Sino)
Pdcd1	2.60	2.59			2.93	B cell development pathway
Cd80	2.59	1.60			3.14	B cell development pathway Downstream signaling events of BCR
Camk4	2.58	3.63			2.63	BCR signaling pathway (Sino)
Fos	2.55	2.21			2.36	BCR signaling pathway (Sino + KEGG)
Adgre4		2.55				BCR signaling pathway (Sino)
Lcp2	2.54	2.31			2.61	BCR signaling pathway (Sino) Antigen activation of BCR
Irf4	2.54	1.99			2.52	BCR signaling pathway (KEGG)
Cd3d	2.50	2.78			3.73	BCR signaling pathway (Sino)
Cyp7b1		2.50			4.26	BCR signaling pathway (Sino)
Adap2	2.48	2.04			1.83	BCR signaling pathway (Sino)
Lat	2.44	4.02				BCR signaling pathway (Sino) Antigen activation of BCR
Ptprc	2.44	2.35			2.56	BCR signaling pathway (Sino + KEGG) B cell development pathway
Cd84	2.44	2.19			2.73	B cell development pathway
Ptpn18	2.44	2.09			3.36	BCR signaling pathway (KEGG)
Tnfrsf13b	2.44	2.00			2.74	B cell development pathway
Egr1	2.41	2.05			2.65	BCR signaling pathway (Sino)
Camk2b	2.39	2.12			2.54	BCR signaling pathway (Sino)
Pag1	2.37	2.38			1.94	BCR signaling pathway (KEGG)
Lilra6	2.35	2.35			2.39	BCR signaling pathway (KEGG)
Pik3cg	2.34	2.33			2.33	BCR signaling pathway (KEGG)
Cd244a	2.34	2.01			2.06	B cell development pathway
Cd5	2.32	2.70			2.77	B cell development pathway
Was	2.32	2.15			2.30	BCR signaling pathway (Sino)
Plcg2	2.32	2.03			1.92	BCR signaling pathway (KEGG)

						Downstream signaling events of BCR Antigen activation of BCR
Icos	2.28	3.41			2.39	B cell development pathway Downstream signaling events of BCR
Il4ra	2.27	2.11			1.87	B cell development pathway
Syk	2.26	2.34			1.81	BCR signaling pathway (Sino + KEGG) Antigen activation of BCR
Rassf5	2.19	1.83			2.44	BCR signaling pathway (Sino)
Rasgrp1	2.17	1.80			2.21	Downstream signaling events of BCR
Il10	2.17	1.76			2.26	B cell development pathway
Il7r	2.16	2.12			1.79	B cell development pathway
Il3ra	2.16	2.03			2.41	B cell development pathway
Cd69	2.14	1.55			2.56	B cell development pathway
Pou2f2	2.12	2.61				B cell receptor signaling pathway (KEGG)
Cd81	2.09	1.95			2.24	B cell receptor signaling pathway (KEGG)
Ptpn6	2.06	1.95			1.81	BCR signaling pathway (Sino + KEGG) Downstream signaling events of BCR Antigen activation of BCR
Vav3	2.04	1.97			1.73	BCR signaling pathway (KEGG) Antigen activation of BCR
Cd1d1	2.03	1.79			2.48	B cell development pathway
Lck	2.02	1.87			2.23	BCR signaling pathway (Sino) Downstream signaling events of BCR
Blnk	2.02	1.74				BCR signaling pathway (KEGG) Downstream signaling events of BCR Antigen activation of BCR
Cd86	2.02	1.72			2.12	B cell development pathway Downstream signaling events of BCR
Prkcb	2.01	2.41				BCR signaling pathway (Sino + KEGG) Downstream signaling events of BCR

Cd48	2.01	1.97			1.99	B cell development pathway
Cd4	1.99	1.85			2.16	BCR signaling pathway (Sino) B cell development pathway
Thy1	1.97	2.07			1.91	B cell development pathway
Vav1	1.97	1.63	-1.61		3.17	BCR signaling pathway (Sino + KEGG) Antigen activation of BCR Downstream signaling events of BCR
Spn	1.95	1.84			1.94	B cell development pathway
Cd72		1.93				BCR signaling pathway (KEGG)
Pik3ap1	1.89	1.96			1.68	BCR signaling pathway (KEGG) Downstream signaling events of BCR Antigen activation of BCR
Rasgrp3					1.86	BCR signaling pathway (KEGG) Downstream signaling events of BCR
Prkch	1.84	1.98			1.73	BCR signaling pathway (Sino)
Card11		1.83	2.01			BCR signaling pathway (KEGG) Downstream signaling events of BCR
Pax5			1.82		-1.87	B cell development pathway
Hcls1	1.79		-1.99		3.56	BCR signaling pathway (KEGG)
Map4k1					1.78	BCR signaling pathway (KEGG)
Cd34		1.77				B cell development pathway
Nfatc2	1.73	1.65				BCR signaling pathway (KEGG) Antigen activation of BCR
Nfkbia	1.73		-1.73		2.99	BCR signaling pathway (Sino + KEGG) Downstream signaling events of BCR
Hgf		1.71				Downstream signaling events of BCR
Rps6ka1	1.67	1.65			1.49	BCR signaling pathway (KEGG)
Lat2	1.66	1.52			1.87	BCR signaling pathway (Sino + KEGG)
Pik3cd	1.65	1.61				BCR signaling pathway (KEGG) Downstream signaling events of BCR Antigen activation of BCR
Tlr9		1.65	1.59			BCR signaling pathway (Sino)
Inpp5d	1.63		-2.35		3.83	BCR signaling pathway (KEGG)

Kit		1.63				B cell development pathway Downstream signaling events of BCR
Pnck			1.63		-1.95	BCR signaling pathway (Sino)
Malt1					1.63	BCR signaling pathway (Sino + KEGG) Downstream signaling events of BCR
Lyn	1.61	1.46			1.77	BCR signaling pathway (Sino + KEGG) Antigen activation of BCR Downstream signaling events of BCR
Cd83		1.59				B cell development pathway
Ikbke	1.54		-1.94	1.61	2.99	BCR signaling pathway (Sino)
Camk2a			1.54			BCR signaling pathway (Sino + KEGG)
Prr5	1.50					Downstream signaling events of BCR
Rac3			1.50			BCR signaling pathway (Sino + KEGG)
Egfr					1.48	Downstream signaling events of BCR
Prkcg		1.46				BCR signaling pathway (Sino)
Cd93	1.44	1.26	-1.40		2.03	B cell development pathway
Adap1	1.42	1.43			1.49	BCR signaling pathway (Sino)
Prkcd	1.41	1.28				BCR signaling pathway (Sino + KEGG)
Nfkbie	1.41				1.45	BCR signaling pathway (KEGG) Downstream signaling events of BCR
Cd38	1.40		-1.39		1.94	B cell development pathway
Pdgfb	1.38	1.44			1.43	Downstream signaling events of BCR
Tlr5		1.36	1.40			BCR signaling pathway (Sino)
Dapp1	1.34	1.33			1.37	BCR signaling pathway (KEGG) Downstream signaling events of BCR Antigen activation of BCR
Psmb10					1.34	Downstream signaling events of BCR
Mtor			1.33		-1.47	BCR signaling pathway (Sino)

						Downstream signaling events of BCR
Cdkn1a	1.32				1.61	Downstream signaling events of BCR
Trpc1			1.29		-1.39	Downstream signaling events of BCR Antigen activation of BCR
Pik3r1	1.28				1.48	BCR signaling pathway (Sino + KEGG) Downstream signaling events of BCR Antigen activation of BCR
Shc1			1.28		-1.43	BCR signaling pathway (KEGG) Downstream signaling events of BCR Antigen activation of BCR
Sh3bp2	1.27	1.27	1.25			BCR signaling pathway (KEGG)
Pip4k2a	1.27	1.22			1.28	Downstream signaling events of BCR
Nr4a1		1.27				Downstream signaling events of BCR
Il6ra			1.27		-1.50	B cell development pathway
Rel		1.26				BCR signaling pathway (Sino + KEGG) Downstream signaling events of BCR
Ubb			1.26		-1.32	Downstream signaling events of BCR
Psmd10	1.24				1.42	Downstream signaling events of BCR
Ppp2r5d			1.24		-1.39	Downstream signaling events of BCR
Phlpp2			1.24		-1.36	Downstream signaling events of BCR
Pdgfa	1.23		-1.33		1.63	Downstream signaling events of BCR
Pdk1			1.23		-1.46	BCR signaling pathway (Sino)
Sos1			1.23		-1.23	BCR signaling pathway (KEGG) Downstream signaling events of BCR Antigen activation of BCR
Tecr			1.21			BCR signaling pathway (KEGG)

Sh3kbp1					1.21	Downstream signaling events of BCR Antigen activation of BCR
Vav2	1.20	1.22				BCR signaling pathway (KEGG) Antigen activation of BCR
Stat3	1.20				1.23	B cell development pathway
Akt3			1.20		-1.43	BCR signaling pathway (Sino + KEGG) Downstream signaling events of BCR
Foxo4			1.20		-1.39	Downstream signaling events of BCR
Frs2			1.20		-1.31	Downstream signaling events of BCR
Elk1			1.20			BCR signaling pathway (Sino + KEGG)
Map3k1					1.20	BCR signaling pathway (KEGG)
Clta	1.19	1.14			1.32	BCR signaling pathway (Sino)
Gtf2i			1.18		-1.33	BCR signaling pathway (KEGG)
Src			1.18		-1.30	Downstream signaling events of BCR
Map3k3			1.18		-1.29	BCR signaling pathway (Sino)
Tsc2			1.18		-1.20	Downstream signaling events of BCR
Akt1s1			1.17		-1.20	BCR signaling pathway (Sino) Downstream signaling events of BCR
Dok1					1.17	BCR signaling pathway (KEGG)
Mdm2	1.16			1.17	1.30	Downstream signaling events of BCR
Pik3cb				1.17		BCR signaling pathway (Sino + KEGG) Downstream signaling events of BCR
Rasa1			1.16		-1.14	BCR signaling pathway (KEGG)
Grb2	1.15	1.10			1.26	BCR signaling pathway (KEGG) Downstream signaling events of BCR Antigen activation of BCR
Mapk12			1.15		-1.29	BCR signaling pathway (Sino)
Rapgef1			1.14		-1.19	BCR signaling pathway (KEGG)
Csk	1.13	1.13	1.15			BCR signaling pathway (KEGG)

Itpr1	1.12		1.14			Downstream signaling events of BCR Antigen activation of BCR
Ago1			1.12		-1.21	Downstream signaling events of BCR
Capn1			1.12		-1.21	BCR signaling pathway (Sino)
Traf6			1.12		-1.13	BCR signaling pathway (KEGG)
Calm3			1.12			BCR signaling pathway (Sino + KEGG) Downstream signaling events of BCR Antigen activation of BCR
Gnai3			1.11		-1.20	BCR signaling pathway (Sino)
Nfatc3			1.11		-1.19	BCR signaling pathway (Sino + KEGG) Antigen activation of BCR
Apbb1ip	1.10	1.07				BCR signaling pathway (Sino)
Gab2			1.10			BCR signaling pathway (Sino + KEGG)
Akt1			1.09		-1.15	BCR signaling pathway (Sino + KEGG) Downstream signaling events of BCR
Mapk8					1.09	BCR signaling pathway (Sino + KEGG)
Capns1	1.08	1.07				BCR signaling pathway (Sino)
Cdc42		1.08	-1.12		1.23	BCR signaling pathway (Sino + KEGG)
Inppl1			1.08			BCR signaling pathway (KEGG)
Mapk14		1.07	1.16		-1.12	BCR signaling pathway (Sino + KEGG)
Mapk7		-1.06	-1.13		1.12	BCR signaling pathway (Sino)
Max		-1.06	-1.11			BCR signaling pathway (KEGG)
Psmc2	-1.07	-1.06			-1.08	Downstream signaling events of BCR
Mef2d	-1.07	-1.06				BCR signaling pathway (KEGG)
Ppp3r1		-1.07	-1.11			BCR signaling pathway (Sino + KEGG) Antigen activation of BCR
Ywhab	-1.08	-1.07	-1.10			BCR signaling pathway (Sino)
Csnk2a1	-1.08		-1.11			BCR signaling pathway (KEGG)
Psma3	-1.08					Downstream signaling events of BCR

Psmb1			-1.08			Downstream signaling events of BCR
Ppp2cb			-1.08			Downstream signaling events of BCR
Bcap29		-1.08				BCR signaling pathway (Sino)
Psmc5		-1.08	-1.12			Downstream signaling events of BCR
Mapkap 1	-1.09	-1.07			-1.10	Downstream signaling events of BCR
Pip5k1a	-1.09		1.07		-1.17	BCR signaling pathway (KEGG) Downstream signaling events of BCR
Mapk9		-1.09	-1.14		1.12	BCR signaling pathway (Sino + KEGG)
Jun		-1.09				BCR signaling pathway (Sino + KEGG)
Psmd12		-1.09				Downstream signaling events of BCR
Nck1			-1.09			BCR signaling pathway (KEGG) Downstream signaling events of BCR
Creb1			-1.09			BCR signaling pathway (Sino + KEGG) Downstream signaling events of BCR
Psmd2			-1.09			Downstream signaling events of BCR
Calm2	-1.10	-1.07	-1.11			BCR signaling pathway (Sino + KEGG) Downstream signaling events of BCR Antigen activation of BCR
Prkci	-1.10	-1.13	-1.12			BCR signaling pathway (Sino)
Bcap31	-1.10				-1.12	BCR signaling pathway (Sino)
Pdpk1	-1.10		1.10		-1.21	BCR signaling pathway (KEGG) Downstream signaling events of BCR
Psme3		-1.10				Downstream signaling events of BCR
Psmd3		-1.10				Downstream signaling events of BCR
Psmd9		-1.10				Downstream signaling events of BCR

Bcl2l1			-1.10		1.14	BCR signaling pathway (Sino)
Tln2	-1.11	-1.16			-1.23	BCR signaling pathway (Sino)
E2f3	-1.11					BCR signaling pathway (KEGG)
Ppp2r1a	-1.11		1.10		-1.22	Downstream signaling events of BCR
Ppp2ca		-1.11				Downstream signaling events of BCR
Pten			-1.11			BCR signaling pathway (Sino + KEGG) Downstream signaling events of BCR
Rap1a			-1.11			BCR signaling pathway (Sino)
Psmb4			-1.11			Downstream signaling events of BCR
Calm1			-1.11		1.16	BCR signaling pathway (Sino + KEGG) Downstream signaling events of BCR Antigen activation of BCR
Psmc4					-1.11	Downstream signaling events of BCR
Ptpn11	-1.12	-1.08			-1.10	BCR signaling pathway (Sino + KEGG) Downstream signaling events of BCR
Gab1	-1.12		1.10		-1.23	BCR signaling pathway (Sino + KEGG) Downstream signaling events of BCR
Ppp3ca		-1.12	-1.27		1.19	BCR signaling pathway (Sino + KEGG) Antigen activation of BCR
Fbxw11		-1.12				Downstream signaling events of BCR
Atf4		-1.12	-1.19			BCR signaling pathway (Sino)
Plcg1	-1.13	-1.11	1.16		-1.32	BCR signaling pathway (KEGG) Downstream signaling events of BCR Antigen activation of BCR
Tnrc6b	-1.13					Downstream signaling events of BCR
Kras	-1.13				-1.13	BCR signaling pathway (Sino + KEGG)

						Downstream signaling events of BCR
Map2k3		-1.13				BCR signaling pathway (Sino)
Creb3l2		-1.13			-1.18	BCR signaling pathway (Sino)
Actn4		-1.13			-1.18	BCR signaling pathway (Sino)
Nfkb1			-1.13		1.16	BCR signaling pathway (Sino + KEGG) Downstream signaling events of BCR
Map3k7					-1.13	BCR signaling pathway (Sino + KEGG) Downstream signaling events of BCR
Bcl10			-1.14		1.14	BCR signaling pathway (KEGG) Downstream signaling events of BCR
Camk1	-1.14	-1.12				BCR signaling pathway (Sino)
Psme4		-1.12			-1.19	Downstream signaling events of BCR
Tnrc6c	-1.14				-1.13	Downstream signaling events of BCR
Pip4k2b		-1.14				Downstream signaling events of BCR
Map2k2			-1.14			BCR signaling pathway (Sino + KEGG)
Braf					-1.15	BCR signaling pathway (KEGG)
Ppp2r5a			-1.15		1.15	Downstream signaling events of BCR
Mlst8	-1.15	-1.08			-1.23	Downstream signaling events of BCR
Capn2	-1.15	-1.13			-1.19	BCR signaling pathway (Sino)
Prkce		-1.16				BCR signaling pathway (Sino)
Rps6kb1			-1.15		1.14	BCR signaling pathway (Sino)
Sem1			-1.15		1.17	Downstream signaling events of BCR
Nras			-1.16		1.13	BCR signaling pathway (Sino + KEGG) Downstream signaling events of BCR
Cdkn1b			-1.16			Downstream signaling events of BCR
Btrc					-1.17	Downstream signaling events of BCR

Pik3r2	-1.17	-1.12	1.14		-1.33	BCR signaling pathway (Sino + KEGG) Downstream signaling events of BCR
Crk	-1.17	-1.13				BCR signaling pathway (KEGG)
Map3k2	-1.17	-1.18				BCR signaling pathway (Sino)
Pdgfrb		-1.18	-1.30			Downstream signaling events of BCR
Erbb2		-1.18				Downstream signaling events of BCR
Pik3ca		-1.18	-1.25			BCR signaling pathway (Sino + KEGG) Downstream signaling events of BCR
Mapk1			-1.18			BCR signaling pathway (Sino + KEGG) Downstream signaling events of BCR
Rap1b			-1.18		1.34	BCR signaling pathway (Sino)
Fgfr1	-1.20	-1.19				Downstream signaling events of BCR
Phlpp1	-1.20	-1.21			-1.25	Downstream signaling events of BCR
Trib3	-1.21	-1.19				Downstream signaling events of BCR
Mov10	-1.22	-1.16			-1.22	Downstream signaling events of BCR
Insr					-1.22	Downstream signaling events of BCR
Foxo3					-1.24	Downstream signaling events of BCR
Ezr					-1.24	BCR signaling pathway (Sino)
Myc	-1.25	-1.17			-1.34	BCR signaling pathway (KEGG)
Camk1d		-1.17				BCR signaling pathway (Sino)
Prkca	-1.25	-1.18			-1.36	BCR signaling pathway (Sino)
Pir	-1.25	-1.25	-1.28			BCR signaling pathway (Sino)
Ppp2r5e					-1.26	Downstream signaling events of BCR
Itpr3	-1.26	-1.28			-1.32	Downstream signaling events of BCR Antigen activation of BCR
Ppp3cb			-1.27		1.21	BCR signaling pathway (KEGG) Antigen activation of BCR

Rac1			-1.27		1.23	BCR signaling pathway (Sino + KEGG)
Bad					-1.30	Downstream signaling events of BCR
Cul1					-1.30	Downstream signaling events of BCR
Pdgfra			-1.38		1.30	Downstream signaling events of BCR
Pip5k1c		-1.39	-1.41			BCR signaling pathway (KEGG) Downstream signaling events of BCR
Capn5	-1.40	-1.35			-1.61	BCR signaling pathway (Sino)
Sos2					-1.43	BCR signaling pathway (KEGG)
Cblb			-1.44		1.63	Downstream signaling events of BCR Antigen activation of BCR
Sh3bp5			-1.45		1.81	BCR signaling pathway (KEGG)
Orai1			-1.49		1.82	BCR signaling pathway (Sino) Downstream signaling events of BCR Antigen activation of BCR
Hbegf			-1.66		1.95	Downstream signaling events of BCR
Txk			-1.67		2.61	Antigen activation of BCR
Nrg2		-1.69				Downstream signaling events of BCR
Btc					-1.70	Downstream signaling events of BCR
Cd40			-1.70		2.01	BCR signaling pathway (Sino) B cell development pathway
Prdm1			-1.71		2.13	B cell development pathway
Fyn			-1.71		2.02	BCR signaling pathway (KEGG) Downstream signaling events of BCR Antigen activation of BCR
Itpr2			-1.72		1.72	Downstream signaling events of BCR Antigen activation of BCR
Map2k6		-1.78	-2.63		2.22	BCR signaling pathway (Sino + KEGG)
Ets1			-2.31		2.06	BCR signaling pathway (Sino + KEGG)
Sla2			-5.04		4.11	BCR signaling pathway (Sino)

Depletion of B cells results in loss of therapeutic efficacy

While B cells play many different roles in the body, their primary function is in antibody production. To follow-up on the results of RNA sequencing analysis and to determine whether or not B cells play a key part in the efficacy of our combination therapies, we performed B cell depletion studies. Subcutaneous E0771 tumors were grown in C57/Bl6 mice and circulating B cells were depleted using an anti-CD20 antibody (Figure 3.6A).[34] Analysis of the overall survival shows that the depletion of B cells diminished therapeutic outcome in tumor-bearing mice (Figure 3.6B and C, Fig. S3.5). Depletion was confirmed via flow cytometry (Figure 3.6D) and an isotype antibody was used as a control. Bulk antibody production levels were also assessed using an indirect ELISA assay. Serum was taken from naïve mice, tumor-bearing mice and from therapeutically treated mice on day 15 and protein lysates from E0771 cells were used to coat the plates. Results of the ELISA assay indicates that FEC alone has no effect on antibody production levels. However, treatment with oHSV-1, CP, FEC + oHSV-1 and FEC + oHSV-1 + CP all show a statistically significant increase in antibody production levels, which is lower in the absence of circulating B cells (Figure 3.6E). Since oHSV-1 or CP alone confer no therapeutic benefit, these data suggest that antibody production, while affected by our therapies, is not the most important function of B cells in relation to our therapeutic efficacy.

To further assess the role B cells play in our treatment, mice were injected with either an anti-CD20 antibody or an isotype antibody, treated with saline or FEC + oHSV-1 and tumors harvested on day 7. Quantification of IHC images shows that B cell

depletion results in decreased levels of tumor-infiltrating T cells and increased levels of $Ly6G^+$ myeloid cells (Figure S3.6A). Immunofluorescence (IF) staining was performed on whole tumor sections and stained for CD3, CD8, PNAd, Pax5 and CD11b. Analysis of multiplex images further corroborates the IHC quantification data and shows that mice treated with FEC + oHSV-1, in the presence of the isotype antibody, had formation of immature tertiary lymphoid structures (as evidenced by the presence of $PNAd^+$ high endothelial venules) (Figure S3.6B). Conversely, mice treated with FEC + oHSV-1, in the presence of the anti-CD20 antibody, have no PNAd present and no organized lymphoid aggregates (Figure S3.6C).

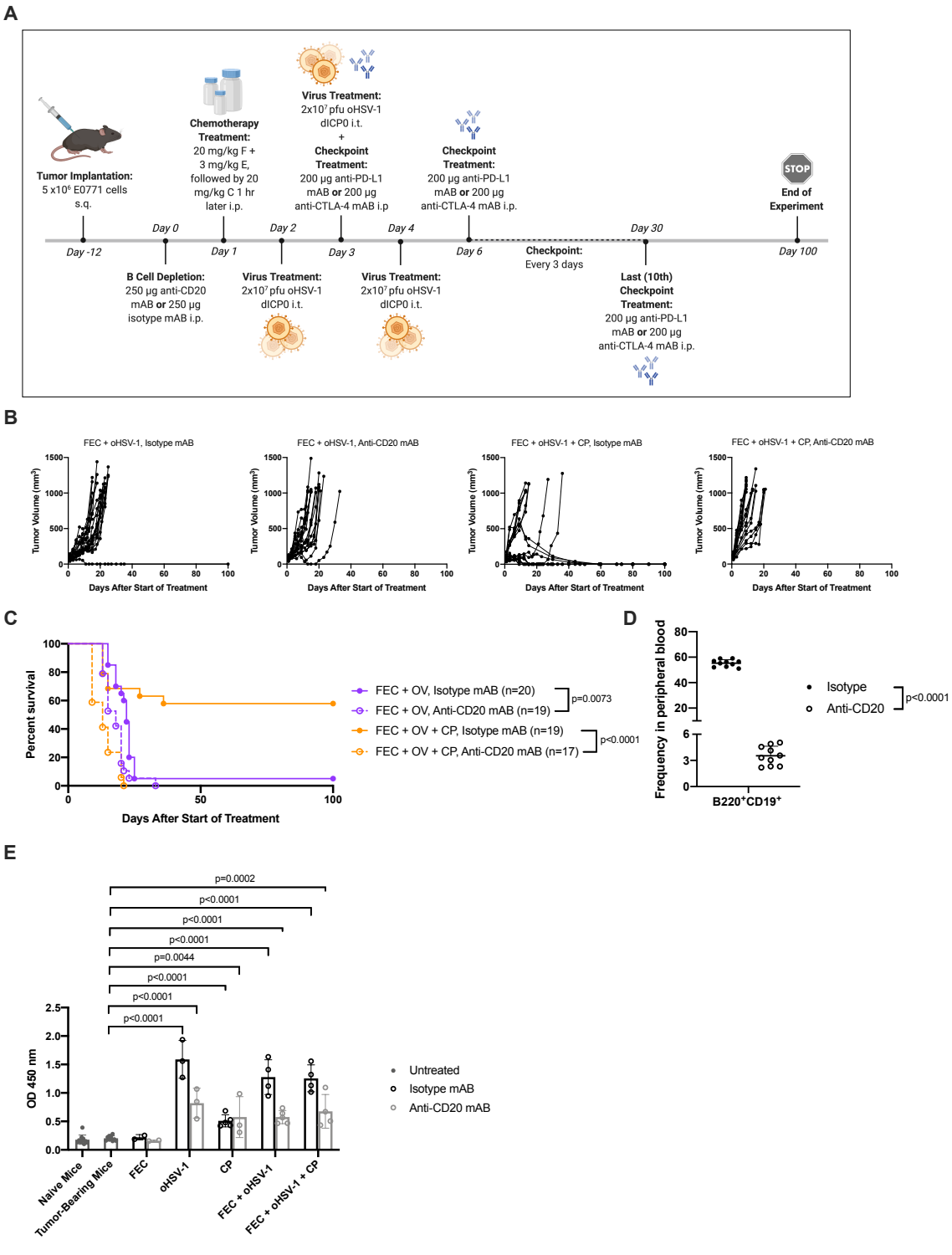
A
Tumor Implantation:
5 x10⁶ E0771 cells
s.q.
Chemotherapy Treatment:
20 mg/kg F +
3 mg/kg E,
followed by 20
mg/kg C 1 hr
later i.p.
Virus Treatment:
2x10⁷ pfu oHSV-1
dICP0 i.t.
+
Checkpoint Treatment:
200 µg anti-PD-L1
mAB or 200 µg
anti-CTLA-4 mAB i.p
Checkpoint Treatment:
200 µg anti-PD-L1
mAB or 200 µg
anti-CTLA-4 mAB i.p.
STOP
End of Experiment
Day -12
Day 0
Day 1
Day 2
Day 3
Day 4
Day 6
Checkpoint:
Every 3 days
Day 30
Day 100
B Cell Depletion:
250 µg anti-CD20
mAB or 250 µg
isotype mAB i.p.
Virus Treatment:
2x10⁷ pfu oHSV-1
dICP0 i.t.
Virus Treatment:
2x10⁷ pfu oHSV-1
dICP0 i.t.
Last (10th) Checkpoint Treatment:
200 µg anti-PD-L1
mAB or 200 µg
anti-CTLA-4 mAB i.p.
B
FEC + oHSV-1, Isotype mAB
FEC + oHSV-1, Anti-CD20 mAB
FEC + oHSV-1 + CP, Isotype mAB
FEC + oHSV-1 + CP, Anti-CD20 mAB
Tumor Volume (mm³)
Days After Start of Treatment
C
Percent survival
Days After Start of Treatment
FEC + OV, Isotype mAB (n=20)
FEC + OV, Anti-CD20 mAB (n=19)
FEC + OV + CP, Isotype mAB (n=19)
FEC + OV + CP, Anti-CD20 mAB (n=17)
p=0.0073
p<0.0001
D
Frequency in peripheral blood
B220⁺CD19⁺
Isotype
Anti-CD20
p<0.0001
E
OD 450 nm
p=0.0002
p<0.0001
p<0.0001
p<0.0001
p=0.0044
p<0.0001
p<0.0001
p<0.0001
Naive Mice
Tumor-Bearing Mice
FEC
oHSV-1
CP
FEC + oHSV-1
FEC + oHSV-1 + CP
Untreated
Isotype mAB
Anti-CD20 mAB

Fig. 3.6. Depletion of B cells results in loss of efficacy in mice treated with FEC + oHSV-1.

(**A**) C57/Bl6 mice bearing E0771 tumors were treated with either an anti-CD20 antibody or isotype antibody, followed by treatment with saline, FEC, oHSV-1, CP, FEC + oHSV-1 or FEC + oHSV-1 + CP therapy. *Created using BioRender.com. (**B**) Tumor volumes were measured every 2-3 days from the start of treatment until mice reached endpoint. Each line represents individual mice within the group. (**C**) Kaplan- Meier survival curves of combination therapy treatments, with both the depletion and isotype antibodies. (**D**) Flow cytometry confirmed that a singular dose of an anti-CD20 antibody is sufficient to deplete B cells within 24 hours of administration. (**E**) Bar plot showing bulk IgG production levels from naïve mice, tumor-bearing mice and therapeutically treated mice. *Mantel-Cox test was used for statistical analyses in (**C**), two-tailed paired t test was used for statistical analyses in (**D**) and two-tailed unpaired t test was used for statistical analyses in (**E**). Error bars are representative of the standard deviation.

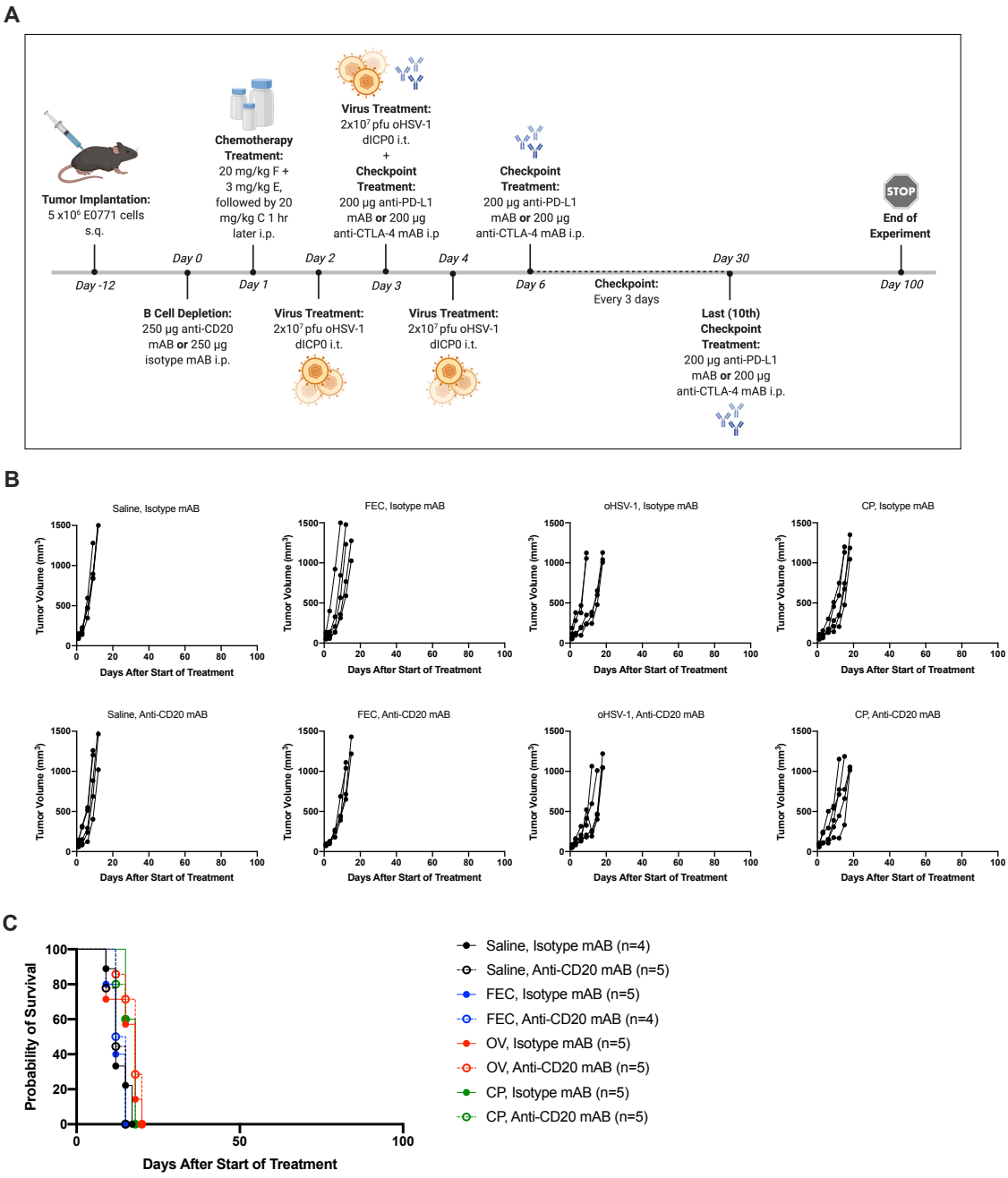

Fig. S3.5. B cells are required for therapeutic efficacy of combination therapies.

(**A**) C57/Bl6 mice bearing E0771 tumors were treated with anti-CD20 mAB or isotype mAB 24hr prior to the start of treatment. Groups of mice were then treated with saline,

FEC, oHSV-1, CP, FEC + oHSV-1 or FEC + oHSV-1 + CP. *Created using BioRender.com. (**B**) Tumor volumes were measured every 2-3 days from the start of treatment until mice reached endpoint (tumor volume > 1000 mm^3). Each line represents individual mice within the group. (**B**) Kaplan- Meier survival curves of each group.

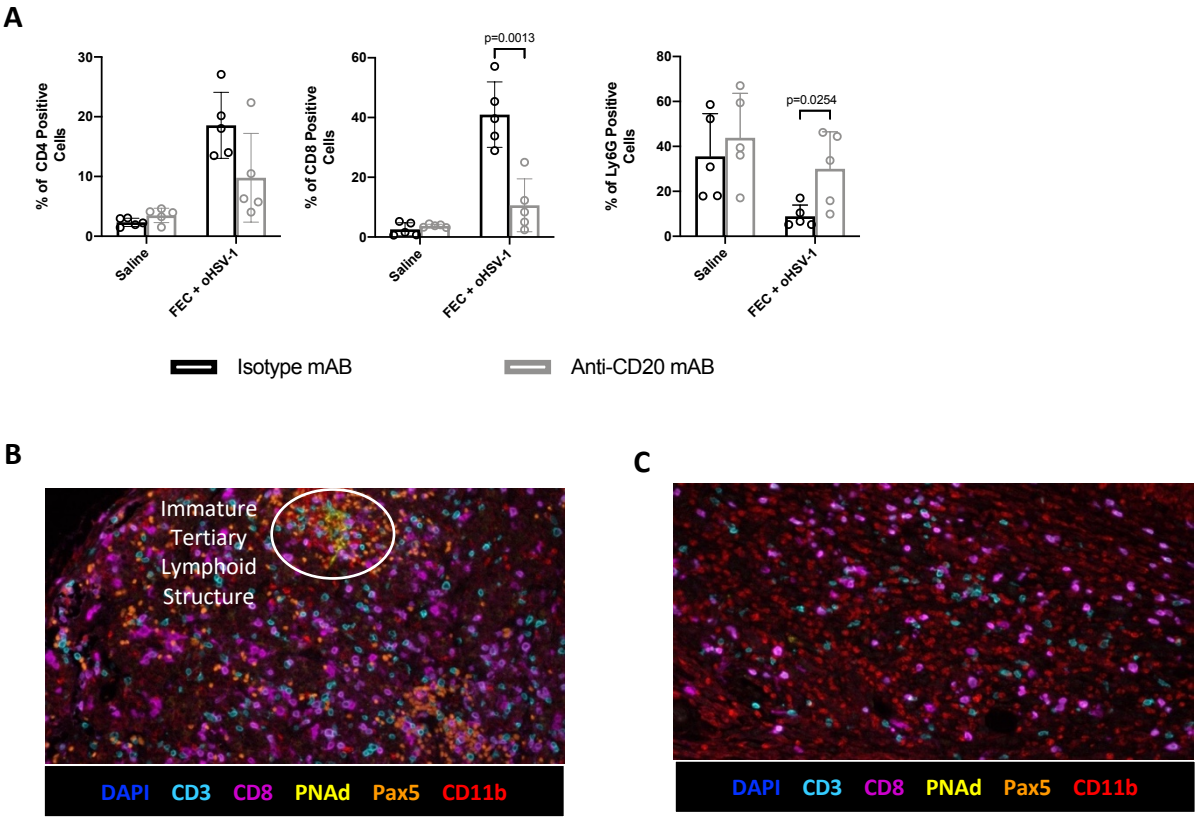

Fig. S3.6. Depletion of B cells results in disruption of immune cell organization.

(**A**) Whole tumor sections were scanned and quantified using HALO quantification software. Each symbol represents an individual mouse within that group. (**B**) Multi-panel IF staining with DAPI, as well as antibodies to stain for CD3 (light blue), CD8 (magenta), PNAd (yellow), Pax5 (orange) and CD11b (red). *Two-tailed unpaired t test was used for statistical analyses. Error bars represent the standard deviation.

B cells are required for control of MDSCs and resultant therapeutic efficacy

Depletion of circulating B cells results in a complete loss of therapeutic efficacy and disruption to immune cell organization in mice treated with FEC + oHSV-1 therapy. What remains unknown is how the addition of FEC mechanistically alters therapeutic outcome to oHSV-1 therapy and what effector cell functions are being regulated by tumor-infiltrating B cells (TIL-Bs). We performed a deeper assessment into the differentially expressed gene pool from RNA sequencing data, paying particular attention to the differences between oHSV-1 and FEC + oHSV-1 therapy. In this comparison we see many genes that are implicated in immunosuppressive MDSCs. Interestingly, some of these genes (*S100A8*, *CXCL2*, *CXCL1*, *Ly6G*, *Slpi*, *Fpr2*) are upregulated in oHSV-1 vs. saline but downregulated in FEC + oHSV-1 vs. oHSV-1 (Table 3.1, Figure 3.7A), suggesting that FEC + oHSV-1 therapy is able to not only upregulate B cell receptor signaling pathways, but also regulate the maturation and migration of MDSCs. It is well established in the literature that some chemotherapies (including 5-fluorouracil in particular) directly deplete MDSCs in both animal models as well as in patients[35–37]. However, in such studies chemotherapy is given in dose-dense cytotoxic regimens. In our hands, chemotherapy is being used as a low dose, immune-stimulatory intervention and shows no therapeutic efficacy alone, suggesting that it is unable to suppress MDSCs without the addition of oHSV-1.

To further investigate the relationship between these distinct cell types, we performed immune analysis studies. E0771 tumors were grown in C57/Bl6 mice and treated with saline, FEC, oHSV-1, CP, FEC + oHSV-1 or FEC + oHSV-1 + CP in both

the presence (isotype mAb) and absence (anti-CD20 mAb) of circulating B cells. Blood was drawn on days 6, 10 and 15 and peripheral blood mononuclear cells (PBMCs) were analyzed via flow cytometry. While this analysis confirmed the depletion of circulating B cells in mice treated with our anti-CD20 mAB (Figure 3.7B), it also revealed a striking and consistent difference in the population of MDSCs ($Ly6G^{hi}Ly6C^{int}$ cells) between mice treated with isotype and anti-CD20 antibodies (Figure 3.7C). Analysis of the frequency of these populations shows that circulating B cells in isotype-treated mice decrease over time in all treatment groups, except for those mice treated with FEC + oHSV-1 + CP (Figure 3.7D). On the contrary, mice treated with the triple combination therapy see a re-population of circulating B cells by day 15. The frequency of MDSCs in the blood (Figure 3.7E) confirms that there is rapid expansion of the granulocytic MDSC population, with the frequency more than doubling in B cell-depleted mice treated with triple therapy. Levels of other immune cell populations in the blood (CD4s, CD8s, monocytes and DCs) are consistent with expected findings, with no clear disturbance in their frequencies in the absence of B cells (Figure S3.7).

To rule out the clonal effect and assess whether or not the correlation between B cells and MDSCs holds true across more than one TNBC tumor model, we also conducted immune analysis using the PY230 murine breast cancer line (Figure S3.8). Here too, we see that when mice are treated with FEC + oHSV-1 + CP and depleted of circulating B cells, there is a prominent expansion of MDSCs in the blood. These data suggest that the correlation between B cells and MDSCs is not due to tumor clonality, but rather carries over between different models.

Table 1. MDSC Genes Differentially Expressed Between FEC + oHSV-1 and oHSV-1 treatments.

Gene	O Vs. S	F + O Vs. O	Function
S100A9	2730.36	-9.79	Associated with MDSC-mediated resistance to chemotherapy [38,39] Implicated in MDSC-driven metastasis [40] Associated with MDSC activation and suppressive function [41]
CXCL3	411.80	-5.87	MDSC activation and recruitment [42,43]
CXCR2	345.58	-6.20	Phenotypic marker of MDSCs [44] Myeloid cell differentiation and migration in the tumor microenvironment [43,45] MDSC recruitment [46]
CSF3	282.48	-9.38	Gene encoding G-CSF, critical to the accumulation of MDSCs [40]
S100A8	242.56	-6.44	Implicated in MDSC-driven metastasis [40]
CXCL2	233.83	-5.11	MDSC proliferation and chemotaxis [38,43] MDSC activation and recruitment [43]
CXCL1	120.11	-7.78	MDSC activation and recruitment [43]
TREM1	45.37	-3.01	MDSC marker [47]
NOS2	44.63	-4.06	MDSC-driven metastasis and T-cell suppression [40]
ARG2	41.34	-3.11	Associated with MDSC-mediated suppression [41]
LY6G	16.52	-7.04	Phenotypic marker of MDSCs [43,44] MDSC-driven metastasis [40]
SLPI	10.04	-1.96	MDSC differentiation [48,49]
FPR2	9.38	-2.00	Receptor for SAA3, a well-known inflammatory factor that connects MDSCs with cancer progression [50]
IL1R1	5.43	-4.11	MDSC-driven metastasis [51]
ADAM19	5.34	-3.47	STAT pathway differentiation of MDSCs [52]
SERPIND1	4.41	-4.23	MDSC proliferation and migration [53]
ITGB2	3.73	-1.98	MDSC effector function [54]
LY6C1	3.05	-4.17	Phenotypic marker of MDSCs [38,43,44,55]
PEAR1	2.76	-3.47	MDSC differentiation [56]
FYN	2.02	-1.71	Differentiates MDSCs from DCs [57]
CD38	1.94	-1.39	Phenotypic marker of MDSCs [44]
SOCS1	1.65	-1.25	MDSC induction [58]
ATRAID	1.22	-1.21	MDSC differentiation [44,59,60]

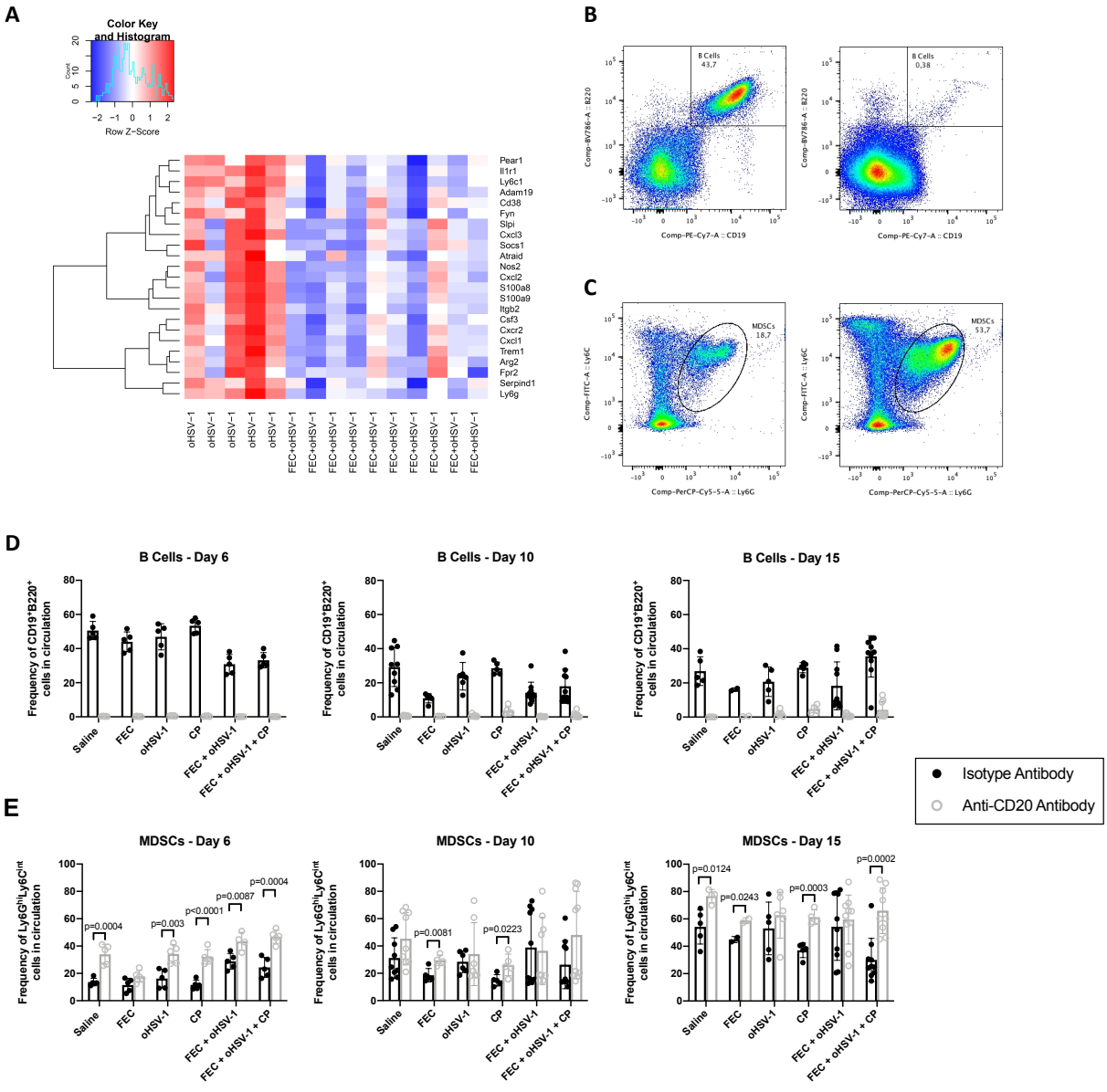

Fig. 3.7. Absence of circulating B cells results in rapid expansion of granulocytic MDSCs.

C57/Bl6 mice bearing E0771 tumors were treated with either an anti-CD20 mAB or isotype mAB, followed by treatment with saline, FEC, oHSV-1, CP, FEC + oHSV-1 or FEC + oHSV-1 + CP. Blood was drawn on days 6, 10 and 15 and analyzed via flow

cytometry. (**A**) Heat map showing selected MDSC-related genes and their expression across all oHSV-1 and FEC+ oHSV-1 samples, as determined by whole tumor RNA sequencing analysis. (**B**) Representative flow plot showing the gating strategy for B cells ($CD19^{+}B220^{+}$ cells) in mice treated with the isotype mAB (left) and an anti-CD20 mAB (right). (**C**) Representative flow plot showing the gating strategy for MDSCs ($Ly6G^{hi}Ly6C^{int}$ cells) in mice treated with the isotype mAB (left) and the anti-CD20 mAB (right). (**D**) Bar plots showing the frequency of B cells in circulation across all timepoints. **(E**) Bar plots showing the frequency of MDSCs in circulation across all timepoints. *Two-tailed unpaired t test was used for statistical analyses. Error bars are representative of standard deviation.

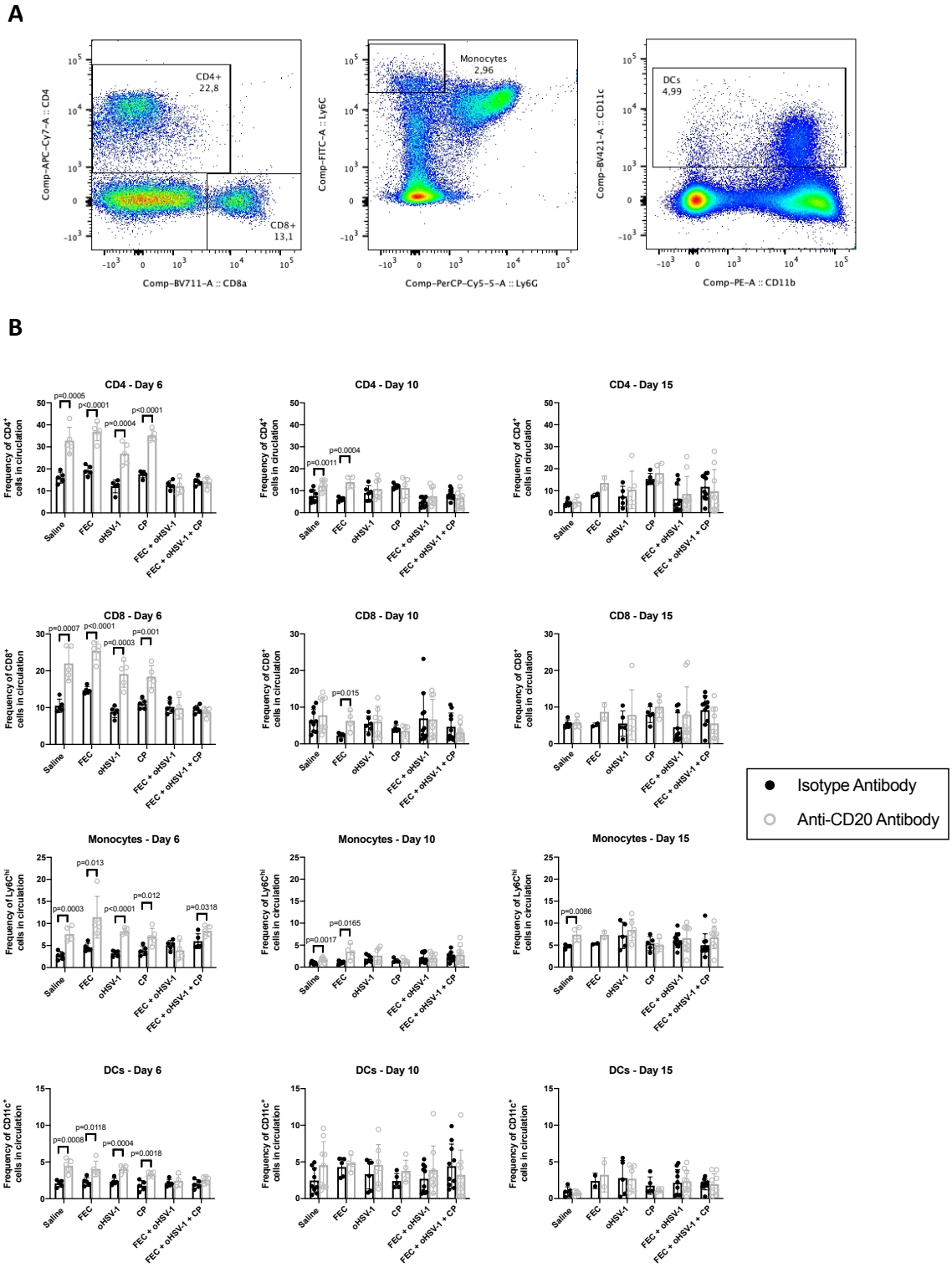

Fig. S3.7. Immune analysis of $CD4^+$, $CD8^+$, monocytes and DCs.

C57/Bl6 mice bearing E0771 tumors were treated with saline, FEC, oHSV-1, CP, FEC + oHSV-1 or FEC + oHSV-1 + CP. Half of the mice were treated with an isotype mAB and half were treated with an anti-CD20 mAB. Blood was drawn on days 6, 10 and 15 and analyzed via flow cytometry. (**A**) Representative flow plot showing the gating strategy for $CD4^+$, $CD8^+$, monocytes ($Ly6C^{hi}Ly6G^-$ cells) and DCs ($CD11c^+$). (**B**) Bar plots showing the frequency of immune cells in circulation across all timepoints. Two-tailed unpaired t test was used for statistical analyses. Error bars are representative of standard deviation.

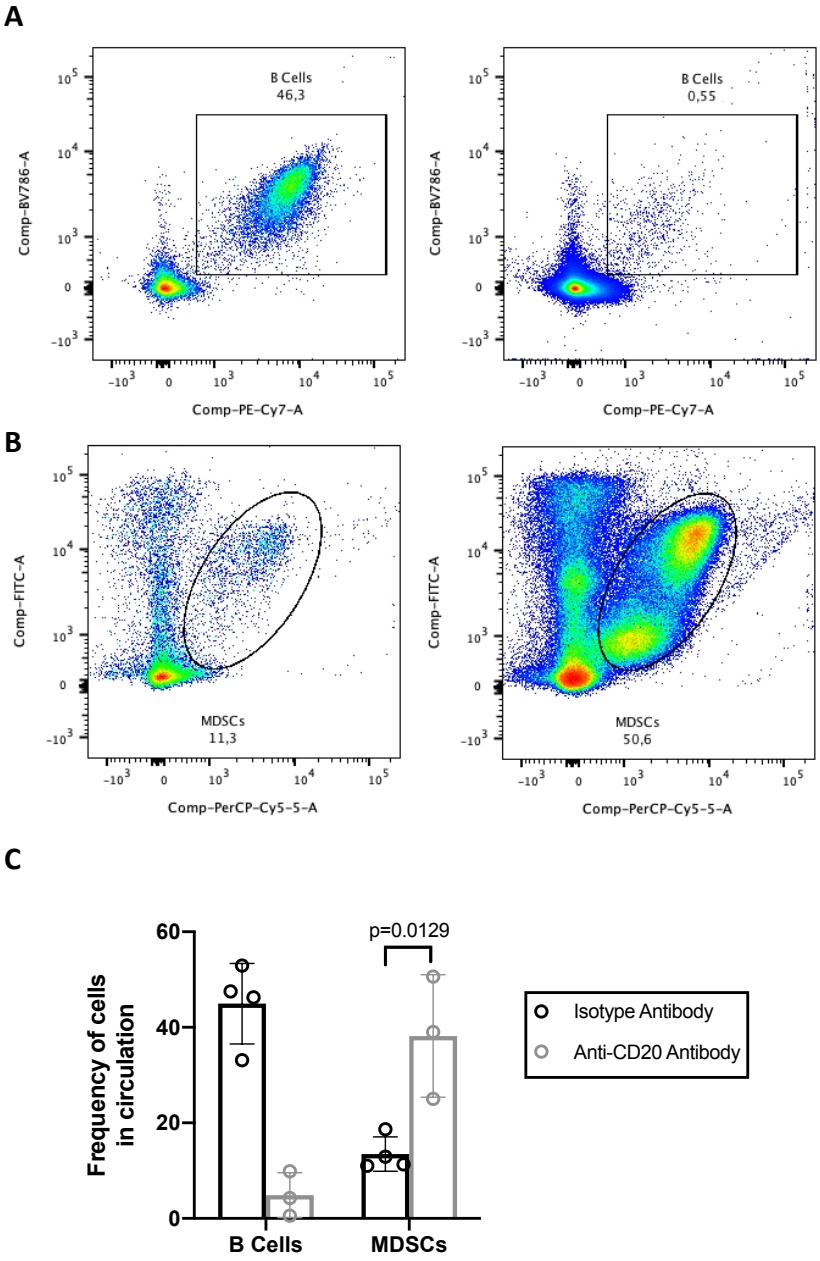

Fig. S3.8. Immune analysis of B cells and MDSCs in PY230 tumors.

C57/Bl6 mice bearing PY230 tumors were treated with FEC + oHSV-1 + CP. Half of the mice were treated with an isotype mAB and half were treated with an anti-CD20 mAB. Blood was drawn on day 29 and analyzed via flow cytometry. (**A**) Representative flow

plots showing the gating strategy for B cells ($CD19^+B220^+$ cells). The left plot shows a mouse treated with isotype mAB and the right plot shows a mouse treated with anti-CD20 mAB. (**B**) Representative flow plots showing the gating strategy for MDSCs ($Ly6C^{int}Ly6G^{hi}$ cells). The left plot shows a mouse treated with isotype mAB and the right plot shows a mouse treated with anti-CD20 mAB. (**C**) Frequency of B cells and MDSCs, as determined by flow cytometry. Two-tailed unpaired t test was used for statistical analyses. Error bars are representative of standard deviation.

B cells are required to alleviate tumor immunosuppressive mechanisms

To assess whether changes seen in the peripheral blood were consistent and representative of what was happening in the tumor, immune analysis was performed on TILs. E0771 tumors were grown in C57/Bl6 mice and treated with saline, FEC, oHSV-1, CP, FEC + oHSV-1 or FEC + oHSV-1 + CP in both the presence (isotype mAb) and absence (anti-CD20 mAb) of circulating B cells. Mice were sacrificed on day 10 and TILs were processed and stained for analysis via flow cytometry. Consistent with previous findings, treatment with FEC + oHSV-1 or FEC + oHSV-1 + CP increases the level of TIL-Bs (Figure 3.8A), particularly those of a memory phenotype ($CD19^+CD27^+$). Interestingly, whether or not mice were depleted of circulating B cells did not significantly affect the level of TIL-Bs. However, in line with findings from the peripheral blood, depletion of circulating B cells did result in a rapid expansion of MDSCs (Figure 3.8B, C). Irrespective of whether mice were treated with the depletion antibody or not, the triple combination therapy was also shown to significantly reduce immunosuppressive populations in the tumor, such as the $CD244.2^+$ immunoregulatory

receptor, $PDL1^+$ immune checkpoint and $F4/80^+$ tumor-associated macrophages. The relationship between B cells and myeloid cells was further shown in both splenocytes (Figure 3.8E, F) and tumor-draining lymph nodes (TDLNs) (Figure 3.8G-I). The levels of other immune cell populations in the tumor, spleen and TDLN (CD4s, CD8s and DCs) are consistent with expected findings, with no clear disturbance in their frequencies in the absence of B cells (Figure S3.9).

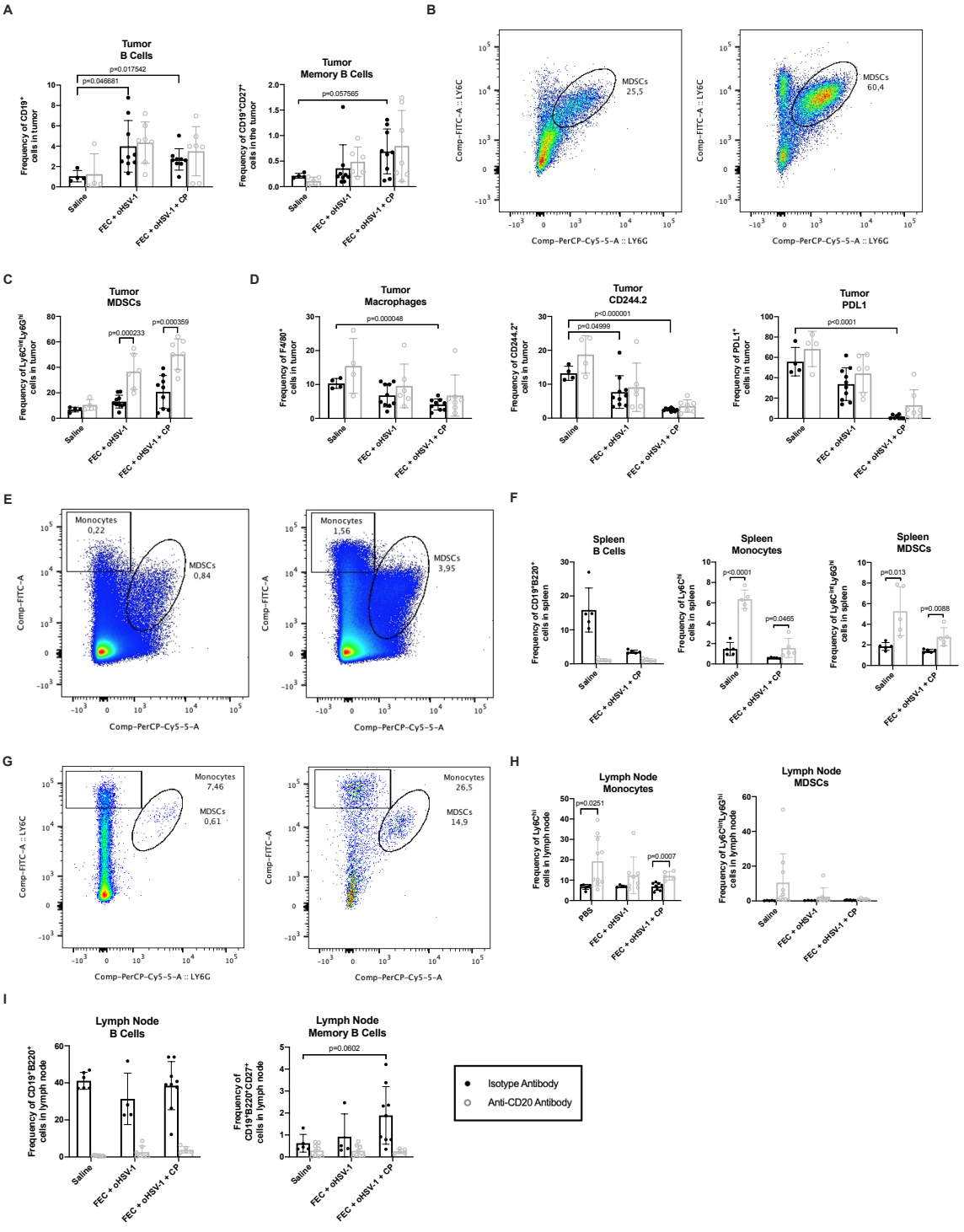
A
Tumor
B Cells
p=0.017542
p=0.046681
Frequency of CD19+ cells in tumor
Saline
FEC + oHSV-1
FEC + oHSV-1 + CP
Tumor
Memory B Cells
p=0.057565
Frequency of CD19+CD27+ cells in the tumor
B
MDSCs
25,5
MDSCs
60,4
Comp-FITC-A :: LY6C
Comp-PerCP-Cy5-5-A :: LY6G
C
Tumor
MDSCs
p=0.000233
p=0.000359
Frequency of Ly6Chi/Ly6Ghi cells in tumor
D
Tumor
Macrophages
p=0.000048
Frequency of F4/80+ cells in tumor
Tumor
CD244.2
p<0.000001
p=0.04999
Frequency of CD244.2+ cells in tumor
Tumor
PDL1
p<0.0001
Frequency of PDL1+ cells in tumor
E
Monocytes
0,22
MDSCs
0,84
Monocytes
1,56
MDSCs
3,95
Comp-FITC-A
Comp-PerCP-Cy5-5-A
F
Spleen
B Cells
Frequency of CD19+B220+ cells in spleen
Spleen
Monocytes
p<0.0001
p=0.0465
Frequency of Ly6Chi cells in spleen
Spleen
MDSCs
p=0.013
p=0.0088
Frequency of Ly6Chi/Ly6Ghi cells in spleen
G
Monocytes
7,46
MDSCs
0,61
Monocytes
26,5
MDSCs
14,9
Comp-FITC-A :: LY6C
Comp-PerCP-Cy5-5-A :: LY6G
Comp-FITC-A
Comp-PerCP-Cy5-5-A
H
Lymph Node
Monocytes
p=0.0251
p=0.0007
Frequency of Ly6Chi cells in lymph node
PBS
Lymph Node
MDSCs
Frequency of Ly6Chi/Ly6Ghi cells in lymph node
I
Lymph Node
B Cells
Frequency of CD19+B220+ cells in lymph node
Lymph Node
Memory B Cells
p=0.0602
Frequency of CD19+B220+CD27+ cells in lymph node
Isotype Antibody
Anti-CD20 Antibody

Fig. 3.8. FEC + oHSV-1 + CP increases TIL-Bs and reduces immunosuppressive cell populations in E0771 tumors

C57/Bl6 mice bearing E0771 tumors were treated with either an anti-CD20 mAB or isotype mAB, followed by treatment with saline, FEC + oHSV-1 or FEC + oHSV-1 + CP. Mice were sacrificed on day 10, tumors were processed, and TILs were stained for analysis via flow cytometry. (**A**) Bar plots showing the frequency of B cells ($CD19^+$) and memory B cells ($CD19^+CD27^+$) in the tumor. (**B**) Representative flow plot showing the gating strategy for MDSCs ($Ly6G^{hi}Ly6C^{int}$) in mice treated with the isotype mAB (left) and the anti-CD20 mAB (right). (**C**) Bar plots showing the frequency of MDSCs in the tumor. (**D**) Bar plots showing the frequency of macrophages ($F4/80^+$), $CD244.2^+$ cells and $PDL1^+$ cells. (**E**) Representative flow plot showing the gating strategy for monocytes ($Ly6C^{hi}$) and MDSCs in splenocytes. (**F**) Bar plots showing the frequency of B cells ($CD19^+B220^+$), monocytes and MDSCs in splenocytes. (**G**) Representative flow plot showing the gating strategy for MDSCs in TDLNs. (**H**) Bar plots showing the frequency of monocytes and MDSCs in TDLNs. (**I**) Bar plots showing the frequency of B cells and memory B cells in TDLNs. *Two-tail unpaired t test was used for statistical analyses. Error bars are representative of standard deviation.

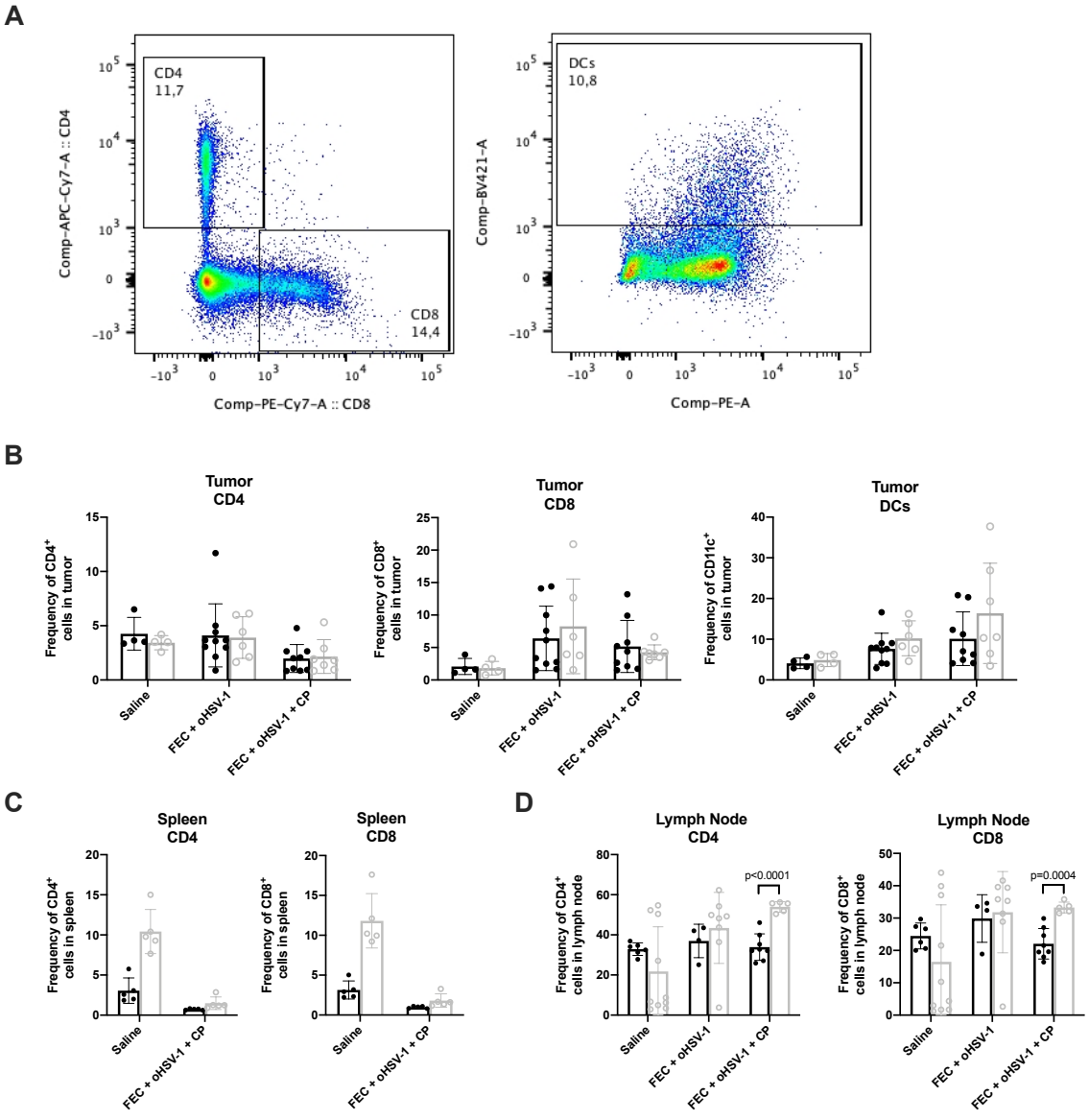

Fig. S3.9. Immune analysis of $CD4^+$, $CD8^+$ and DCs in the tumor, spleen and TDLN.

C57/Bl6 mice bearing E0771 tumors were treated with saline, FEC + oHSV-1 or FEC + oHSV-1 + CP. Half of the mice were treated with an isotype mAB and half were treated with an anti-CD20 mAB. Mice were sacrificed and organs harvested on day 10 for analysis via flow cytometry. (**A**) Representative flow plot showing the gating strategy for

$CD4^+$, $CD8^+$ and DCs ($CD11c^+$). (**B**) Bar plots showing the frequency of immune cells in the tumor. (**C**) Bar plots showing the frequency of immune cells in the spleen. (**D**) Bar plots showing the frequency of immune cells in the TDLN. *Two-tailed unpaired t test was used for statistical analyses. Error bars are representative of standard deviation.

FEC + oHSV-1 responders present with a B cell gene signature and control of MDSCs

Consistent with clinical outcomes, mice treated with FEC + oHSV-1 have dichotomous responses to therapy, shown by the survival outcomes (Figure 3.1), IHC quantification (Figure 3.4) and gene expression profiles (Figure 3.5). To further identify genomic features influencing outcome to therapy, we have sub-grouped these mice into what we believe to be responders and non-responders to treatment, as based on their likeness to the gene expression profiles of saline treated mice (Figure 3.9A). Pathway enrichment analysis of the RNA sequencing data for responders vs. non-responders shows upregulation of pathways involved in immune cell migration, maturation and signaling (Figure 3.9B). Deeper assessment of the differentially expressed gene list shows that responders have upregulation of many genes associated with B cell receptor signaling pathways (Figure 3.9C), as consistent with previous findings. Additional to this and perhaps even more notable, the responders also downregulate *Siglec15*, a critical immune suppressor that is commonly upregulated on human cancer cells and tumor-infiltrating myeloid cells[61].

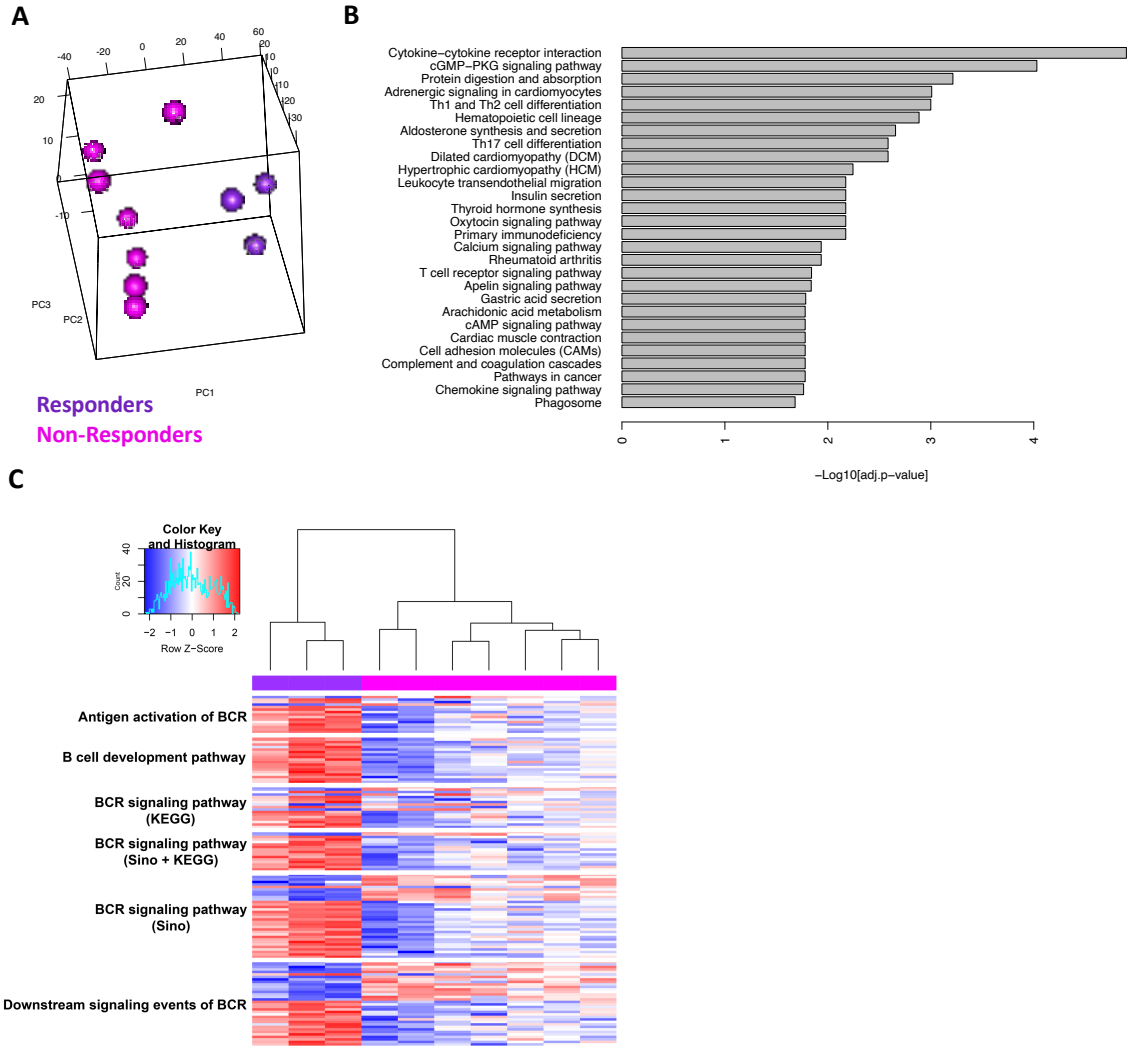

Fig. 3.9. FEC + oHSV-1 induces dichotomous response, with responders having upregulation of B cell receptor signaling pathways and downregulation of genes associated with immunosuppressive phenotypes.

(**A**) 3-D cluster plot showing the RNA expression correlations between mice treated with FEC + oHSV-1 (non-responders = pink; responders = purple). (**B**) Bar plot illustrating the results of pathway enrichment analysis performed on samples from responders, compared

to non-responders. (**C**) Heat map showing the normalized expression values of genes associated with B cell receptor signaling pathways, across all FEC + oHSV-1 samples. *BCR = B Cell Receptor.

3.3. Discussion

Immune checkpoint blockade has surged to the forefront of cancer therapy with astonishing clinical success rates and low toxicity profiles. However, this highly efficacious therapy only works in a fraction of patients and we have yet to fully elucidate the underlying biology that allows some patients to respond to therapy, while others do not. Helmink and colleagues have eloquently shown that B cells play an important role in promoting efficacious responses to immune checkpoint blockade in melanoma and renal cell carcinoma patients[62]. In line with these findings, our data suggest that promoting a B cell signature within the tumor allows for successful treatment with combination immunotherapy platforms. Using the clinical chemotherapy cocktail FEC, in combination with oHSV-1, we are able to elicit the upregulation of B cell receptor signaling pathways that allows our otherwise non-responsive TNBC tumors to respond to CP. In particular, mice treated with the triple combination therapy see a re-population of circulating B cells over time and an increase in memory B cells within the tumor, suggesting that the sustained presence of B cells may be required to achieve durable responses and improved prognostic outcomes.

In vivo depletion studies in which an anti-CD20 antibody was used to deplete mice of circulating B cells have shown that groups of mice that would otherwise achieve complete responses to treatment instead have a complete loss of therapeutic efficacy.

Deeper investigation into this phenomenon revealed a strong correlation between the presence of B cells and control of immunosuppressive MDSCs. These data suggest that B cells are required to suppress the rapid expansion of immunosuppressive myeloid cell populations in the TME. Indeed, RNA sequencing data identified that FEC + oHSV-1 is able to not only upregulate genes associated with the B cell lineage, but also to downregulate genes that are known to be key players in tumor immunosuppression. When further looking at the population of mice with the most distinct RNA profile (as thought to be responders to treatment) we find that amongst the downregulated MDSC genes is *Siglec15*, a known immune suppressor broadly expressed on human cancer cells and tumor infiltrating myeloid cells[61]. As Chen and colleagues have shown, Siglec15 overexpression has been documented in numerous human cancers and its expression is mutually exclusive of PD-L1, suggesting that it may be a potential therapeutic target for patients who are refractive to anti-PD-1/PD-L1 checkpoint blockade therapy[63]. Interestingly, our therapy downregulates this key immune modulator, suggesting a therapeutic platform that can be used to target this pathway of tumor immune escape. Along with downregulation of Siglec15, immune analysis studies showed that our triple combination therapy significantly reduces levels of CD244.2, an immunoregulatory receptor found on a variety of immune cells, including exhausted $CD8^+$ T cells and MDSCs[64].

Current immunotherapies do not target or consider B cells, despite their predominance in the TME and key role in the adaptive immune response. In TNBC, evidence suggests that TIL-Bs generate a robust humoral response to amplify antitumor

immunity[65] and mediate immunotherapy outcomes[66]. TIL-Bs have been correlated with enhanced overall survival[67], but findings in the literature suggest conflicting roles with TIL-Bs having both pro- and anti-tumorigenic functions. TIL-Bs have been identified as mediators of malignancy in several cancer types, with TIL-B depletion yielding positive outcomes[68]. Conversely, coordinated antibody and T cell responses have been documented in cancer patients and TIL-Bs have been correlated with improved outcome[62,66,69–71]. Further, clinical studies have reported that TIL-Bs are influenced by the TME and immunotherapy, a discovery consistent with our findings.

MDSCs are a heterogenous population of immature myeloid cells that accumulate in tumor beds and lymphoid organs (such as the spleen) of tumor-bearing hosts. MDSCs have long been attributed to tumor immunosuppression, most commonly due to their ability to suppress T cell-mediated immune responses. However, studies have also shown that granulocytic MDSCs can suppress antitumor B cell responses, predominantly through the secretion of nitric oxide (NO), arginase (Arg) and IL1[72–74]. While there are no documented studies to our knowledge looking at the reverse regulation of this phenomenon, our data suggests that while MDSCs can suppress TIL-Bs through the secretion of NO, Arg and IL1 perhaps the opposite is also true. We have shown that our therapeutic platform upregulates B cell receptor signaling pathways, suppressing key genes such as *NOS2*, *Arg2* and *IL1R1* (Table 3.1), which we believe to be essential for the regulation and control of MDSCs.

We have used a multi-pronged therapeutic approach to treat triple negative breast tumors (Figure 3.10). In this approach, we have combined low dose chemotherapies that

work to enhance tumor immunogenicity and antigen presentation aiding in BCR-recognition of TAAs. This, coupled with our oncolytic virotherapy initiates a cascade of DC and B cell recruitment and ultimately clonal expansion of B cells. B cell and T cell priming results in the release of antitumor chemokines driving effector cell function, while simultaneously suppressing cytokines responsible for the accumulation of MDSCs in the TME. This immune-activating cascade of events leads to an immune landscape conducive to successful treatment with CP.

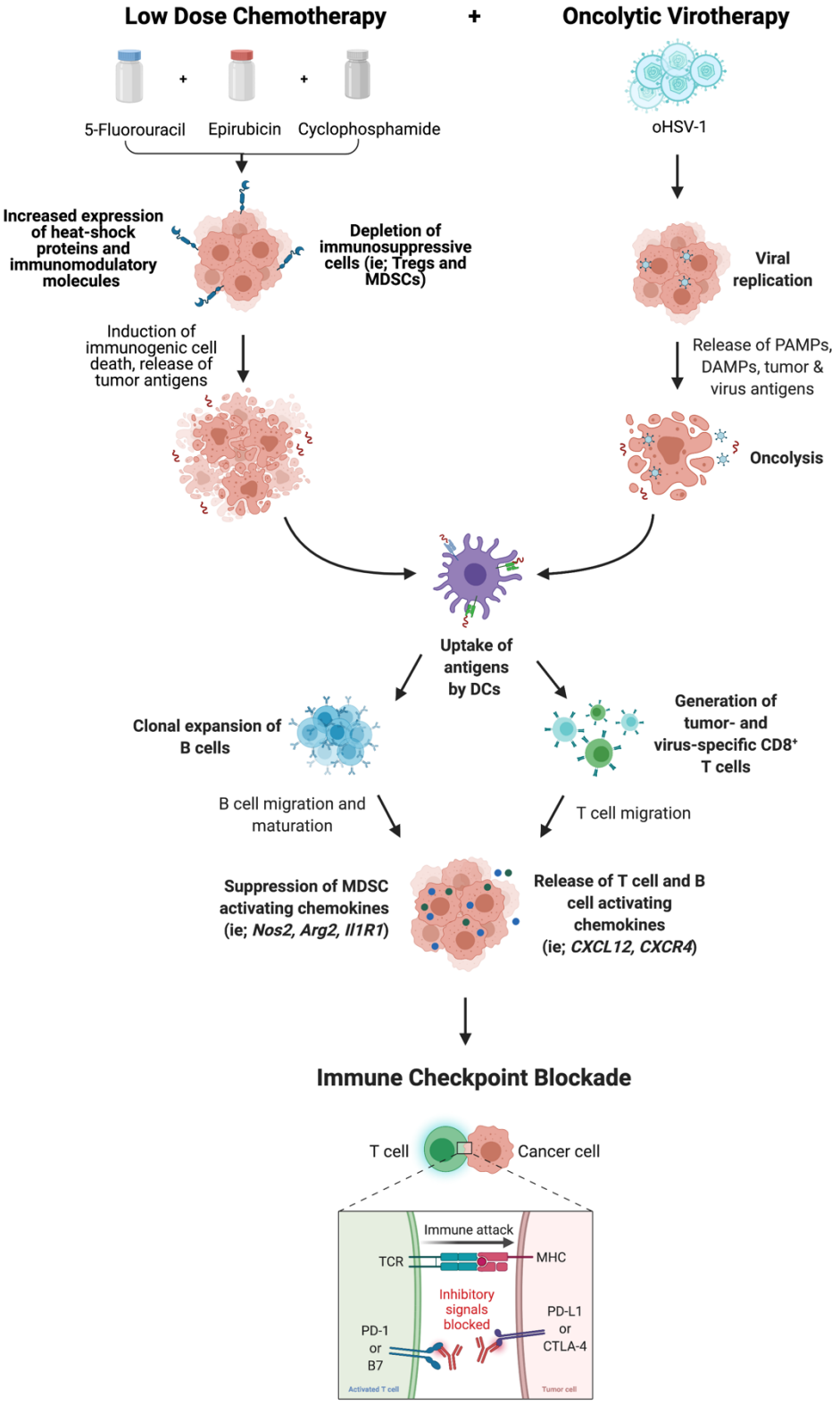
Low Dose Chemotherapy
+
Oncolytic Virotherapy
5-Fluorouracil
Epirubicin
Cyclophosphamide
oHSV-1
Increased expression of heat-shock proteins and immunomodulatory molecules
Depletion of immunosuppressive cells (ie; Tregs and MDSCs)
Viral replication
Induction of immunogenic cell death, release of tumor antigens
Release of PAMPs, DAMPs, tumor & virus antigens
Oncolysis
Uptake of antigens by DCs
Clonal expansion of B cells
Generation of tumor- and virus-specific CD8+ T cells
B cell migration and maturation
T cell migration
Suppression of MDSC activating chemokines (ie; Nos2, Arg2, Il1R1)
Release of T cell and B cell activating chemokines (ie; CXCL12, CXCR4)
Immune Checkpoint Blockade
T cell
Cancer cell
Immune attack
TCR
MHC
Inhibitory signals blocked
PD-1 or B7
PD-L1 or CTLA-4
Activated T cell
Tumor cell

Fig. 3.10. Schematic of therapy-induced immune activation

Our studies are limited by the nature of murine hosts and their inability to fully recapitulate human biology. Our data were generated from subcutaneous tumors and should be further analyzed in metastatic and spontaneously arising tumor models to assess these core immunological interactions in a more naturally occurring setting. We aim to further assess these fascinating findings as we continue to phenotype our B cell populations and assess their interactions with various myeloid cell populations in cancer-bearing hosts. We believe that clinical studies should focus not only on the levels of T cells and their correlated effects to prognostic outcomes, but also look at B cells as a key biomarker to predict responses to immunotherapy treatments.

3.4. Materials and Methods

Cell Lines

Human osteosarcoma cells from a fifteen-year old Caucasian female (U2OS; ATCC, Manassas, VA) were maintained in Dulbecco's modified Eagle's media (DMEM) supplemented with 10% fetal bovine serum (FBS, ATCC 30-2020) 2 mmol/l L-glutamine, 100 U/ml penicillin, 100 μg/ml streptomycin (Gibco, Grand Island, NY). Vero cells originating from the kidney of an adult monkey (ATCC, Manassas, VA) were maintained in DMEM supplemented with 10% FBS 2 mmol/l L-glutamine, 100 U/mL penicillin, 100 μg/mL streptomycin (Gibco, Grand Island, NY). Murine medullary breast adenocarcinoma cells isolated as a spontaneous tumor from a C57/Bl6 mouse (E0771; CH3 Biosystems, Amherst, NY) were maintained in roswell park memorial institute

(RPMI) medium supplemented with 10% FBS, 10 mM HEPES, 100U/mL penicillin, 100 μg/mL streptomycin and 2 mmol/l L-glutamine. Murine breast adenocarcinoma cells derived from an MMTV-PyMT tumor were maintained in Ham's F-12K Medium supplemented with 5% FBS and 0.1% MITO + serum extender (Corning #355006). All cell lines were grown at 37 °C with 5% CO_2.

Mouse Experiments

Mice were maintained at the McMaster University Central Animal Facility and all the procedures were performed in full compliance with the Canadian Council on Animal Care and approved by the Animal Research Ethics Board of McMaster University. Six- to eight-week-old female C57/Bl6 mice (Charles River Laboratories, Wilmington, MA) were used to implant 5×10^6 E0771 cells subcutaneously on the left flank. Mice were weighed and all found to be approximately 20 g in size. Mice were housed in groups, 5 / cage, fed a normal diet and kept at room temperature. To minimize experimental variability, low passage E0771 cells were used for subcutaneous injections. Twelve days after injection, the tumors reached treatable average tumor volume (50-100 mm^3). Mice were blindly randomized prior to the start of treatment. In experimental groups receiving FEC treatment, mice were treated on day 1 with 20 mg/kg 5-fluorouracil in 200 μL saline, followed by 3 mg/kg epirubicin in 200 μL saline, followed by 20 mg/kg cyclophosphamide in 200 μL saline 1 h later. In experimental groups receiving AC treatment, mice were treated on day 1 with 3 mg/kg doxorubicin in 200 μL saline, followed by 20 mg/kg cyclophosphamide in 200 μL saline 1 h later. All chemotherapy injections were given intraperitoneally (i.p.). Experimental groups receiving oHSV-1

were treated with 2×10^7 pfu oHSV-1 dICP0 in 50 µL PBS intratumorally (i.t.) on days 2, 3 and 4. Experimental groups receiving immune checkpoint blockade therapy were treated with α-CTLA-4 (BioCell, BE0131) and α-PD-L1 (BioCell, BE101) antibodies (200 µg / 200 µL PBS, each) starting on day 3, every 3 days until mice reached endpoint or a total of 10 doses had been given. For B cell depletion studies, mice were treated on day 0 with a singular dose of 250 µg of α-CD-20 (Biolegend, 152104) or isotype (Biolegend, 400566) antibody. For all mouse studies, tumors were measured every 2 – 3 days and mice having a tumor volume of 1000 mm^3 were classified as end point.

Drug Preparation

5-fluorouracil stock powder (Sigma Aldrich, F6627) was stored at 4 °C and dissolved in sterile saline to a concentration of 2 mg/mL. Epirubicin stock powder (Cayman Chemicals, 12091) was stored at -20 °C and dissolved in sterile saline to a concentration of 0.3 mg/mL. Cyclophosphamide stock powder (Sigma Aldrich, C0768) was stored at 4 °C and dissolved in sterile saline to a concentration of 2 mg/mL. Doxorubicin stock powder (Sigma Aldrich, D1515) was stored at 4 °C and dissolved in sterile saline to a concentration of 0.3 mg/mL. α-CTLA-4 (BioCell, BE0131) and α-PD-L1 (BioCell, BE0101) antibodies solutions were diluted to 1 mg/mL with sterile PBS. All solutions were prepared fresh for each experiment.

Virus Preparation

Recombinant HSV-1 was generated by homologous recombination using infectious DNA of luciferase-expressing wild-type HSV-1 KOS/Dluc/oriL[75]. HSV-1 dNLS encodes a

GFP-tagged protein that lacks the ICP0 NLS region and a portion of the C-terminal oligomerization domain[76]. HSV-1 dICP0 contains a deletion of the entire *ICP0* coding region. All HSV-1 *ICP0* mutants were propagated and tittered on U2OS cells in the presence of 3 mmol/l hexamethylene bisacetamide (Sigma, St Louis, MO). Wild-type HSV-1 strain KOS was propagated and titered on Vero cells. All viruses were purified and concentrated via sucrose cushion ultracentrifugation and purified virus was resuspended in PBS and stored at -80 °C.

Rechallenge Experiment

Mice that achieved a complete response to therapy (tumor-free mice) and naïve mice, as control, were subcutaneously implanted subcutaneously with 5×10^6 E0771 cells in the left flank. Tumors were measured every 3 – 4 days for a minimum of 4 weeks.

Cytokines Analysis

Mice were anaesthetized and euthanized before resection of the tumors. As previously described[77], tumors were cut into small pieces and homogenized in the presence of tissue extraction solution (50mM Tris, pH 7.4, 250mM NaCl, 5mM EDTA, 2 mM Na3VO4, 1mM NaF, 20mM Na4P2O7, 1mM beta-glycerophosphate, 1% NP-40). Homogenized tumors were incubated on ice for 30 min. Whole-tumor lysates were clarified by three sequential centrifugations at 14,000 rpm for 10 min at 4 °C. Tumor homogenates were diluted to achieve equal amounts of protein concentration. Forty-four-Plex murine cytokine/chemokine analysis was done by Eve Technologies (Calgary, Alberta, Canada).

Histology and Image Analysis

Treated and control tumors were resected on day 7, fixed in 10% formalin for 48 h and then transferred to 70% ethanol until histological processing. Tumor tissue was embedded in paraffin and 4-μm sections were prepared. Tissue sections were processed for hematoxylin staining and IHC using Automated Leica Bond Rx stainer with Epitope Retrieval Buffer 2 (Leica, AR9640). All antibodies were diluted in IHC/ISH Super Blocker (Leica, PV6199). Primary antibodies and working dilutions were as follows: α-CD3 (1:150; Abcam, ab16669), α-CD4 (1:800; eBio, 14-9766), α-CD8a (1:1000; eBio, 14-0808), α-FOXP3 (1:100; eBio, 14-5773-82) and α-Ly6G (1:1000; Biolegend, 127602). Secondary antibody and working dilution: rabbit α-rat antibody (1:100; Vector Labs, BA-4001). Bond Refine Polymer Detection kit (Leica, DS9800) was used. Additional tissue sections were processed for immunofluorescence (IF) staining. Slides were incubated at 37 °C overnight, deparaffinized and rinsed with distilled water (dH_2O). Slides were fixed in 10% neutral buffered formalin (NBF) for 20 minutes and rinsed with dH_2O. Antigen retrieval was performed using the decloaking chamber plus with Diva decloaker (Biocare). Slides were added to the Intellipath FLX rack, rinsed with dH_2O and covered with TBS buffer. Slides were loaded into the pre-programmed, reagent-loaded Intellipath FLX. Endogenous peroxidase blocking was performed by adding peroxidazed-1 for 5 minutes at room temperature (RT), followed by nonspecific blocking with Rodent Block M for 30 minutes at RT. Primary antibody staining was performed in five rounds: CD3 (1:600, Spring Bioscience Corp., M3074), PNAd (1:200, Biolegend, 120802), Pax5 (1:1000, Abcam, EPR3730), CD8 (1:200, Cell Signaling Technologies, 98941S), CD11b (1:7500, Abcam, EPR1344). Each round was followed by application of Mach2 Rb HRP

for 10 minutes at RT and fluorophore incubation for 10 minutes at RT. Diluted IF counterstain DAPI was applied for 5 minutes at RT and slides were rinsed with water. Finally, Vectashield mounting media and cover slip were applied and slides were stored in the dark at RT. All images were scanned with Vectra3 and annotated using Phenochart software.

RNA Sequencing

Mice were sacrificed on day 5 and tumors harvested for RNA sequencing analysis. Tumors were homogenized in 1 mL trizol (Thermo Fisher Scientific, #15-596-018). 375 µL was transferred to 1250 µL trizol and mized well. RNA was first extracted using chloroform and then following the manufacturer's instructions using an RNeasy RNA extraction kit (Qiagen). cDNA libraries were created by polyA enrichment using NEBNext poly(A) magnetics isolation module (NEB) and reverse transcribed using NEBNext ultra II directional RNA library prep kit (NEB) according to the manufacturer's instructions. cDNA libraries were sequenced using an Illumina HiSeq rapid V2 (1 x 50 bp sequence reads) at the Farncombe Metagenomics Facility (McMaster University). The sequencing was run in 2 batches. Sequencing yielded ~15 x 10^6 reads/sample. First, reads were filtered by quality (at least 90% of the bases must have a quality score of 20 and higher). Then the mapping of the remaining reads was performed using HISAT2[78] with hg38 (UCSC) reference genome; reads were counted by using HTSeq count[79]. Genes which did not show sufficiently large counts were removed using filterByExpr function in EdgeR package[80,81] in R, resulting in 13,079 and 12,334 genes in the first and second batches, respectively. These remaining count values were normalized with TMM

normalization method[82] and then transformed with voom transformation[83]. 12,334 genes were shared between the first and second batches and were used for batch effect removal using ComBat[84], with experiment date used as the batch information. Limma package[85] in R was used to examine differential expression between the groups of interest; p-values obtained from the analysis were corrected with BH correction for multiple testing[86], and corrected values <0.05 were considered to be significant.

ELISA Assay

Cell lysates of E0771 tumor cells were prepared by sonication. Polystyrene 96-well microtiter plates (Nunc MaxiSorp; Thermo Fischer Scientific) were coated overnight at 4 ℃ with 100 µL of E01771 tumor cell lysate (5 µg/mL in PBS). The wells were washed 3x with wash buffer (0.05% Tween in PBS) and blocked with 300 µL of blocking buffer (1% bovine serum albumin (BSA) in PBS) for 3h at RT. The wells were washed 3x with wash buffer. 50 µL of a 1/50 dilution of each test or control mouse serum, diluted in 1% BSA-PBS, was added in triplicate and incubated for 3 hours at RT. The wells were washed 3x with wash buffer, and 100 µL of horseradish peroxidase conjugated goat anti-mouse IgG Fc antibody (1:10,000; Thermofisher Scientific, cat# A16084) diluted in blocking buffer was added for 1 hr at RT. Wells were washed 3x with wash buffer and 3,3′,5,5′-Tetramethylbenzidine (TMB; BD Biosciences) substrate solution was added for 20 minutes at RT. Stop solution (2N H_2SO_4) was added to each well to stop the reaction and the 450 nm and 540 nm OD was read using a SpectraMax i3 Microplate Autoreader (Molecular Devices).

Flow Cytometry Analysis

Organs were harvested from animals at given time points. Tumors were minced with a razor blade in RPMI media. 100 µL liberase (Sigma Aldrich, #5401054001) was added for digestion and samples incubated for 20 min at 37 °C. The cell suspension was passed over a 100 micron filter and rinsed with 5 mL of RPMI. Samples were spun at 1500 RPM for 5 min. Spleens and lymph nodes were pressed between two glass slides to extract cells and 150 µL of blood was collected from the periorbital sinus. Red blood cells from all samples were lysed using ACK buffer. The PBMCs were treated with anti-CD16/CD32 (Fc block; BD Biosciences, #553141) and surface stained with fluorescently conjugated antibodies for FVS (BD Biosciences, #564406), CD19 (Fisher Scientific, #14-019-482), B220 (BD Biosciences, #563894), CD27 (BD Biosciences, #558754), CD4 (BD Biosciences, #561830), CD8 (BD Biosciences, #563046), CD11b (BD Biosciences, #553311), Ly6C (BD Biosciences, #553104), Ly6G (BD Biosciences, #560602), CD11c (BD Biosciences, #562782), F4/80 (BD Biosciences, #743282), CD244.2 (BD Biosciences, #740860) and PD-L1 (BD Biosciences, #563369). LSRFortessa flow cytometer with FACSDiva software (BD Biosciences) was used for data acquisition and FlowJo Mac, version 10.0 software was used for data analysis.

Quantification and Statistical Analysis

IHC slides were digitalized using the Olympus VS120-L100-W automated slide scanner. They were batch-scanned on the brightfield setting at 20x magnification. The color camera used was the Pike 505C VC50. HALO Image Analysis Software (Indica Labs, HALO v2.2) was used to analyze digital histology image. Cytonuclear cell count algorithms were developed to determine the amount of CD3, CD4, CD8a, FOXP3 and

Ly6G positive cells and total cell number present in a given sample of tissue. Percentage of positive cells were calculated relative to total cell number[87]. For each statistical analysis used, normality of the distributions and variance assumptions were tested before running the statistical analyses. Multiple t-tests were used to determine the statistical significance of the differences in means. The log-rank (Mantel-Cox) test was used to determine statistical significance for the difference in Kaplan-Meier survival curves between treatments. All the tests were two-sided. The null hypothesis was rejected for p-values less than 0.05. All data analyses were carried out using GraphPad Prism (La Jolla, CA, USA).

Supplementary Materials

Fig. S1. Preliminary dose optimization studies for AC and FEC chemotherapy regimens.

Fig. S2. Administration of singular checkpoint antibodies shows no therapeutic efficacy.

Fig. S3. FEC + oHSV + CP significantly changes the expression of many cytokines in tumor-bearing mice.

Fig. S4. H&E staining reveals increased necrotic tissue in FEC + oHSV-1 + CP treated mice.

Fig. S5. B cells are required for therapeutic efficacy of combination therapies.

Fig. S6. Depletion of B cells results in disruption of immune cell organization.

Fig. S7. Immune analysis of $CD4^+$, $CD8^+$, monocytes and DCs.

Fig. S8. Immune analysis of B cells and MDSCs in PY230 tumors.

Fig. S9. Immune analysis of $CD4^+$, $CD8^+$ and DCs in the tumor, spleen and TDLN.

Table S1. Differentially expressed genes associated with B cell pathways.

Data file S1. RNA sequencing of whole tumor digests.

Supplementary Data 1. Raw data for all figures.

Supplemental Table 1. Antibodies used in manuscript.

References

1. Wang, X. *et al.* Immunological therapy: A novel thriving area for triple-negative breast cancer treatment. *Cancer Letters* (2019). doi:10.1016/j.canlet.2018.10.042

2. Stagg, J. & Allard, B. Immunotherapeutic approaches in triple-negative breast cancer: Latest research and clinical prospects. *Therapeutic Advances in Medical Oncology* (2013). doi:10.1177/1758834012475152

3. Schmid, P. *et al.* Atezolizumab and nab-paclitaxel in advanced triple-negative breast cancer. *N. Engl. J. Med.* (2018). doi:10.1056/NEJMoa1809615

4. Taube, J. M. *et al.* Differential expression of immune-regulatory genes associated with PD-L1 display in melanoma: Implications for PD-1 pathway blockade. *Clin. Cancer Res.* (2015). doi:10.1158/1078-0432.CCR-15-0244

5. Diaz-Montero, C. M. *et al.* Increased circulating myeloid-derived suppressor cells correlate with clinical cancer stage, metastatic tumor burden, and doxorubicin-cyclophosphamide chemotherapy. *Cancer Immunol. Immunother.* (2009). doi:10.1007/s00262-008-0523-4

6. Markowitz, J., Wesolowski, R., Papenfuss, T., Brooks, T. R. & Carson, W. E. Myeloid-derived suppressor cells in breast cancer. *Breast Cancer Research and Treatment* (2013). doi:10.1007/s10549-013-2618-7

7. Kroemer, G., Senovilla, L., Galluzzi, L., André, F. & Zitvogel, L. Natural and therapy-induced immunosurveillance in breast cancer. *Nature Medicine* (2015). doi:10.1038/nm.3944

8. DeNardo, D. G. *et al.* Leukocyte complexity predicts breast cancer survival and functionally regulates response to chemotherapy. *Cancer Discov.* (2011). doi:10.1158/2159-8274.CD-10-0028

9. Lee, M. *et al.* Presence of tertiary lymphoid structures determines the level of tumor-infiltrating lymphocytes in primary breast cancer and metastasis. *Mod. Pathol.* (2019). doi:10.1038/s41379-018-0113-8

10. Song, I. H. *et al.* Predictive value of tertiary lymphoid structures assessed by high endothelial venule counts in the neoadjuvant setting of triple-negative breast cancer. *Cancer Res. Treat.* (2017). doi:10.4143/crt.2016.215

11. Cuddington, B. P. & Mossman, K. L. Oncolytic bovine herpesvirus type 1 as a broad spectrum cancer therapeutic. *Current Opinion in Virology* (2015). doi:10.1016/j.coviro.2015.03.010

12. Hummel, J. L., Safroneeva, E. & Mossman, K. L. The role of ICP0-Null HSV-1 and interferon signaling defects in the effective treatment of breast adenocarcinoma. *Mol. Ther.* (2005). doi:10.1016/j.ymthe.2005.07.533

13. Sobol, P. T. *et al.* Adaptive antiviral immunity is a determinant of the therapeutic success of oncolytic virotherapy. *Mol. Ther.* (2011). doi:10.1038/mt.2010.264

14. Workenhe, S. T. *et al.* Immunogenic HSV-mediated Oncolysis shapes the antitumor immune response and contributes to therapeutic efficacy. *Mol. Ther.* (2014). doi:10.1038/mt.2013.238

15. van Vloten, J. P., Workenhe, S. T., Wootton, S. K., Mossman, K. L. & Bridle, B. W. Critical Interactions between Immunogenic Cancer Cell Death, Oncolytic Viruses, and the Immune System Define the Rational Design of Combination Immunotherapies. *J. Immunol.* (2018). doi:10.4049/jimmunol.1701021

16. Workenhe, S. T. & Mossman, K. L. Rewiring cancer cell death to enhance oncolytic viro-immunotherapy. *Oncoimmunology* (2013). doi:10.4161/onci.27138

17. Workenhe, S. T. & Mossman, K. L. Oncolytic virotherapy and immunogenic cancer cell death: Sharpening the sword for improved cancer treatment strategies. *Molecular Therapy* (2014). doi:10.1038/mt.2013.220

18. Workenhe, S. T., Pol, J. G., Lichty, B. D., Cummings, D. T. & Mossman, K. L. Combining oncolytic HSV-1 with immunogenic cell death-inducing drug mitoxantrone breaks cancer immune tolerance and improves therapeutic efficacy. *Cancer Immunol. Res.* (2013). doi:10.1158/2326-6066.CIR-13-0059-T

19. Workenhe, S. T., Verschoor, M. L. & Mossman, K. L. The role of oncolytic virus immunotherapies to subvert cancer immune evasion. *Future Oncology* (2015). doi:10.2217/fon.14.254

20. Vacchelli, E. *et al.* Trial watch: Chemotherapy with immunogenic cell death inducers. *OncoImmunology* (2012). doi:10.4161/onci.1.2.19026

21. Sukkurwala, A. Q. *et al.* Screening of novel immunogenic cell death inducers within the NCI mechanistic diversity set. *Oncoimmunology* (2014). doi:10.4161/onci.28473

22. Vacchelli, E. *et al.* Trial watch: Chemotherapy with immunogenic cell death inducers. *OncoImmunology* (2014). doi:10.4161/onci.27878

23. Eid, R. A., Razavi, G. S. E., Mkrtichyan, M., Janik, J. & Khleif, S. N. Old-School Chemotherapy in Immunotherapeutic Combination in Cancer, A Low-cost Drug Repurposed. *Cancer Immunol. Res.* (2016). doi:10.1158/2326-6066.CIR-16-0048

24. Landreneau, J. P. *et al.* Immunological Mechanisms of Low and Ultra-Low Dose Cancer Chemotherapy. *Cancer Microenviron.* (2015). doi:10.1007/s12307-013-0141-3

25. Galluzzi, L., Buqué, A., Kepp, O., Zitvogel, L. & Kroemer, G. Immunological Effects of Conventional Chemotherapy and Targeted Anticancer Agents. *Cancer Cell* (2015). doi:10.1016/j.ccell.2015.10.012

26. Sow, H. S. & Mattarollo, S. R. Combining low-dose or metronomic chemotherapy with anticancer vaccines: A therapeutic opportunity for lymphomas. *OncoImmunology* (2013). doi:10.4161/onci.27058

27. Torres, S., Trudeau, M., Eisen, A., Earle, C. C. & Chan, K. K. W. Adjuvant taxane-based chemotherapy for early stage breast cancer: a real-world comparison

of chemotherapy regimens in Ontario. *Breast Cancer Res. Treat.* (2015). doi:10.1007/s10549-015-3441-0

28. Wu, Y. *et al.* Repeated cycles of 5-fluorouracil chemotherapy impaired anti-tumor functions of cytotoxic T cells in a CT26 tumor-bearing mouse model. *BMC Immunol.* (2016). doi:10.1186/s12865-016-0167-7

29. Cyprian, F. S., Akhtar, S., Gatalica, Z. & Vranic, S. Targeted immunotherapy with a checkpoint inhibitor in combination with chemotherapy: A new clinical paradigm in the treatment of triple-negative breast cancer. *Bosnian Journal of Basic Medical Sciences* (2019). doi:10.17305/bjbms.2019.4204

30. Dill, E. A. *et al.* PD-L1 Expression and Intratumoral Heterogeneity Across Breast Cancer Subtypes and Stages: An Assessment of 245 Primary and 40 Metastatic Tumors. *Am. J. Surg. Pathol.* (2017). doi:10.1097/PAS.0000000000000780

31. Vikas, P., Borcherding, N. & Zhang, W. The clinical promise of immunotherapy in triple-negative breast cancer. *Cancer Manag. Res.* (2018). doi:10.2147/CMAR.S185176

32. Takada, K. *et al.* Use of the tumor-infiltrating CD8 to FOXP3 lymphocyte ratio in predicting treatment responses to combination therapy with pertuzumab, trastuzumab, and docetaxel for advanced HER2-positive breast cancer. *J. Transl. Med.* (2018). doi:10.1186/s12967-018-1460-4

33. Miyashita, M. *et al.* Prognostic significance of tumor-infiltrating CD8+ and FOXP3+ lymphocytes in residual tumors and alterations in these parameters after

neoadjuvant chemotherapy in triple-negative breast cancer: A retrospective multicenter study. *Breast Cancer Res.* (2015). doi:10.1186/s13058-015-0632-x

34. Chen, Y. Q. *et al.* Tumor-released autophagosomes induces CD4+ T cell-mediated immunosuppression via a TLR2-IL-6 cascade. *J. Immunother. Cancer* (2019). doi:10.1186/s40425-019-0646-5

35. Le, H. K. *et al.* Gemcitabine directly inhibits myeloid derived suppressor cells in BALB/c mice bearing 4T1 mammary carcinoma and augments expansion of T cells from tumor-bearing mice. *Int. Immunopharmacol.* (2009). doi:10.1016/j.intimp.2009.03.015

36. Vincent, J. *et al.* 5-Fluorouracil selectively kills tumor-associated myeloid-derived suppressor cells resulting in enhanced T cell-dependent antitumor immunity. *Cancer Res.* (2010). doi:10.1158/0008-5472.CAN-09-3690

37. Sawant, A. *et al.* Enhancement of antitumor immunity in lung cancer by targeting myeloid-derived suppressor cell pathways. *Cancer Res.* (2013). doi:10.1158/0008-5472.CAN-13-0987

38. Yang, Z. *et al.* Myeloid-derived suppressor cells-new and exciting players in lung cancer. *Journal of Hematology and Oncology* (2020). doi:10.1186/s13045-020-0843-1

39. Feng, P. H. *et al.* CD14+S100A9+ monocytic myeloid-derived suppressor cells and their clinical relevance in non-small cell lung cancer. *Am. J. Respir. Crit. Care Med.* (2012). doi:10.1164/rccm.201204-0636OC

40. Ouzounova, M. *et al.* Monocytic and granulocytic myeloid derived suppressor cells differentially regulate spatiotemporal tumour plasticity during metastatic cascade. *Nat. Commun.* (2017). doi:10.1038/ncomms14979

41. Chen, X. *et al.* Induction of myelodysplasia by myeloid-derived suppressor cells. *J. Clin. Invest.* (2013). doi:10.1172/JCI67580

42. Lin, L. *et al.* Accumulation of tumor infiltrating myeloid-derived suppressor cells associates with changes in the immune landscape of clear cell renal cell carcinoma. *J. Clin. Oncol.* (2018). doi:10.1200/jco.2018.36.6_suppl.655

43. Katoh, H. *et al.* CXCR2-Expressing Myeloid-Derived Suppressor Cells Are Essential to Promote Colitis-Associated Tumorigenesis. *Cancer Cell* (2013). doi:10.1016/j.ccr.2013.10.009

44. Talmadge, J. E. & Gabrilovich, D. I. History of myeloid-derived suppressor cells. *Nature Reviews Cancer* (2013). doi:10.1038/nrc3581

45. Han, X. *et al.* CXCR2 expression on granulocyte and macrophage progenitors under tumor conditions contributes to mo-MDSC generation via SAP18/ERK/STAT3. *Cell Death Dis.* (2019). doi:10.1038/s41419-019-1837-1

46. Raccosta, L. *et al.* The oxysterol-cxcr2 axis plays a key role in the recruitment of tumor-promoting neutrophils. *J. Exp. Med.* (2013). doi:10.1084/jem.20130440

47. Ford, J. *et al.* Enhanced Triggering Receptor Expressed on Myeloid Cells 1 (TREM-1) and Soluble TREM-1 Levels in the Myeloid Cells of Tumor-Bearing Mice and Patients with Renal Cell Carcinoma (100.8). *J. Immunol.* **184**, (2010).

48. Azzaoui, I. *et al.* T-cell defect in diffuse large B-cell lymphomas involves expansion of myeloid-derived suppressor cells. *Blood* (2016). doi:10.1182/blood-2015-08-662783

49. Majchrzak-Gorecka, M., Majewski, P., Grygier, B., Murzyn, K. & Cichy, J. Secretory leukocyte protease inhibitor (SLPI), a multifunctional protein in the host defense response. *Cytokine and Growth Factor Reviews* (2016). doi:10.1016/j.cytogfr.2015.12.001

50. Lee, J. M. *et al.* Serum amyloid A3 exacerbates cancer by enhancing the suppressive capacity of myeloid-derived suppressor cells via TLR2-dependent STAT3 activation. *Eur. J. Immunol.* (2014). doi:10.1002/eji.201343867

51. Malgulwar, P. B. *et al.* Transcriptional co-expression regulatory network analysis for Snail and Slug identifies IL1R1, an inflammatory cytokine receptor, to be preferentially expressed in ST-EPN-RELA and PF-EPN-A molecular subgroups of intracranial ependymomas. *Oncotarget* (2018). doi:10.18632/oncotarget.26211

52. de Almeida Nagata, D. E. *et al.* Regulation of Tumor-Associated Myeloid Cell Activity by CBP/EP300 Bromodomain Modulation of H3K27 Acetylation. *Cell Rep.* (2019). doi:10.1016/j.celrep.2019.03.008

53. Guo, Q. *et al.* SERPIND1 Affects the Malignant Biological Behavior of Epithelial Ovarian Cancer via the PI3K/AKT Pathway: A Mechanistic Study. *Front. Oncol.* (2019). doi:10.3389/fonc.2019.00954

54. Elpek, K. G. *et al.* The tumor microenvironment shapes lineage, transcriptional,

and functional diversity of infiltrating myeloid cells. *Cancer Immunol. Res.* (2014). doi:10.1158/2326-6066.CIR-13-0209

55. Bronte, V. *et al.* Recommendations for myeloid-derived suppressor cell nomenclature and characterization standards. *Nature Communications* (2016). doi:10.1038/ncomms12150

56. Cui, Y. F. *et al.* Platelet endothelial aggregation receptor-1 (PEAR1) is involved in C2C12 myoblast differentiation. *Exp. Cell Res.* (2018). doi:10.1016/j.yexcr.2018.03.027

57. Gato-Cañas, M. *et al.* A core of kinase-regulated interactomes defines the neoplastic MDSC lineage. *Oncotarget* (2015). doi:10.18632/oncotarget.4746

58. Zhang, C. xia *et al.* STING signaling remodels the tumor microenvironment by antagonizing myeloid-derived suppressor cell expansion. *Cell Death Differ.* (2019). doi:10.1038/s41418-019-0302-0

59. Laoui, D. *et al.* Mononuclear phagocyte heterogeneity in cancer: Different subsets and activation states reaching out at the tumor site. *Immunobiology* (2011). doi:10.1016/j.imbio.2011.06.007

60. Bronte, V. & Zanovello, P. Regulation of immune responses by L-arginine metabolism. *Nature Reviews Immunology* (2005). doi:10.1038/nri1668

61. Wang, J. *et al.* Siglec-15 as an immune suppressor and potential target for normalization cancer immunotherapy. *Nat. Med.* (2019). doi:10.1038/s41591-019-0374-x

62. Helmink, B. A. *et al.* B cells and tertiary lymphoid structures promote immunotherapy response. *Nature* (2020). doi:10.1038/s41586-019-1922-8

63. Ren, X. Immunosuppressive checkpoint Siglec-15: a vital new piece of the cancer immunotherapy jigsaw puzzle. *Cancer Biol. Med.* (2019). doi:10.20892/j.issn.2095-3941.2018.0141

64. Agresta, L. *et al.* CD244 represents a new therapeutic target in head and neck squamous cell carcinoma. *J. Immunother. Cancer* (2020). doi:10.1136/jitc-2019-000245

65. Garaud, S. *et al.* Tumor-infiltrating B cells signal functional humoral immune responses in breast cancer. *JCI Insight* (2019). doi:10.1172/jci.insight.129641

66. Bruno, T. C. New predictors for immunotherapy responses sharpen our view of the tumour microenvironment. *Nature* (2020). doi:10.1038/d41586-019-03943-0

67. Tsou, P., Katayama, H., Ostrin, E. J. & Hanash, S. M. The emerging role of b cells in tumor immunity. *Cancer Research* (2016). doi:10.1158/0008-5472.CAN-16-0431

68. Liudahl, S. M. & Coussens, L. M. B cells as biomarkers: Predicting immune checkpoint therapy adverse events. *Journal of Clinical Investigation* (2018). doi:10.1172/JCI99036

69. Petitprez, F. *et al.* B cells are associated with survival and immunotherapy response in sarcoma. *Nature* (2020). doi:10.1038/s41586-019-1906-8

70. Cabrita, R. *et al.* Tertiary lymphoid structures improve immunotherapy and survival in melanoma. *Nature* (2020). doi:10.1038/s41586-019-1914-8

71. Gnjatic, S. *et al.* Survey of naturally occurring CD4+ T cell responses against NY-ESO-1 in cancer patients: Correlation with antibody responses. *Proc. Natl. Acad. Sci. U. S. A.* (2003). doi:10.1073/pnas.1133324100

72. Crook, K. R. *et al.* Myeloid-derived suppressor cells regulate T cell and B cell responses during autoimmune disease. *J. Leukoc. Biol.* (2015). doi:10.1189/jlb.4a0314-139r

73. Rastad, J. L. & Green, W. R. Myeloid-derived suppressor cells in murine AIDS inhibit B-cell responses in part via soluble mediators including reactive oxygen and nitrogen species, and TGF-β. *Virology* (2016). doi:10.1016/j.virol.2016.08.031

74. Lelis, F. J. N. *et al.* Myeloid-derived suppressor cells modulate B-cell responses. *Immunol. Lett.* (2017). doi:10.1016/j.imlet.2017.07.003

75. Summers, B. C. & Leib, D. A. Herpes Simplex Virus Type 1 Origins of DNA Replication Play No Role in the Regulation of Flanking Promoters. *J. Virol.* (2002). doi:10.1128/jvi.76.14.7020-7029.2002

76. Halford, W. P., Püschel, R. & Rakowski, B. Herpes simplex virus 2 ICP0- mutant viruses are avirulent and immunogenic: Implications for a genital herpes vaccine. *PLoS One* (2010). doi:10.1371/journal.pone.0012251

77. Workenhe, S. T. *et al.* De novo necroptosis creates an inflammatory environment mediating tumor susceptibility to immune checkpoint inhibitors. *Commun. Biol.*

(2020). doi:10.1038/s42003-020-01362-w

78. Kim, D., Langmead, B. & Salzberg, S. L. HISAT: A fast spliced aligner with low memory requirements. *Nat. Methods* (2015). doi:10.1038/nmeth.3317

79. Anders, S., Pyl, P. T. & Huber, W. HTSeq-A Python framework to work with high-throughput sequencing data. *Bioinformatics* (2015). doi:10.1093/bioinformatics/btu638

80. McCarthy, D. J., Chen, Y. & Smyth, G. K. Differential expression analysis of multifactor RNA-Seq experiments with respect to biological variation. *Nucleic Acids Res.* (2012). doi:10.1093/nar/gks042

81. Robinson, M. D., McCarthy, D. J. & Smyth, G. K. edgeR: A Bioconductor package for differential expression analysis of digital gene expression data. *Bioinformatics* (2009). doi:10.1093/bioinformatics/btp616

82. Robinson, M. D. & Oshlack, A. A scaling normalization method for differential expression analysis of RNA-seq data. *Genome Biol.* (2010). doi:10.1186/gb-2010-11-3-r25

83. Law, C. W., Chen, Y., Shi, W. & Smyth, G. K. Voom: Precision weights unlock linear model analysis tools for RNA-seq read counts. *Genome Biol.* (2014). doi:10.1186/gb-2014-15-2-r29

84. Johnson, W. E., Li, C. & Rabinovic, A. Adjusting batch effects in microarray expression data using empirical Bayes methods. *Biostatistics* (2007). doi:10.1093/biostatistics/kxj037

85. Ritchie, M. E. *et al.* Limma powers differential expression analyses for RNA-sequencing and microarray studies. *Nucleic Acids Res.* (2015). doi:10.1093/nar/gkv007

86. Benjamini, Y. & Hochberg, Y. Controlling the False Discovery Rate: A Practical and Powerful Approach to Multiple Testing. *J. R. Stat. Soc. Ser. B* (1995). doi:10.1111/j.2517-6161.1995.tb02031.x

87. Fedchenko, N. & Reifenrath, J. Different approaches for interpretation and reporting of immunohistochemistry analysis results in the bone tissue - a review. *Diagnostic pathology* (2014). doi:10.1186/s13000-014-0221-9

Acknowledgments: Alyssa Vito was the recipient of the Vanier Canada Graduate Scholarship. The authors wish to acknowledge Spencer Revill for his work on the IHC images and quantification. The authors wish to acknowledge the BC Cancer Agency's Molecular and Cellular Immunology Core facility, Victoria, Canada for their work on the multi-panel IF images. **Funding**: This work was sponsored by operating grants from the Canadian Cancer Society Research Institute (formerly the Canadian Breast Cancer Research Alliance); grant #319377 and #706280. **Author contributions**: Conceptualization, A.V. and K.M.; Methodology, A.V., O.S., S.W. and K.M.; Investigation, A.V., O.S., N.E., S.W., A.P., K.M., D.H.; Writing – Original Draft, A.V.; Writing – Review & Editing, A.V., O.S., N.E., S.W., B.N., Y.W. and K.M.; Funding Acquisition, S.W. and K.M.; Resources, Y.W., and K.M.; Supervision, Y.W. and K.M.

Competing interests: The authors declare no competing interests. **Data and materials availability**: Complete RNA sequencing data set can be found here: https://www.ncbi.nlm.nih.gov/geo/query/acc.cgi?acc=GSE152698.

CHAPTER FOUR: S100A8/A9 AS MEDIATORS OF RESPONSE TO IMMUNOTHERAPY TREATMENT

Preamble

This chapter presents unpublished work that is currently under preparation. The version of record **Vito A**, El-Sayes N, Salem O, Wan Y, Mossman KL. S100A8/A9 as mediators of response to immunotherapy treatment.

AV conceived and designed the project, acquired and analyzed the data, interpreted the results and wrote the manuscript. NES acquired data and revised the manuscript. OS acquired data and revised the manuscript. YW supervised the study and revised the manuscript. KLM supervised the study and revised the manuscript.

Our literature review showed conflicting reports of the function of S100A8/A9 in the context of cancer. Hence, the aim of this work was to determine whether S100A8/A9 contribute to pro- or antitumorigenic functions in breast cancer. As S100A8/A9 are strongly linked to myeloid cell populations, we were further interested in their expression on various myeloid cells, which we assessed via flow cytometry. Utilizing next generation transcriptome-wide gene-level expression profiling, we showed that FEC + oHSV-1 therapy upregulated both S100A8/A9 and that this expression was irrespective of the location of the tumor (subcutaneous or orthotopic implantation), indicating that it was therapeutically induced. Review of data obtained from the TCGA database suggested that high levels of S100A8/A9 in breast tumors correlates with improved survival outcomes. Overall, this work added to our understanding of S100A8/A9 in the context of cancer and identified these key proteins as potential biomarkers of prognostic outcomes.

S100A8/A9 as mediators of response to immunotherapy treatments

Alyssa Vito[1,2], Omar Salem[1,2], Nader El-Sayes[1,2], Yonghong Wan[1,2] and Karen Mossman[1,2*]

[1]McMaster Immunology Research Centre, McMaster University, Hamilton, Ontario, L8S 4K1, Canada.

[2]Department of Medicine, McMaster University, Hamilton, Ontario, L8S 4K1, Canada.

*Corresponding author. Email: mossk@mcmaster.ca

Abstract

The era of immunotherapy has seen an insurgence of novel therapies driving oncologic research and clinical management. Immune checkpoint blockade (ICB) has undoubtedly been one of the most efficacious treatments discovered, with widespread clinical use across a variety of cancer types. Unfortunately, ICB only works in a small percentage of patients and has therefore been trialed primarily in combination with other therapeutic modalities, rather than as a standalone treatment. We have previously reported that a combination of low dose chemotherapy (FEC) and oncolytic virotherapy (oHSV-1) can be used to sensitize otherwise non-responsive tumors to ICB and that tumor-infiltrating B cells are required for efficacy of our therapeutic regimen in a murine model of triple negative breast cancer (TNBC). Further, we have shown that in the absence of circulating B cells, mice undergo rapid expansion of myeloid-derived suppressor cells (MDSCs), though the exact mechanism of MDSC modulation remains unknown. In the studies herein we have performed gene expression profiling using microarray analyses and

investigated the differential gene expression between tumors treated with FEC + oHSV-1, versus untreated tumors. Notably, two of the top upregulated genes were S100A8 and S100A9, calcium-binding proteins reported to have both pro- and antitumorigenic functions. In our studies, S100A8/A9 correlate with a shift to less immunosuppressive myeloid phenotypes, reduced immunosuppression and increased mechanisms of tumor cell killing. This correlation is in line with clinical data from breast cancer patients obtained from the Cancer Genome Atlas database and suggests that S100A8/A9 may facilitate responses to immunotherapy treatments and in particular, ICB.

4.1. Introduction

In recent years we have seen an insurgence of novel immunotherapies in both preclinical and clinical development, revolutionizing cancer therapy and clinical management of the disease. However, only a small percentage of patients benefit from these highly efficacious therapies and recent focus has shifted towards the need for a more comprehensive understanding of the immune system and immune interactions within the ever-changing tumor microenvironment (TME)[1]. With renewed attention to fundamental tumor immunology, myeloid cells have presented as a vital population of cells that drive the immune response, promote activation and expansion of effector T cells, and also simultaneously play a role in the maintenance of tissue homeostasis and in promoting immune tolerance[2]. Indeed, tumor-infiltrating myeloid cells are abundantly found in the tumor stroma and their levels strongly correlate with patient outcomes in many forms of cancer[3]. Additionally, tumors can co-opt myeloid cells to promote cancer growth and increase metastatic potential[3]. Recent years have uncovered a crucial role of

myeloid cell-driven immune escape in the TME, and it has become widely recognized that myeloid cells play a central, yet not fully understood, role in the response to many cancer therapies.

S100A8 and S100A9 are calcium binding proteins belonging to the S100 family. They often exist as a heterodimer and have minimal function in the homodimer state, due to instability[4]. The heterodimer is constitutively expressed by myeloid cells, functioning as a calcium sensor with roles in cytoskeletal rearrangement and metabolic pathways. In response to inflammation and cellular stress, S100A8/A9 is released from the cytoplasm and actively participates in the modulation of immune homeostasis by stimulating leukocyte recruitment and inducing cytokine secretion[4]. While these proteins have been extensively studied across various disease types, their exact role in inflammatory and malignant conditions continues to be controversial in the literature. In particular, S100A8 and S100A9 have been described as having both pro- and antitumorigenic functions[5,6].

Clinically, accumulation of S100A8 and S100A9 has been documented in many different forms of cancer including colon, pancreatic, bladder, ovarian, breast and skin[7,8]. Duan and colleagues have demonstrated that S100A9 is a prominent regulator of myeloid-derived suppressor cell (MDSC)-mediated immune suppression in colorectal cancer patients[9]. Similarly, other studies have highlighted the pro-tumorigenic role of S100A8/A9 in promoting cellular migration and ultimately, tumor metastasis[10,11]. Opposed to these functions, others have shown that S100A8 exhibits potent chemotactic activity, promoting cytotoxic immune cell recruitment to sites of inflammation[12].

We have previously reported an immunotherapy platform targeting immune-bare triple negative breast cancer (TNBC) tumors using a clinical chemotherapy cocktail (FEC; 5-fluorouracil, epirubicin, cyclophosphamide) in combination with an oncolytic Herpes Simplex-1 virus (oHSV-1)[13]. In this prior work, we focused on the ability of this therapeutic combination to sensitize tumors to immune checkpoint blockade (ICB) and the requirement of tumor-infiltrating B cells to combat MDSC-driven immunosuppression. In the current studies, we have focused on myeloid cell gene signatures and the ability of FEC + oHSV-1 therapy to switch the immunological landscape of a tumor from that of immunosuppressive myeloid phenotypes to those with antitumorigenic functions. Indeed, *S100A8* and *S100A9* were among the top upregulated genes in tumors treated with FEC + oHSV-1 therapy and their increased levels correlates with improved outcomes in our model.

Preliminary data for this work was conducted in subcutaneous tumors, which fail to accurately recapitulate de novo tumor formation and lack other cell types that may be found in naturally occurring TMEs. To assess the locational differences between subcutaneous tumors and those in the more appropriate location of the mammary fat pad, genome-wide transcriptome analysis was performed in both subcutaneous and orthotopically-implanted tumors. While these studies are specific to breast cancer, the underlying immunological functions of S100A8 and S100A9 biology can carry through to other solid tumor phenotypes as well.

4.2. Results

Treatment with FEC + oHSV-1 upregulates S100A8 and S100A9

We have previously reported that FEC + oHSV-1 therapy upregulates many immune pathways and leads to improved prognostic outcomes[13]. To validate previously published findings from RNA sequencing data, we performed gene expression profiling using microarray technique. C57/Bl6 mice were implanted with E0771 cells subcutaneously on the left flank and treated with either PBS (n=5) or FEC + oHSV-1 (n=10). Tumors were harvested on day 5 and RNA was extracted from whole tumor digests. Principal component analysis of the data shows that mice treated with FEC + oHSV-1 cluster distinctly from those treated with PBS (Figure 4.1A). Pathway enrichment analysis shows that our therapy switches the myeloid phenotype in the tumor from an immunosuppressive to inflammatory state. This switch is characterized by STAT5 and STAT3 signaling with a strong inflammatory response and upregulation of genes associated with apoptosis. This correlates strongly with increased levels of *S100A8* and *S100A9*, which are known to drive apoptotic pathways when found at high concentrations[4,14–16]. Indeed, of the top upregulated genes (Figure 4.1B), many are associated with macrophages (*SAA3*, *LCN2*, *CXCL2*, *IL1B, IL1A*, *CCL3*, *CXCL3, CLEC4E, ACOD1*), key myeloid-derived cells known to play a primary role in epigenetic reprogramming[17–19]. Furthermore, pathway enrichment analysis also revealed a strong downregulation of MTORC1 signaling, a known driver of myeloid cell differentiation to the immunosuppressive MDSC phenotype (Figure 4.1C).

We have previously shown that FEC + oHSV-1 therapy is able to cure 10 – 20 % of mice treated. Consistent with these findings, we see that the RNA profile of FEC + oHSV-1 mice shows 80% of mice clustered more similarly to PBS-treated mice, with

20% of mice having a distinct expression profile (Figure 4.1D). To determine whether these results were biased by the subcutaneous nature of the tumors, orthotopic implantation was used to more closely mimic the true microenvironment of breast tumors (Figure S4.1). Data are consistent between both implantation models, but more pronounced in tumors derived from the mammary fat pad.

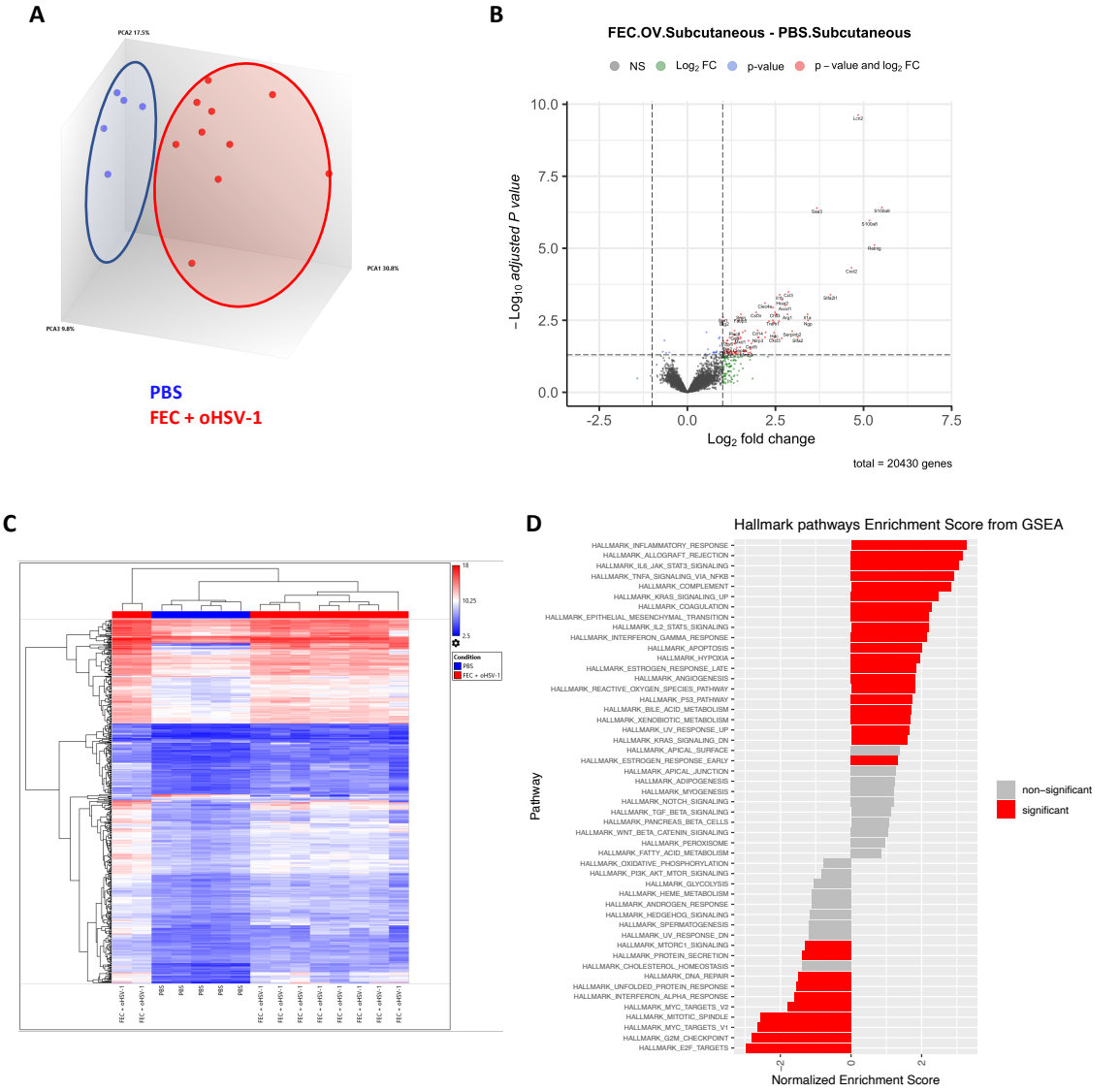

Fig. 4.1. FEC + oHSV-1 therapy upregulates many immune pathways and processes

C57/Bl6 mice bearing E0771 subcutaneous tumors were treated with either PBS, or FEC + oHSV-1. Tumors were harvested on day 5 and RNA was extracted from whole tumor digests and sent for sequencing.

(**A**) 3-D cluster plot showing the RNA expression correlations between mice treated with PBS (blue; n=5) and FEC + oHSV-1 (red; n=10). (**B**) Volcano plot showing differentially expressed genes between tumors treated with FEC + oHSV-1 and PBS. (**C**) Heat map showing the normalized expression values of genes across all samples. (**D**) Bar plot illustrating the results of hallmark pathway enrichment analysis performed on samples from mice treated with FEC + oHSV-1, compared to those treated with PBS alone.

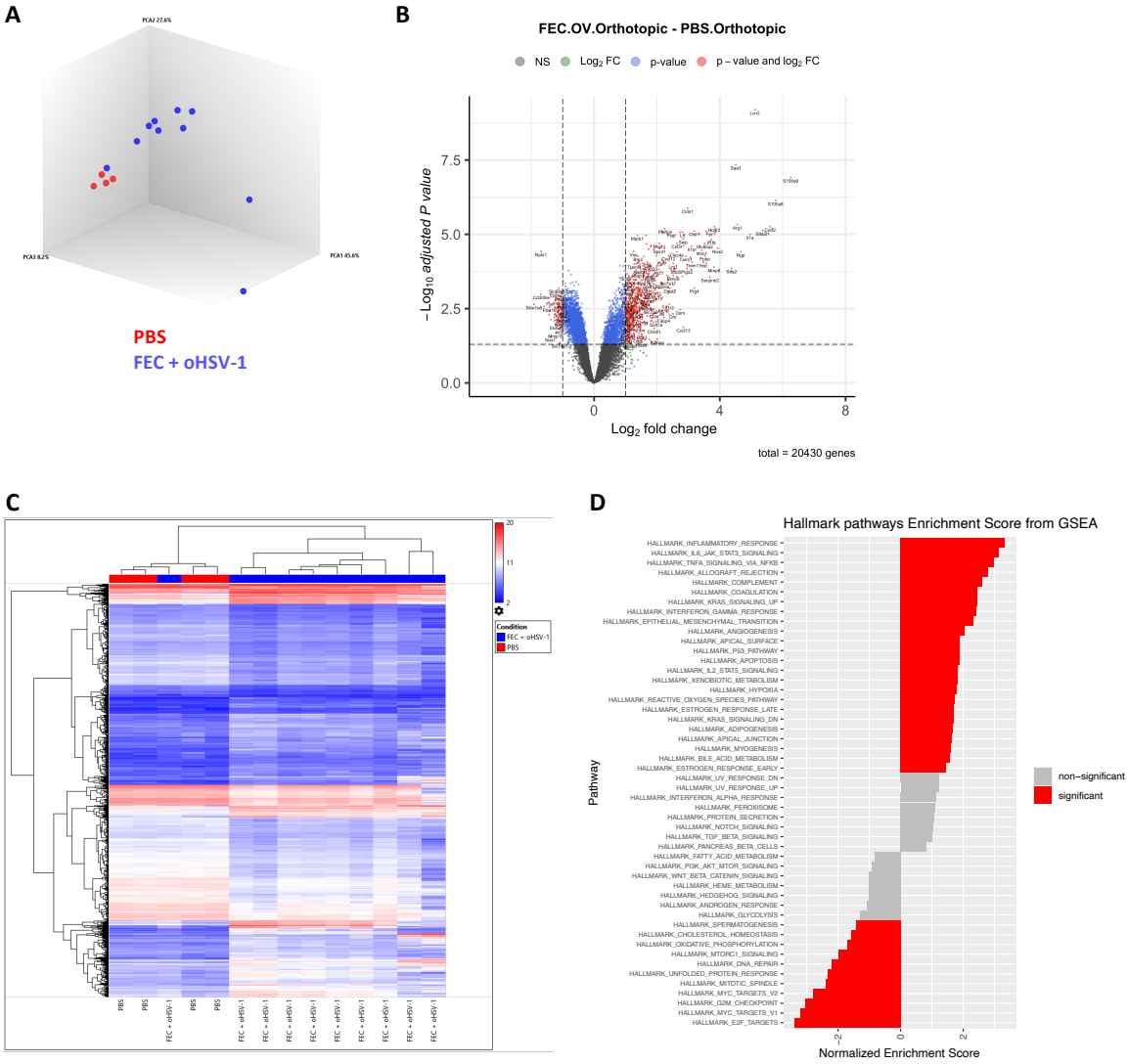

Fig. S4.1. FEC + oHSV-1 therapy upregulates many immune pathways and processes

C57/Bl6 mice bearing E0771 orthotopic tumors were treated with either PBS, or FEC + oHSV-1. Tumors were harvested on day 5 and RNA was extracted from whole tumor digests and sent for sequencing.

(**A**) 3-D cluster plot showing the RNA expression correlations between mice treated with PBS (blue; n=5) and FEC + oHSV-1 (red; n=10). (**B**) Volcano plot showing differentially

expressed genes between tumors treated with FEC + oHSV-1 and PBS. (**C**) Heat map showing the normalized expression values of genes across all samples. (**D**) Bar plot illustrating the results of hallmark pathway enrichment analysis performed on samples from mice treated with FEC + oHSV-1, compared to those treated with PBS alone.

FEC + oHSV-1 improves overall survival outcomes and increases S100A9

Consistent with our previous findings[13], mice treated with FEC + oHSV-1 therapy show delayed tumor progression and 10 – 20% durable cures (Figure 4.2) and increased levels of circulating S100A8/A9 (Figure 4.3). In particular, we found that S100A8/A9 expression on F4/80$^+$ macrophages peaked at day 10, which is consistent with the timeline of peak CD8$^+$ T cell levels in our model (Figure S4.2)[13]. These findings are in line with the RNA transcriptome profile, indicating that macrophages are responsible for the shift in myeloid cell differentiation.

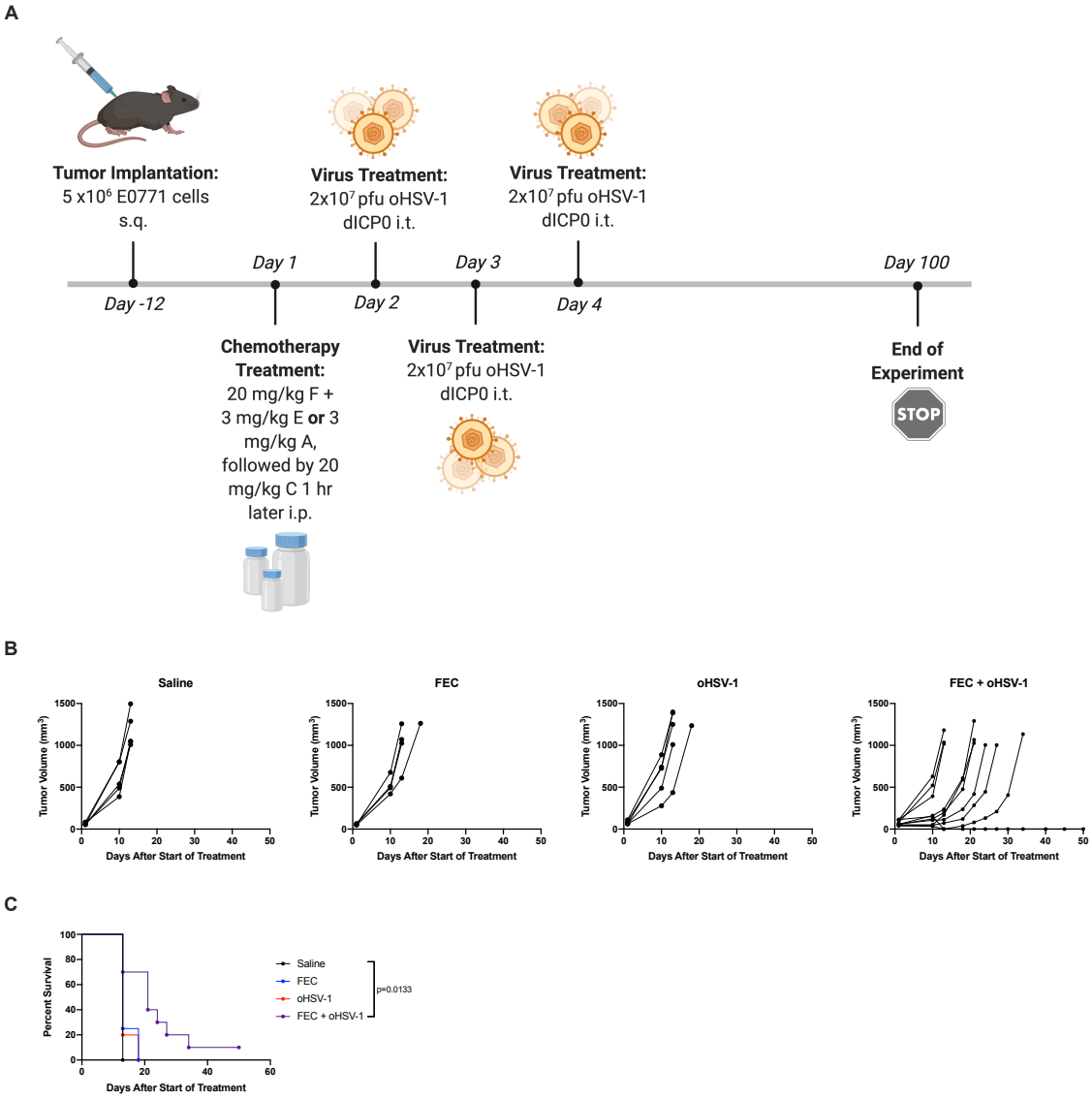

Fig. 4.2. FEC + oHSV-1 slows tumor growth and improves overall survival outcomes

(**A**) C57/Bl6 mice bearing E0771 tumors were treated with saline, chemotherapy (FEC), oncolytic virus (oHSV-1) or chemotherapy + oncolytic virus (FEC + oHSV-1). *Created using BioRender.com. (**B**) Tumor volumes were measured ever 2-3 days from the start of treatment until mice reached endpoint. Each line represents an individual mouse within

the group. (**C**) Kaplan-Meier survival curves of each group. *Mantel-Cox test was used for statistical analyses.

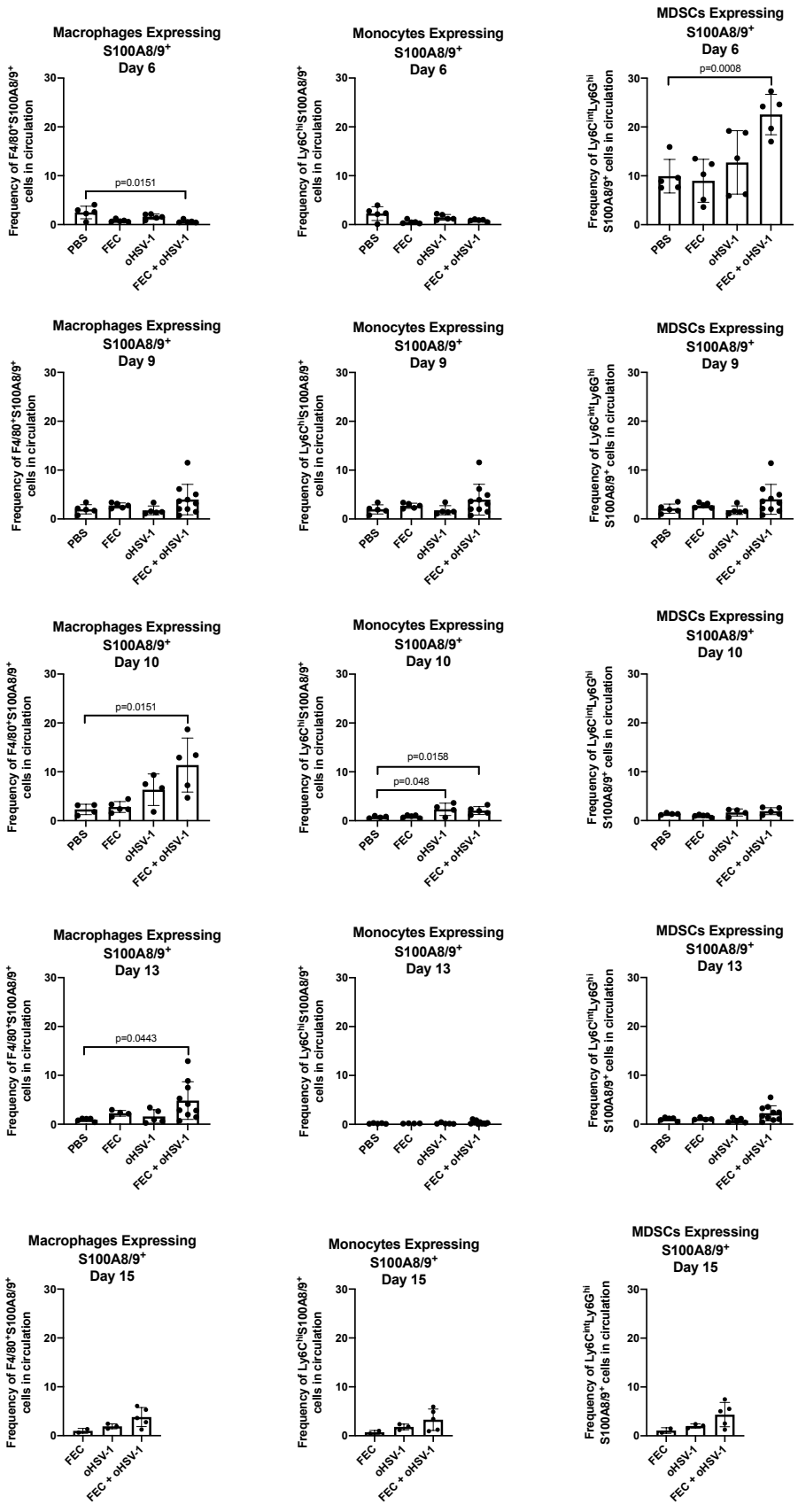
Macrophages Expressing S100A8/9+ Day 6
Frequency of F4/80+S100A8/9+ cells in circulation
p=0.0151
Monocytes Expressing S100A8/9+ Day 6
Frequency of Ly6Chi S100A8/9+ cells in circulation
MDSCs Expressing S100A8/9+ Day 6
Frequency of Ly6CintLy6Ghi S100A8/9+ cells in circulation
p=0.0008
Macrophages Expressing S100A8/9+ Day 9
Monocytes Expressing S100A8/9+ Day 9
MDSCs Expressing S100A8/9+ Day 9
Macrophages Expressing S100A8/9+ Day 10
p=0.0151
Monocytes Expressing S100A8/9+ Day 10
p=0.0158
p=0.048
MDSCs Expressing S100A8/9+ Day 10
Macrophages Expressing S100A8/9+ Day 13
p=0.0443
Monocytes Expressing S100A8/9+ Day 13
MDSCs Expressing S100A8/9+ Day 13
Macrophages Expressing S100A8/9+ Day 15
Monocytes Expressing S100A8/9+ Day 15
MDSCs Expressing S100A8/9+ Day 15
PBS
FEC
oHSV-1
FEC + oHSV-1

Fig. 4.3. FEC + oHSV-1 increases circulating levels of S100A9

C57/Bl6 mice bearing E0771 tumors were treated with PBS, FEC, oHSV-1 or FEC + oHSV-1. Blood was drawn on days 6, 9, 10, 13 and 15 and analyzed via flow cytometry. Bar plots showing the frequencies of F4/80^{+}S100A8/A9^{+}, Ly6C^{hi}S100A8/A9^{+} and Ly6C^{int}Ly6G^{hi}S100A8/A9^{+} cells in circulating PBMCs. Dots are representative of individual mice. Error bars are representative of the standard deviation. Two-tailed unpaired t test was used for statistical analyses.

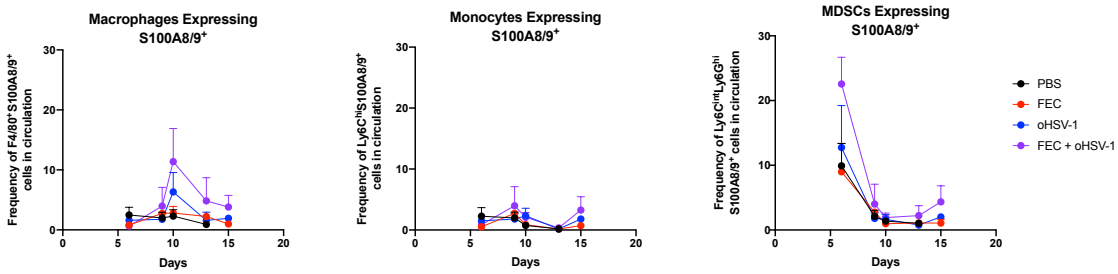

Fig. S4.2. FEC + oHSV-1 increase in circulating levels of S100A9

C57/Bl6 mice bearing E0771 tumors were treated with PBS, FEC, oHSV-1 or FEC + oHSV-1. Blood was drawn on days 6, 9, 10, 13 and 15 and analyzed via flow cytometry. Line graphs are representative of the mean frequency of F4/80^{+}S100A8/A9^{+}, Ly6C^{hi}S100A8/A9^{+} and Ly6C^{int}Ly6G^{hi}S100A8/A9^{+} cells in circulating PBMCs for all mice in each group. Error bars are representative of the standard deviation.

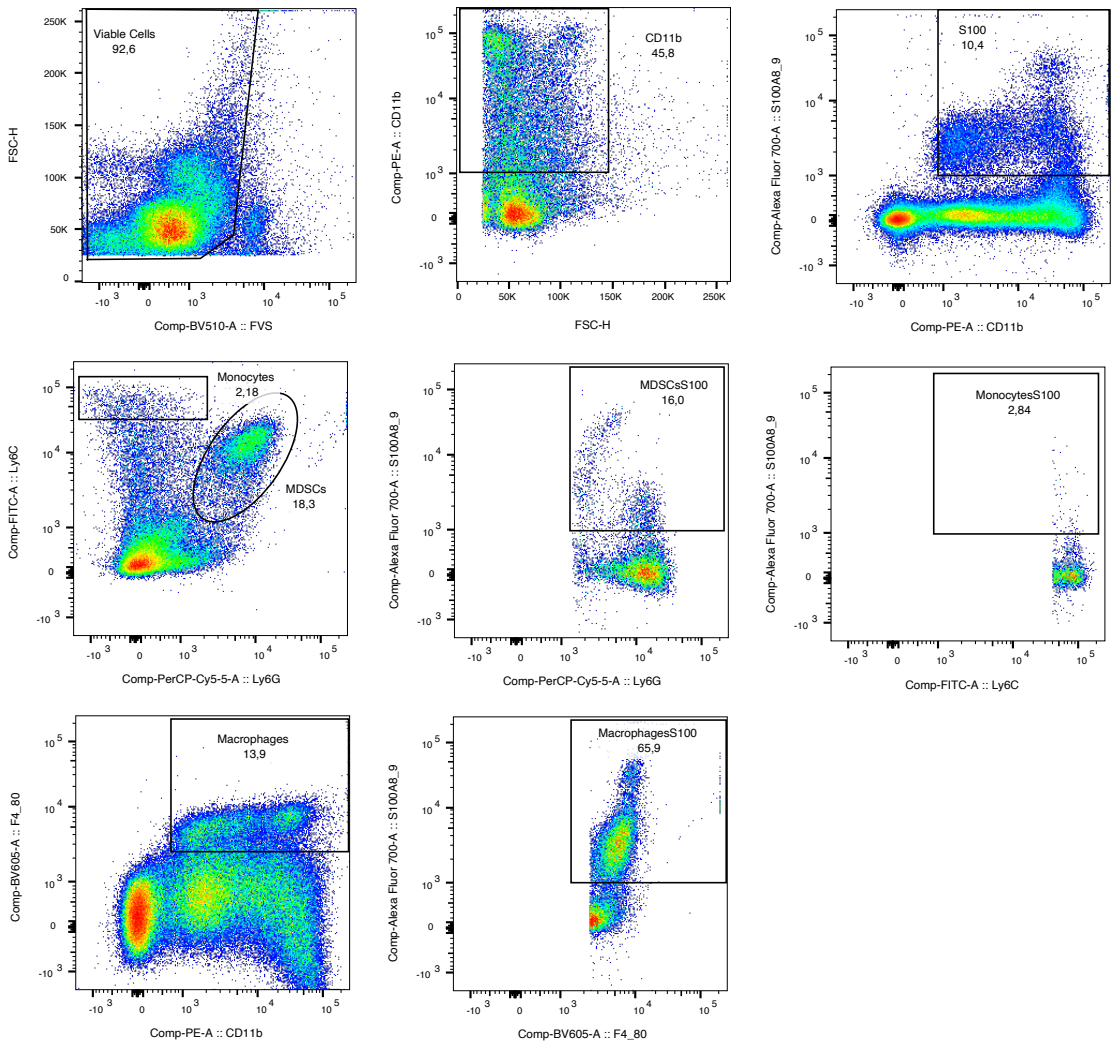

Fig. S4.3. Flow cytometry gating strategy

High expression levels of S100A8 and S100A9 correlate with improved prognostic outcomes in breast cancer

It has been well established in both preclinical and clinical studies that many forms of cancer show increased expression levels of S100A8 and S100A9. However, whether or not this high expression correlates with improved prognostic outcomes

remains elusive in the literature. Using data from The Cancer Genome Atlas (TCGA)[20], we have investigated prognostic outcomes of patients with high and low expression of S100A8 and S100A9 in breast cancer (Figure 4). As indicated by the survival outcomes, breast cancer patients with high levels of S100A8 and S100A9 have improved survival outcomes, which is consistent with our findings in a murine model of TNBC.

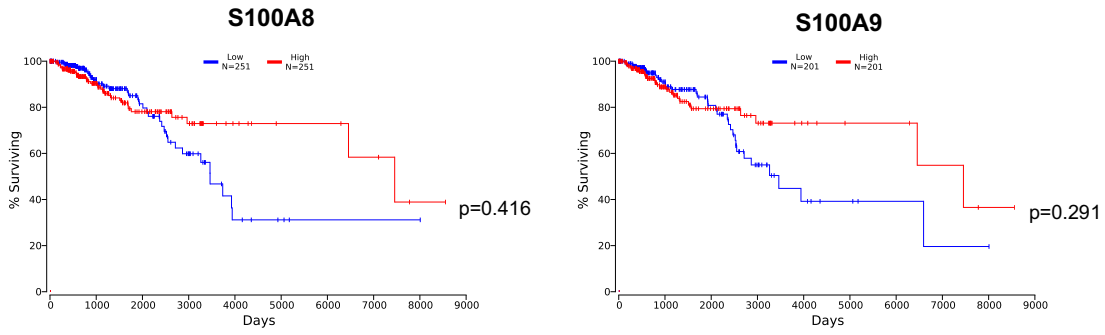

Fig. 4.4. High level of S100A8 and S100A9 in breast cancer correlate with improved survival outcomes

Kaplan-Meier survival curve of breast cancer patients segregated into low and high expression of S100A8 and S100A9. The results shown here are based upon data generated by the TCGA Research Network: https://www.cancer.gov/tcga.

4.3. Discussion

Immunotherapy has continued to cement itself as a pillar of cancer care with widespread clinical success in a variety of cancer types. However, responses to immunotherapy treatments, and in particular ICB, vary greatly between patients and drivers of therapeutic response remain largely elusive to date. While myeloid cells have arisen as potent regulators of tumor evolution, their plasticity and metabolic heterogeneity

means they are heavily influenced by the TME and cellular populations they come in contact with[21]. S100A8 and S100A9, multifunction proteins expressed by myeloid cells at various differentiation states, have controversial roles reported in the literature and may contribute to both pro- and antitumorigenesis.

We have previously reported a combination of FEC + oHSV-1 as being capable of sensitizing tumors to ICB. To further investigate this phenomenon, herein we have described the RNA profile of tumors treated with either FEC + oHSV-1 therapy or PBS and the myeloid gene signature associated with our therapeutic platform. Notable from our findings, FEC + oHSV-1 significantly downregulated MTORC1 signaling. Indeed, S100A9 has been shown to control MTORC1 modulation of MDSCs[22–24]. Additionally, recently published studies also dictate that therapies that can successfully sensitize breast tumors to ICB do so through epigenetic reprogramming of myeloid cells in the TME, shifting tumor-associated macrophages (TAMs) to an anti-tumor M1 phenotype and promoting STAT3-mediated suppression of myeloid cells[25]. These findings are in line with our analysis of cellular populations in PBMCs.

4.4. Materials and Methods

Cell Lines

Human osteosarcoma cells from a fifteen-year old Caucasian female (U2OS; ATCC, Manassas, VA) were maintained in Dulbecco's modified Eagle's media (DMEM) supplemented with 10% fetal bovine serum (FBS, ATCC 30-2020) 2 mmol/l L-glutamine, 100 U/ml penicillin, 100 μg/ml streptomycin (Gibco, Grand Island, NY). Vero

cells originating from the kidney of an adult monkey (ATCC, Manassas, VA) were maintained in DMEM supplemented with 10% FBS 2 mmol/l L-glutamine, 100 U/ml penicillin, 100 μg/ml streptomycin (Gibco, Grand Island, NY). Murine medullary breast adenocarcinoma cells isolated as a spontaneous tumor from a C57/Bl6 mouse (E0771; CH3 Biosystems, Amherst, NY) were maintained in roswell park memorial institute (RPMI) medium supplemented with 10% FBS, 10 mM HEPES, 200 μM geneticin and 2 mmol/l L-glutamine. All cell lines were grown at 37 °C with 5% CO_2.

Mouse Experiments

Mice were maintained at the McMaster University Central Animal Facility and all the procedures were performed in full compliance with the Canadian Council on Animal Care and approved by the Animal Research Ethics Board of McMaster University. Six- to eight-week-old female C57/Bl6 mice (Charles River Laboratories, Wilmington, MA) were used to implant 5×10^6 E0771 cells subcutaneously on the left flank or orthotopically. Mice were weighed and all found to be approximately 20 g in size. Mice were housed in groups, 5 / cage, fed a normal diet and kept at room temperature. To minimize experimental variability, low passage E0771 cells were used for subcutaneous injections. Twelve days after injection, the tumors reached treatable average tumor volume (50-100 mm^3). Mice were blindly randomized prior to the start of treatment. In experimental groups receiving FEC treatment, mice were treated on day 1 with 20 mg/kg 5-fluorouracil in 200 μL saline, followed by 3 mg/kg epirubicin in 200 μL saline, followed by 20 mg/kg cyclophosphamide in 200 μL saline 1 h later. All chemotherapy injections were given intraperitoneally (i.p.). Experimental groups receiving oHSV-1

were treated with 2×10^7 pfu oHSV-1 dICP0 in 50 µL PBS intratumorally (i.t.) on days 2, 3 and 4. For all mouse studies, tumors were measured every 2 – 3 days and mice having a tumor volume of 1000 mm^3 were classified as end point.

Drug Preparation

5-fluorouracil stock powder (Sigma Aldrich, F6627) was stored at 4 °C and dissolved in sterile saline to a concentration of 2 mg/mL. Epirubicin stock powder (Cayman Chemicals, 12091) was stored at -20 °C and dissolved in sterile saline to a concentration of 0.3 mg/mL. Cyclophosphamide stock powder (Sigma Aldrich, C0768) was stored at 4 °C and dissolved in sterile saline to a concentration of 2 mg/mL.

Virus Preparation

Recombinant HSV-1 was generated by homologous recombination using infectious DNA of luciferase-expressing wild-type HSV-1 KOS/Dluc/oriL[26]. HSV-1 dNLS encodes a GFP-tagged protein that lacks the ICP0 NLS region and a portion of the C-terminal oligomerization domain[27]. HSV-1 dICP0 contains a deletion of the entire *ICP0* coding region All HSV-1 *ICP0* mutants were propagated and tittered on U2OS cells in the presence of 3 mmol/l hexamethylene bisacetamide (Sigma, St Louis, MO). Wild-type HSV-1 strain KOS was propagated and tittered on Vero cells. All viruses were purified and concentrated via sucrose cushion ultracentrifugation and purified virus was resuspended in PBS and stored at -80 °C.

Flow Cytometry Analysis

150 µL blood was collected from the periorbital sinus. Red blood cells from all samples were lysed using ACK buffer. The PBMCs were treated with anti-CD16/CD32 (Fc block) and surface stained with fluorescently conjugated antibodies for FVS (BD Biosciences, #564406), CD11b (BD Biosciences, #553311), Ly6C (BD Biosciences, #553104), Ly6G (BD Biosciences, #560602), F4/80 (BD Biosciences, #743282), S100A8/A9 (Novus Biologicals, #NBP2-47667AF700). LSRFortessa flow cytometer with FACSDiva software (BD Biosciences) was used for data acquisition and FlowJo Mac, version 10.0 software was used for data analysis.

Statistical Analysis

For each statistical analysis used, normality of the distributions and variance assumptions were tested before running the statistical analyses. Multiple t-tests were used to determine the statistical significance of the differences in means. The log-rank Mantel-Cox test and the Gehan-Breslow-Wilcoxon test were used to determine statistical significance for the difference in Kaplan-Meier survival curves between treatments. All the tests were two-sided. The null hypothesis was rejected for p-values less than 0.05. All data analyses were carried out using GraphPad Prism.

Supplementary Materials

Fig. S4.1. FEC + oHSV-1 therapy upregulates many immune pathways and processes

Fig. S4.2. FEC + oHSV-1 increase in circulating levels of S100A9

Fig. S4.3. Flow cytometry gating strategy

References

1. Waldman, A. D., Fritz, J. M. & Lenardo, M. J. A guide to cancer immunotherapy: from T cell basic science to clinical practice. *Nature Reviews Immunology* (2020). doi:10.1038/s41577-020-0306-5

2. Amodio, G. *et al.* Role of myeloid regulatory cells (MRCs) in maintaining tissue homeostasis and promoting tolerance in autoimmunity, inflammatory disease and transplantation. *Cancer Immunology, Immunotherapy* (2019). doi:10.1007/s00262-018-2264-3

3. Engblom, C., Pfirschke, C. & Pittet, M. J. The role of myeloid cells in cancer therapies. *Nature Reviews Cancer* (2016). doi:10.1038/nrc.2016.54

4. Wang, S. *et al.* S100A8/A9 in inflammation. *Frontiers in Immunology* (2018). doi:10.3389/fimmu.2018.01298

5. Bagheri, V. & Apostolopoulos, V. Pro-inflammatory S100A9 Protein: a Double-Edged Sword in Cancer? *Inflammation* (2019). doi:10.1007/s10753-019-00981-8

6. Srikrishna, G. S100A8 and S100A9: New insights into their roles in malignancy. *Journal of Innate Immunity* (2011). doi:10.1159/000330095

7. Gebhardt, C., Németh, J., Angel, P. & Hess, J. S100A8 and S100A9 in inflammation and cancer. *Biochem. Pharmacol.* (2006). doi:10.1016/j.bcp.2006.05.017

8. Salama, I., Malone, P. S., Mihaimeed, F. & Jones, J. L. A review of the S100 proteins in cancer. *European Journal of Surgical Oncology* (2008). doi:10.1016/j.ejso.2007.04.009

9. Huang, M. *et al.* S100A9 Regulates MDSCs-Mediated Immune Suppression via the RAGE and TLR4 Signaling Pathways in Colorectal Carcinoma. *Front. Immunol.* (2019). doi:10.3389/fimmu.2019.02243

10. Saha, A. *et al.* Lack of an endogenous anti-inflammatory protein in mice enhances colonization of B16F10 melanoma cells in the lungs. *J. Biol. Chem.* (2010). doi:10.1074/jbc.M109.083550

11. Ang, C. W. *et al.* Smad4 loss is associated with fewer S100A8-positive monocytes in colorectal tumors and attenuated response to S100A8 in colorectal and pancreatic cancer cells. *Carcinogenesis* (2010). doi:10.1093/carcin/bgq137

12. Goyette, J. & Geczy, C. L. Inflammation-associated S100 proteins: New mechanisms that regulate function. *Amino Acids* (2011). doi:10.1007/s00726-010-0528-0

13. Vito, A. *et al.* B cell involvement renders triple negative breast cancer sensitive to immune checkpoint blockade through downregulation of myeloid-derived suppressor cells. *Commun. Biol.* (2021).

14. Ghavami, S. *et al.* S100A8/A9: A Janus-faced molecule in cancer therapy and tumorgenesis. *European Journal of Pharmacology* (2009). doi:10.1016/j.ejphar.2009.08.044

15. Ghavami, S. *et al.* S100A8/A9 at low concentration promotes tumor cell growth via RAGE ligation and MAP kinase-dependent pathway. *J. Leukoc. Biol.* (2008). doi:10.1189/jlb.0607397

16. Turovskaya, O. *et al.* RAGE, carboxylated glycans and S100A8/A9 play essential roles in colitis-associated carcinogenesis. *Carcinogenesis* (2008). doi:10.1093/carcin/bgn188

17. Rodriguez, R. M., Suarez-Alvarez, B. & Lopez-Larrea, C. Therapeutic Epigenetic Reprogramming of Trained Immunity in Myeloid Cells. *Trends in Immunology* (2019). doi:10.1016/j.it.2018.11.006

18. Chen, S., Yang, J., Wei, Y. & Wei, X. Epigenetic regulation of macrophages: from homeostasis maintenance to host defense. *Cellular and Molecular Immunology* (2020). doi:10.1038/s41423-019-0315-0

19. Álvarez-Errico, D., Vento-Tormo, R., Sieweke, M. & Ballestar, E. Epigenetic control of myeloid cell differentiation, identity and function. *Nature Reviews Immunology* (2015). doi:10.1038/nri3777

20. Anaya, J. OncoLnc: Linking TCGA survival data to mRNAs, miRNAs, and lncRNAs. *PeerJ Comput. Sci.* (2016). doi:10.7717/peerj-cs.67

21. Sieow, J. L., Gun, S. Y. & Wong, S. C. The sweet surrender: How myeloid cell metabolic plasticity shapes the tumor microenvironment. *Frontiers in Cell and Developmental Biology* (2018). doi:10.3389/fcell.2018.00168

22. Trikha, P. & Carson, W. E. Signaling pathways involved in MDSC regulation. *Biochimica et Biophysica Acta - Reviews on Cancer* (2014). doi:10.1016/j.bbcan.2014.04.003

23. ZHONG, X., XIE, F., CHEN, L., LIU, Z. & WANG, Q. S100A8 and S100A9

promote endothelial cell activation through the RAGE-mediated mammalian target of rapamycin complex 2 pathway. *Mol. Med. Rep.* (2020). doi:10.3892/mmr.2020.11595

24. Ohata, H. *et al.* NOX1-Dependent mTORC1 Activation via S100A9 Oxidation in Cancer Stem-like Cells Leads to Colon Cancer Progression. *Cell Rep.* (2019). doi:10.1016/j.celrep.2019.06.085

25. Sidiropoulos, D. N. *et al.* Phenotypic shifts of tumor associated macrophages and STAT3 mediated suppression of myeloid derived suppressor cells drive sensitization of HER2 + tumor immunity. *bioRxiv* (2021).

26. Summers, B. C. & Leib, D. A. Herpes Simplex Virus Type 1 Origins of DNA Replication Play No Role in the Regulation of Flanking Promoters. *J. Virol.* (2002). doi:10.1128/jvi.76.14.7020-7029.2002

27. Halford, W. P., Püschel, R. & Rakowski, B. Herpes simplex virus 2 ICP0- mutant viruses are avirulent and immunogenic: Implications for a genital herpes vaccine. *PLoS One* (2010). doi:10.1371/journal.pone.0012251

Acknowledgments: Alyssa Vito was the recipient of the Vanier Canada Graduate Scholarship. **Funding**: This work was sponsored by operating grants from the Canadian Cancer Society Research Institute (formerly the Canadian Breast Cancer Research Alliance); grant #319377 and #706280. **Author contributions**: Conceptualization, A.V. and K.M.; Methodology, A.V.; Investigation, A.V., O.S., N.E.; Writing – Original Draft, A.V.; Writing – Review & Editing, A.V., O.S., N.E., Y.W. and K.M.; Funding

Acquisition, K.M.; Resources, Y.W. and K.M.; Supervision, Y.W. and K.M. **Competing interests**: The authors declare no competing interests.

CHAPTER FIVE: COMBINED RADIONUCLIDE THERAPY AND IMMUNOTHERAPY FOR TREATMENT OF TRIPLE NEGATIVE BREAST CANCER

Preamble

This is a pre-copyedited, author-produced version of an article submitted for peer-review to the International Journal of Molecular Sciences. The version of record **Vito A**, Rathmann S, Mercanti N, El-Sayes N, Mossman KL, Valliant J. Combined radio-immunotherapy for treatment of triple negative breast cancer.

AV conceived and designed the project, acquired and analyzed the data, interpreted the results and wrote the manuscript. SR conceived and designed the project, acquired the data and wrote the manuscript. NM acquired the data. NES acquired the data. KLM supervised the study, interpreted the results and revised the manuscript. JV supervised the study, interpreted the results and revised the manuscript.

Our literature review showed many preclinical and clinical studies assessing the synergistic benefit of radiotherapies and immunotherapies. We used a radiolabeled biomolecule for targeted radiotherapy and combined this with ICB. Survival studies in TNBC tumor-bearing mice showed that radiotherapy was able to sensitize tumors to respond to ICB. IHC was used to look at the TME and showed that combination therapy was able to induce infiltration of immune cells into the otherwise immune-bare landscape. Flow cytometry studies further showed that the combination of radiotherapy and ICB decreased levels of MDSCs, allowing for improved therapeutic efficacy, a finding consistent with the remainder of work in this thesis.

Combined Radionuclide Therapy and Immunotherapy for Treatment of Triple Negative Breast Cancer

Alyssa Vito[1†], Stephanie Rathmann[2†], Natalie Mercanti[2], Nader El-Sayes[1], Karen Mossman[1*] and John Valliant[2*]

[1]Department of Medicine, McMaster Immunology Research Centre, McMaster University, Hamilton, Ontario, L8S 4K1, Canada.

[2]Department of Chemistry and Chemical Biology, McMaster University, Hamilton, ON, Canada.

[†]The authors contributed equally to this publication.

*Corresponding author. Email: valliant@mcmaster.ca, mossk@mcmaster.ca

Abstract

Triple negative breast cancer (TNBC) is an aggressive subtype of the disease with poor clinical outcomes and limited therapeutic options. Immune checkpoint blockade (CP) has surged to the forefront of cancer therapies with widespread clinical success in a variety of cancer types. However, the percentage of TNBC patients that benefit from CP as a monotherapy is low and clinical trials have shown the need for combined therapeutic modalities. Specifically, there has been interest in combining CP therapy with radiation therapy where clinical studies primarily with external beam have suggested their therapeutic synergy, contributing to the development of anti-tumor immunity. Here, we have developed a therapeutic platform combining radionuclide therapy (RT) and

immunotherapy utilizing a radiolabelled biomolecule and CP in an E0771 murine TNBC tumor model. Survival studies show that while neither monotherapy is able to improve therapeutic outcomes, the combination of RT + CP extended overall survival. Histologic analysis showed that RT + CP increased necrotic tissue within the tumor and decreased levels of F4/80+ macrophages. Flow cytometry analysis of the peripheral blood also showed that RT + CP suppressed macrophages and myeloid-derived suppressive cells, both of which actively contribute to immune escape and tumor relapse.

5.1. Introduction

Breast cancer is the most common cancer among women worldwide, accounting for more than 2 million new cases and 600,000 deaths annually [1]. Triple negative breast cancer (TNBC) accounts for 10 – 20% of all breast cancers, has a higher risk in women under the age of 40, demonstrates substantial tumor heterogeneity and is often identified as being high grade [2]. TNBC patients routinely undergo extensive, highly toxic treatment regimens and have the highest risk of relapse amongst all breast cancer types [3,4]. Furthermore, recently approved therapies for TNBC are limited (olaparib, atezolizumab and sacituzumab-govitecan) and only benefit 10 – 20% of patients, highlighting the need for improved therapies for TNBC patients. To this end, a deeper understanding of the immune landscape in TNBC patients is required to develop novel, effective therapies.

Recent years have seen the emergence of immunotherapies in both preclinical and clinical development, revolutionizing the way we think about treating cancer patients. One such therapy, immune checkpoint blockade (CP), uses antibodies to block inhibitory pathways on immune cells and has shown widespread clinical success with durable cures across a variety of cancer types [5,6]. However, the percentage of patients that respond to CP is low and even those patients who initially display tumor regression often succumb to relapsed disease [5,7]. As the field of immuno-oncology continues to grow, so too does our understanding of immunotherapies and the challenges associated with achieving durable and complete responses to treatment. In an effort to combat clinical barriers to CP

efficacy, there has been an emergence of new paradigms incorporating traditional therapies into immunotherapy regimens [8–10].

Radiation therapy has been a mainstay treatment for many forms of cancer since the late 1800s. Historically, radiation has been thought to work solely through direct contact-based killing, but there has long been the postulation of immune involvement through the hypothesis of the abscopal effect [11]. The abscopal effect occurs when an irradiated tumor initiates a cascade of events with the release of damage-associated molecular patterns (DAMPs) such as high mobility group box 1 (HMGB1), adenosine triphosphate (ATP) and heat shock proteins (HSPs). These DAMPs act on receptors that are expressed on dendritic cells (DCs), leading to antigen presentation, tumor-specific killing from cytotoxic T cells and ultimately anti-tumor activity (Figure 5.1). The abscopal effect was first clinically documented in 1953 [12], but interest waned with rare occurrences noted and difficulties in recapitulating the phenomenon in preclinical models. Now, in the era of immunotherapy there is a much deeper understanding of the immune system and the interplay of cells in the tumor microenvironment (TME) and the abscopal effect has once again been brought to the forefront of oncologic research.

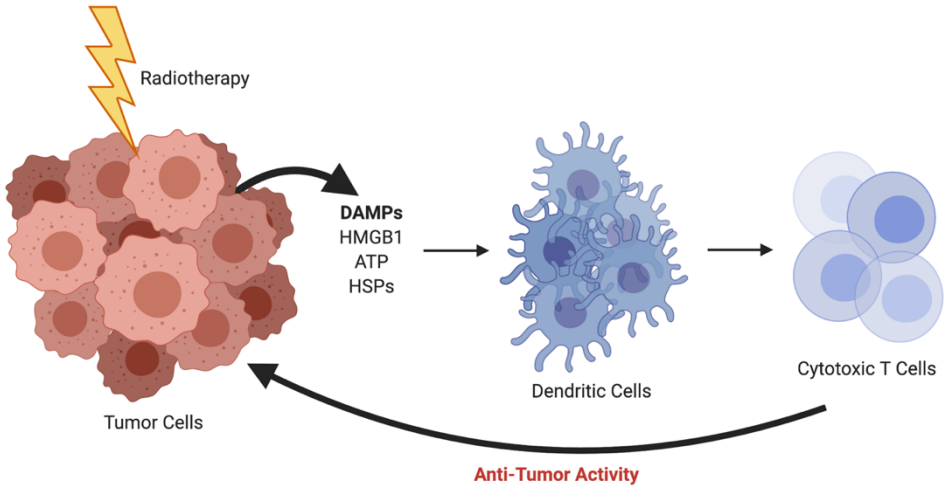

Fig. 5.1. Radiotherapy-induced abscopal effect resulting in anti-tumor activity. *Created using BioRender.com

Clinical studies have shown that the combination of radiotherapy and immunotherapy synergizes for enhanced anti-tumor activity and improved prognostic outcomes [13,14]. In a phase I clinical trial, patients with metastatic or nonresectable melanoma tumors were treated with anti-CTLA-4 and anti-PD-1 checkpoint antibodies and a small cohort of patients was also given radiation therapy [15]. This study noted a significant improvement in overall survival percentages in the patient population receiving the dual therapy. Similarly, in a phase II clinical trial, patients with metastatic TNBC (mTNBC) were treated with anti-PD-1 checkpoint antibodies and fractionated external beam radiation therapy [16]. The overall response rate of the patients was 17.6% with 3 responders achieving a 100% reduction in tumor volume outside of the irradiated

field. It is important to note that the patients enrolled in the study were unselected for PD-L1 expression and had failed previous first line therapies.

Here, we outline a therapeutic platform using cytotoxic radiation to sensitize otherwise non-responsive tumors to CP. In particular, we chose to investigate whether continuous cell irradiation, through the use of internal radionuclide therapy (RT), would synergize with dual anti-CTLA-4 and anti-PD-L1 checkpoint therapy. In order to maximize and better control the radiation dose to the tumor, we used intratumoral delivery of the beta emitter, lutetium-177, linked to a biomolecule. Albumin, an abundant blood protein, was used as a biocompatible protein anchor to prolong retention of the radionuclide in the tumor. With respective to potential translation, intratumoral injections of albumin radiopharmaceuticals for sentinel node imaging in breast cancer are routinely performed in the clinic [17] while materials labeled with beta emitting isotopes are routinely being delivered in a similar manner for liver cancers.

5.2. Results

Tunable platform for intratumoral administration of radiotherapeutic

Due to the rich history and proven track record in medical practice, we chose to use albumin as the protein anchor to prolong the retention of the radionuclide within the TME and provide greater control over the administered dose when compared to intravenous (iv) administration [18–20]. To increase the versatility of our platform and ensure that protein integrity is maintained during synthesis, bovine serum albumin (BSA) was first functionalized with trans-cyclooctene (TCO). This TCO-BSA conjugate can

then undergo a rapid, room temperature inverse electron-demand Diels-Alder (IEDDA) reaction in which the TCO moiety forms a covalent linkage with its coupling partner, a tetrazine, which in this case is radiolabelled with lutetium-177 (Figure 5.2). This type of two step functionalization minimizes the risk of a non-specific binding interaction of the radionuclide with BSA. To prepare TCO-BSA, BSA was combined with a TCO-NHS ester and the mixture allowed to incubate overnight at room temperature. TCO-BSA was purified by dialysis and the conjugation confirmed by matrix-assisted laser desorption ionization mass spectrometry (MALDI-MS; Figure S5.1). The tetrazine was synthesized as previously described [21], and the radiolabelled product produced by adding [177Lu]LuCl3 (Figure 5.3) at 60 ºC for 5 minutes, resulting in a radiochemical yield of >99%. The radiolabelled small molecule was incubated with TCO-BSA for ten minutes at room temperature, followed by purification using a high molecular weight spin filter. The resultant radiochemical yield was 46 ± 5% based on the amount of activity isolated from the spin filter.

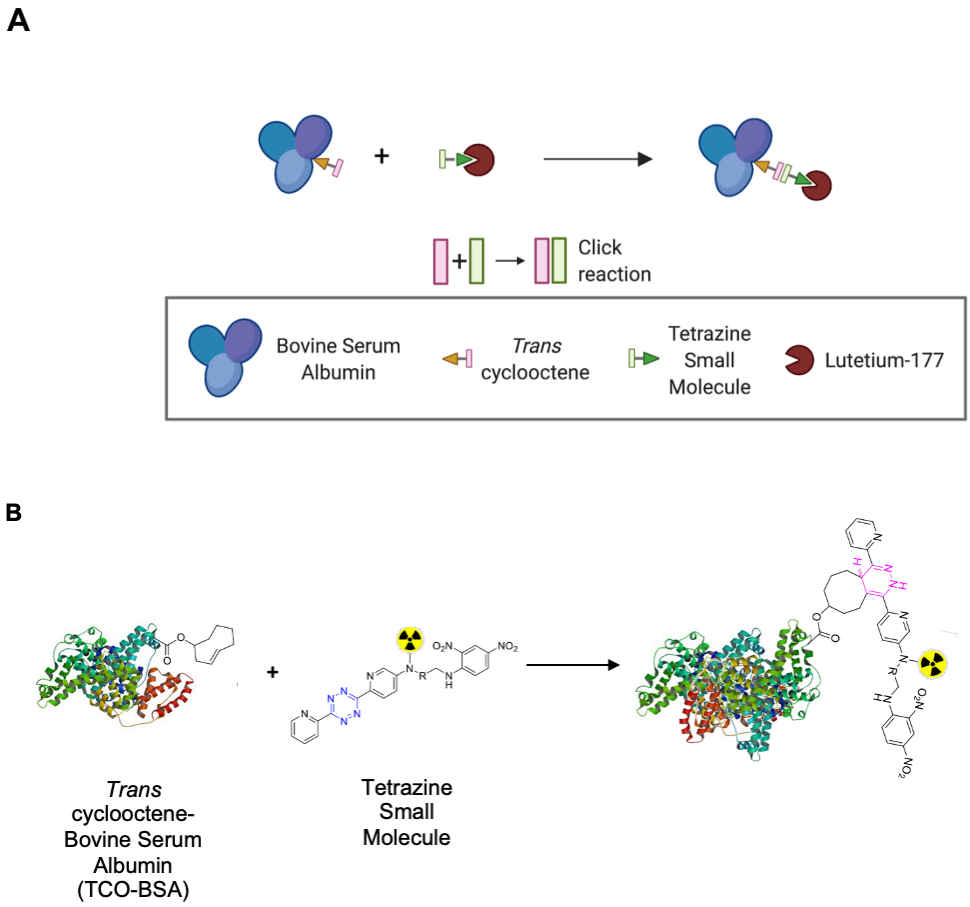

Fig. 5.2. Schematic representation showing the inverse electron-demand Diels-Alder reaction between the trans-cyclooctene and tetrazine-based moieties.

(**A**) Simplified schematic of the overall conjugation and labelling strategy. (**B**) Schematic showing the key functional groups used to label albumin.

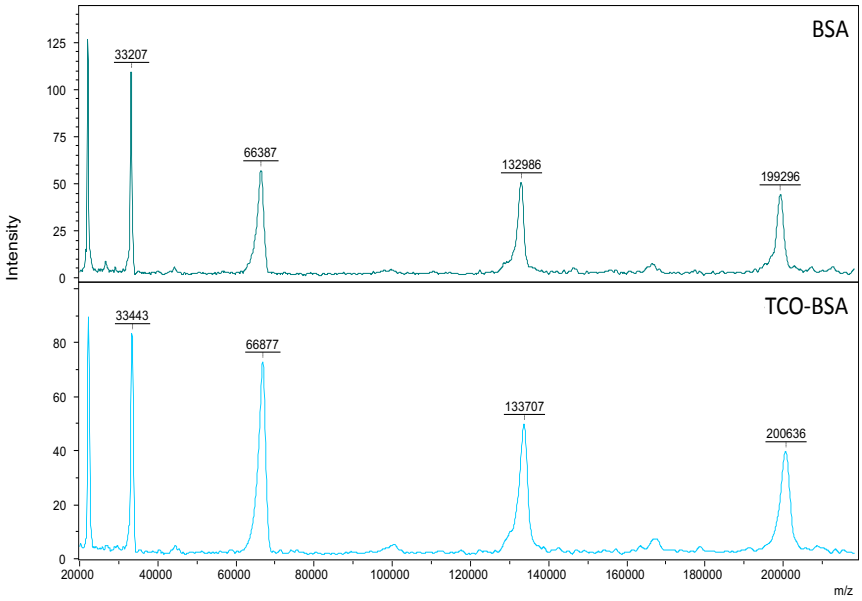

Fig. S5.1. MALDI-MS confirms conjugation of TCO to BSA

BSA (top spectrum) was conjugated with TCO (bottom spectrum) and analyzed via MALDI-MS, indicating an average of 3.2 TCO groups per BSA.

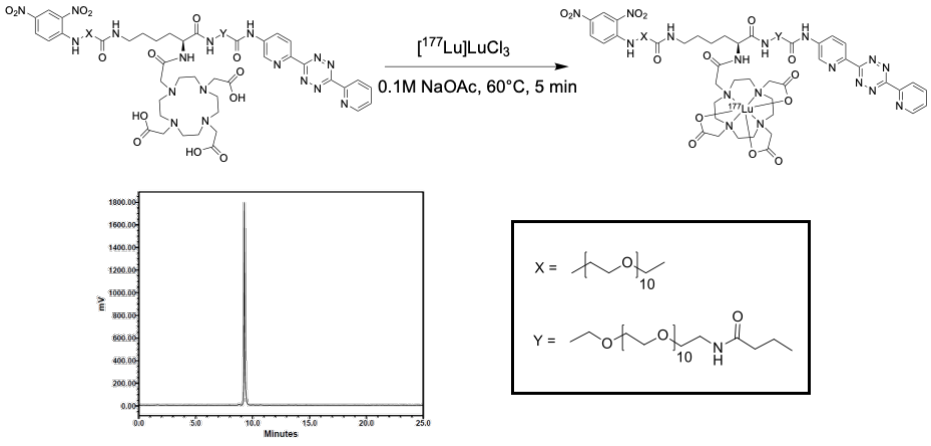

Fig. 5.3. Radiolabelling scheme and radio-HPLC chromatogram of the tetrazine small molecule labelled with lutetium-177.

RT immobilizes in the tumor microenvironment

To evaluate the spatial distribution of the compound within the tumor, qualitative autoradiography studies were performed. Subcutaneous E0771 tumors were grown in C57/Bl6 mice. Mice were treated with a single intratumoral injection of RT when palpable tumors arose (12 days after implantation) and groups of mice were sacrificed at 24, 72 and 120 hours (Figure 5.4). These images revealed that the compound was able to distribute well throughout the tumor after a single injection, which is evident out to 120 hours. To quantitatively evaluate the long-term retention of the RT in the tumor as well as to assess uptake in non-tumor tissues, biodistribution studies were performed. RT showed high retention in the tumor out to 120 hours as well as high tumor to non-tumor ratios, which are ideal for therapy (Figure S5.2, Table S5.1, n=3).

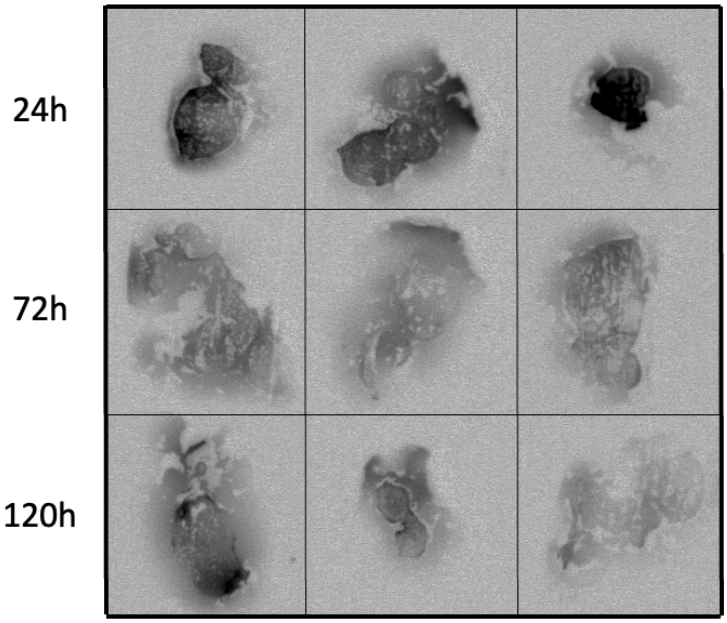

Fig. 5.4. Autoradiography of tumors treated with a single intratumoral injection of RT shows distribution in the TME.

C57/Bl6 mice bearing subcutaneous E0771 tumors were treated with a single intratumoral dose of RT (0.15 MBq – 0.30 MBq). Mice were sacrificed at 24, 72 and 120 hours after treatment and tumors were harvested and flash frozen for autoradiography. Each image represents a slice of an individual tumor. The darker the area, the more radioactive decay that was detected in that area.

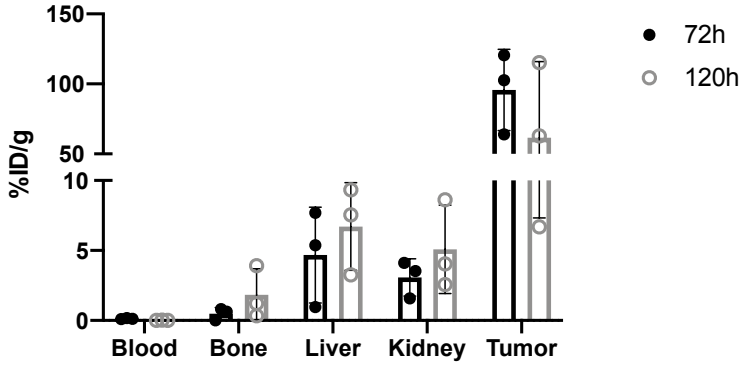

Fig. S5.2. Biodistribution studies show retention of RT in the tumor

Balb/c mice bearing subcutaneous 4T1 tumors were administered 0.22 MBq (SD ± 0.16 MBq) intratumorally. Groups of mice (n=3) were sacrificed 72 and 120 hours after treatment and tissues were harvested to assess tumor retention and uptake in non-target tissues.

Table S5.1. Biodistribution studies. %ID/g values for the complete tissue list, for each mouse (n=3 per timepoint).

Tissue	72 h			120 h		
Blood	0.18	0.12	0.10	0.01	0.03	0.01
Adipose	0.00	0.58	0.55	0.71	1.21	0.45
Adrenals	0.00	0.97	0.83	2.32	3.18	0.87
Bone	0.00	0.63	0.82	1.22	3.92	0.34
Brain	0.00	0.02	0.01	0.01	0.12	0.04
Gall Bladder	0.00	1.88	0.00	6.82	6.99	0.60
Heart	0.00	0.73	1.02	1.37	1.40	0.34
Kidneys	1.58	3.53	4.11	4.05	8.63	2.56
Large Intestine + Caecum	0.26	0.47	0.60	0.50	0.75	0.32
Liver	0.96	5.37	7.70	7.55	9.34	3.25
Lungs	0.00	0.61	1.03	0.84	1.08	0.21
Pancreas	0.00	0.66	0.90	0.87	1.02	0.23
Skeletal Muscle	0.00	0.39	0.55	6.46	18.85	0.25
Small Intestine	0.19	0.35	0.49	0.41	0.55	0.11
Spleen	0.00	2.27	3.46	2.57	3.69	0.70
Stomach	0.32	0.26	0.45	0.64	0.48	0.14
Thyroid/Trachea	0.00	0.67	1.17	0.69	1.23	1.08
Tumor	63.95	102.63	120.56	6.69	115.25	62.89
Urine + Bladder	2.18	8.79	0.94	4.68	11.09	2.60

Radiotherapy results in improved prognostic outcomes

While radionuclide therapy may be administered as a single or fractionated dose in the clinic, studies suggest improved therapeutic efficacy and enhanced antitumor immunity with fractioned regimens, employing intratumoral injections of as little as 2 MBq per dose in murine xenograft models [22–25]. In an effort to determine the most efficacious dosing regimen for our RT, dose optimization studies were performed. C57/Bl6 mice bearing E0771 subcutaneous tumors on the left flank were treated with RT intratumorally and monitored for overall survival. Preliminary studies utilized a two-dose

regimen, with single doses up to 0.74 MBq (Figure S5.3). This range of radioactivity was insufficient to slow tumor progression and therefore, the maximum dose was increased to 3.33 MBq and administered as a single dose to monitor host toxicity and tolerability (Figure S5.4). Mice tolerated treatment well with no acute toxicity seen. Moving to multi-dosing to promote improved efficacy and sustained tumor regression, two doses, with doses ranging from 0 – 4.44 MBq, were given five days apart. This regimen resulted in delayed tumor progression and improved survival outcome (Figure 5.5).

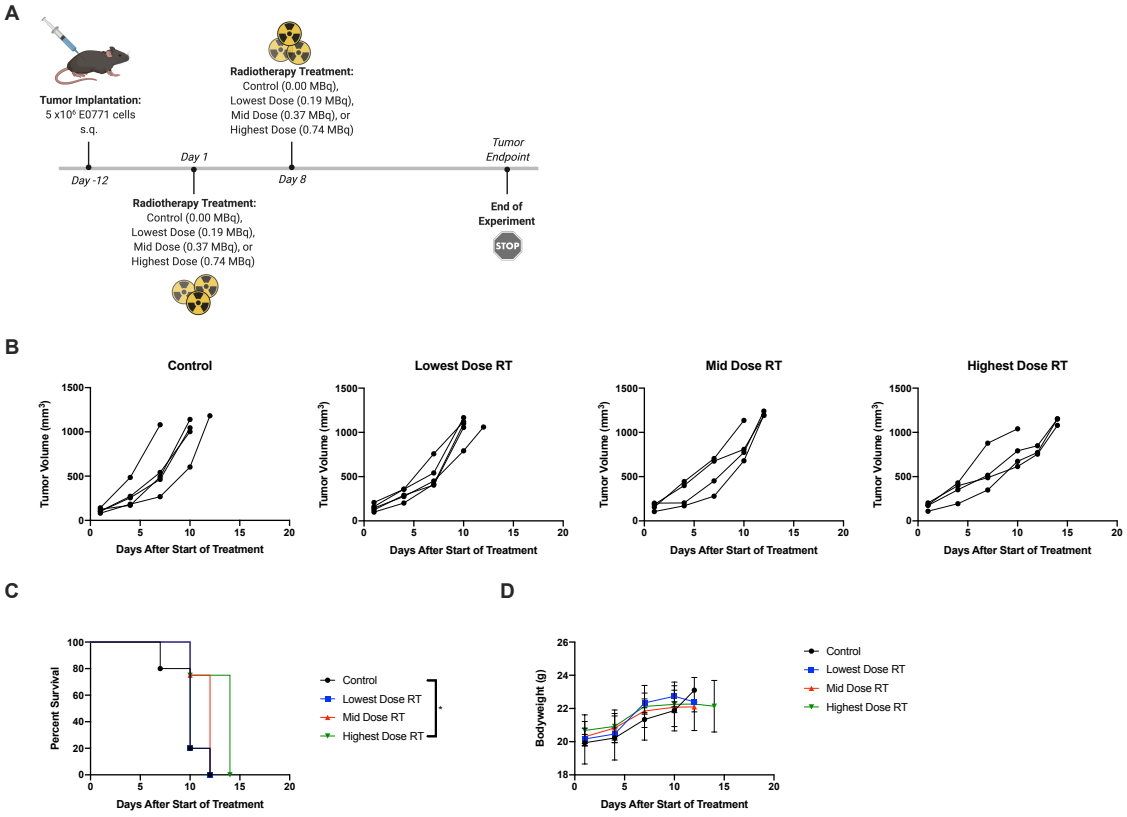

Fig. S5.3. Preliminary dose optimization studies for RT regimens

(**A**) C57/Bl6 mice bearing E0771 tumors were treated with control, lowest dose RT, mid dose RT or highest dose RT. Each treatment schedule outlines a separate experiment. (**B**)

Tumor volumes were measured every 2-3 days from the start of treatment until mice reached endpoint. Each line represents an individual mouse within the group. (**C**) Kaplan-Meier survival curves of each group. (**D**) Average bodyweights for all groups.

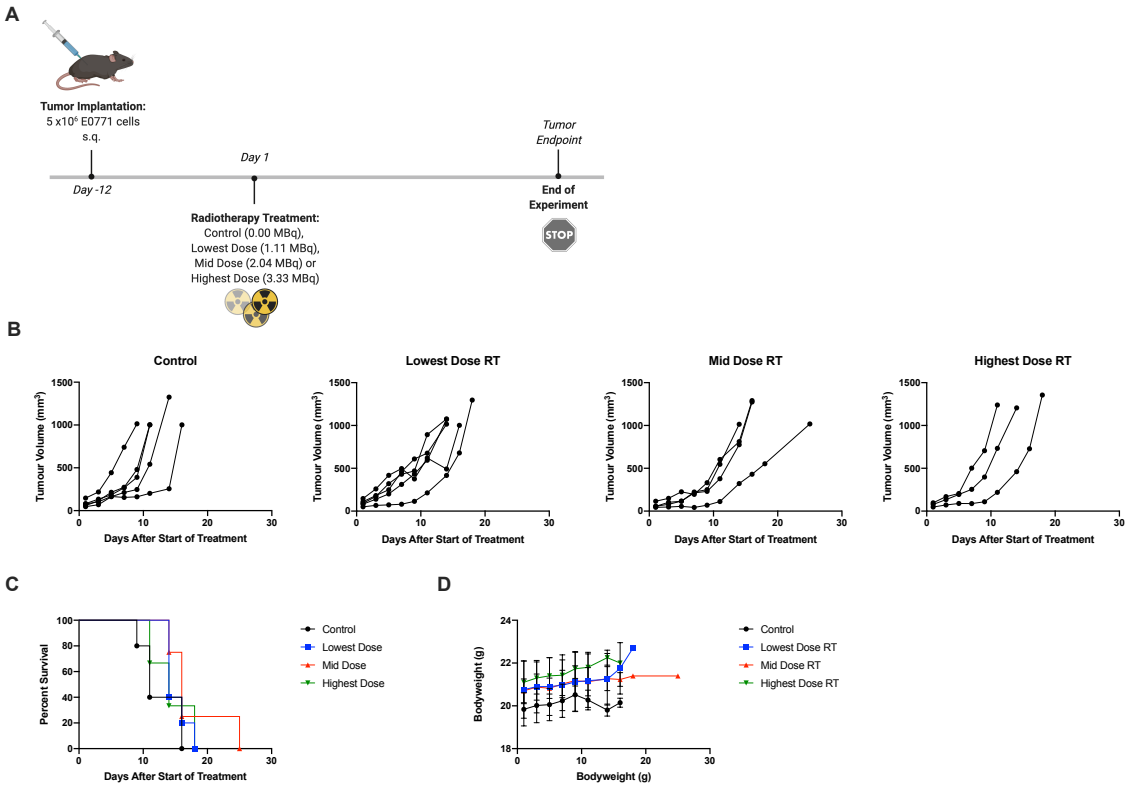

Fig. S5.4. Dose optimization studies for RT regimens

(**A**) C57/Bl6 mice bearing E0771 tumors were treated with control, lowest dose RT, mid dose RT or highest dose RT. Each treatment schedule outlines a separate experiment. (**B**) Tumor volumes were measured every 2-3 days from the start of treatment until mice reached endpoint. Each line represents an individual mouse within the group. (**C**) Kaplan-Meier survival curves of each group. (**D**) Average bodyweights for all groups.

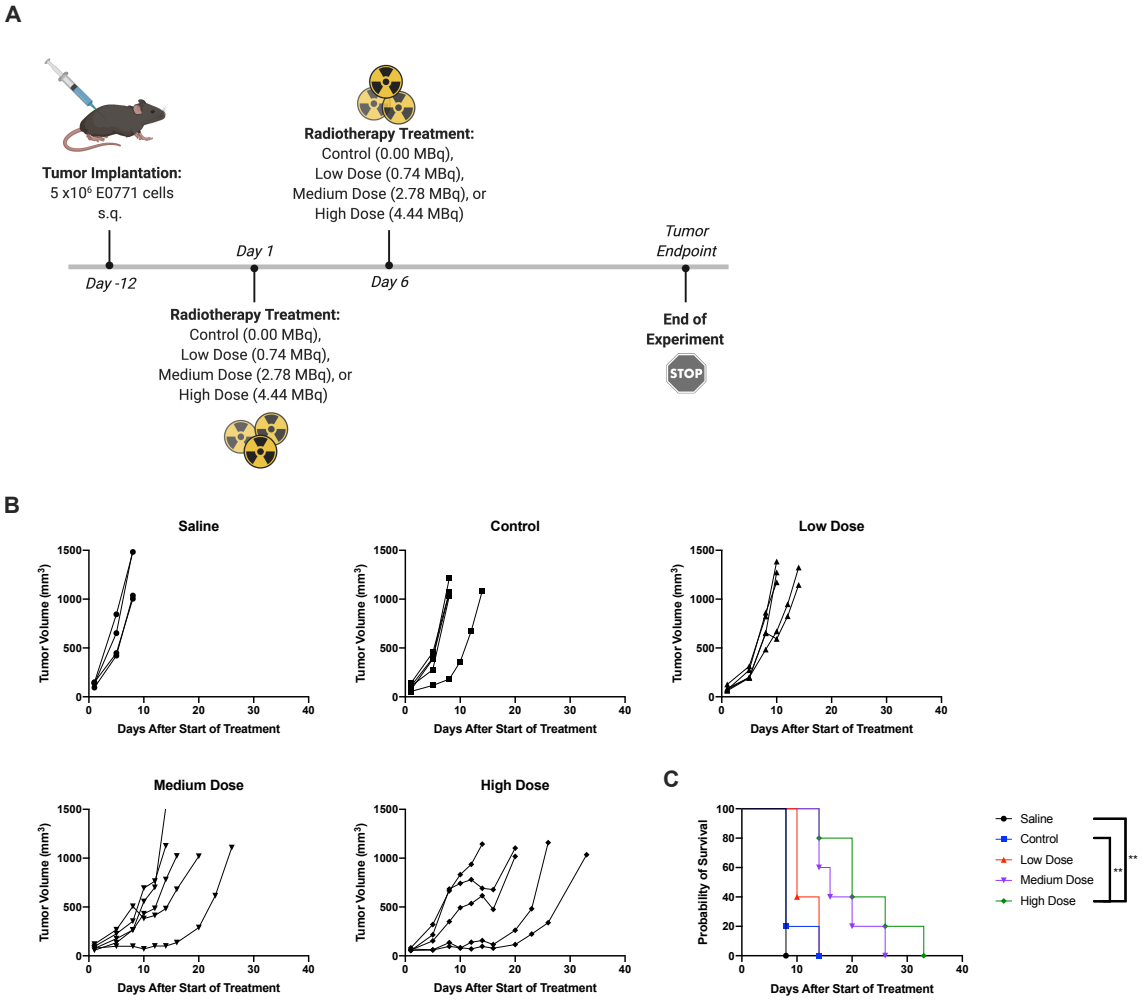

Fig. 5.5. Two administrations of the highest dose RT improved survival outcomes (**A**) C57/Bl6 mice bearing subcutaneous E0771 tumors on the left flank were treated with PBS, control (non-radioactive compound), low dose (0.74 MBq), medium dose (2.78 MBq) or high dose (4.44 MBq) on days 1 and 6. (**B**) Tumor volumes were measured every 2-3 days from the start of treatment until mice reached endpoint. Each line represents an individual mouse within the group. (**C**) Kaplan-Meier survival curves of each group. **P<0.01.

RT + CP improves overall survival in tumor-bearing mice

As CP continues to gain traction as a viable therapeutic option, using PD-L1 expression as a predictive biomarker has become more commonplace. TNBC tumors do indeed express PD-L1 [26], however, the expression is low and it is not homogenously distributed throughout the tumor, but rather found in focal areas in a small proportion of cancer cells [27]. Further to this, clinical trials have reported both the efficiency and necessity of combined therapeutic modalities, as TNBC patients often have short-lived responses to CP on its own [28]. Based on our preliminary studies, we hypothesized that high dose RT is capable of sensitizing tumors to CP. Survival studies were performed with the addition of dual CP targeting the non-redundant pathways of cytotoxic T-lymphocyte antigen 4 and programmed death ligand-1 (with anti-CTLA4 and anti-PD-L1 antibodies, respectively). While neither control (non-radioactive TCO-BSA), RT alone, CP alone or vehicle control + CP showed therapeutic efficacy, the combination of RT + CP resulted in greatly improved overall survival (Figure 5.6).

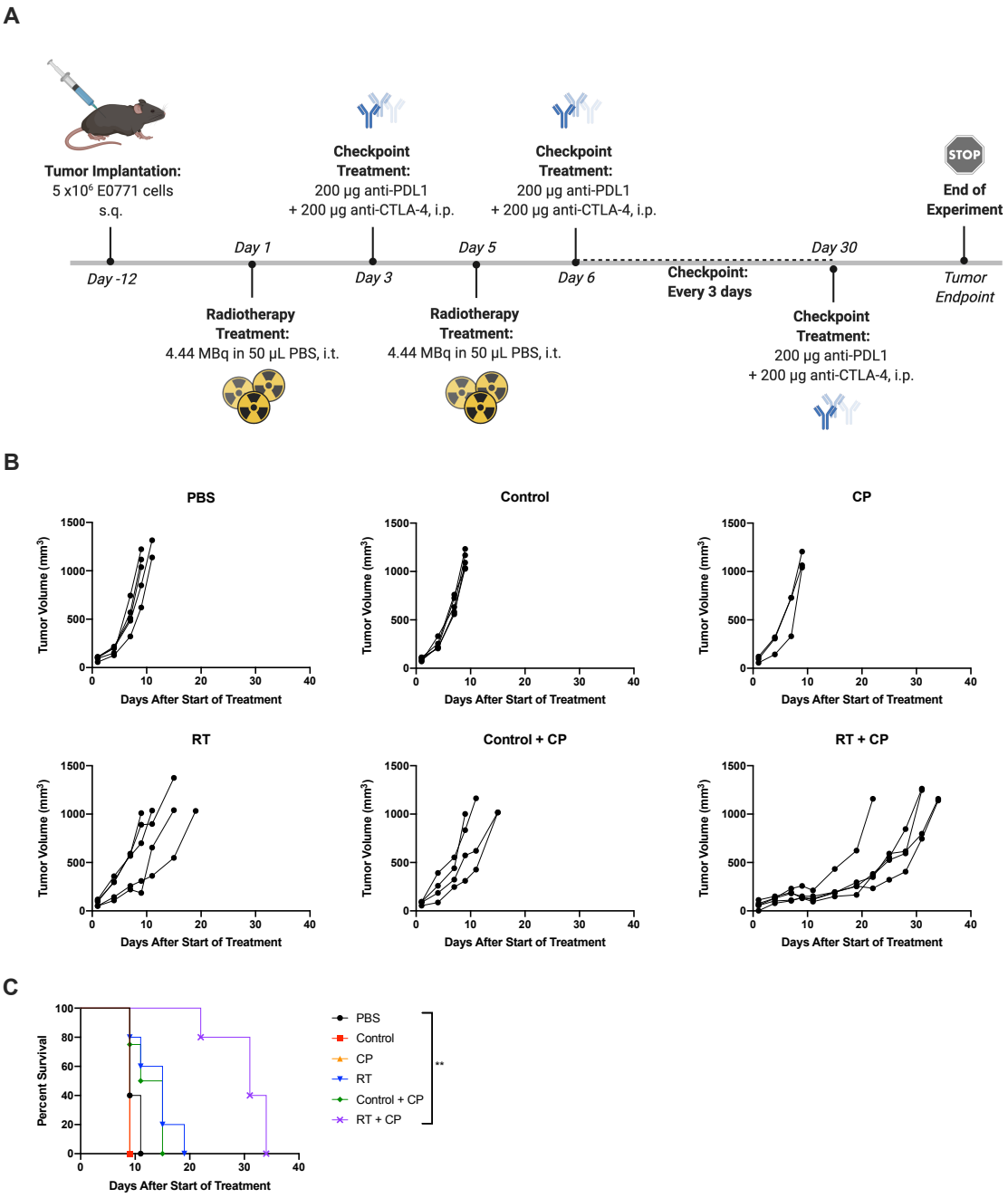

Fig. 5.6. RT + CP significantly improves overall survival.

(**A**) C57/Bl6 mice bearing E0771 tumors were treated with PBS, control, CP (anti-CTLA4 and anti-PD-L1), RT, control + CP or RT + CP. (**B**) Tumor volumes were measured every 2-3 days from the start of treatment until mice reached endpoint. Each

line represents an individual mouse within the group. (**C**) Kaplan- Meier survival curves of each group. **P<0.001.

Radiotherapy + CP increases TILs in otherwise immune-bare tumors

To further investigate the impact of each component of our therapy to the TME, histologic assessment was performed. Tumors were harvested on day 7 from mice treated with PBS, control, CP, RT, control + CP and RT + CP. Analysis of whole tumor sections harvested and stained with hematoxylin and eosin (H&E) shows that mice treated with PBS or the control compound have large tumors with many multi-nucleated cells, suggesting rapid cellular division. Mice treated with CP, RT or control + CP present with pockets of necrosis and many multi-nucleated cells surrounding these areas, suggesting that although these therapies may induce acute necrosis in areas of the tumor, these mice still have rapid tumor kinetics and disease progression. As expected from survival study outcomes, tumors harvested from mice that were treated with RT + CP present with increased necrosis and shrinking cellular structures; likely a direct result of their response to therapy.

Tumors were further stained with CD4, CD8, and F4/80 to assess immune cell infiltrates in the tumor. Mice treated with PBS or the control compound present with moderate levels of $CD4^+$ and $CD8^+$ cells with densely populated areas of $F4/80^+$ macrophages. Mice treated with CP therapy have increased levels of $CD4^+$ and $CD8^+$ cells and substantial increases of $F4/80^+$ macrophages. Interestingly, mice that were treated with RT alone have significantly decreased levels of $CD4^+$ and $CD8^+$ cells, with a moderate decrease in $F4/80^+$ macrophages. Control + CP tumors appeared very similar to

those treated with CP alone, suggesting that CP was able to increase the level of $CD4^+$, $CD8^+$ and $F4/80^+$ cells in the tumor. Mice treated with RT + CP have moderate levels of $CD4^+$ and $CD8^+$ cells (similar to PBS treated mice), but decreased levels of $F4/80^+$ macrophages.

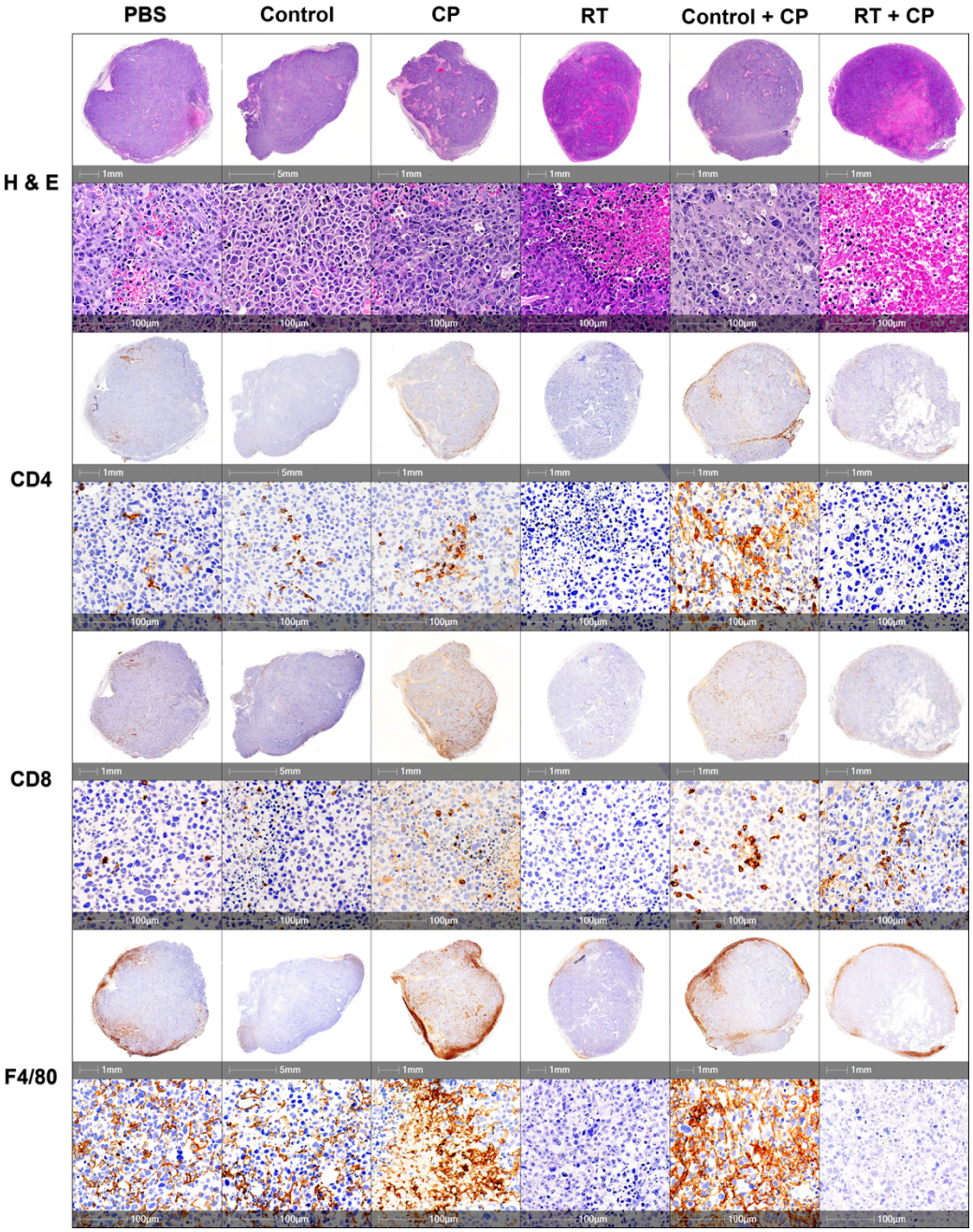

Fig. 5.7. IHC analysis of immune cell infiltrates

C57/Bl6 mice bearing E0771 tumors were treated with PBS, control, CP, RT, control + CP or RT + CP and tumors were harvested on day 7. Tumors were sectioned and stained with H&E, CD4, CD8 and F4/80 for pathologic analysis. Each representative image shows a whole section of an individual tumor from the given group.

RT + CP decreases immunosuppressive MDSCs in the peripheral blood

To investigate the systemic effects of therapeutic intervention, we performed immune analysis studies. E0771 tumors were grown in C57/Bl6 mice and treated with PBS, control, CP, RT, control + CP and RT + CP. RT doses were kept consistent with previous studies in Figures 6 and 7. Blood was drawn on days 4 and 9 and peripheral blood mononuclear cells (PBMCs) were analyzed via flow cytometry. While no significant difference was seen in $CD4^+$ or $CD8^+$ T cells, RT and RT + CP did significantly reduce macrophages ($F4/80^+$ cells) on day 4. Interestingly, while no therapy was able to suppress myeloid-derived suppressor cells (MDSCs; $Ly6G^{hi}Ly6C^{int}$ cells) at day 4, both control + CP and RT + CP significantly decrease the frequency of circulating MDSCs by day 9 (Figure 5.8).

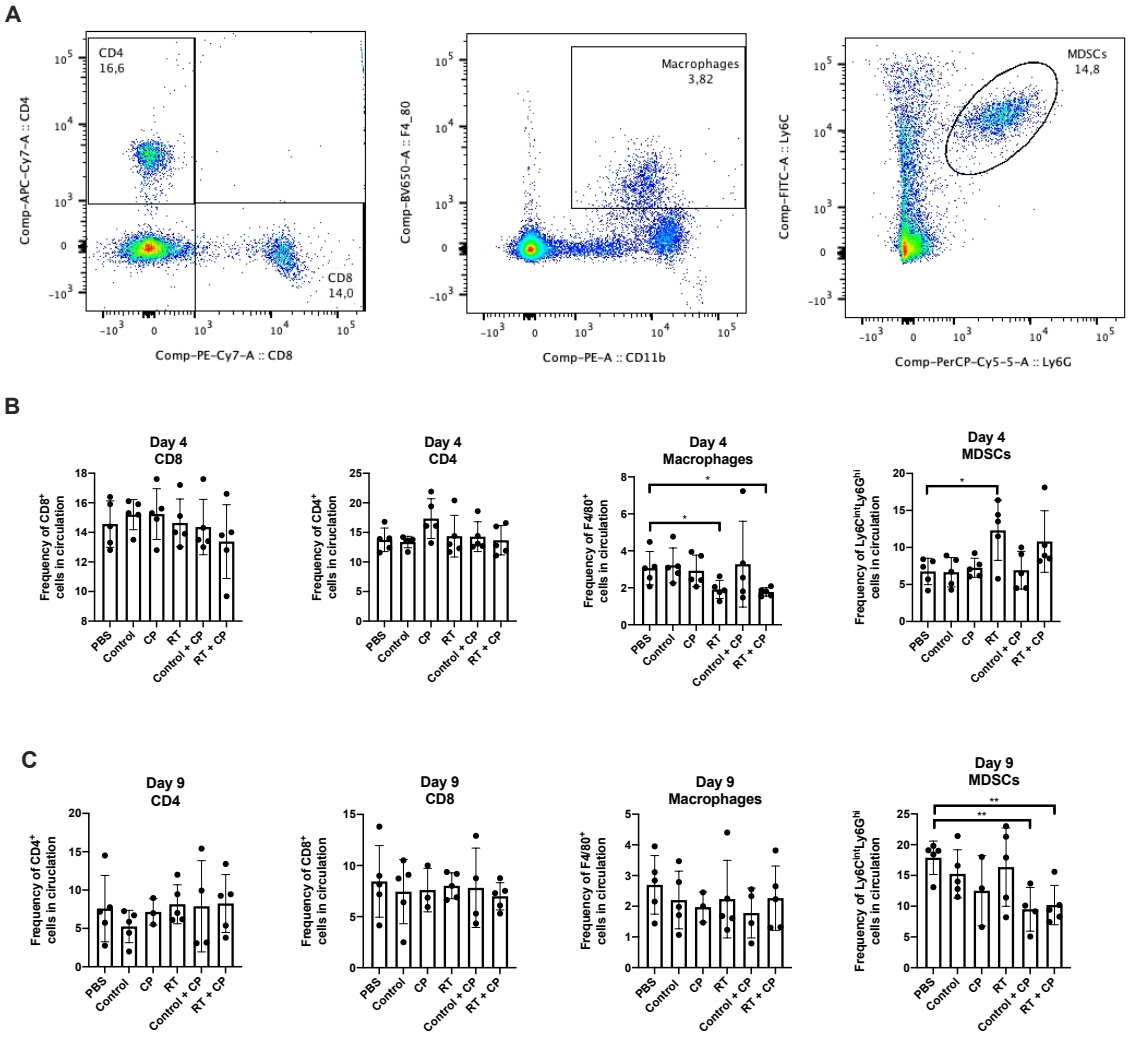

Fig. 5.8. RT + CP decreases immunosuppressive MDSCs in the peripheral blood

C57/Bl6 mice bearing E0771 tumors were treated with either PBS, Control, CP, RT, Control + CP or RT + CP. Blood was drawn on days 4 and 9 and analyzed via flow cytometry. (**A**) Representative flow plots showing the gating strategy for $CD4^+$ T cells, $CD8^+$ T cells, $F4/80^+$ macrophages and $Ly6G^{hi}Ly6C^{int}$ MDSCs. (**B**) Bar plots showing the frequency of cells in circulation on day 4. **(E)** Bar plots showing the frequency of cells in circulation on day 9. *P<0.05; **P<0.01.

5.3. Discussion

Clinical studies have detailed the synergistic benefit of combined external beam radiation therapy and immunotherapy [29–34]. Hodge and colleagues demonstrated that external beam radiation of tumors can alter tumor phenotype, rendering it susceptible to immune-mediated killing [35]. While external beam radiation has been a mainstay, first line therapy for many types of cancer for more than 100 years, it comes with unfavorable side effects such as damage to surrounding tissues and limited utility in metastatic disease. To combat this, researchers have shifted towards the development of internal RT, which can deliver cytotoxic levels of radiation directly to disease sites with a high level of specificity. Indeed, RT can be highly selective not only due to the nature of the targeting vector chosen, but also through the choice of radionuclide used. For example, beta emitting radioisotopes are unable to drive therapeutic response in hypoxic tumors [36,37]. In such an instance, the radionuclide can be changed to an alpha emitter, such as actinium-225, for improved efficacy and decreased toxicity to the patient. This allows for the development and utilization of a single tunable probe, which can then be personalized for optimal effectiveness for individual cancers.

In this paper, we have investigated the combined effects of RT with the beta-emitting radionuclide lutetium-177 and CP immunotherapy using anti-PD-L1 and anti-CTLA-4 in an E0771 murine TNBC tumor model. While CP alone showed no survival benefit in our model, the combination of control + CP did show modest benefit, likely due to increased T cell-mediated killing from CP therapy. However, this benefit was not translated into significant improvements in overall survival, which was only seen with the

combination of RT + CP. While studies have documented correlations between increased levels of T cells and improved overall survival in TNBC patients [38], this alone is often insufficient to overcome intrinsic resistance mechanisms and tumor relapse. Indeed, resistance mechanisms are most commonly driven by the immunosuppressive TME, where MDSCs and tumor-associated macrophages (TAMs) play a crucial role. MDSC frequency is directly correlated with tumor progression, recurrence, poor prognosis and decreased efficacy of immunotherapies [39]. In our therapeutic combination, we have shown that RT + CP is able to suppress the frequency of MDSCs in peripheral blood, potentially contributing to the observed improved therapeutic efficacy in the form of increased survival. While we do also see suppression of MDSCs in the control + CP group, this does not correlate with a benefit in overall survival and may simply be the effect of increase T cell killing due to CP administration. Additionally, in TNBC, TAMs have been shown to promote tumor growth and progression, while also modulating the levels of PD-L1 expression [40]. In our studies, we have shown that both RT and RT + CP suppresses peripheral macrophages as early as day 4 (Figure 5.8), suggesting that early treatment with RT aids in alleviating TAM-modulation of PD-L1 suppressive functions, though more experiments are required to properly investigate this phenomenon. Immunotherapies aim to stimulate the immune system to mount a systemic anti-tumor immune response to recognize and destroy tumor cells within the body. Consideration of the abscopal effect and the possibility that RT can truly induce a bona fide anti-tumor immune response greatly expands the breadth of application for this therapeutic platform as it need not be used solely for primary lesions but can also induce regression of distant

microscopic lesions as well. While this work was completed in a transplantable murine model of TNBC, these studies can be applied to many solid tumor types, increasing the potential translatability of our findings. Additionally, the use of non-radiolabeled BSA was shown to have no influence on therapeutic outcomes or tumor kinetics (as assessed with our control groups). For clinical translation, the BSA derivative can be replaced with the corresponding human serum albumin analogue.

Our studies are limited by the nature of murine hosts and their inability to accurately represent human biology. Indeed, cancer metastasis is a major cause of failed therapeutic intervention and cancer-related deaths [41,42] and our data was conducted in a subcutaneous tumor model representative of primary tumor formation. For enhanced translative capacity, our therapeutic platform should be studied in metastatic and spontaneously arising tumor models to better recapitulate de novo tumor formation in a host. In these models, we would treat the primary tumor and monitor response in metastatic lesions in terms of both the size and number of lesions formed.

5.4. Materials and Methods

Cell Lines

Murine medullary breast adenocarcinoma cells isolated as a spontaneous tumor from a C57/Bl6 mouse (E0771; CH3 Biosystems, Amherst, NY) were maintained in roswell park memorial institute (RPMI) medium supplemented with 10% FBS, 10 mM HEPES, 200 μM geneticin and 2 mM L-glutamine. Murine mammary gland breast cancer cells isolated as a spontaneous tumor from a Balb/c mouse (4T1; ATCC® CRL2539™) were

maintained in RPMI medium supplemented with 10% FBS, 2 mM L-glutamine, 100U/mL penicillin and 100 μg/mL streptomycin. All cells were grown at 37 °C with 5% CO_2.

Chemistry General

Chemicals and reagents for synthesis were purchased from Sigma-Aldrich and Conjuprobe and used without further purification. ^{177}Lu[Lu] was produced by the McMaster Nuclear Reactor (MNR, Hamilton, Ontario) using the ^{176}Lu (p,γ) reaction and was provided as a solution of [^{177}Lu]$LuCl_3$ in 0.01 M HCl. Radio-TLC was performed using a Bioscan AR-2000 imaging scanner on iTLC-SG glass microfiber chromatography paper (SGI0001, Agilent Technologies) plates using 0.1 M EDTA as the eluent. For each TLC performed, plates were spotted with approximately 2 μL (~3.7 kBq) and run for 5 minutes. MALDI data were obtained using a Bruker Ultraflextreme spectrometer.

In Vivo Therapy Experiments

Mice were maintained at the McMaster University Central Animal Facility and all the procedures were performed in full compliance with the Canadian Council on Animal Care and approved by the Animal Research Ethics Board and the Health Physics Department of McMaster University. Six- to eight-week-old female C57/Bl6 mice (Charles River Laboratories, Wilmington, MA) were used to implant 5×10^6 E0771 cells subcutaneously on the left flank. Mice were weighed and all found to be approximately 20 g in size. Mice were housed in groups, 5 / cage, fed a normal diet and kept at room temperature. To minimize experimental variability, low passage E0771 cells were used for subcutaneous

injections. Twelve days after injection, the tumors reached treatable average tumor volume (50-100 mm^3). Mice were blindly randomized prior to the start of treatment, but not blinded one treatments commenced. In experimental groups receiving control treatment, mice were treated on day 1 and day 5 with DNP-DOTA-BSA (100 µg / 50 µL PBS, intratumorally). Experimental groups receiving RT treatment were treated on day 1 and day 5 with ~4.44 MBq of ^{177}Lu-DNP-DOTA-BSA (100 µg / 50 µL PBS, intratumorally). Experimental groups receiving CP were treated with α-CTLA-4 (BioXCell, BE0131) and α-PD-L1 (BioXCell, BE101) antibodies (200 µg / 200 µL PBS each, intraperitoneally) starting on day 3, every 3 days until mice reached endpoint or a total of 10 doses had been given. For all mouse studies, tumors were measured every 2 – 3 days and mice having a tumor volume of 1000 mm^3 were classified as end point.

Radiochemistry Methods

To a solution of tetrazine small molecule (100 µg, 48.0 nmol) in 100 µL of 0.1 M NaOAc (pH 5.5) was added [^{177}Lu]$LuCl_3$ (31-74 MBq). The reaction mixture was heated to 60°C for 5 min at which point a radio-TLC (cellulose/silica plate) was run in 0.1 M EDTA solution. The radiochemical yield of the reaction was determined to be >99% with >99% radiochemical purity. The radiolabelled tetrazine was added to a solution of TCO-BSA (2 mg/mL) in saline at room temperature for 10 minutes. The reaction was added to a 50 kDa spin filter and centrifuged at 4000 rpm for 10 minutes, which had been previously activated with 1.00 mL of saline. The supernatant was washed twice with 1 mL of sterile saline and centrifuged as stated above, followed by resuspension in sterile saline for injection. The conjugation efficiency of the reaction was 46 ± 5% (n=3).

Autoradiography

C57Bl/6 mice bearing an E0771 flank tumor were administered a single dose of radiolabelled BSA (0.15 – 0.33 MBq / 100 µg, intratumorally) on day 12 of growth when the tumors were palpable (~100 mm^3). The mice were sacrificed after 24, 72 or 120 hours (n=3) at which point the tumors were harvested, placed on a cryomold and submerged in optimal cutting temperature compound. The cryomold was then wrapped in plastic wrap, and flash frozen in liquid nitrogen for 15 seconds. The tumors were sent for analysis where they were sliced and placed on a phosphor screen for 10 days.

Biodistribution Studies

Female, 5-6 week old Balb/c mice ordered from Charles River Laboratory (Kingston, NY) were inoculated with 1×10^6 4T1 breast cancer cells in the right flank. On day 7 of growth, the mice were administered radiolabelled BSA (0.07-0.33 MBq / 100 µg, intratumorally). At 72 and 120 h post-injection (n = 3 per time point), mice were anesthetized with 3% isoflurane and euthanized by cervical dislocation. Blood, adipose, adrenals, bone, brain, gall bladder, heart, kidneys, large intestine and caecum (with contents), liver, lungs, pancreas, skeletal muscle, small intestine (with contents), spleen, stomach (with contents), thyroid/trachea, urine + bladder, tumor and tail were collected, weighed and counted in a gamma counter. Decay correction was used to normalize organ activity measurements to time of dose preparation for data calculations with respect to injected dose (i.e. %ID/g).

Histology

Non-radioactive tumors were resected on day 7, fixed in 10% formalin for 48 h and then transferred to 70% ethanol for immediate histological processing. Radioactive tumors were resected on day 7, fixed in 10% formalin, decayed for 3 months and then transferred to 70% ethanol for histological processing. Tumor tissue was embedded in paraffin and 4-μm sections were prepared. Tissue sections were processed for hematoxylin staining and IHC using Automated Leica Bond Rx stainer with Bond Refine Polymer Detection kit (Leica, DS9800). All antibodies were diluted in IHC/ISH Super Blocker (Leica, PV6199). Primary antibodies and working dilutions using HIER Retrieval Buffer 2 (Leica, AR9640) were as follows: CD3 (1:150; Abcam, ab16669), CD4 (1:800; eBio, 14-9766), CD8a (1:1000; eBio, 14-0808). For F4/80 (1:500; AbD Serotec, MCA497R) an Enzyme 1 pre-treatment was performed before staining with antibody (AR9551). Antibodies CD4, CD8a,CD19 and F4/80 all required a secondary antibody before polymer detection using Rabbit anti-rat (Vector labs BA4001) at a dilution of 1:100. Immunohistochemistry slides were digitalized using the Olympus VS120-L100-W automated slide scanner. They were batch-scanned on the brightfield setting at 20x magnification. The color camera used was the Pike 505C VC50.

Flow Cytometry Analysis

150 μL blood was collected from the periorbital sinus. Red blood cells from all samples were lysed using ACK buffer. The PBMCs were treated with anti-CD16/CD32 (Fc block) and surface stained with fluorescently conjugated antibodies for FVS (BD Biosciences, #564406), CD4 (BD Biosciences, #561830), CD8 (BD Biosciences, #563046), CD11b (BD Biosciences, #553311), Ly6C (BD Biosciences, #553104), Ly6G (BD Biosciences,

#560602), F4/80 (BD Biosciences, #743282). LSRFortessa flow cytometer with FACSDiva software (BD Biosciences) was used for data acquisition and FlowJo Mac, version 10.0 software was used for data analysis.

Statistical Analysis

For each statistical analysis used, normality of the distributions and variance assumptions were tested before running the statistical analyses. Multiple t-tests were used to determine the statistical significance of the differences in means. The log-rank Mantel-Cox test and the Gehan-Breslow-Wilcoxon test were used to determine statistical significance for the difference in Kaplan-Meier survival curves between treatments. All the tests were two-sided. The null hypothesis was rejected for p-values less than 0.05. All data analyses were carried out using GraphPad Prism.

Supplementary Materials: The following are available online at www.mdpi.com/xxx/s1, Fig. S1: MALDI-MS confirms conjugation of TCO to BSA, Fig. S2: Biodistribution studies show retention of RT in the tumor, Table S1: Biodistribution studies. %ID/g values for the complete tissue list, for each mouse (n=3 per timepoint). Fig. S3: Preliminary dose optimization studies for RT regimens, Fig. S4: Dose optimization studies for RT regimens.

Author Contributions: Conceptualization, A.V., S.R., K.M. and J.V.; Methodology, A.V. and S.R.; Investigation, A.V., S.R., N.M. and N.E.; Writing – Original Draft, A.V. and S.R.; Writing – Review & Editing, A.V., S.R., N.M., N.E., K.M. and J.V.; Funding Acquisition, K.M. and J.V.; Resources, K.M. and J.V.; Supervision, K.M. and J.V.

Funding: This work was sponsored by operating grants from the Canadian Cancer Society Research Institute; grant #706280 and #7038587.

Institutional Review Board Statement: In this section, please add the Institutional Review Board Statement and approval number for studies involving humans or animals. Please note that the Editorial Office might ask you for further information. Please add "The study was conducted according to the guidelines of the Declaration of Helsinki, and approved by the Institutional Review Board (or Ethics Committee) of NAME OF INSTITUTE (protocol code XXX and date of approval)." OR "Ethical review and approval were waived for this study, due to REASON (please provide a detailed justification)." OR "Not applicable." for studies not involving humans or animals. You might also choose to exclude this statement if the study did not involve humans or animals.

Acknowledgments: Alyssa Vito was the recipient of the Vanier Canada Graduate Scholarship. The authors would like to acknowledge the core histology facility at McMaster University for their work processing histologic samples and the MPIC Facility for scanning of IHC slides.

Conflicts of Interest: The authors declare no conflict of interest. The funders had no role in the design of the study; in the collection, analyses, or interpretation of data; in the writing of the manuscript, or in the decision to publish the results.

References

1. Ferlay, J.; Colombet, M.; Soerjomataram, I.; Mathers, C.; Parkin, D.M.; Piñeros, M.; Znaor, A.; Bray, F. Estimating the global cancer incidence and mortality in 2018:

GLOBOCAN sources and methods. *Int. J. Cancer* 2019.

2. Wang, X.; Qi, Y.; Kong, X.; Zhai, J.; Li, Y.; Song, Y.; Wang, J.; Feng, X.; Fang, Y. Immunological therapy: A novel thriving area for triple-negative breast cancer treatment. *Cancer Lett.* 2019.

3. Stagg, J.; Allard, B. Immunotherapeutic approaches in triple-negative breast cancer: Latest research and clinical prospects. *Ther. Adv. Med. Oncol.* 2013.

4. Dawson, S.J.; Provenzano, E.; Caldas, C. Triple negative breast cancers: Clinical and prognostic implications. *Eur. J. Cancer* **2009**, doi:10.1016/S0959-8049(09)70013-9.

5. Robert, C. A decade of immune-checkpoint inhibitors in cancer therapy. *Nat. Commun.* 2020.

6. Darvin, P.; Toor, S.M.; Sasidharan Nair, V.; Elkord, E. Immune checkpoint inhibitors: recent progress and potential biomarkers. *Exp. Mol. Med.* 2018.

7. Nowicki, T.S.; Hu-Lieskovan, S.; Ribas, A. Mechanisms of Resistance to PD-1 and PD-L1 Blockade. *Cancer J. (United States)* 2018.

8. Mahoney, K.M.; Rennert, P.D.; Freeman, G.J. Combination cancer immunotherapy and new immunomodulatory targets. *Nat. Rev. Drug Discov.* 2015.

9. Melero, I.; Berman, D.M.; Aznar, M.A.; Korman, A.J.; Gracia, J.L.P.; Haanen, J. Evolving synergistic combinations of targeted immunotherapies to combat cancer. *Nat. Rev. Cancer* 2015.

10. Kalbasi, A.; June, C.H.; Haas, N.; Vapiwala, N. Radiation and immunotherapy: A

synergistic combination. *J. Clin. Invest.* 2013.

11. Afshar, S.F.; Zawaski, J.A.; Inoue, T.; Rendon, D.A.; Zieske, A.W.; Punia, J.N.; Sabek, O.M.; Gaber, M.W. Investigating the Abscopal Effects of Radioablation on Shielded Bone Marrow in Rodent Models Using Multimodality Imaging. *Radiat. Res.* **2017**, doi:10.1667/RR14692.1.

12. MOLE, R.H. Whole body irradiation; radiobiology or medicine? *Br. J. Radiol.* **1953**, doi:10.1259/0007-1285-26-305-234.

13. Larson, S.M.; Carrasquillo, J.A.; Cheung, N.K. V.; Press, O.W. Radioimmunotherapy of human tumours. *Nat. Rev. Cancer* 2015.

14. Sharkey, R.M.; Goldenberg, D.M. Cancer radioimmunotherapy. *Immunotherapy* 2011.

15. Choi, J.; Beaino, W.; Fecek, R.J.; Fabian, K.P.L.; Laymon, C.M.; Kurland, B.F.; Storkus, W.J.; Anderson, C.J. Combined VLA-4–targeted radionuclide therapy and immunotherapy in a mouse model of melanoma. *J. Nucl. Med.* **2018**, doi:10.2967/jnumed.118.209510.

16. Ho, A.Y.; Barker, C.A.; Arnold, B.B.; Powell, S.N.; Hu, Z.I.; Gucalp, A.; Lebron-Zapata, L.; Wen, H.Y.; Kallman, C.; D'Agnolo, A.; et al. A phase 2 clinical trial assessing the efficacy and safety of pembrolizumab and radiotherapy in patients with metastatic triple-negative breast cancer. *Cancer* **2020**, doi:10.1002/cncr.32599.

17. Bakker, R.C.; Lam, M.G.E.H.; van Nimwegen, S.A.; Rosenberg, A.J.W.P.; van Es, R.J.J.; Nijsen, J.F.W. Intratumoral treatment with radioactive beta-emitting

microparticles: a systematic review. *J. Radiat. Oncol.* **2017**, doi:10.1007/s13566-017-0315-6.

18. Ulrich, G.; Dudeck, O.; Furth, C.; Ruf, J.; Grosser, O.S.; Adolf, D.; Stiebler, M.; Ricke, J.; Amthauer, H. Predictive value of intratumoral 99mTc-macroaggregated albumin uptake in patients with colorectal liver metastases scheduled for radioembolization with 90Y-microspheres. *J. Nucl. Med.* **2013**, doi:10.2967/jnumed.112.112508.

19. Caraceni, P.; Tufoni, M.; Bonavita, M.E. Clinical use of albumin. *Blood Transfus.* 2013.

20. Garin, E.; Palard, X.; Rolland, Y. Personalised dosimetry in radioembolisation for HCC: Impact on clinical outcome and on trial design. *Cancers (Basel).* 2020.

21. Rathmann, S. Development of a Versatile Platform for Combination Targeted Radionuclide and Immune Cell Recruitment Therapies using Bio-orthogonal Chemistry, McMaster University, 2020.

22. Vilchis-Juárez, A.; Ferro-Flores, G.; Santos-Cuevas, C.; Morales-Avila, E.; Ocampo-García, B.; Díaz-Nieto, L.; Luna-Gutiérrez, M.; Jiménez-Mancilla, N.; Pedraza-López, M.; Gómez-Oliván, L. Molecular targeting radiotherapy with Cyclo-RGDfK(C) peptides conjugated to 177Lu-labeled gold nanoparticles in tumor-bearing mice. *J. Biomed. Nanotechnol.* **2014**, doi:10.1166/jbn.2014.1721.

23. Hoskin, P.J.; Hopkins, K.; Misra, V.; Holt, T.; Mcmenemin, R.; Dubois, D.; Mckinna, F.; Foran, B.; Madhavan, K.; Macgregor, C.; et al. Effect of Single-Fraction vs

Multifraction Radiotherapy on Ambulatory Status among Patients with Spinal Canal Compression from Metastatic Cancer: The SCORAD Randomized Clinical Trial. *JAMA - J. Am. Med. Assoc.* **2019**, doi:10.1001/jama.2019.17913.

24. Palayoor, S.T.; John-Aryankalayil, M.; Makinde, A.Y.; Falduto, M.T.; Magnuson, S.R.; Coleman, C.N. Differential expression of stress and immune response pathway transcripts and miRNAs in normal human endothelial cells subjected to fractionated or single-dose radiation. *Mol. Cancer Res.* **2014**, doi:10.1158/1541-7786.MCR-13-0623.

25. Schaue, D.; Ratikan, J.A.; Iwamoto, K.S.; McBride, W.H. Maximizing tumor immunity with fractionated radiation. *Int. J. Radiat. Oncol. Biol. Phys.* **2012**, doi:10.1016/j.ijrobp.2011.09.049.

26. Cyprian, F.S.; Akhtar, S.; Gatalica, Z.; Vranic, S. Targeted immunotherapy with a checkpoint inhibitor in combination with chemotherapy: A new clinical paradigm in the treatment of triple-negative breast cancer. *Bosn. J. Basic Med. Sci.* 2019.

27. Dill, E.A.; Gru, A.A.; Atkins, K.A.; Friedman, L.A.; Moore, M.E.; Bullock, T.N.; Cross, J. V.; Dillon, P.M.; Mills, A.M. PD-L1 Expression and Intratumoral Heterogeneity Across Breast Cancer Subtypes and Stages: An Assessment of 245 Primary and 40 Metastatic Tumors. *Am. J. Surg. Pathol.* **2017**, doi:10.1097/PAS.0000000000000780.

28. Vikas, P.; Borcherding, N.; Zhang, W. The clinical promise of immunotherapy in triple-negative breast cancer. *Cancer Manag. Res.* **2018**, doi:10.2147/CMAR.S185176.

29. Finkelstein, S.E.; Fishman, M. Clinical opportunities in combining immunotherapy with radiation therapy. *Front. Oncol.* **2012**,

doi:10.3389/fonc.2012.00169.

30. Hodge, J.W.; Guha, C.; Neefjes, J.; Gulley, J.L. Synergizing radiation therapy and immunotherapy for curing incurable cancers: Opportunities and challenges. *Oncology* 2008.

31. Schiavone, M.B.; Broach, V.; Shoushtari, A.N.; Carvajal, R.D.; Alektiar, K.; Kollmeier, M.A.; Abu-Rustum, N.R.; Leitao, M.M. Combined immunotherapy and radiation for treatment of mucosal melanomas of the lower genital tract. *Gynecol. Oncol. Reports* **2016**, doi:10.1016/j.gore.2016.04.001.

32. Ferrara, T.A.; Hodge, J.W.; Gulley, J.L. Combining radiation and immunotherapy for synergistic antitumor therapy. *Curr. Opin. Mol. Ther.* 2009.

33. Finkelstein, S.E.; Salenius, S.; Mantz, C.A.; Shore, N.D.; Fernandez, E.B.; Shulman, J.; Myslicki, F.A.; Agassi, A.M.; Rotterman, Y.; Devries, T.; et al. Combining immunotherapy and radiation for prostate cancer. *Clin. Genitourin. Cancer* 2015.

34. Hiniker, S.M.; Knox, S.J. Immunotherapy and radiation. *Semin. Oncol.* **2014**, doi:10.1053/j.seminoncol.2014.09.019.

35. Chakraborty, M.; Abrams, S.I.; Coleman, C.N.; Camphausen, K.; Schlom, J.; Hodge, J.W. External beam radiation of tumors alters phenotype of tumor cells to render them susceptible to vaccine-mediated T-cell killing. *Cancer Res.* **2004**, doi:10.1158/0008-5472.CAN-04-0073.

36. Saha, G.B. *Physics and radiobiology of nuclear medicine*; 2013; ISBN 9781461440123.

37. Marcu, L.; Bezak, E.; Allen, B.J. Global comparison of targeted alpha vs targeted beta therapy for cancer: In vitro, in vivo and clinical trials. *Crit. Rev. Oncol. Hematol.* 2018.

38. Gao, G.; Wang, Z.; Qu, X.; Zhang, Z. Prognostic value of tumor-infiltrating lymphocytes in patients with triple-negative breast cancer: A systematic review and meta-analysis. *BMC Cancer* **2020**, doi:10.1186/s12885-020-6668-z.

39. Kang, C.; Jeong, S.Y.; Song, S.Y.; Choi, E.K. The emerging role of myeloid-derived suppressor cells in radiotherapy. *Radiat. Oncol. J.* **2020**, doi:10.3857/roj.2019.00640.

40. Santoni, M.; Romagnoli, E.; Saladino, T.; Foghini, L.; Guarino, S.; Capponi, M.; Giannini, M.; Cognigni, P.D.; Ferrara, G.; Battelli, N. Triple negative breast cancer: Key role of Tumor-Associated Macrophages in regulating the activity of anti-PD-1/PD-L1 agents. *Biochim. Biophys. Acta - Rev. Cancer* 2018.

41. Hanahan, D.; Weinberg, R.A. Hallmarks of cancer: The next generation. *Cell* 2011.

42. Chaffer, C.L.; Weinberg, R.A. A perspective on cancer cell metastasis. *Science (80-.).* 2011.

CHAPTER SIX: CONCLUSIONS AND FUTURE DIRECTIONS

6.1. Impact and Clinical Translation

6.1.1. B Cell Involvement Renders Triple Negative Breast Cancer Sensitive to Immune Checkpoint Blockade Through Downregulation of Myeloid-Derived Suppressor Cells

While immunotherapies have surged to the forefront of oncology research, their focus has largely been on strategies to improve the functionality and activation of T cells, with limited assessment of other immune subsets that may also contribute to antitumor immunity. Indeed, current immunotherapies do not target B cells, despite their predominance in the TME and key role in the adaptive immune response. Recent studies have detailed the role of B cells in promoting responses to immunotherapy treatments and their potential use as predictive biomarkers for response to treatment[1]. Helmink and colleagues performed bulk RNA sequencing and found that B cell markers were the most differentially expressed genes in the tumors of responders versus non-responders[2]. They further assessed the functional contributions of B cells via bulk and single-cell RNA sequencing and demonstrated clonal expansion and unique functional states of B cells within responders. In particular, they identified that a switch to memory B cells was enriched in responding patients. This data was performed on patients with melanoma and renal cell carcinoma but is highly consistent with findings from our studies in TNBC (Chapter 3), suggesting that this B cell-centric signature may have important clinical impact across multiple tumor types.

Petitprez et al. studied the gene expression profiles in 608 tumors across various subtypes of soft-tissue sarcoma. They found that a subset of patients was characterized by the presence of TLS that were rich in B cells and that B cells were the strongest prognostic factor, even in the context of high or low $CD8^+$ T cells[3]. This B-cell-rich subset of patients demonstrated improved overall survival and a high response rate to anti-PD1 ICB in a phase 2 clinical trial, highlighting the significance of B cells and TLS as drivers of response to ICB. This data is in line with our findings (Chapter 3) in which we show that FEC + oHSV-1 therapy increases B cell receptor signaling, sensitizing tumors to ICB.

Authors Nielsen and Nelson have eloquently outlined potential mechanisms by which B cells might enhance cellular immunity, including serving as APCs, organizing TLS and secreting polarizing cytokines[4]. These postulated mechanistic roles of B cells build upon many studies in the field, with B cells and TLS shown to be key promoters of T cell-mediated antitumor immunity[4–6]. While our data is in line with and supportive of these findings, we have proposed an additional function of B cells in modulating immunosuppressive phenotypes in the TME. In particular, we have proposed that B cells regulate the differentiation of MDSCs, via the downregulation of key cytokines and chemokines such as Arg1 and iNOS2. While previous studies have focused on B cell-mediated polarization of T cells towards different functional phenotypes, we have proposed that B cells can also function to polarize differentiating myeloid cells, shifting their polarization to less immunosuppressive phenotypes and decreasing the accumulation of immature MDSCs in the TME. While we have not fully characterized the mechanism

of this regulation, this is the first study to our knowledge to highlight this extremely impactful role of B cells. MDSCs are already a well-characterized biomarker of disease with higher levels being directly correlated with poorer prognostic outcomes and our work shows that B-cell-based immunotherapies may be useful in overcoming MDSC-mediated therapeutic resistance.

We chose to investigate the immune outcome of combination therapies routinely used in the clinic for assessment of current clinical practice and ease of translation of our findings. Indeed, FEC is one of the most commonly used chemotherapy regimens for TNBC patients[7], our oncolytic virus is the same backbone as the FDA approved oHSV (T-Vec)[8] and our ICB antibodies (anti-PD-L1 and anti-CTLA4) are FDA approved for various types of cancer[9–11]. While we continue to see the emergence of more clinical trials employing various combination strategies (most commonly chemotherapy and ICB) for TNBC patients, our work highlights the potential impact of adding oHSV-1 to these platforms for enhanced response to ICB. Additionally, we have shown the importance of B cells in driving therapeutic efficacy and would suggest adding B cells as predictive biomarkers of treatment outcomes.

6.1.2. S100A8A9 as Mediators of Response to Immunotherapy Treatments

S100A8/A9 is a heterodimer of the two calcium-binding proteins S100A8 and S100A9 originally discovered as an immunogenic protein secreted by neutrophils[12]. Since the discovery it has emerged as a critical mediator of inflammation in acute and chronic inflammatory conditions. However, its role in tumorigenesis has been understudied with conflicting reports in the literature of it having both pro- and antitumorigenic functions[13–

[15]. S100A9 is currently used a predictive biomarker of therapeutic responses to inflammatory diseases[14]. Our data supports increased levels of S100A8/A9 as driving improved responses to immunotherapy treatments through macrophages. These findings are highly impactful to the field as S100A9 may be a useful predictive biomarker for response to immunotherapy treatments in TNBC. Indeed, these findings could easily be assessed in clinical trials by analyzing S100A9 levels in serum of patients prior to and after treatment with immunotherapies.

6.1.3. Combined Internal Radionuclide Therapy and Immunotherapy for Treatment of Triple Negative Breast Cancer

Recent years have seen an insurgence of clinical trials combining radiation therapy and immunotherapy. While these two therapies often intertwine in the clinic, little is known about immune outcomes of these combined modalities and there are few studies in the literature with preclinical assessment of them together. There has been a shift away from external beam radiation towards more precise, targeted platforms. In our work, we have used BSA as a protein anchor to allow for optimal delivery of our radiotherapeutic within the site of the tumor, decreasing toxicity to non-target tissues. Since albumin is already used in a variety of pharmaceuticals, we believe this construct allows for rapid clinical translation[16,17]. Additionally, we have used immune checkpoint antibodies that are already used in many clinical trials for various types of cancer, further extending the clinical translatability of this work.

6.2. Study Limitations

The tumor model used throughout the work contained in this dissertation was the E0771 syngeneic murine model. While E0771 cells mimic the aggressive nature of TNBC tumors, the model has two prominent limitations: it is poorly metastatic and requires transplantation. As metastatic disease is a major clinical challenge and TNBC itself is inherently prone to metastasis, immunotherapies that limit metastases are greatly needed. Further, transplantable models fail to recapitulate *de novo* tumor formation with co-evolving tumor-host interactions[18,19]; the immune environment within transplanted and spontaneous tumors differ significantly. In several autochthonous mammary tumor models, disease progression mimics that of humans at the molecular and morphological levels and correlates with clinical outcomes[20,21].

Another limitation of the work performed in this dissertation is the limited number of tumor models used. While PY230 tumors were also used in the manuscript in Chapter 3 to rule out the clonal effect, these are also breast tumors and therefore we cannot rule out that our findings may be cancer type dependent. Additionally, the work described in chapter 5 combining radiotherapy and immunotherapy was limited in terms of immune assessment by the nature of working with radioactive samples.

6.3. Future Directions

In the work presented in this dissertation I have provided insight into different therapeutic platforms aiming to target MDSCs in tumor-bearing hosts. Additionally, an interesting phenomenon was reported in which our platform of FEC + oHSV-1 therapy upregulated B cell receptor signaling pathways, resulting in indirect control of MDSCs in the tumor. While we tried to show this interesting finding, we did not fully elucidate the

mechanism behind it or the interactions between these two key immune cell types that allowed for modulation in the TME.

Future studies should focus on three main points: 1) Sub-setting B cells in our tumor model and identifying the specific subset required for therapeutic efficacy; 2) Sub-setting the myeloid cells in our tumor model and identifying the specific timeline of differentiation and heterogeneity within that population; and 3) Identifying mechanistic correlations between B cells and MDSCs that drives therapeutic efficacy.

To sub-set B cells, we can utilize multi-panel flow cytometry with a comprehensive panel of markers associated with different B cells as well as multi-spectral IF imaging. These studies should span multiple timepoints to see how the populations shift with tumorigenesis, treatment and in mice with durable responses to therapy. Myeloid cell sub-setting can also be done with multi-panel flow cytometry using a comprehensive panel of markers associated with myeloid phenotypes. This should be assessed in the peripheral blood, spleens and tumors of tumor-bearing hosts as well as in the peripheral blood and spleens of naïve hosts. Identifying the mechanistic correlations between B cells and MDSCs is the most interesting and complex challenge for future directions of this work. Mice should be treated with either saline or FEC + oHSV-1 + CP. Both treatment groups should have 5 mice treated with an isotype antibody and 5 mice treated with an anti-CD20 antibody prior to the start of treatment. On day 10 post the start of treatment mice should be sacrificed and MDSCs should be isolated from the tumors and spleens. These MDSCs should then be co-cultured with T cells ex vivo to assess their level of immunosuppression (using T cell proliferation as a readout). Additionally, the

same four groups of mice can be used for flow cytometry and IHC analysis of the bone marrow. Using markers for myeloid cells, B cells and proliferation (Ki67), IHC and flow cytometry can assess the change in myeloid and B cell precursors in the bone marrow in treated versus untreated mice and in mice with or without B cells.

6.4. Concluding Remarks

Oncolytic virotherapy has been studied in the Mossman Lab for many years. Prior to my joining the lab, combination approaches of low-dose chemotherapy and OV therapy had been employed and exhibited potential synergistic activity in murine models. To build upon previous work done in the lab, assess therapies being used in current clinical practice and discover novel findings with widespread applicability, I chose to perform preliminary studies using an oHSV-1 combined with chemotherapy regimens routinely used for TNBC patients. I quickly learned that reverse-translating chemotherapy regimens from humans to mice was more than challenging and simplified the overall therapeutic regimen. In my studies using FEC + oHSV-1 to sensitize tumors to CP therapy I performed RNA sequencing studies, which allowed me to introduce an element of genuine discovery into the project. From this point, all studies conducted in my PhD (and contained within this thesis) truly followed the data as they were presented.

This body of work utilizes therapeutic platforms to sensitize otherwise non-responsive tumors to CP therapy. It assesses the underlying immunological traits associated with therapeutic efficacy, with a general tie of needing to overcome the immunosuppression in the TME. I further delved into the heterogeneity of myeloid cells and in particular the S100A8/A9 proteins, which are linked directly to MDSC levels and

have controversial reports as to their anti- and/or pro-tumorigenic functions in the literature.

References

1. Bruno, T. C. New predictors for immunotherapy responses sharpen our view of the tumour microenvironment. *Nature* (2020). doi:10.1038/d41586-019-03943-0
2. Helmink, B. A. *et al.* B cells and tertiary lymphoid structures promote immunotherapy response. *Nature* (2020). doi:10.1038/s41586-019-1922-8
3. Petitprez, F. *et al.* B cells are associated with survival and immunotherapy response in sarcoma. *Nature* (2020). doi:10.1038/s41586-019-1906-8
4. Nielsen, J. S. & Nelson, B. H. Tumor-infiltrating B cells and T cells: Working together to promote patient survival. *OncoImmunology* **1**, 1623–1625 (2012).
5. Bruno, T. C. *et al.* Antigen-presenting intratumoral B cells affect CD4+ TIL phenotypes in non–small cell lung cancer patients. *Cancer Immunol. Res.* **5**, 898–907 (2017).
6. Nelson, B. H. CD20 + B Cells: The Other Tumor-Infiltrating Lymphocytes . *J. Immunol.* **185**, 4977–4982 (2010).
7. Torres, S., Trudeau, M., Eisen, A., Earle, C. C. & Chan, K. K. W. Adjuvant taxane-based chemotherapy for early stage breast cancer: a real-world comparison of chemotherapy regimens in Ontario. *Breast Cancer Res. Treat.* (2015). doi:10.1007/s10549-015-3441-0
8. Andtbacka, R. H. I. *et al.* Talimogene laherparepvec improves durable response rate in patients with advanced melanoma. *J. Clin. Oncol.* (2015).

doi:10.1200/JCO.2014.58.3377

9. Pfirschke, C. *et al.* Immunogenic Chemotherapy Sensitizes Tumors to Checkpoint Blockade Therapy. *Immunity* (2016). doi:10.1016/j.immuni.2015.11.024
10. Rowshanravan, B., Halliday, N. & Sansom, D. M. CTLA-4: A moving target in immunotherapy. *Blood* (2018). doi:10.1182/blood-2017-06-741033
11. Aguiar, P. N., De Mello, R. A., Hall, P., Tadokoro, H. & De Lima Lopes, G. PD-L1 expression as a predictive biomarker in advanced non-small-cell lung cancer: Updated survival data. *Immunotherapy* (2017). doi:10.2217/imt-2016-0150
12. Gebhardt, C., Németh, J., Angel, P. & Hess, J. S100A8 and S100A9 in inflammation and cancer. *Biochem. Pharmacol.* (2006). doi:10.1016/j.bcp.2006.05.017
13. Turovskaya, O. *et al.* RAGE, carboxylated glycans and S100A8/A9 play essential roles in colitis-associated carcinogenesis. *Carcinogenesis* (2008). doi:10.1093/carcin/bgn188
14. Wang, S. *et al.* S100A8/A9 in inflammation. *Frontiers in Immunology* (2018). doi:10.3389/fimmu.2018.01298
15. Zhao, F. *et al.* S100A9 a new marker for monocytic human myeloid-derived suppressor cells. *Immunology* (2012). doi:10.1111/j.1365-2567.2012.03566.x
16. Ulrich, G. *et al.* Predictive value of intratumoral 99mTc-macroaggregated albumin uptake in patients with colorectal liver metastases scheduled for radioembolization with 90Y-microspheres. *J. Nucl. Med.* (2013). doi:10.2967/jnumed.112.112508
17. Caraceni, P., Tufoni, M. & Bonavita, M. E. Clinical use of albumin. *Blood*

Transfusion (2013). doi:10.2450/2013.005s

18. Schreiber, K., Rowley, D. A., Riethmüller, G. & Schreiber, H. Cancer Immunotherapy and Preclinical Studies: Why We Are Not Wasting Our Time with Animal Experiments. *Hematology/Oncology Clinics of North America* (2006). doi:10.1016/j.hoc.2006.03.001
19. Willimsky, G. *et al.* Immunogenicity of premalignant lesions is the primary cause of general cytotoxic T lymphocyte unresponsiveness. *J. Exp. Med.* (2008). doi:10.1084/jem.20072016
20. Stewart, T. J. & Abrams, S. I. Altered Immune Function during Long-Term Host-Tumor Interactions Can Be Modulated to Retard Autochthonous Neoplastic Growth. *J. Immunol.* (2007). doi:10.4049/jimmunol.179.5.2851
21. Talmadge, J. E., Singh, R. K., Fidler, I. J. & Raz, A. Murine models to evaluate novel and conventional therapeutic strategies for cancer. *American Journal of Pathology* (2007). doi:10.2353/ajpath.2007.060929